# AUTOMOTIVE CLIMATE CONTROL BASED ON THERMAL STATE ESTIMATION

A DISSERTATION

SUBMITTED TO THE DEPARTMENT OF MECHANICAL ENGINEERING

OF GLASGOW UNIVERSITY

IN COMPLETE FULFILLMENT OF THE REQUIREMENTS

FOR THE DEGREE OF

DOCTOR OF PHILOSOPHY

By

Benjamin A. Saunders

June 2002



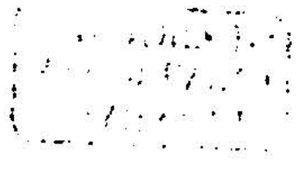

Dedicated To:

My Brother: Angus Alexander Saunders

My Mother: Margaret Susan Saunders

and

In Memory Of My Father: The Late Alfred Roy Saunders

# Abstract

The motivation for the current study is to provide an information base on which to predict the implementation of future automotive HVAC (Heating Ventilation and Air-Conditioning) systems. Thermal state estimation is identified as the key technology in the future development of comfort control and so this investigation concentrates on the current state of the art in thermal state estimation. The aim of this thesis is to provide a detailed review of the requirements involved in estimating thermal state, to investigate the control of thermal state via the cabin environment and to examine user interactions as a source of personalizing the control response. This thesis presents a number of novel contributions in this area.

This thesis contributes a detailed comparison of three of the most popular techniques: the PMV (Predicted Mean Vote), the TSV (Thermal Sensation Vote) and a neural network approach. The TSV thermal state estimation is then used in a novel way by combining it with a state-space controller for the control of thermal state via the temperature of the cabin environment.

The accuracies and performance of the three thermal state estimation methods are presented. Only a few data sets were used but the values comply with results in the literature. In addition to the analytical results the context of the discussions also focus on the implementation issues. The PMV method seemed to have marginally better performance. However, the TSV method was the most direct to implement and to calculate. Control of a test subject's thermal state within a Mercedes-Benz S-class test car was demonstrated successfully using the TSV method for estimation and feedback into a state-space controller.

The second part of this thesis considers fuzzy logic and the concept of gathering control information directly from the user. A rearrangement of the Fuzzy Model Reference Learning Controller (FMRLC) method leads to a new solution of learning interactions. The method is termed "Fuzzy User Reference Learning Controller" (FURLC). The performance of the technique is tested by applying it to learn to estimate the thermal state of a test subject. These tests were carried out by first subjecting the controller to a teaching data set and then

turning the learning rule off and testing with verification data. The method is designed for "on-line" learning however the learning rule was switched off to allow a direct comparison with the neural network approach presented earlier. The controller performs well on estimating thermal state and after three passes with the teaching data outperforms the neural network approach.

The TSV calculation, together with the cabin air temperature, is then combined with the fuzzy controller to form a feedback control loop. The fuzzy logic controller was applied directly to learning the interactions of the user. Only a few results were gathered, nevertheless, the controller demonstrates successfully that personal preferences in the operation of the automotive HVAC system can be learnt from user interactions.

The final chapter provides an algorithmic performance comparison. The PMV, TSV, State-Space controller and the FURLC algorithm were all programmed into a microprocessor. An interface consisting of a 2x16 digit display and a 9-key keypad was also included. The computation times and memory requirements of the algorithms were determined and compared. The PMV method required the most time due to it's iterative nature. The algorithm code for the TSV method is the shortest and uses the least amount of memory. The FURLC method compares well against the TSV and the PMV thermal state methods and also against the state-space controller.

# Preface

This is my contribution to the area of automotive environmental control. When I started this work I was reminded of the quote from Hitch-Hiker's Guide to the Galaxy by the late Douglas Adams:

> "He had found a Nutri-Matic machine which had provided him with a plastic cup filled with a liquid that was almost, but not quite, unlike tea. The way it functioned was very interesting. When the Drink button was pressed it made an instant but highly detailed examination of the subject's taste buds, a spectroscopic analysis of the subject's metabolism and then sent tiny experimental signals down the neural pathways to the taste centres of the subject's brain to see what was likely to go down well. However no one new quite why it did this because it invariably delivered a cupful of liquid that was almost, but not quite, unlike tea."

Douglas Adams, "Hitch-Hiker's Guide to the Galaxy", *Pan Books, London*, pp. 94 - 95, (1980).

One must always be aware that ultimate control and prediction techniques are sometimes let down by the actuators they control. Just as this jocular quote from the Hitch-Hiker's Guide to the Galaxy exemplifies, the ultimate tea making machine can only make the best of the ingredients it has been given. Similarly the ultimate air-conditioning controller can only do as much as the limitation on the air-conditioning plant will allow. The control aims of modern day heating and air-conditioning systems in cars is becoming more and more sophisticated and involves the understanding of what thermal comfort really is. To achieve a thermal comfort controller one must consider the heat transfer boundaries involved (skin temperature), check the current physical state of the test subject (activity level and metabolism) and in essence predict the psychological preference "to see what is likely to go down well".

What is suggested later in this thesis, however, is a prediction of the psychological preference based on previous user interactions with the system. Thus the appreciation of the control is

not in terms of the satisfaction with the system performance. (When control is not adequate the user can interact but when the system performance is not adequate the user can do nothing - and the controller can not learn to provide a better result than the system can provide).

## Thesis Contributions

This thesis represents my own contributions in the area of automotive environmental control. To make it clear what these contributions are the following section will concisely describe the contributions from each chapter.

Chapter 1 contributes a clarification of the terms used in thermal comfort analysis.

Chapter 2 contributes a descriptive experience of the control of an HVAC system and provides a discussion on the observed thermal state votes.

Chapter 3 contributes a review of three thermal state estimation methods and provides for the first time an evaluated performance and implementation comparison.

Chapter 4 contributes and verifies a thermal state control method using the TSV estimation. It proves feasibility of the control of thermal state using a linear state-space controller.

Chapter 5 contributes a new method of learning user interactions and shows how this could be implemented in the automotive cabin.

Chapter 6 contributes a systems level performance comparison between the thermal state estimation methods. It also provides a realization of the typical amount of resources required at the systems level for thermal state estimation and control.

The overall aim of this thesis is to provide a detailed review of the requirements involved in estimating thermal state, to investigate the control of thermal state via the cabin environment and to examine user interactions as a source of personalizing the control response. The motivation for the current study is to provide an information base on which to predict future automotive HVAC system requirements from an implementation perspective. To make these predictions the current state of the art in thermal state estimation is an important key because it is the future of developing "climate control" into "comfort control".

The overall contributions of this thesis achieve this aim by providing performance data and

operational requirements from a diverse selection of preferred methods. The feasibility of the control of thermal state (chapter 4) is an important contribution that demonstrates the definite future of automotive environmental control.

## List of Abbreviations

| Abbreviation | Full Description |
|---|---|
| HVAC | Heating Ventilation and Air Conditioning |
| PMV | Predicted Mean Vote |
| PPD | Predicted Percentage of Dissatisfied |
| TSV | Thermal Sensation Vote |
| PRBS | Pseudo Random Binary Signal |
| ARX | Auto Regression with eXogeneous variables |
| FMRLC | Fuzzy Model Reference Learning Control |
| FURLC | Fuzzy User Reference Learning Control |

# Acknowledgements

I hereby acknowledge the contributions to my work and offer my thanks to the people who have helped and supported me during my work over the last 3 years.

My Supervisors:

Professor K. J. Hunt
Mr. Steve McAslan

The Funding Organizations: EPSRC (Engineering and Physical Science Research Council) and Motorola

Motorola and DaimlerChrysler for additional experimental support and infrastructure.

Additional Support:

Dr. Klaus-Peter Kuhn
Mr. Andreaus Prtel Dip.Ing.
Mr. Martyn Gallop
Mr. Kenneth Stevenson
Mr. Thomas Schauer
Ms. Katherine I. Baxter
Mr. Alexander Roger

Test Subjects:

Mr. Nills-Otto Negaard
Mr. Thomas Breivik
Dr. William Holderbaum
Mr. Dustin Vink
Mr. Andrew Goh
Mr. Myak Stellter
Mr. Georg Bedal
Mr. Sven Langerer

There are many more people who have contributed in an indirect way and deserve my thanks also – Thank you.

# Contents

# List of Tables

# List of Figures

# 1 Introduction Background and Definitions

This chapter is a brief outline of the history of automotive Heating Ventilation and Air-Conditioning (HVAC) systems and their control. This chapter will then present some definitions used in the thermal state estimation research. This is to provide background information for the following chapters.

This chapter contributes a clarification of the terms used in thermal comfort analysis.

## 1.1 Introduction

Automotive Heating, Ventilation and Air Conditioning (HVAC) is an important system to automotive manufacturers and to their customers. Substantial research has been done to develop this system (for example [1], [2] and [3]). Climate control systems are also being investigated for electric vehicles (see [4] and [5]). The thermodynamics involved is standard and the dynamics of modern systems can be described simply, for a brief overview see appendix A. The main operational objective of the system is the supply of heated or cooled air to the passengers at the desired temperature and air velocity and at the desired location. The control of the system in terms of its operational aim has been achieved using modern control techniques. Advances in microprocessor technology have influenced most automotive systems and it is now common to see actuators with built in microcontrollers. The advantages of microcontrollers has reduced the burden on the overall control of the system: containing the problem of local control and offering embedded interface software for higher level control decisions.

Engineers working on the control of automotive HVAC systems are now addressing the basic aim of HVAC (What is it really trying to do?) not just the control of its operation. The answer to their question is that the system modifies the cabin environment of the automobile

for the benefit of the passengers. Passenger thermal comfort is now an important aspect in the engineering of automobiles in which intelligent systems make travel more pleasurable and reduce driver distraction. Most HVAC systems currently available also offer additional operational functions designed to improve drivability rather than passenger comfort, (for example the front windscreen de-mister which even has its own air outlet, but is now integrated into the control system for general thermal comfort as well as for it's own specialised function of de-misting). The specialised functions for improving driveability are not considered by this study.

Thermal comfort research has been extensive and research has expanded in the area of automotive climate control (e.g. [6] and [7]). Many papers have drawn attention to the fact that the current technology used in HVAC systems for buildings is inapplicable to the automobile. The main difference is that the occupants of a room have an expected work level and clothing resistance. Since the HVAC system outputs in a building creates a uniform environment, often for many occupants at the same time, steady state equations of human thermal state can be used in the control of the system. The automotive passengers are in close confrontation with the air outlet vents of the systems and thermal disturbances from solar gain can be dramatic. Furthermore automotive HVAC systems allow individual preferences to be addressed. Current state of the art shows that the utilisation of thermal comfort control in the automobile is close to becoming practicable. Recent research has shown a variety of thermal control strategies being applied (including the use of neural networks and fuzzy logic) and a variety of approaches (including the use of infrared sensors to observe the facial position and skin temperature).

### 1.1.1 History of Automotive Air Conditioning Systems

The modification of the environment of a cabin for the benefit of the passengers has been engineered since the very beginning. It started out simply with vents, or gaps, in the floor of the cabin in an attempt to increase air circulation. This also allowed a lot of dust to enter with the air and there was no real attempt to modify the condition of the air. In 1884 William Whiteley installed blocks of ice under a horse drawn carriage. Using a fan driven from the main axle, air was forced over the ice and thus cooled before entering the cabin. This idea was developed for the automobile carriage and the company Nash devised a system using the "Weather Eye" effect of cooling the air (by passing it over water).

In 1902 Willis Carrier invented the first air-conditioning machine for reducing humidity in a printing company. He later patented his invention calling it an "Apparatus for Treating Air" and it was Stuart W. Cramer who first used the term "Air Conditioning" in 1906. The

1939 Packard was the first car to have an actual refrigerant evaporator coil fitted, which took up the whole boot space. Manual control consisted solely of a blower switch. In 1941 Cadillac also offered an air-cooling system, but no compressor clutch meant the only way of disengaging the system was to take the belt off from under the bonnet manually (when the car was switched off). After World War II users were offered more control over the system but the controls, being close to the system at the rear of the car, were not easily accessible for the driver. With the invention of the Rotary Compressor in 1957 air conditioning units became smaller, quieter and more efficient. The biggest growth in air conditioning units, according to the Motor Service Manual, was between 1966 and 1987 with an increase of close to 550%. It is estimated that over 80% of cars today use air-conditioning systems.

### 1.1.2 History and Current State of the Art in Thermal State Estimation

Thermal state, sensation and comfort have been studied since at least the 1930's with pioneers such as Gagge, Dage and Neilson with initial publications in the Journal of Nutrition and Physiology. Other early researchers include P. O. Fanger, R. G. Nevins, C.-E. A. Winslow and L. P. Herrington. Thermal state started becoming of interest to the engineering researchers when air conditioning systems developed into a commercial product. The control of a comfortable environment is a well-established topic for the control engineer and standards have already been defined (such as the ASHRAE standard 55 - 66 1966 which will be quoted later in this chapter).

In order to establish a control strategy the variables involved must be clearly identified. A block diagram of the factors affecting thermal comfort is presented in figure 1.1. Thermal comfort is affected by body physiology notably internal heat, skin temperature and sweat secretion. Activity level, clothing resistance and external variables are also important. It is worth noting that the human body adapts to its environment and there are many physiological and psychological processes affecting comfort, termed in the figure as situation perception.

The external variables, air humidity, temperature and velocity are all controllable outputs from the car's HVAC system. The radiation variable is difficult and expensive to control, it is, however, the control of the other three external variables, with respect to radiation, clothing resistance and activity level, combined with a directional element which constitutes the task of comfort control. It was Fanger in [8] that brought together the six principal variables of thermal state estimation listed below. Prior to this, experimental work had been restricted to experiments of two or three of these variables at any one time.

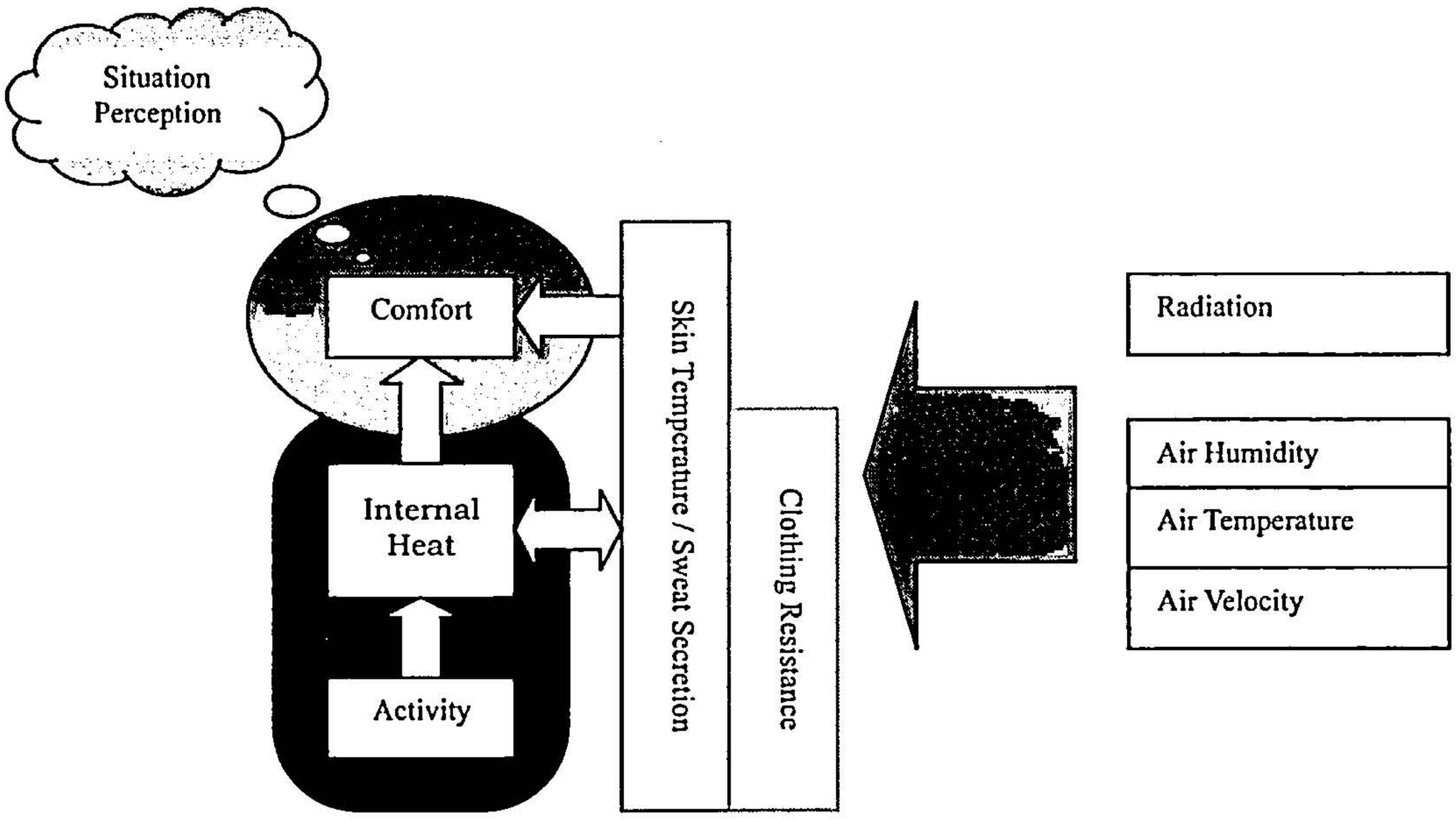


Figure 1.1: Simplified diagram of factors affecting personal comfort

1. Air Temperature.
2. Mean Radiant Temperature.
3. Relative Air Velocity.
4. Humidity (Partial Vapour Pressure).
5. Activity Level (Internal Heat Production).
6. Insulation Value of Clothing.

This list constitutes the 6 principal variables used later in the Predicted Mean Vote approach to thermal state estimation.

Research into the calculation of thermal state of a human subject is extensive. Paper [9] exhibits a comparative study of three different techniques and makes a distinction between the passive calculation of heat transfer and the study of the neural response. The passive study revolves around the energy transfer processes between the core of the body and the environment outside the body though the skin. In most cases, parameters are then correlated with empirical data to reference a thermal state index. Such studies have supplied extensive empirical data, [10] confirms that differences between people from different parts of the world is negligible.

There are many parameters to consider in the thermal balance equation. Simplifications can be carried out as [11] shows by using a one dimensional heat conduction equation and assuming the head as a cylinder. The modelling process can become more and more complex,

as shown in [12], and even include radiation heat loss [13] and evaporative heat loss [14] from the skin.

Physiological research in the field of body temperature regulation has presented a complex set of non-linear processes that are difficult to model directly. There have been many attempts in the past (since 1923) by physiologists and engineers to simplify the problem (such as [15] and [16]).

A literature review on thermal comfort in 1990 by J. L. M. Hensen [17] suggests that there were two accepted solutions. One by Fanger using his "Comfort Equation" [8], associated "Predicted Mean Vote" and "Predicted Percentage of Dissatisfied" and the other method is the J. B. Pierce two-node model of human thermoregulation, [18] and [19] (see also [20] and [21]). Since this literature review in 1990 there have been other methods published demonstrating the evaluation of thermal state. For example [22] in 1995 put forward the concept of equivalent temperature.

With present day computational technology available to engineers, simulation of components can be done easily and quickly. Simulation is useful for both control design and component and system evaluation purposes and for both these reasons simulation of the automotive HVAC system has been demonstrated. Papers [23] and [24] both describe simulations of the cabin compartment in addition to the simulation of the air conditioning unit and this is a more extensive approach than earlier papers. Both papers however, are more concerned with what is happening within the air conditioning system and not so much with system output control. The first paper described the compartment model as only having two controllable variables, cooling load and temperature drop and in the second paper the desire was in obtaining a system capacity level. These two papers, however, do suggest that when designing new systems engineers are becoming more interested in the influence of what is happening in the passenger cabin. The development of such models and simulations is just as relevant in the development of air conditioning system control strategies.

## 1.2 Definitions of Thermal Description Terms

There has been much confusion in the literature in segregating the definitions of thermal comfort, thermal state and thermal sensation. One of the most famous papers in the literature, [8], proposes a thermal state equation and calls it a comfort equation. Similarly an equation proposed by [25] is used to calculate a thermal sensation value which appears to be more like a thermal state value. In the context of this thesis the meanings of the terms

thermal state, thermal sensitivity, thermal sensation and thermal comfort will be discussed and clarified and where appropriate given numerical scales. When referring to material taken from the literature, the names of the variables used by the original authors will be kept to maintain consistency in the global community but it should be clear by the context what each variable represents.

### 1.2.1 Thermal State

Thermal state is one of the most used concepts in current research in the control of HVAC systems. It quantifies an abstract psychological measure of feeling. It is quite reasonable to expect that the reaction of the human body to the state of the environment plays an important role in the personal estimation of thermal state. This connection is the basis for most thermal state estimation techniques, which relate the thermal balance equation between the person's body and the environment to thermal state estimate through a statistically proved equation. Human bodies are very individual with anatomical and physiological differences, even two bodies that are quite similar is structure and operation may be in different modes of operation – such as being hungry or tired. Coupling these differences with differences in psychological influences and the personal estimation of thermal state does become an individual measure. This is what is meant by calling it an abstract psychological measure of feeling.

The concept of thermal state has been around long before any air conditioning systems and is described as the degree of warmth or coldness, of the entire body, felt by a person. Although thermal state is essentially an abstract feeling most bodies are built roughly the same and physiological reactions to the environment have a much greater influence than the psychological differences. It has already been said that statistical differences from people around the world are negligible with reference to [10]. A subtle consequence of this may be recognized by noting the interesting way the linguistic terms of many languages have certain parallels. In English there are four main terms: hot, warm, cool and cold. Similarly, in German there are the same four directly translated terms. In Chinese there are similarly the same directly translated four terms, see figure 1.2. This global consensus may give more confidence in using the statistically proved thermal state estimation equations.

| 热 | 暖 | 凉 | 冷 |
|---|---|---|---|
| *Rè* | *Nuǎn* | *Liáng* | *Lěng* |
| Hot | Warm | Cool | Cold |

Figure 1.2: Chinese symbols for the 4 linguistic thermal descriptions

For the researchers it is more convenient to represent the thermal state in terms of a numerical value and so the linguistic terms are compared to a scale. It is assumed that the linguistic terms are linearly spaced such that warm is half the feeling of Hot etc. and the scale is expanded adding intermediate terms. There are slight variations on the scale used but most follow the same general format. The scale used throughout this thesis is presented in table 1.1. The thermal state scale is more commonly referred to as the *thermal state index.*

| Linguistic Values | Numerical Values |
|---|---|
| Very Hot | +5 |
| Hot | +4 |
| Very Warm / Slightly Hot | +3 |
| Warm | +2 |
| Slightly Warm | +1 |
| Neutral | 0 |
| Slightly Cool | -1 |
| Cool | -2 |
| Very Cool / Slightly Cold | -3 |
| Cold | -4 |
| Very Cold | -5 |

Table 1.1: Thermal state index

During the experiments in this thesis the subjects were asked to supply estimates of their own personal thermal state. The estimates of a subject determining personal feelings are termed *votes.* The acquisition of the thermal state votes was achieved by directly uploading the estimate during the experiment at the time the estimate was made. In some of the latter experiments a touch display screen was available and was programmed to accept thermal vote inputs and a timer was used to help to regulate the thermal state voting of the subjects. The subjects were asked to interpolate between the standard values to as accurate a vote as possible.

### 1.2.2 Thermal Sensitivity

Thermal sensitivity is used to describe the accuracy of the test subject in estimating thermal state. A non sensitive person will not recognize small changes and will make larger jumps in thermal state votes while a more sensitive person will be able to identify slight changes in thermal state and will be more confident in voting to a greater accuracy.

### 1.2.3 Thermal Sensation

Thermal sensation is quite often taken to mean thermal state. It might be argued by some researchers that thermal state is not a feeling but an actual physical state of the person's body and that the person's own feeling about the state of their body is a sensation of this physical state.

The word sensation has a Latin link with the word sense, as in the sense of touch or any of the five main senses, with the meaning of the recognition and evaluation of an external parameter. However people also have a conscious awareness of situations which lead to internal reactions such as a sense of guilt or a sense of humour, thus sensation also takes the meaning of the ability to interpret situations with an evaluated response. The following quote encapsulates both these ideas:

> Sensation: The recognition and evaluation of an *external event* which leads to, but does not include, a reacting feeling.

With this interpretation, thermal sensation is defined as the ability to recognize and evaluate the degree of thermal transfer from or into the environment from the body and evaluate the effect of this on the body's thermal state value.

Poker players may have a high level of situation recognition but can suppress their own feelings – they can sense when the game is becoming more serious but they do not allow themselves to become nervous. This demonstrates that sensation and the actual feelings are separate however in cases of sensing the environment it is not so easy to make such a clear division. There may even be some grey area between sensation and feeling. The difference between thermal state and thermal sensation and the grey area between can be demonstrated by examining different response to the same environment in table 1.2.

| | |
|---|---|
| "The air feels warm": | is a thermal sensation response. |
| "The air is heating me up": | is a thermal sensation response coupled with a thermal state evaluation. |
| "I am becoming warmer": | is a thermal state response coupled with a thermal sensation evaluation. |
| "I feel slightly warm": | is a thermal state response. |

Table 1.2: Demonstration of the difference between thermal state and thermal sensation

The two middle examples show the combined evaluation of thermal sensation and thermal state being used together.

### 1.2.4 Thermal Comfort

Thermal comfort is more easily recognized because it is based on a scale of comfort, or a comfort index. A high comfort level for the driver and passengers is the objective of all luxury automobile manufacturers. Thermal comfort has been increasing in importance in the research of HVAC systems, not just in the automotive industry, and is currently formally defined by the ASHRAE, standard 55 - 66 1966 (see also [26]):

> Thermal comfort is a condition of mind which expresses satisfaction with the thermal environment.

Even this academically accepted definition implies a subjective evaluation, this however has not deterred researchers in attempting to quantify thermal comfort and to correlate it to environmental and physical parameters. Examples of direct quantification of comfort by [27] and [28] are presented in table 1.3. Using such indexes many researchers have questioned their subjects on thermal comfort and it seems the most popular, and simplistic approach is to ask:

"How comfortable do you feel in the current environment?"

| Comfort Scale used by [27] | | Comfort Scale used by [28] | |
|---|---|---|---|
| Linguistic Value | Numeric Value | Linguistic Value | Numeric Value |
| Very Comfortable | 3 | — — — | ... |
| Comfortable | 2 | — — — | ... |
| Slightly Comfortable | 1 | — — — | ... |
| Neutral | 0 | Comfortable | 0 |
| Slightly Uncomfortable | -1 | Slightly Uncomfortable | -1 |
| Uncomfortable | -2 | Uncomfortable | -2 |
| Very Uncomfortable | -3 | Very Uncomfortable | -3 |

Table 1.3: Thermal comfort scales from the literature

Difficulty arises in the first case when realistically trying to consider what "neutral" comfort feels like and if you are already thermally comfortable then can you be made more comfortable? The second case avoids these issues by concentrating on the discomfort of the subjects and using comfort as the topmost level and as soon as the subject is not comfortable they are considered uncomfortable (rather than having a neutral level). In this approach higher levels of comfort will be plateaued by the numerical interpretation but as long as the subject is not

uncomfortable then perhaps the subject is also content within the current environment. It is perhaps of more interest to examine the comfort range when the subject is uncomfortable.

It is suggested by the author that the comfort scale should be a double-sided fuzzy index (an expansion of the second scale in table 1.3). This is simply explained by considering the linguistic value of "slightly comfortable" which implicitly suggests that there is something that is stopping the subject from being 100% comfortable – there is some uncomfortable aspect. This concept is illustrated in figure 1.3 by showing the overlapping comfort and discomfort scales.

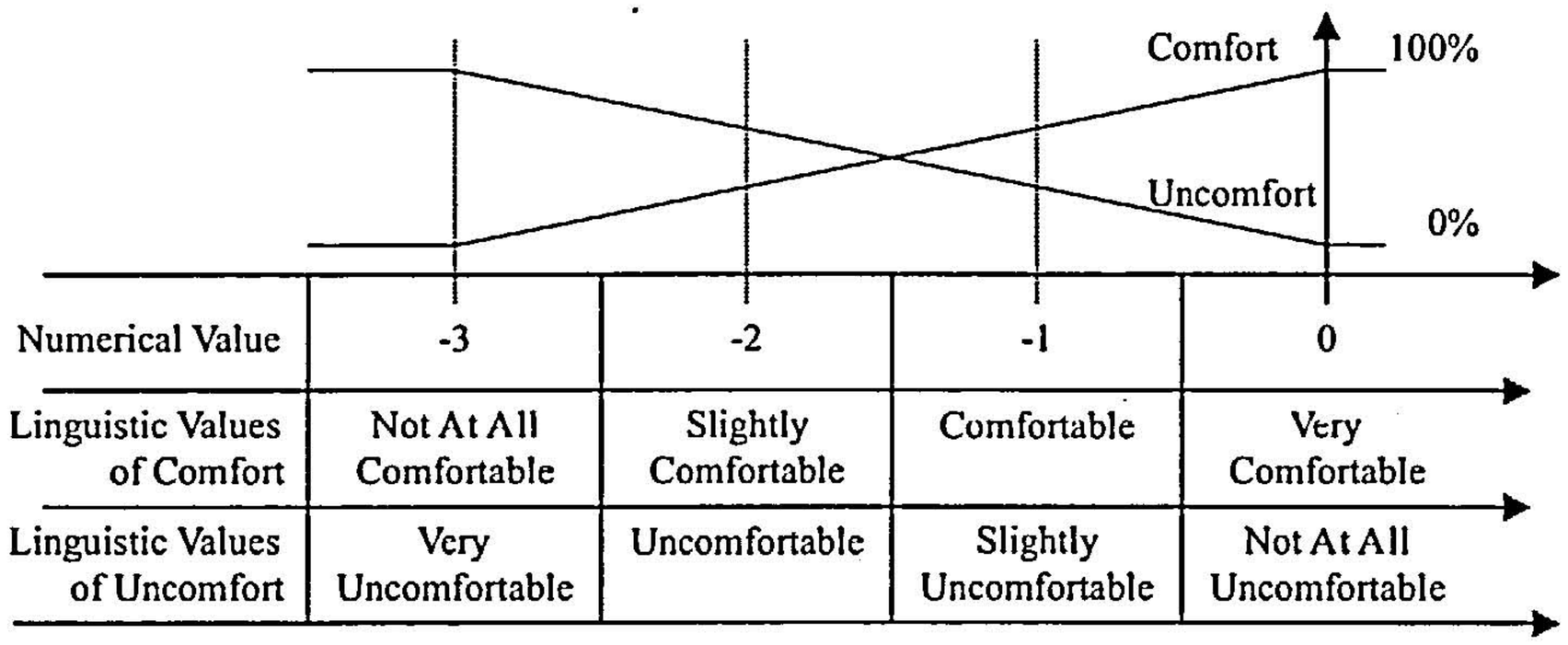


Figure 1.3: Thermal comfort represented as a fuzzy variable

Perhaps what is more interesting to the researcher are the points on the comfort scale which excite a reaction, as long as the subject is comfortable then the subject should also be content with the current HVAC settings. When the subject becomes less comfortable (or more uncomfortable) then the subject is more likely to desire a change in the operation of the HVAC system. This raises another point about satisfaction with the HVAC system. Even modern day automotive HVAC systems can not react immediately to a step change and can take a few minutes to reach the desired temperature. During this time the subject may still be uncomfortable. However, they are expecting the system to respond, and may even sense the change, and so are *satisfied* with the current desired temperature input level. A distinction between the satisfaction with the system and the satisfaction with the environment may be an important future step.

Another way of representing comfort is in terms of a preferred modification to the current environment (which includes the idea of satisfaction). Often a subject's complaint of a particular environment is in terms of a personal evaluation of thermal state with reference to a desired thermal state. For example the subject might say "I am feeling slightly too warm" or "I would prefer to be cooler" which are both indications of comfort but with a personal suggestion from the subject why total comfort (100%) has not been reached. The suggestion

could be anything which affects the users perception of the environment, for example complaints of being "too sticky" or "too dry" could be humidity or air flow problems. Thus in the case where humidity and air flow are kept constant a better scale of comfort might be the one presented in table 1.4.

| Numerical Comfort Value: | -3 | -2 | -1 | 0 | -1 | -2 | -3 |
|---|---|---|---|---|---|---|---|
| Numerical Comfort State: | -3 | -2 | -1 | 0 | 1 | 2 | 3 |
| Linguistic Values: | Much too Cool | too Cool | Slightly too Cool | About Right | Slightly too Warm | too Warm | Much too Warm |

Table 1.4: Thermal comfort scale in terms of thermal state

This is a much more useful scale as it contains more information about how the user is feeling and what the perceived displeasure is. It is also easier for the subject to use as it is less ambiguous.

# Part I

# Thermal State Analysis

# 2 Control of an HVAC Experiment and Observation of Thermal Sensation

The aim of this chapter is to present the method and results of an experiment used in the investigation of thermal state. There are two main objectives in this part of the investigation: to examine the modelling and control aspects of a heating system and to observe and measure a subject's thermal state votes in relation to changes in temperature. Chapters 3 and 5 both use the data collected in this experiment.

The experiments consisted of seating test subjects in a semi-enclosed cabin and directing heated air at their upper body and face. The first objective was fulfilled by implementing a controller to manipulate the air temperature. The controller was synthesised using a polynomial, pole placement approach and was based on an identified plant model. The results from this experiment together with the test subjects thermal state votes during the tests complete the second objective of the investigation.

The results show that modelling and control of the HVAC system has been achieved. The identified model was accurate enough on the verification data and was of a low order. Observing the thermal state votes of the test subjects suggests that most are willing to vote to the nearest decimal place but that this is the limit of their thermal sensitivity. The results also show an interesting phenomenon of the congruity of the facial skin temperature with regards to the local air temperature.

This chapter contributes a descriptive experience of the control of an HVAC system and provides a discussion on the observed thermal state votes.

## 2.1 Introduction

### 2.1.1 Aim of Chapter

The aim of this chapter is to present the method and results of an experiment used in the investigation of thermal state. The experiment set up consisted of an HVAC system which altered the environment inside a semi-enclosed cabin. In order to precisely vary the environment within this cabin it was necessary to implement a controller for the HVAC system. This also gives some useful insight into the control issues involved. The control of the HVAC system in this experiment is not on the same scale as one used in the automotive industry but the control issues are similar. The data collected from this experiment is used in chapters 3 and 5 to investigate different thermal state estimation methods. The experiment also opens discussion on some further aspects of thermal state acquisition.

The development and testing of the experimental framework for investigating thermal state involved:

1. Examining the identification, modelling and control aspects of a heating system.
2. Observing and measuring the changes in a subject's personal thermal state votes in relation to changes in temperature.

### 2.1.2 Background

The experiment described in this chapter has a similar set up to an experiment presented in a paper by Taniguchi et al, [25]. The objectives of [25] are more specific, aiming to show a connection between thermal state and facial skin temperature. The results from this chapter will be used to compare different thermal state estimation techniques. Since [25] presented a successful experimental set-up it was a good basis for the design of a more general experiment. A thermal state estimation method presented in [25] will be explored later in chapter 3.

## 2.2 Experimental Set-Up of an HVAC System

### 2.2.1 Equipment - HVAC System

The experimental set-up consists of a large HVAC unit with one air inlet and one outlet. The air passes over a refrigerant heat exchanger first, for the duration of this experiment the refrigeration subsystem was deactivated and it was assumed that no heat was exchanged. The air then passes through 2 banks of heaters which were controlled via an analogue, 0-1 volt control signal. Both heaters were controlled simultaneously from a single voltage. The air ducting then narrows and channels the air through the fan, the ducting then opens out to its original diameter. Finally the air passes through a flexible ducting tube which can be aimed to direct the air. Additionally infrared lamps were used to simulate heat load from the sun and were also controlled by a 0-1 volt signal. The control of the infrared lamps was implemented by truncating the amplitude of the current of the AC power supply proportionally with respect to the control signal voltage. The experimental setup is illustrated in figure 2.1.

Heated air is directed at the face and upper regions of a subject's body. The subject is seated inside a semi-enclosed cabin consisting of a floor, roof and 3 walls with the front open.

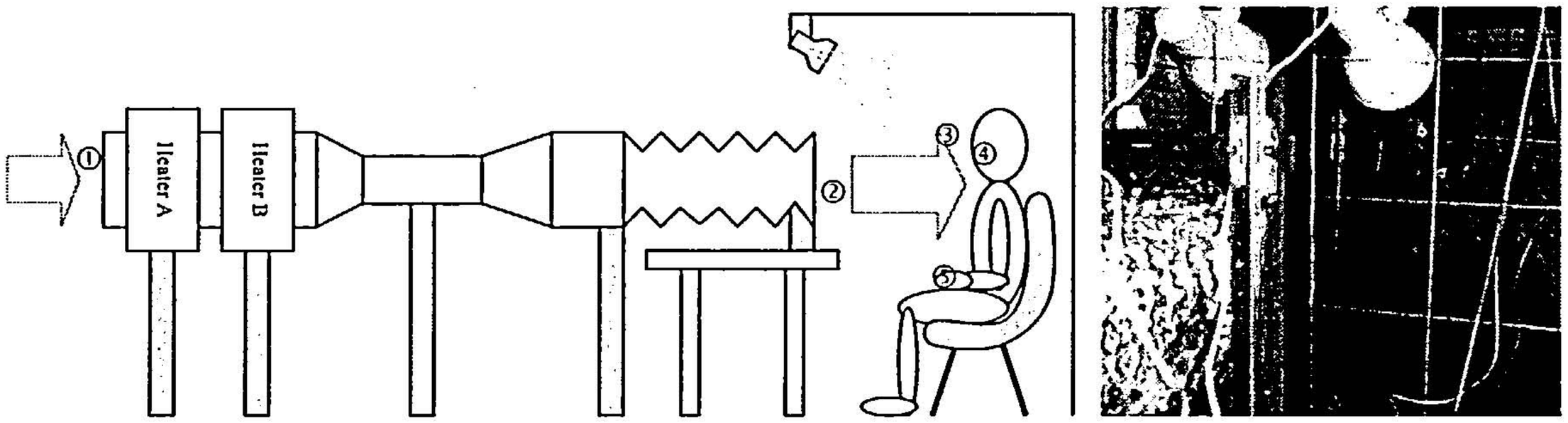


Figure 2.1: Diagram and photo of the experimental setup for evaluating thermal state

The circled numbers in figure 2.1 represent the sensor positions as explained below:

1. Ambient Air Temperature Measurement.
2. Air Temperature Measurement at Nozzle Outlet (measured at the center and at the edge of the flow).
3. Air Temperature Measurement at Face.
4. Face Skin Temperature Measurement (3 positions on the face).
5. Hand Skin Temperature Measurement.

A detailed list of the HVAC plant properties is given in appendix B. These were used to derive a physical model representation of the plant, also presented in appendix B. This model is not used in this chapter but provides an insight into the processes involved and provides information for future reference.

### 2.2.2 Obtaining Measurement from the Temperature Sensors

The air temperature sensors and the skin temperature sensors were all thermistors, which were based on the same operational properties. The temperature was related to the resistance in the thermistors. Figure 2.2 and equation (2.1) shows the circuit diagram and calculation used to extract the resistance of the thermistors using only voltages read through an AD card. The comparative resistance $R_r$ was selected to maximize the accuracy of the A-D converter.

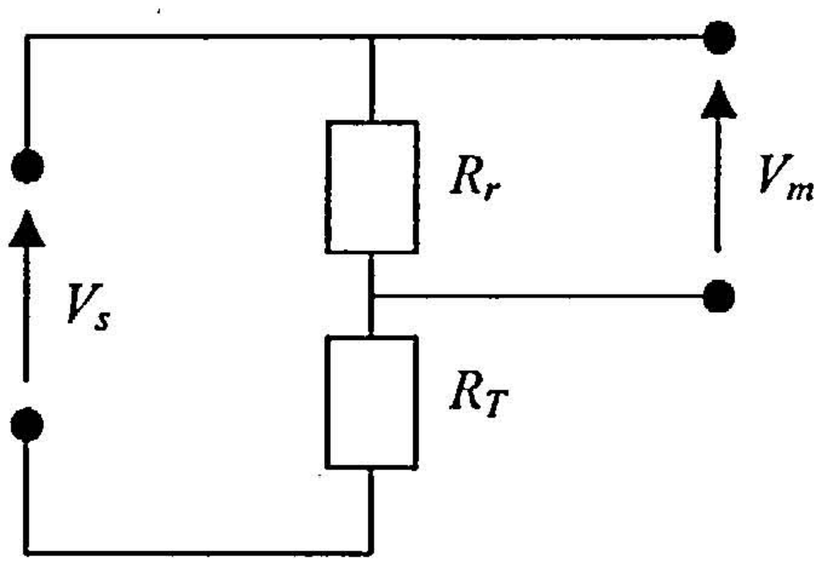


$$R_T = \frac{(V_s - V_m)R_r}{V_m} \tag{2.1}$$

Figure 2.2: Circuit diagram and equation used to calculate the resistance of the temperature thermistors

Some of the properties of the thermistors are listed below:

- Resistance @ 25 °C: 10,000 Ω
- Tolerance: ±0.2 °C from 0 °C to 70 °C
- Operating Range: −55 °C to +150 °C

Once the resistance had been calculated the result was interpolated in a look-up table of resistance versus temperature supplied by the thermistor manufacturer. A section of the table corresponding to the operational range of the sensor is presented in Table 2.1.

The air temperature sensors were left to dangle in the air flow at the desired positions. The sensor wire was attached to a coarse mesh of string close to the sensor location to support the sensor. The wire was stiff enough that the suspended sensor resisted movement in the air flow.

| Temperature | Resistance |
|---|---|
| $-50\,^{o}$C | 667,820.00 Ω |
| ... | ... |
| $10\,^{o}$C | 19,903.64 Ω |
| $15\,^{o}$C | 15,714.03 Ω |
| $20\,^{o}$C | 12,493.78 Ω |
| $25\,^{o}$C | 10,000.00 Ω |
| $30\,^{o}$C | 8,055.95 Ω |
| $35\,^{o}$C | 6,530.20 Ω |
| $40\,^{o}$C | 5,325.04 Ω |
| $45\,^{o}$C | 4,366.87 Ω |
| ... | ... |
| $150\,^{o}$C | 184.79 Ω |

Table 2.1: Temperature related to thermistor resistance

The skin temperature sensors were held against the skin by medical sticky pads. The pads were placed over the outside of the sensor and thus helped to insulate the sensors from external temperatures. Initially only 3 facial skin temperatures were measured as illustrated in figure 2.3.

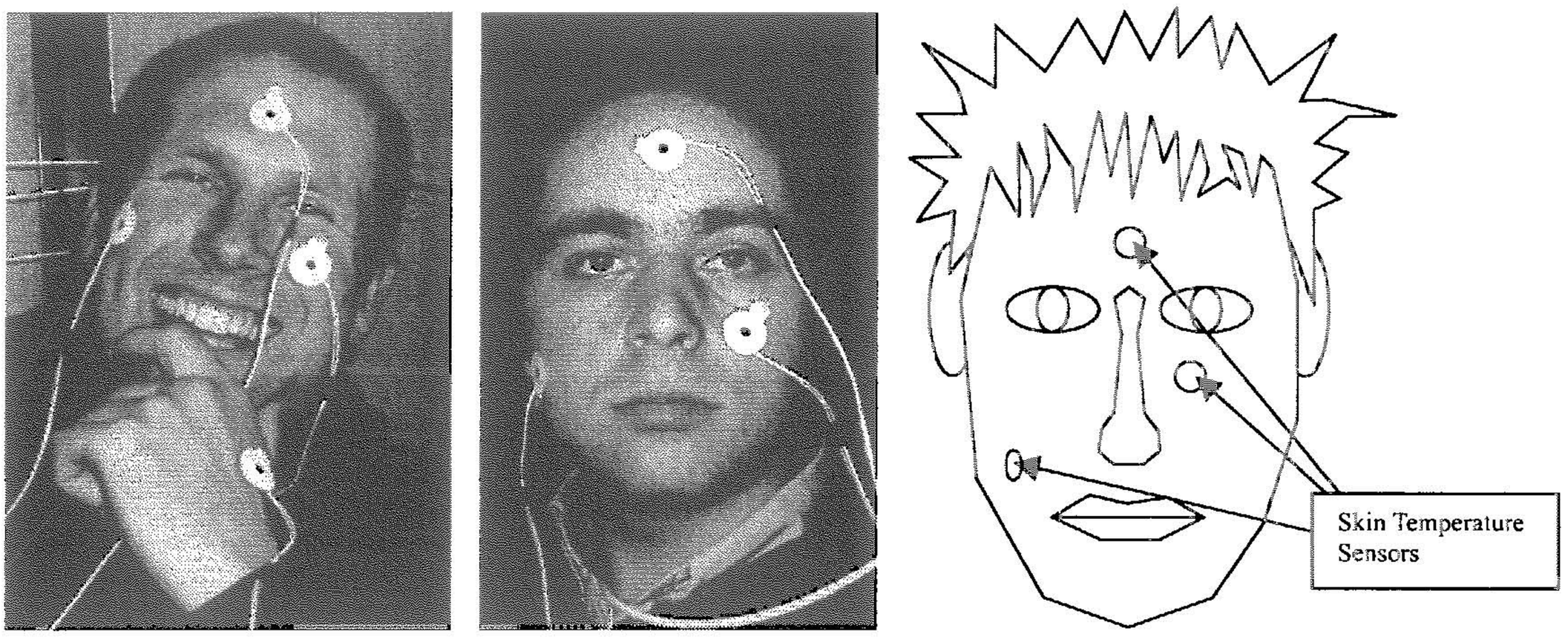


Figure 2.3: Photos and diagram of facial skin temperature sensor locations

All the test subjects were male students aged between 20 and 25 and in good health.

### 2.2.3 Initial Tests (Pre-Experimental)

Once the equipment was set up a simple step test and a random input test were performed to examine the system response, see figure 2.4. The random input was created using a random

generator that set the intervals indicating the time when to toggle between maximum and minimum heater output.

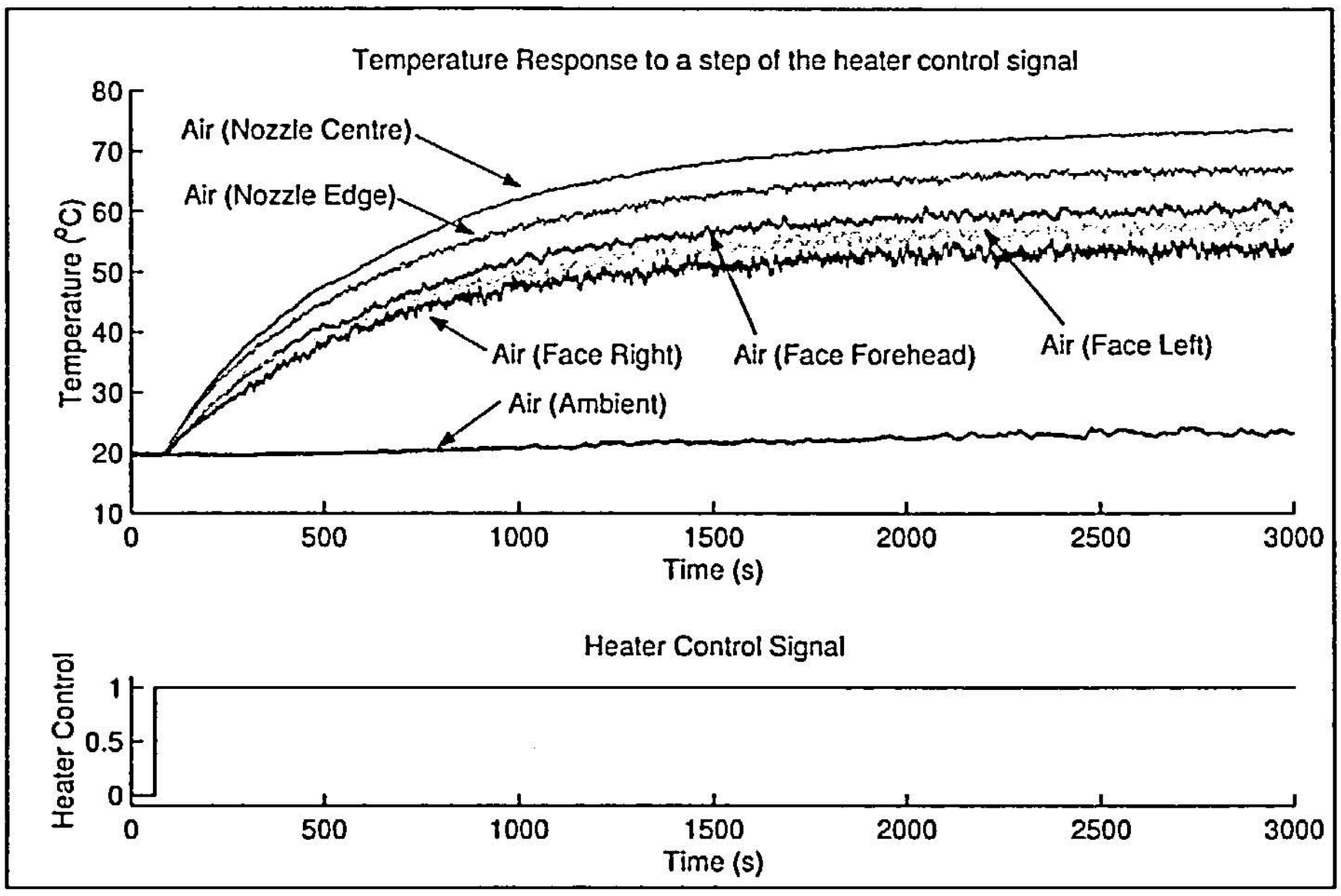


Figure 2.4: Step-Response and Random Input Response of HVAC Plant

The test included a human subject sitting in the experiment cabin and providing personal thermal state votes. The main aim of the initial test was to obtain the rise time and to check the sensor calibration. The step response shows a rise time to the final value of about 3000

seconds. The sensors proved to maintain accuracy when cross checked with the temperature readout from an industrial thermometer.

## 2.3 System Identification: Least Squares ARX Approximation by MATLAB "ident" Tool

An identification method for finding the plant model was preferred to the use of a physical model. The physical model presented in appendix B contains too many uncertain estimates and the final result needed severe over-adjustment of the parameters before the model became reasonably close to the measured system.

The data collected for the identification process is presented in figure 2.5 and shows a step-up step-down input signal followed by a PRBS (Pseudo Random Binary Signal) input at different operating levels.The step responses were included to help in deciding the best controller sampling period. As a rule of thumb the number of samples per rise time should be between 4 and 10 (see [29]). The PRBS part of the input was used for the identification process. The least squares approach was carried out using the "ident" tool in MATLAB. The models were compared against each other at the different operating ranges and on the verification data, see figure [?]. The ident tool provided a "Best Fit" measure for comparing models against measured data which is described as the percentage of output variations that is reproduced by the model. This was used to select the best overall model which was a 4th order model with a 40s sampling time calculated from the data with the input based around the value of 0.4.

The best identified transfer function model is presented in equation (2.2), with the argument $z$ as the z-transform operator:

$$IdentMdl = \frac{3.951z^{-1} + 2.388z^{-2} - 0.09974z^{-3} + 2.875z^{-4}}{1 - 0.3323z^{-1} - 0.1627z^{-2} + 0.02573z^{-3} - 0.2952z^{-4}} \tag{2.2}$$

With a sampling time of 40 seconds.

The identified model can be used to simulate the air temperature of the plant and thus can be verified against previously measured data. Figure 2.6 shows how the simulated air temperature using $IdentMdl$ compares with the measured air temperature.

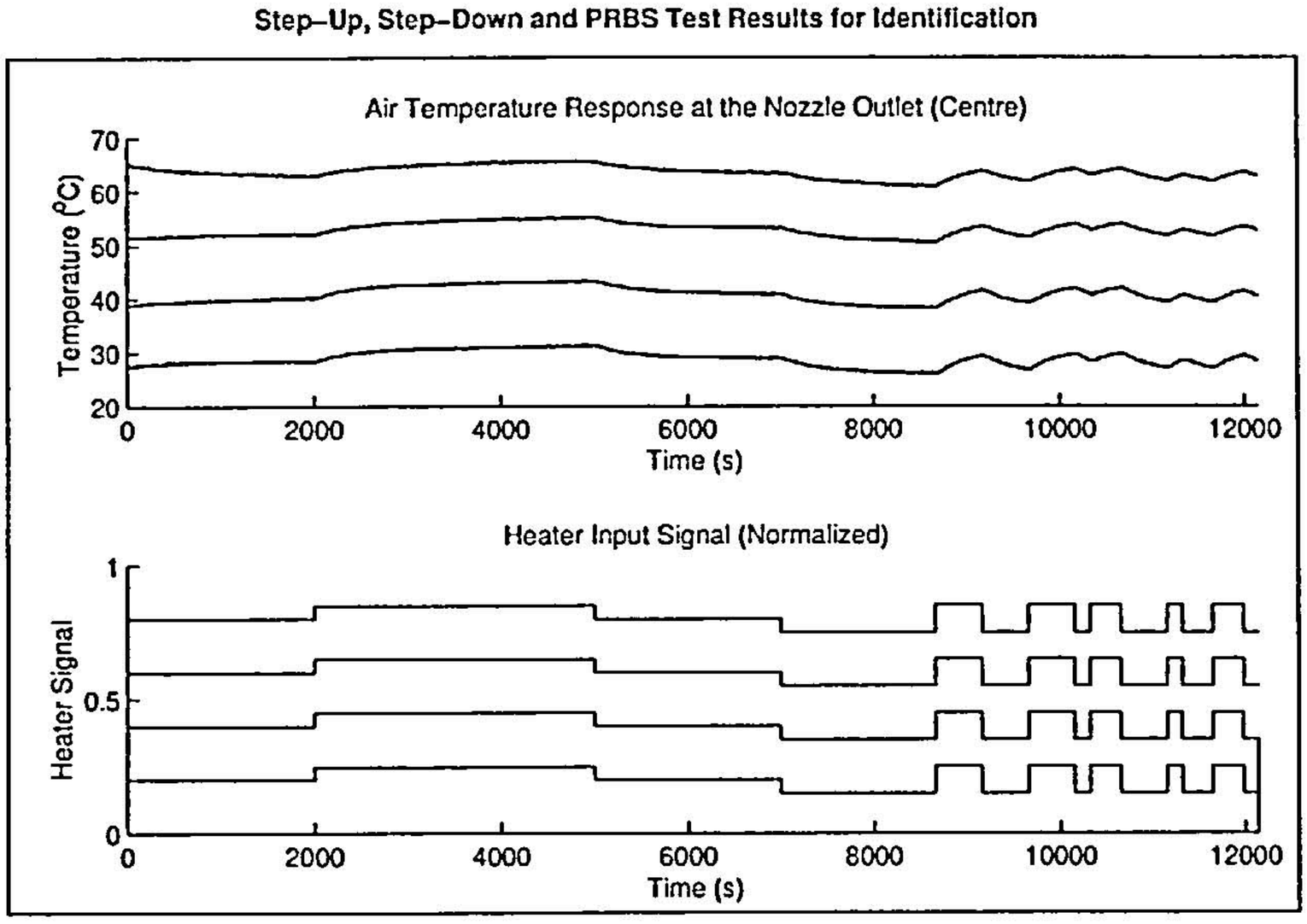


Figure 2.5: Data Collected for identification of the HVAC plant

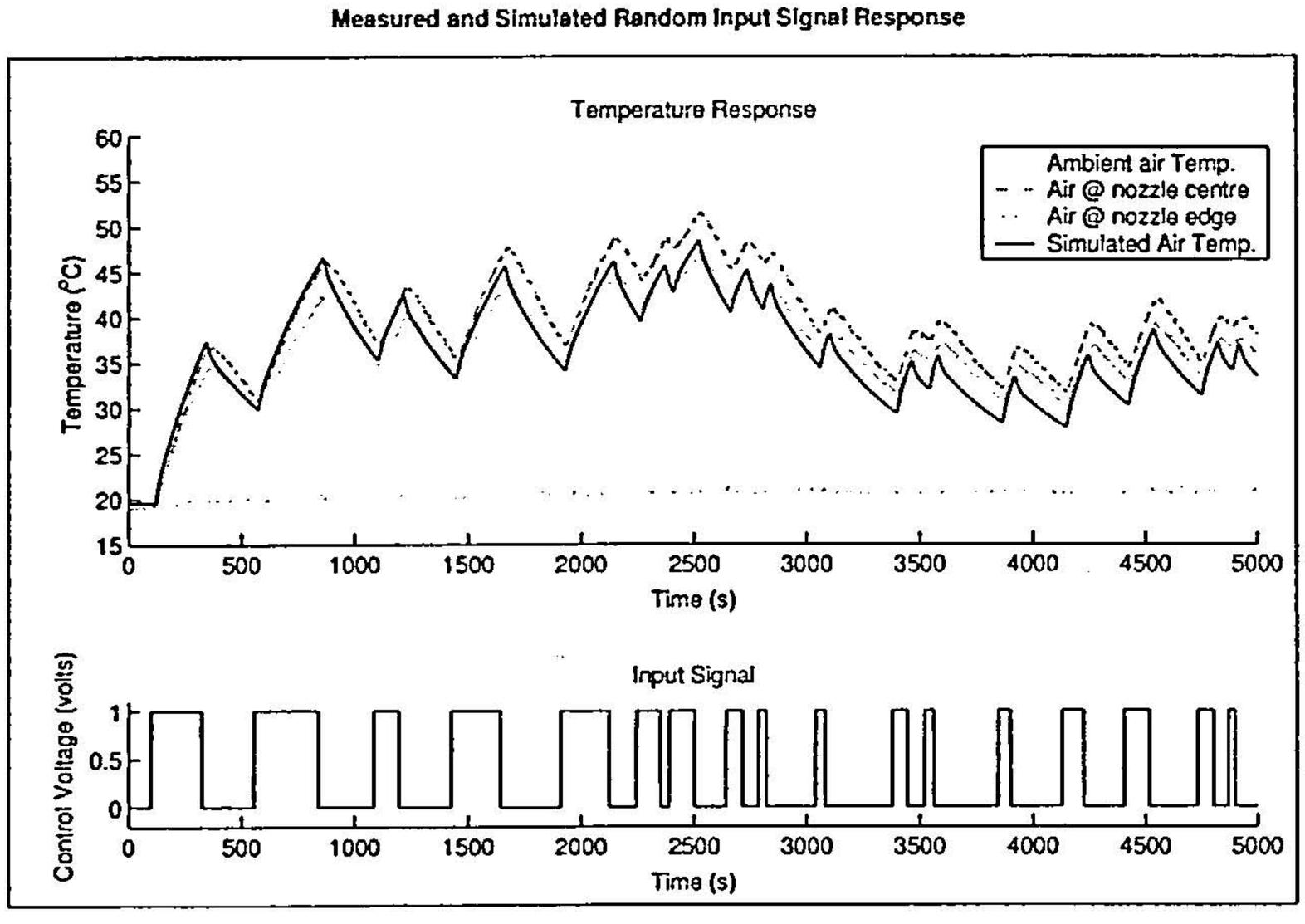


Figure 2.6: Verification of the identified model

## 2.4 RST Control

Desired rise time and overshoot were stipulated and used to form a set of desired poles. The pole-placement technique was then implemented using the polynomial approach (taken from [29]).

### 2.4.1 Polynomial Pole-Placement Theory

Assuming the model of the system has the format

$$A(z^{-1})y(k) = B(z^{-1})u(k) \tag{2.3}$$

Here $A(z^{-1})$ and $B(z^{-1})$ are polynomials with a z-transform argument, $z^{-1}$, such that the pulse-transfer function of the system is $\frac{B(z^{-1})}{A(z^{-1})}$. The system input and output, for time sample $k$, are $u(k)$ and $y(k)$ respectively.

The synthesized controller will have the following format:

$$R(z^{-1})u(k) = T(z^{-1})u_c(k) - S(z^{-1})y(k) \tag{2.4}$$

Here $R(z^{-1})$, $S(z^{-1})$ and $T(z^{-1})$ are designed polynomials and define the feed-forward pulse-transfer function as $H_{ff} = \frac{T(z^{-1})}{R(z^{-1})}$ and the feedback pulse-transfer function as $H_{fb} = \frac{S(z^{-1})}{R(z^{-1})}$. The variable $u_c(k)$ is a control reference signal.

This control structure can be realized graphically as shown in figure 2.7 which also shows the injection of noise, $n(k)$, and plant disturbances, $d'(k)$.

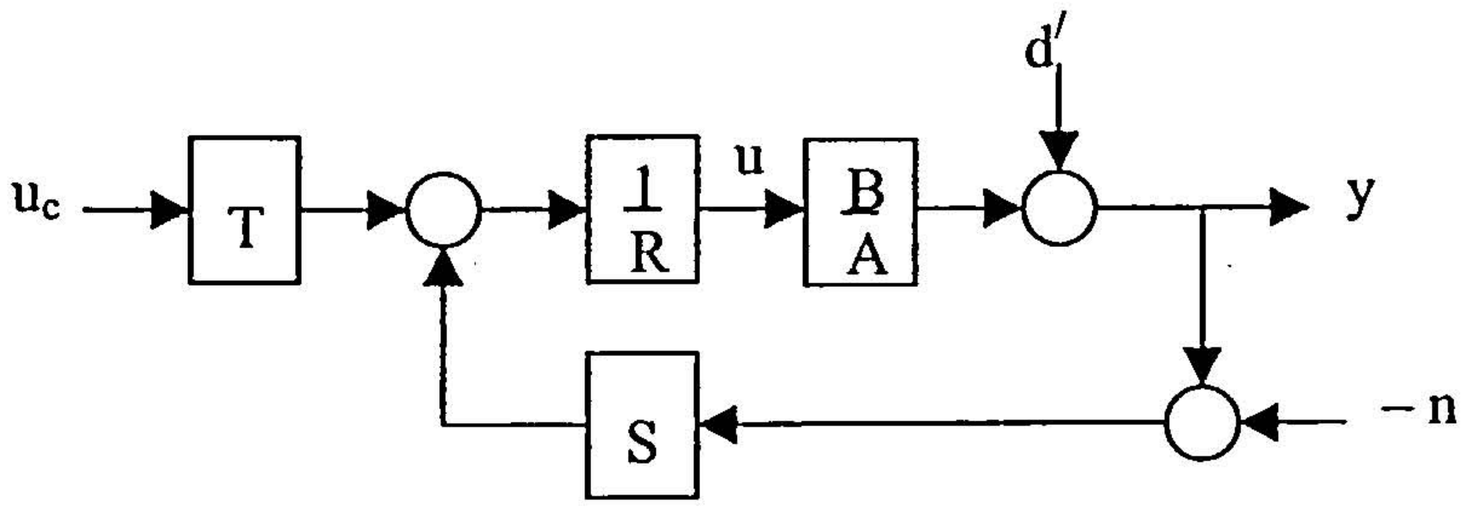


Figure 2.7: Graphical interpretation of implementation of the RST control method, with disturbances

Combining equations (2.3) and (2.4) and eliminating $u(k)$ gives the closed loop system, $u_c(k) \rightarrow y(k)$, in equation (2.5).

$$\left(A(z^{-1})R(z^{-1}) + B(z^{-1})S(z^{-1})\right) y(k) = B(z^{-1})T(z^{-1})u_c(k) \tag{2.5}$$

Thus the characteristic polynomial of the closed loop system, $\left(A(z^{-1})R(z^{-1}) + B(z^{-1})S(z^{-1})\right)$, can be compared to a desired characteristic polynomial, $A_{cl}(z^{-1})$, in order to evaluate $R(z^{-1})$

and $S(z^{-1})$ as in equation (2.6). Equation (2.6) is called the Diophantine Equation. The closed loop characteristic polynomial, $A_{cl}(z^{-1})$, can be factored into a controller polynomial, $A_c(z^{-1})$, and an observer polynomial, $A_o(z^{-1})$. The feed-forward term, $T(z^{-1})$, is usually designed to cancel the observer polynomial.

The Diophantine Equation is

$$A(z^{-1})R(z^{-1}) + B(z^{-1})S(z^{-1}) = A_{cl}(z^{-1}) = A_c(z^{-1})A_o(z^{-1}) \tag{2.6}$$

There are conditions for the existence of solutions to the Diophantine Equation and different methods of finding the solutions such as Euclid's Algorithm or by use of the Sylvester Matrix. When using the polynomial toolbox in MATLAB there exists a function that automatically calculates a particular solution (if one exists).

The notation from now on will be reduced by omitting the polynomial argument, $(z^{-1})$.

The method can be extended by selecting damped stable poles in the process to be cancelled. This is done by extracting the factors of the identified model to be cancelled eg. $A = A^+A^-$ and $B = B^+B^-$. The factors $A^+$ and $B^+$ are the factors to be cancelled and are chosen in monic form. Cancelation takes place by selecting a controller zero to match with a process pole and vice versa. Thus $R$, $S$ and $T$ are redefined with factors as shown:

$$\begin{aligned} R &= B^+\bar{R} \\ S &= A^+\bar{S} \\ T &= A^+\bar{T} \end{aligned} \tag{2.7}$$

Following on, the Diophantine Equation (2.6) is thus modified to show that the the desired characteristic polynomial has factors of the cancelled parts of $A$ and $B$. Thus by removing $A^+B^+$ the Diophantine Equation can still be solved for $\bar{A}_{cl} = (A^-\bar{R} + B^-\bar{S})$ and it is natural to assume that $A_c = B^+\bar{A}_c$ and $A_o = A^+\bar{A}_o$

$$A_{cl} = AR + BS = A^+B^+\left(A^-\bar{R} + B^-\bar{S}\right) = A^+B^+\bar{A}_{cl} \tag{2.8}$$

The technique can be extended further by presenting a reference plant with the desired response to changes in the command signal.

$$y_m = \frac{B_m}{A_m} u_c \tag{2.9}$$

Note that because $B^-$ is not cancelled it must also be a factor of $B_m = \bar{B}_m B^-$ so that the process can follow the model exactly. $R$, $S$ and $T$ are now chosen as:

$$\begin{aligned} R &= A_m B^+ \bar{R} \\ S &= A_m A^+ \bar{S} \\ T &= \bar{B}_m \bar{A}_o \bar{A}_c A^+ \end{aligned} \tag{2.10}$$

When $A$, $B$ are known and properties of $A_{cl}$, $A_m$ and $B_m$ are stipulated the control synthesis then follows a simple path. It is also advantageous to state some of the properties of $R$ and $S$ in advance, for example if we desire integral action then the polynomial $R$ must have $(1-z^{-1})$ as a factor. Thus $R_d$ and $S_d$ shall represent desired factors of $R$ and $S$ respectively.

### 2.4.2 Plant Controller Design

The desired characteristic polynomial was chosen by stipulating the desired rise time and desired damping for both the reference model and the plant control. The reference model dictates the response behaviour to changes in command signal and the plant controller dictates the response behaviour to disturbances. The following values were chosen:

- $Tr_{A_m} = 150$; Desired rise time of attenuation due to control reference changes.
- $D_{A_m} = 0.99$; Desired damping of attenuation due to control reference changes.
- $Tr_{A_{cl}} = 100$; Desired rise time of attenuation due to disturbances.
- $D_{A_{cl}} = 0.99$; Desired damping of attenuation due to disturbances.

The above selection was chosen after an iterative simulation of the closed loop system and testing of the real system. $B_m$ was chosen to be $B^- \cdot G_{sys}$ where $G_{sys}$ is the gain of the system.

The cancellation factors of the plant polynomials were chosen as follows:

- $A^+ = A$ and $A^- = 1$
- $B^+ = 1$ and $B^- = B$

i.e. the poles of the identified system are all cancelled and the numerator is not cancelled at all.

Additional specifications were specified as follows:

- $R_d = (1 - z^{-1})$
- $S_d = 1$

Thus integral action is introduced.

With a 40 second sampling time the transfer function of the reference model $\frac{B_m}{A_m}$ is calculated as:

$$RefMdl = \frac{0.1148z^{-1} + 0.06941z^{-2} - 0.002899z^{-3} + 2.08357z^{-4}}{1 - 0.9754z^{-1} - 0.2403z^{-2}} \tag{2.11}$$

The closed loop control system $\frac{B \cdot T}{A_{cl}} = \frac{B \cdot T}{A \cdot R + B \cdot S}$ is:

$$ClsdLp = \frac{\left[\begin{array}{c} 0.1148z^{-1} - 0.04665z^{-2} - 0.05233z^{-3} + 0.1102z^{-4} - 0.1164z^{-5} + \\ 0.01512z^{-6} + 0.01919z^{-7} - 0.03074z^{-8} + 0.0171z^{-9} - 0.002907z^{-10} \end{array}\right]}{\left[\begin{array}{c} 1 - 1.986z^{-1} + 1.407z^{-2} - 0.3221z^{-3} - 0.3831z^{-4} + \\ 0.5504z^{-5} - 0.3129z^{-6} + 0.08281z^{-7} - 0.008361z^{-8} \end{array}\right]} \tag{2.12}$$

Comparing the pole-zero maps in figure 2.8 of the plant system, the reference model and the final closed loop system, $u_c(k) \rightarrow y(k)$, the cancelled poles can easily be seen. It should be expected since it follows from the definitions of $T = \bar{B}_m A^+ \bar{A}_{cl}$, $B = B^+ B^-$, and of $A_{cl} = A^+ B^+ A_m \bar{A}_{cl}$, that with assumptions of exact cancellation the closed loop control system can be simplified to the control reference model:

$$\frac{B \cdot T}{A_{cl}} = \frac{B \cdot T}{A \cdot R + B \cdot S} = \frac{B^+ B^- \cdot \bar{B}_m A^+ \bar{A}_{cl}}{A^+ B^+ A_m \bar{A}_{cl}} = \frac{B_m}{A_m} \tag{2.13}$$

This assumes that the cancellation is exact. When model error or load change occurs the cancellation is not exact and the model starts to exhibit corrective behaviour as designed by the process control rather than the model control.

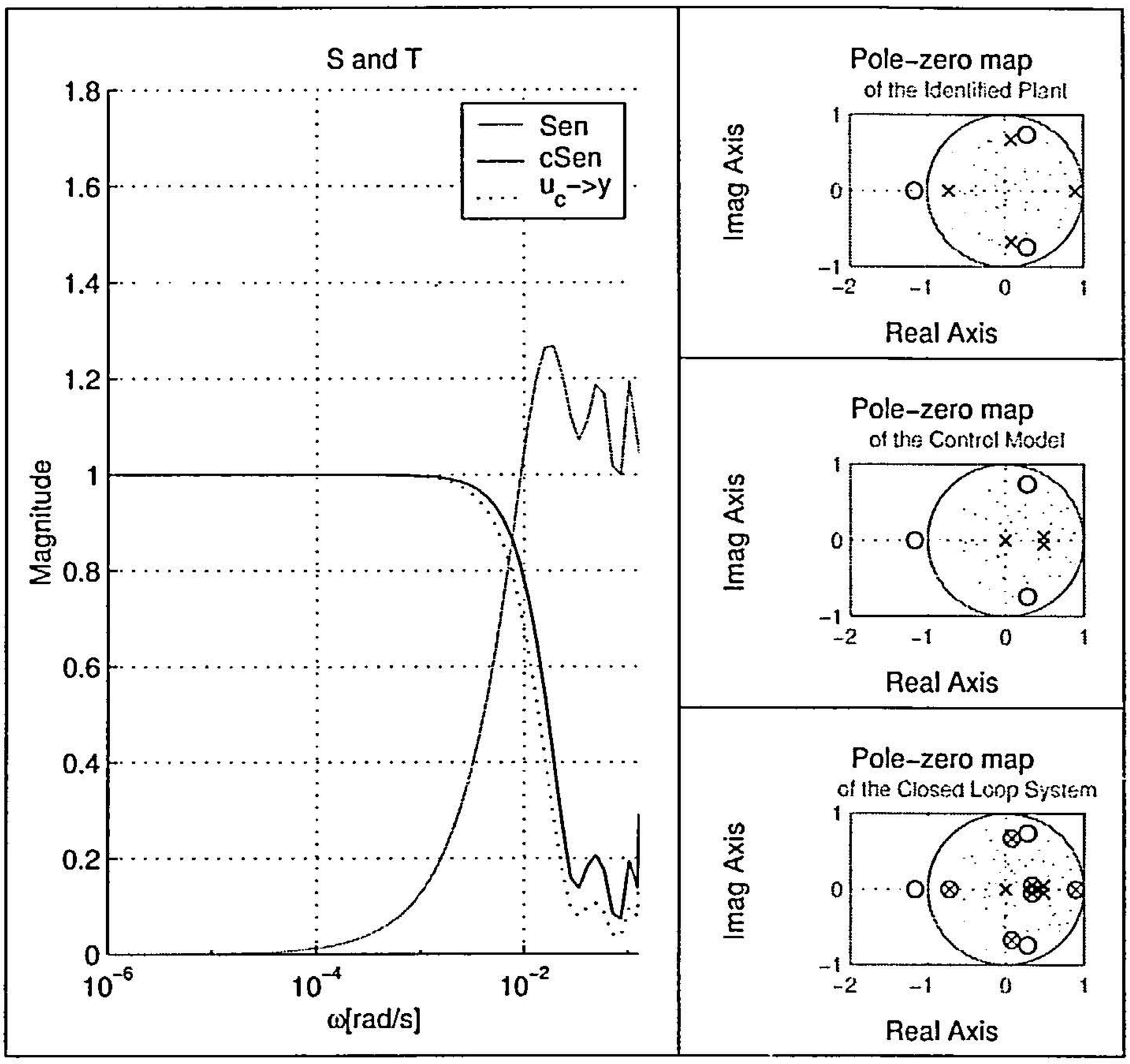


Figure 2.8: T-S Plot of the Controlled Model and Pole-Zero Maps of $IdentMdl$, $RefMdl$ and $ClsdLp$

Figure 2.8 also includes a Nyquist plot of the closed loop transfer function $u_c(k) \rightarrow y(k)$, sensitivity function $Sen$, and complementary sensitivity function $cSen$. In order to determine the sensitivity and complementary sensitivity function it is useful to observe where in the controlled system the model error, $d'$, and noise disturbances, $n$, enter the loop. Figure 2.7 shows the standard injection points.

The sensitivity function is calculated by finding the closed loop transfer function $d'(k) \rightarrow y(k)$.

$$y = \frac{B}{A}\left[\frac{1}{R}\left(T \cdot u_c - S \cdot y\right)\right] + d'$$

$$y = \frac{BT}{AR}u_c - \frac{BS}{AR}y + d'$$

Ignoring the contribution from $u_c$ in the transfer function.

$$y\left(1+\frac{BS}{AR}\right)=d'$$
$$y=\frac{AR}{AR+BS}d' \tag{2.14}$$

Thus the sensitivity function is:

$$Sen=\frac{AR}{AR+BS} \tag{2.15}$$

The complementary sensitivity function is derived from the closed loop transfer function $n(k) \rightarrow y(k)$:

$$cSen=\frac{BS}{AR+BS} \tag{2.16}$$

### 2.4.3 HVAC Plant Air Temperature Control and Results

The synthesized controller was used to regulate the air temperature of the HVAC plant at desired values and respond to step changes satisfactorily. Figure 2.9 verifies that the air temperature is controlled successfully and shows the controller output response.

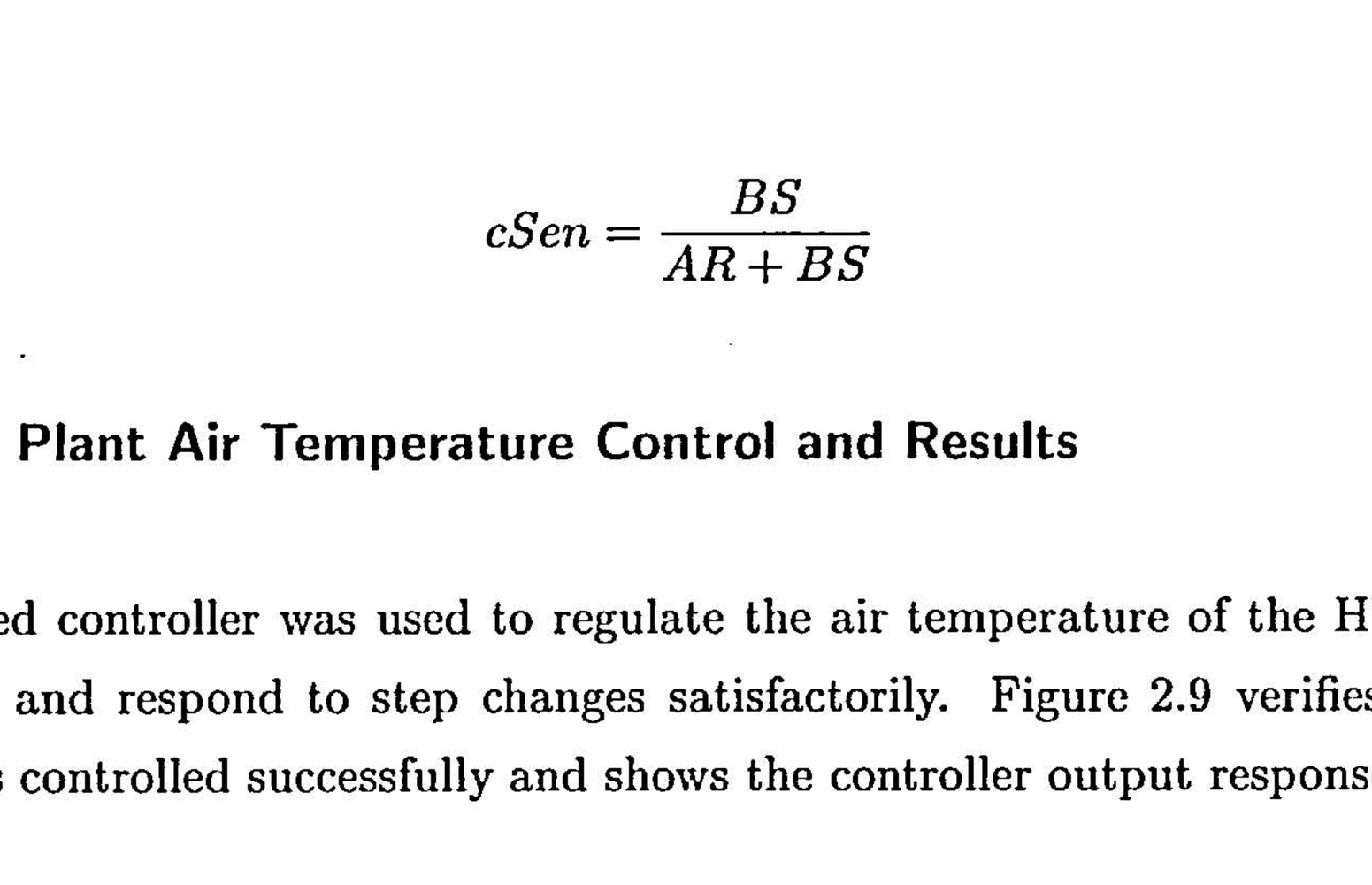


Figure 2.9: Controlled air temperature of the HVAC plant and control output signal

## 2.5 Results and Discussion of Thermal Sensation Voting

Thermal state votes were collected from the test subjects during the three stages of the experimental process, using a random generated binary signal (initial tests), using a PRBS (plant identification) and when the air temperature was controlled using a reference signal (control verification).

The first stage results contain frequent rapid changes and can be used to investigate transient conditions. The last stage of the experiments made it possible for the outlet temperature to be specified and to be regulated and for step changes to be dealt with quickly. This allows examination of the detection of changes in thermal state by the subject and investigation of consistency and speed in reaching steady state equilibrium thermal state.

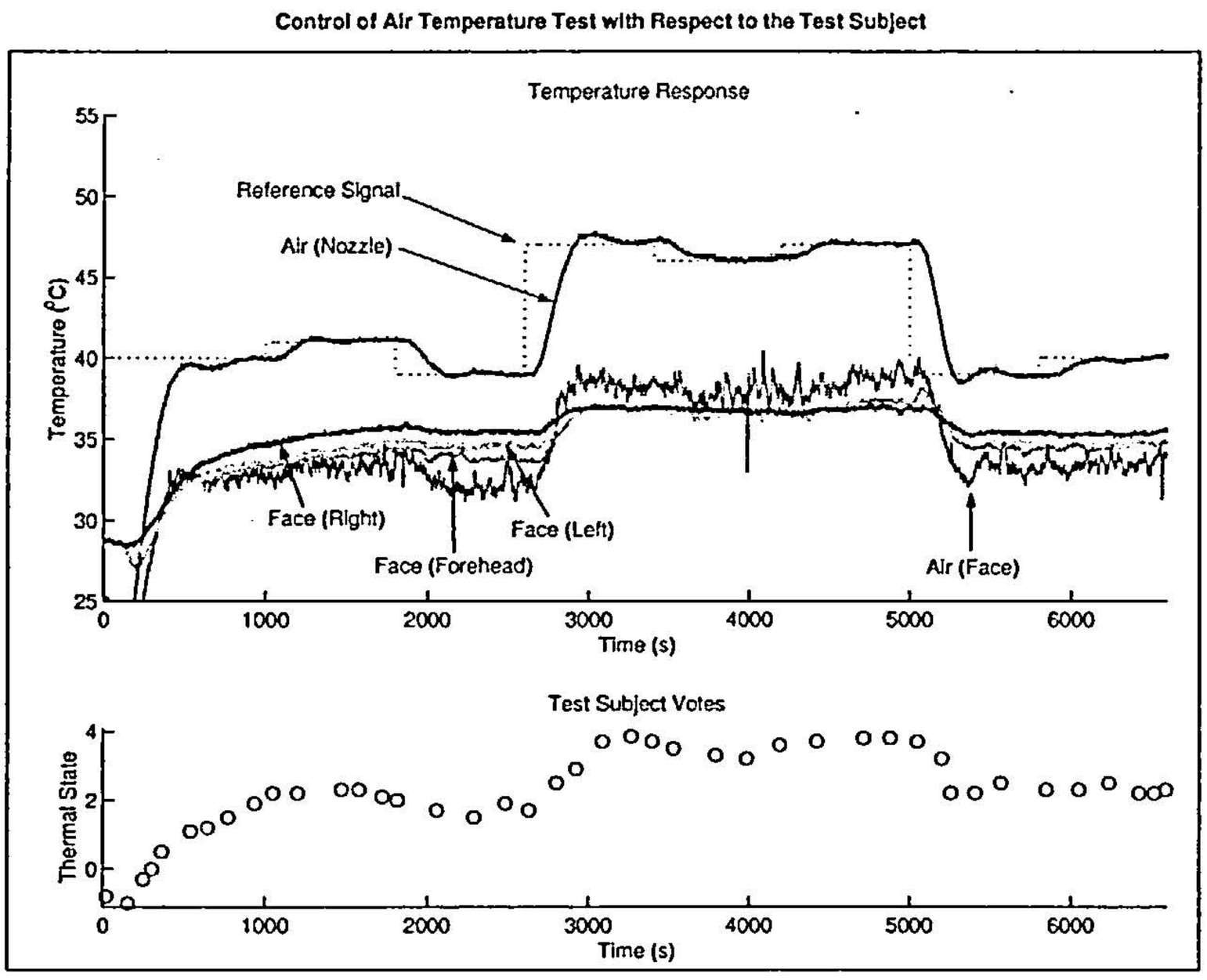


Figure 2.10: Controlled air temperature of the HVAC plant - test 11

Figure 2.10 shows the thermal state votes and face and air temperatures that were recorded during the control test presented in figure 2.9. The plot shows the controller reference and the controlled air temperature at the nozzle outlet. The air temperature close to the subjects face was also recorded. The shape of the reference signal was chosen to examine the effect of small changes and large changes on the facial skin temperature and on the thermal state of the subject.

The small steps changes in temperature in the middle and at the end of the test are not

detected by the user. This is not surprising since the temperature of the air around the subject's face is not greatly affected.

The slightly bigger step ($2^{nd}$ change) has a more prominent effect on the air temperature around the subject's face however the corresponding change in personal vote is vague. The change in thermal vote sees to preempt the step change, which just seems to continue the trend.

The last phase of the test shows that the subject returned to a slightly higher thermal vote than for the same air temperature earlier, after being heated for a while. The thermal state then remains constant until the end of the test.

An interesting phenomenon that appears in the data is the congruity of the facial skin temperature during the middle phase of the test. At the start of the test there is a range in facial skin temperature, but as the air temperature rises above the facial skin temperature the facial skin temperatures converge on the same value and as the air temperature drops below the facial skin temperature the facial skin temperatures drift apart again.

It is suggested that this is due to the physiology of the subject. To start with, the air temperature is lower than the skin temperature and so the skin does not need to cool itself since it is cooled by forced convection of the air (hence different temperature at different locations due to geometry based cooling) but as the air temperature increases the skin starts to actively cool itself locally (not sweating) so that the temperatures at different locations become the same. The most interesting part is that the subject has switched from votes around 2 - "feeling warm" to votes around 4 - "feeling hot". Thus it is hypothesised that the difference in facial skin temperatures and the difference between the mean facial skin temperature and the local air temperature could be used to estimate the thermal state of the subject or at least provide a modifier coefficient to make it more user specific and reduce offset errors.

This phenomenon is supported by data collected from other test subjects but not by all. Some data even shows the reverse scenario such as figure 2.11. The plot shows the separation of the skin temperatures as the air temperature rises above the mean skin temperature. This might be explained if the subject's body was actively warming itself at the lower temperatures.

It is quite difficult to draw conclusions from the thermal voting by this subject during this test. The initial response, up to about 2500 seconds seems fine but then there is a sudden drop in thermal state votes at 3000 seconds. The large step up in reference air temperature does seem to have caused the rise in thermal state. However, just after the small slight

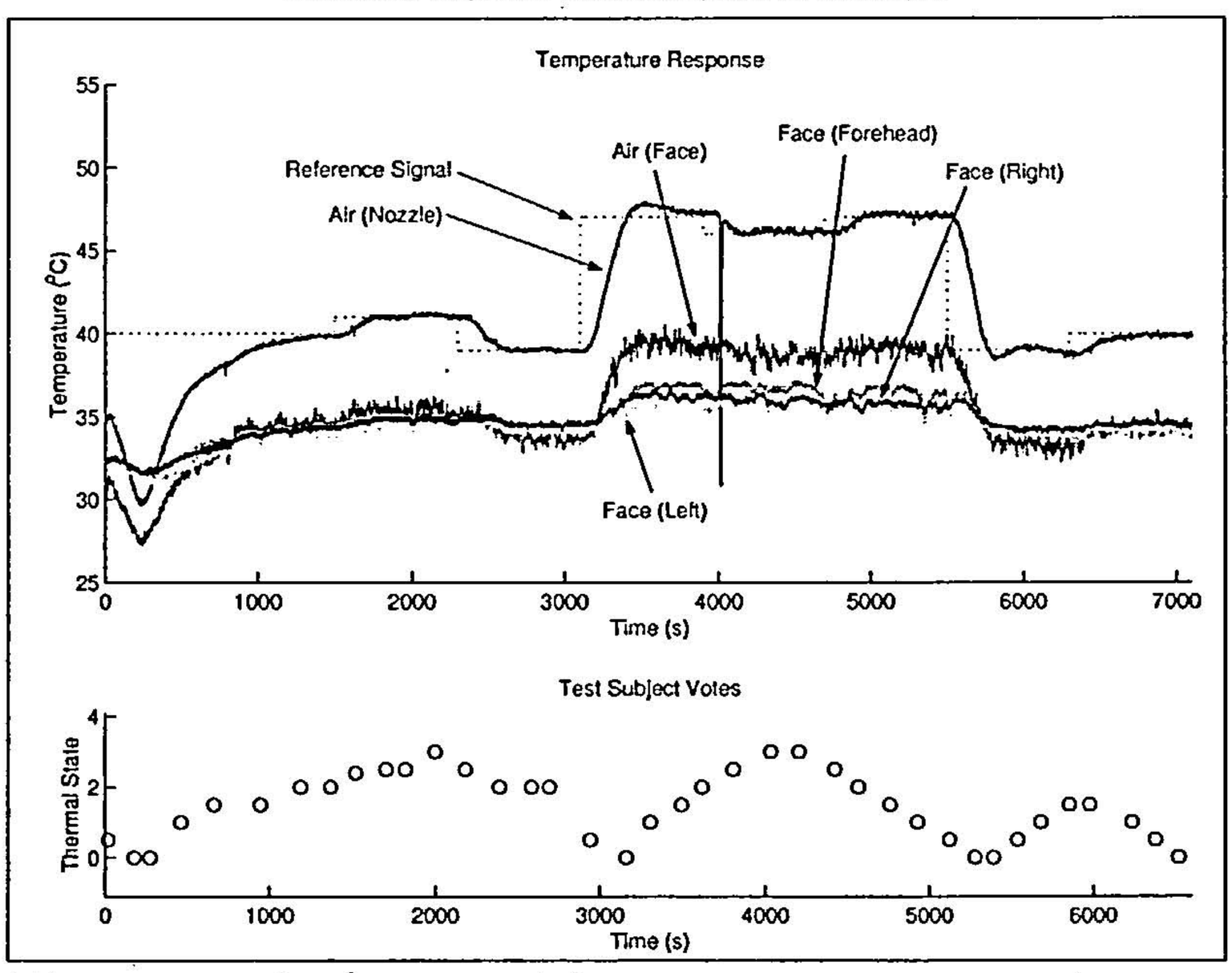


Figure 2.11: Controlled air temperature of the HVAC plant - test 12

change down (at the higher temperature level) the subject's thermal state estimates starts decreasing. The small step back up (at the higher temperature level) has no effect. Just after the drop to the lower temperature level the thermal state response starts to increase again but only for a small peak before returning to zero.

This test data was rejected because it is obvious that the subject did not respond to the test. The reason suggested by the test subject for the lack of response was that the chair seemed to be very cold and made him feel cold. This problem was fixed by using a chair with a padded seat and back rest for insulation. The reason for the disruption to the thermal state is not captured by any of the measured values. All hidden influences affecting thermal state were removed, once identified, so that the results could be correlated to the measured signals. These influencing factors are, nevertheless, an important consideration in determining thermal sate.

The interesting thing about asking a person how they are feeling, in a thermal sense, is that the answer is not definite. When requesting a numerical evaluation, say between -5 ( = cold) and +5 ( = hot), it is not reasonable to ask for five decimal places. The reply will be approximated to a level compromising accuracy with confidence. The optimal effective level of accuracy is thus determined. It is expected that to measure and to control the thermal state to a greater degree of accuracy is pointless since the person using the system will not

appreciate the extra capacity. Most subjects were willing to vote the the nearest decimal place but it was usual to find that there was uncertainty even at this resolution. From the experience of these test it is suggested that this is the general limit of thermal sensitivity, where the accuracy of the test subject is compromised by the confidence in voting. In the case where confidence is compromised for accuracy the subject's consistency needs to be examined.

## 2.6 Conclusions

This chapter describes an experiment that was used to modify the environment of a test subject. The experiment was not to the same scale as a system fitted to a standard automobile. However, similar work has been carried out in the literature and was then verified through application to an automotive cabin. The main aim of the use of this experiment was *not* to provide a comparative system but was simply to investigate the estimation of thermal state. Different methods of thermal state will be investigated in chapter 3.

The development and testing of an experimental framework for investigating thermal state involved:

1. Examining the modelling and control aspects of a heating system.
2. Observing and measuring the changes in a subject's personal thermal state votes in relation to changes in temperature.

To compare the objectives of this chapter with the results obtained it is clear that modelling and control of the HVAC system has been achieved. From the work presented in appendix B it appears that the creation of an accurate physical model is more than a trivial task. Simple assumptions and roughly estimated parameters are not enough to provide an adequately accurate physical model response. "Fiddling" the physical model can help to increase its accuracy, the resulting parameters, however, become unrealistic. The presented attempt at providing a physical model does give insight into the heat transfer thermodynamics and mechanical processes that are involved, which given more time, could be expanded and re-evaluated to provide a better model. The identification process helped to provide a faster solution to finding a model of the plant. The identified model was accurate enough on the tested data and was of a low order.

Control of the HVAC air temperature was successfully achieved using the identified plant model as a basis for control synthesis by pole placement using a polynomial approach. This

is a standard control technique and it shows that control of only the air temperature did not require any special control requirements. From the equations of the physical model it can be seen that control of the air temperature only results in a linear model. It is also seen that if control of the air temperature and the air flow rate is desired simultaneously this will result in non-linear system equations. The limitations on the HVAC plant used in the experiment described in this chapter meant that no investigation into the coupling of the dynamics of air temperature and velocity could be made.

Observing the thermal state votes of the test subjects suggests that most are willing to vote the the nearest decimal place but that this is the limit of their thermal sensitivity. The results also show an interesting phenomenon of the congruity of the facial skin temperature with regards to the local air temperature.

# 3 Thermal Balance Calculations and Thermal State Estimations

Based on the experimental set up described in chapter 2 the aim of this chapter is to provide a comparative study of three methods of thermal state estimation: the established calculation of PMV, a more direct linear calculation based on facial skin temperature and a neural network approach. In chapter 5 a fuzzy approach will also be explained. However, this is a new approach and will be presented in the context of part II of this thesis - Learning User Interactions.

The methods were evaluated in terms of the estimation variance and the error variance and correlation. The average variance of the error is below 0.7. The average variance of error from the PMV is the lowest (below 0.5) but it requires pre-test information and a more diverse set of sensors. The TSV method was found to be the easiest to set up and to implement. The neural network approach required the most work in setting it up due to the fact that it requires a training data set and then needed to be taught. From the test results it appears that for the extra effort in applying the PMV and neural network methods there is no real gain in performance of estimation.

This chapter contributes a review of three thermal state estimation methods and provides for the first time an evaluated performance and implementation comparison.

## 3.1 Introduction

Thermal state estimation is an established area of research and thus many different methods and techniques have been developed. The aim of this chapter is to examine more closely and

compare some of the most popular methods. Data collected from the experiment presented in Chapter 2 is used to generate thermal state estimations using the different techniques and a comparison of the results will be discussed.

This chapter is important because it not not only provides for the first time a performance comparison between the thermal state evaluation results but also provides a critical evaluation and experience in the implementation of the methods. One of the methods is used in a control experiment in chapter 4. The demonstration of these techniques is also required for the performance evaluation of a new method described in chapter 5.

## 3.2 PMV, PPD and Fanger's Comfort Equation

### 3.2.1 Background

The PMV (Predicted Mean Vote) calculation is a modern day version of Fanger's comfort equation and is an established calculation used mainly in the control of HVAC systems for buildings.

In 1967 P. O. Fanger explained in an important paper, [8], that previous research involved experiments that varied only 2 of the 6 principal variables involved while holding all others constant. While providing valuable results this is a slow and expensive method. The principal variables have been presented already, section 1.1.2, and are restated below:

1. Air Temperature.
2. Mean Radiant Temperature.
3. Relative Air Velocity.
4. Humidity (Partial Vapour Pressure).
5. Activity Level (Internal Heat Production).
6. Insulation Value of Clothing.

The paper proposed a new method regarding the subject's skin temperature and sweat secretion as the basis of thermal comfort. From experiments with these parameters a comfort equation was derived in terms of the 6 principal variables. It was presumed that a person would be in a state of thermal comfort for a particular skin temperature, $t_s$, and internal temperature, $t_i$, that are within certain limits, $a$, $b$ and $c$, $d$:

$$a < t_s < b \quad c < t_i < d$$

Internal temperature, $t_i$, can be expressed as a function of skin temperature and either hypothalamic temperature, $t_{hyp}$, or deep skin temperature, $t_{deep}$, depending on which perspective is taken.

$$t_i = f(t_s, t_{hyp}) = f(t_s, t_{deep}) \tag{3.1}$$

With reference to [30] and [31] Fanger deduced that the sweat secretion level, $S$, could also be expressed as a function of hypothalamic temperature or deep skin temperature.

$$S = f(t_{deep}) = f(t_{hyp}) \tag{3.2}$$

By combining these 2 forms, equations (3.1) and (3.2), internal temperature can thus be expressed as a function of skin temperature and sweat secretion. This led to a new set of limits that were determined by experiment.

$t_i = f(t_s, S)$ Hence: $a < t_s < b \quad e < S < f$

Experiments with varying activity levels were then carried out on test groups of college-aged Americans to find the corresponding mean values of $t_s$ and $S$ and the limits $a$, $b$, $e$ and $f$. The results were collected during the last half-hour of the 3-hour experiment when no significant changes took place (i.e. when the subjects were in steady state). Results also showed that there was no significant difference between the values for males and females. Regressions were carried out on the results and the parameters $t_s$ and $S$ were equated in terms of Dubois body surface area, metabolic rate and external mechanical efficiency. The thermal regressions for $t_s$ and $S$ were then used to quantify the elements of the thermal balance equation (3.3).

$$H - D - S_w - R_w - R_d = K = R + C \tag{3.3}$$

Here:

$H =$ Internal heat production in the human body.

$D =$ Heat loss by water vapour diffusion through the skin.

$S_w =$ Heat loss by evaporation of sweat from the surface of the skin.

$R_w =$ Latent respiration heat loss.

$R_d =$ Dry respiration heat loss.

$K =$ Heat transfer from the skin to the outer surface of the clothed body.

$R =$ Heat loss by radiation from the outer surface of the clothed body.

$C =$ Heat loss by convection from the outer surface of the clothed body.

Fanger's comfort equation then evaluates each of the components of the energy balance equation (3.3) in terms of the principal variables to get equation (3.4). This equation is Fanger's Comfort Equation:

$$\begin{aligned}
&\frac{M}{A_{Du}}(1-\eta) - 0.35\left[43 - 0.061\frac{M}{A_{Du}}(1-\eta) - P_a\right] - 0.42\left[\frac{M}{A_{Du}}(1-\eta) - 50\right] - \\
&0.023\frac{M}{A_{Du}}(44 - P_a) - 0.0014\frac{M}{A_{Du}}(34 - t_a) = \frac{35.7 - 0.032\frac{M}{A_{Du}}(1-\eta) - t_{cl}}{0.18 I_{cl}} \\
&= 4.8 \cdot 10^{-8} f_{cl} f_{eff}\left[(t_{cl}+273)^4 - (t_{mrt}+273)^4\right] + f_{cl} h_c (t_{cl} - t_a) \qquad (3.4)
\end{aligned}$$

The variables as defined in [8] are:

$M =$ Metabolic rate.

$A_{Du} =$ Dubois area (the surface area of the nude body).

$\eta =$ External mechanical efficiency of the body.

$P_a =$ Partial pressure of water vapour in the room air.

$t_a =$ Air temperature.

$t_{cl} =$ Outer temperature of clothed body.

$I_{cl} =$ Dimensionless term for the total heat transfer resistance from skin to outer surface of clothed body.

$f_{cl} =$ Ratio of the surface area of the clothed body to the nude body.

$f_{eff} =$ Ratio of the effective radiation area of the clothed body to the surface area of the clothed body.

$t_{mrt} =$ Mean radiant temperature.

$h_c =$ Convective heat transfer coefficient.

Measurements of the principal variables together with some empirical data allow a person's thermal state to be estimated on a thermal state index scale. Over 1300 subjects giving thermal sensation votes have statistically related PMV and the thermal balance equation.

Steady state conditions, however, are assumed and so the equation is only valid for small changes in thermal conditions and it is recommended that time-weighted averages of the variables over the previous hour are used.

### 3.2.2 How it Works

The method of evaluating PMV, equation (3.5), involves solving a recursive equation set, equations (3.5) to (3.8). The British Standard explains how this is done and provides a short code listing written in BASIC for computational calculation.

$$\begin{aligned} PMV &= \left(0.303\,\mathrm{e}^{-0.036M} + 0.028\right)\Big\{(M-W) - 3.05\cdot 10^{-3}\left[5733 - 6.99\,(M-W) - p_a\right] - \\ &\quad 0.42\left[(M-W) - 58.15\right] - 1.7\cdot 10^{-5} M\,(5867 - p_a) - 0.0014M\,(34 - t_a) - \\ &\quad 3.96\cdot 10^{-8} f_{cl}\left[(t_{cl}+273)^4 - (\bar{t}_r + 273)^4\right] + f_{cl} h_c\,(t_{cl} - t_a)\Big\} \end{aligned} \tag{3.5}$$

$$\begin{aligned} t_{cl} &= 35.7 - 0.028\,(M-W) - \\ &\quad I_{cl}\Big\{3.96\cdot 10^{-8} f_{cl}\left[(t_{cl}+273)^4 - (\bar{t}_r+273)^4\right] + f_{cl} h_c\,(t_{cl} - t_a)\Big\} \end{aligned} \tag{3.6}$$

$$h_c = \begin{cases} 2.38\,(t_{cl} - t_a)^{0.25} & \text{for} \quad 2.38\,(t_{cl} - t_a)^{0.25} > 12.1\sqrt{\nu_{ar}} \\ 12.1\sqrt{\nu_{ar}} & \text{for} \quad 2.38\,(t_{cl} - t_a)^{0.25} \leq 12.1\sqrt{\nu_{ar}} \end{cases} \tag{3.7}$$

$$f_{cl} = \begin{cases} 1.05 + 0.645 I_{cl} & \text{for} \quad I_{cl} > 0.078\ m^2\,{}^{o}\mathrm{C}/W \\ 1.00 + 1.290 I_{cl} & \text{for} \quad I_{cl} \leq 0.078\ m^2\,{}^{o}\mathrm{C}/W \end{cases} \tag{3.8}$$

Here:

$PMV =$ Predicted Mean Vote.

$M =$ Metabolic rate in $W/m^2$ of body surface area (1 metabolic unit =1 met = 58.2 $W/m^2$).

$W =$ External work in $W/m^2$.

$I_{cl} =$ Thermal resistance of clothing in $m^2\,{}^{o}\mathrm{C}/W$ (1 clothing unit = 1 clo = 0.155 $m^2\,{}^{o}\mathrm{C}/W$).

$f_{cl} =$ Ratio of skin surface area when clothed to surface area when nude.

$t_a =$ Air temperature in ${}^{o}\mathrm{C}$.

$\bar{t}_r =$ Mean radiant temperature in ${}^{o}\mathrm{C}$.

$\nu_{ar} =$ Relative air velocity in $m/s$.

$p_a =$ Partial water vapour pressure in $Pa$.

$h_c =$ Convective heat transfer coefficient in $W/m^2\,^oC$.

$t_{cl} =$ Surface temperature of the clothing in $^oC$.

$t_o =$ Operative temperature in $^oC$.

The British standard also supplies data sheets for the estimation of some of the variables such as activity levels, table 3.1, and the thermal resistance of clothing, table 3.2.

| Activity Description | Metabolic Rate $W/m^2$ | met |
|---|---|---|
| Reclining | 46 | 0.8 |
| Seated, relaxed | 58 | 1.0 |
| Sedentary activity | 70 | 1.2 |
| Standing, light activity | 93 | 1.6 |

Table 3.1: Estimation of activity level

### 3.2.3 PMV Experimental Results

The clothing of the test subject was observed and by using table 3.2 a total clothing value could be determined for each subject for each test. Activity level according to table 3.1 was estimated as 1.0. The British standard explains that relative humidity only influences thermal state at the extremity values. As the experimental conditions are not designed to vary the humidity level and the natural state of the air during the tests was considered normal, the relative humidity variable was set at a constant 50%. The air velocity has been calculated as presented in table B.2 for different fan speed settings. The fan speed was set at 30% for the duration of the tests. The radiative energy was not measured but the cabin area was semi enclosed and additional heat through radiation was assumed to be negligible. The cabin enclosure's main aim was to reduce draught disturbance. The air temperature is thus the only changing input into the PMV calculation throughout the experimental tests.

Two examples of results collected are shown in figures 3.1 and 3.2. The distribution of the error was calculated to examine the difference between the PMV calculation and the personal estimate from the test subject. In the figures the upper plot shows the personal votes as circles and a raw PMV estimate as the grey line. A filtered PMV estimate with a first order non-phase shifting filter is drawn as the black line. In the bottom plots the histogram of the error is presented on the left together with the distribution curves and on the right is the cumulative frequency curves. In both the bottom plots two curves are drawn, one from the raw data, $\triangle$, and the other is the filtered curve using the first order non-phase

| Garment Description | | Thermal Insulation (clo) |
|---|---|---|
| Underwear | Panties | 0.03 |
| | Underpants (long legs) | 0.10 |
| | Singlet | 0.04 |
| | T-shirt | 0.09 |
| | Shirt (long sleeves) | 0.12 |
| | Panties and bra | 0.03 |
| Shirts - Blouses | Short sleeves | 0.15 |
| | Light-weight (long sleeves) | 0.20 |
| | Normal (long sleeves) | 0.25 |
| | Flannel shirt (long sleeves) | 0.30 |
| | Light-weight blouse (long sleeves) | 0.15 |
| Trousers | Shorts | 0.06 |
| | Light-weight | 0.20 |
| | Normal | 0.25 |
| | Flannel | 0.28 |
| Dresses - Skirts | Light skirts (summer) | 0.15 |
| | Heavy skirt (winter) | 0.25 |
| | Light dress (short sleeves) | 0.20 |
| | Winter dress (long sleeves) | 0.40 |
| | Boiler suit | 0.55 |
| Sweaters | Sleeveless vest | 0.12 |
| | Thin sweater | 0.20 |
| | Sweater | 0.28 |
| | Thick Sweater | 0.35 |
| Jackets | Light jacket (summer) | 0.25 |
| | Normal jacket | 0.35 |
| | Smock | 0.30 |
| High-Insulative, Fibre-Pelt | Boiler suit | 0.90 |
| | Trousers | 0.35 |
| | Jacket | 0.40 |
| | Vest | 0.20 |
| Outdoor Clothing | Coat | 0.60 |
| | Down jacket | 0.55 |
| | Parka | 0.70 |
| | Fibre-pelt overalls | 0.55 |
| Sundries | Socks | 0.02 |
| | Ankle socks (thick) | 0.05 |
| | Long socks (thick) | 0.10 |
| | Nylon stockings | 0.03 |
| | Shoes (thin soled) | 0.02 |
| | Shoes (thick soled) | 0.04 |
| | Boots | 0.10 |
| | Gloves | 0.05 |

Table 3.2: Estimation of clothing rating

shifting filter, $*$. The filtered curve helps to extrapolate the reduction of the width of the histogram's classes to 0 (and the number of data points to $\infty$).

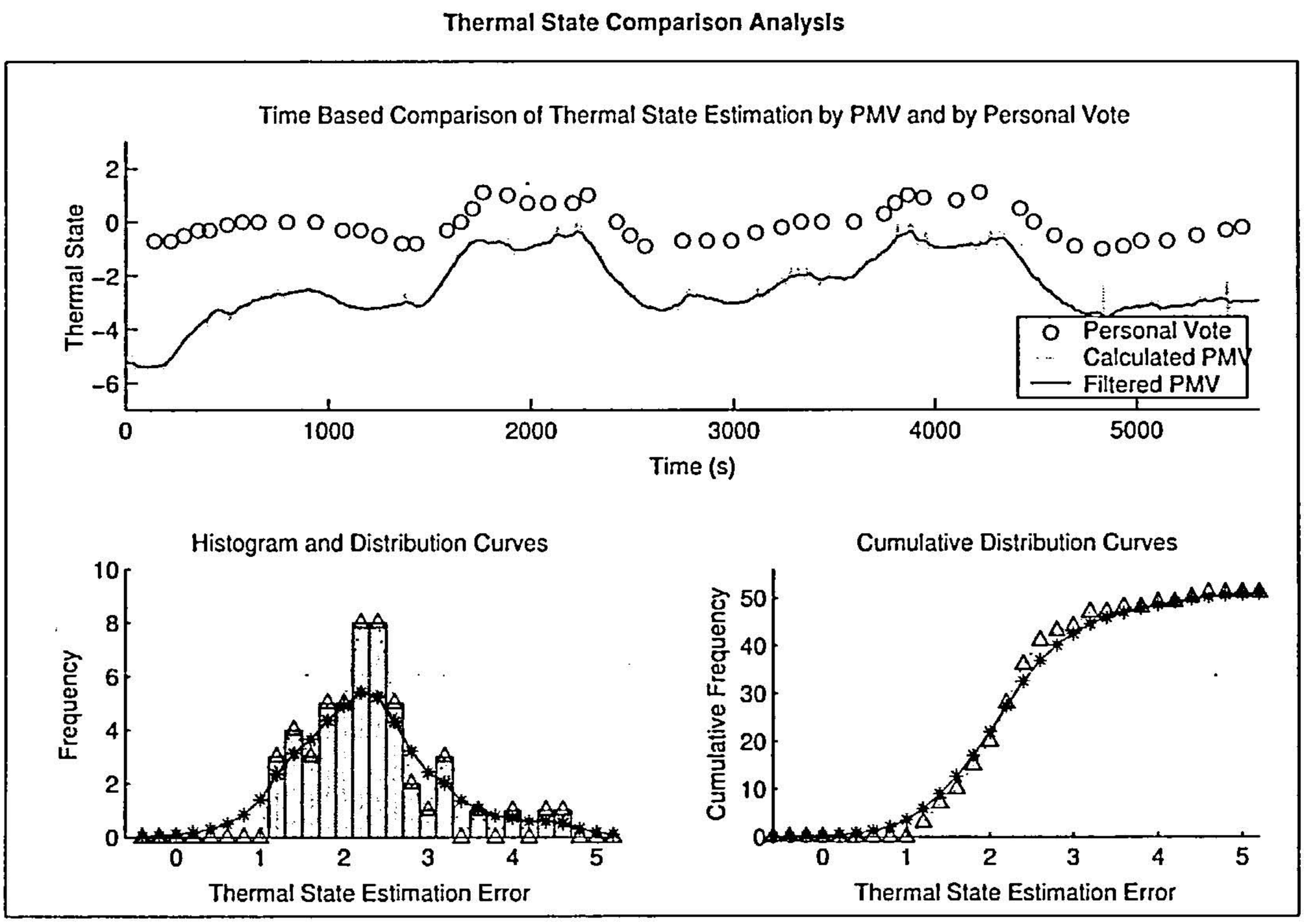


Figure 3.1: Comparison of the PMV thermal state estimate with the personal thermal state vote - test 10

The reason for the difference between the PMV estimate and the personal vote of the test subject might be explained through calibration errors or the fact that the air flow is particularly high (in terms of the method recommendations) or by the fact that the air temperature at the face is significantly different to the temperature at the feet area. It should not be ruled out that the difference could also be due to the test subject giving false votes. This could be because the test subject has poor thermal sensitivity and can not give as accurate a vote as the PMV calculation. A strong psychological influence on the basis of a vote is the value that was voted previously.

It is clear from the plots that there is some sort of offset error. The personal votes of the test subjects are all significantly higher. The thermal state error distribution, in the cases presented, shows how the difference between the PMV estimate and the personal vote is distributed. The distribution curves show very clearly the offset error which can be read off the plot as the value of the x-axis at the distribution peak. The rest of the distribution curve is shaped in a form similar to the normal distribution curve, which is good for evaluating the reliability of the PMV.

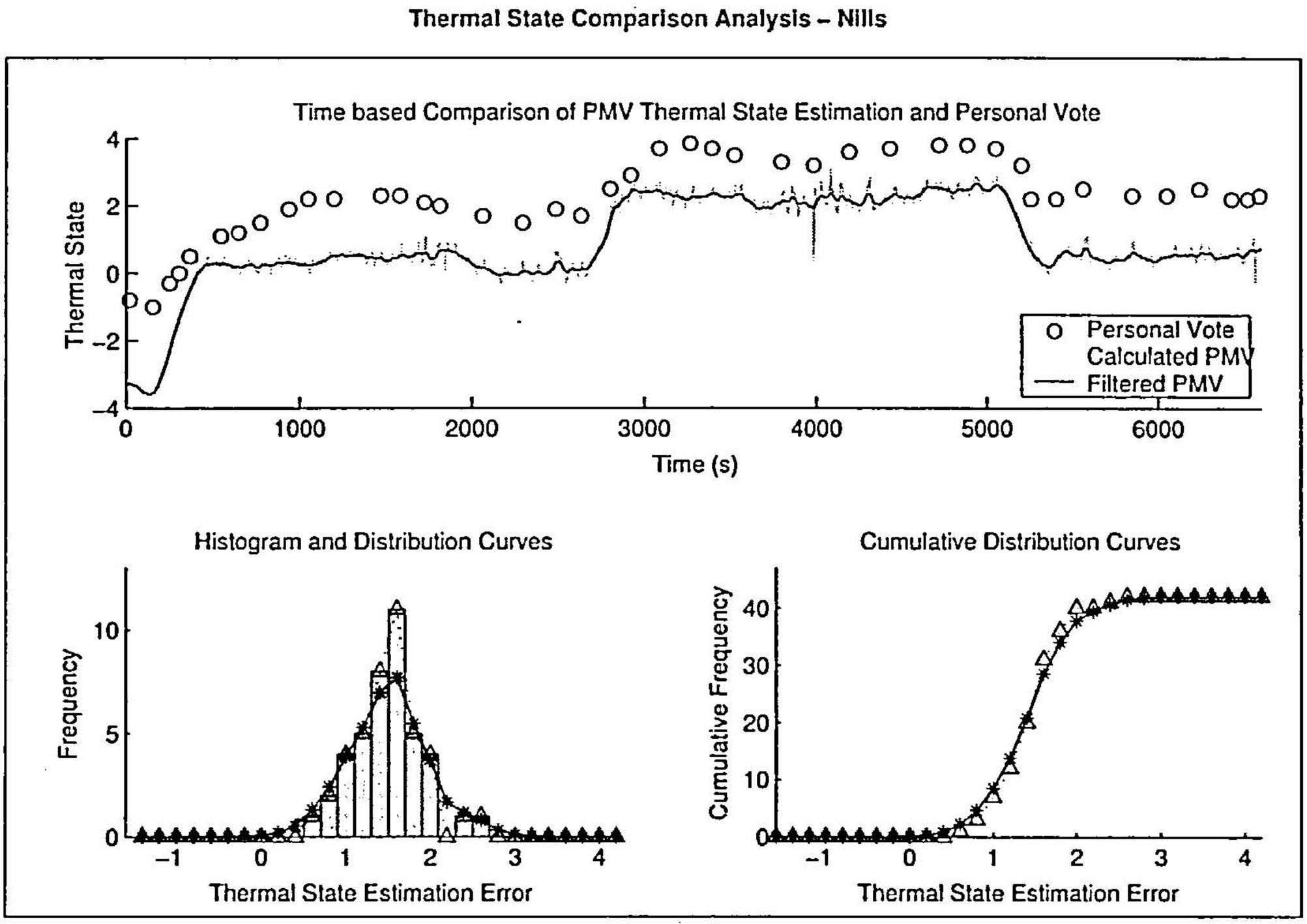


Figure 3.2: Comparison of the PMV thermal state estimate with the personal thermal state vote - test 11

The reliability of the PMV estimate can be evaluated by means of the variance of the error. The variance of the actual data points must also be taken into consideration. A data set where the thermal votes did not change much will not give a good indication of the reliability of the PMV except over that range. The performance of the PMV method can be estimated using a correlation value as well as the variance of the data. The histograms of all the usable results together with the variance and correlation values for the data and for the error between the PMV and the actual votes are presented in table 3.3.

### 3.2.4 Discussion of the PMV Method

#### Discussion of Results

In this experiment air humidity, solar gain and activity rate were *assumed* to be constant through out the test, air velocity and clothing level *were* constant through out the test which means that the PMV value depended entirely on the change in air temperature, measured at the face of the subject. The results show a fair correlation with the actual voting.

| Test Number | Personal Thermal Vote | PMV | Difference (Error) |
|---|---|---|---|
| 03 | 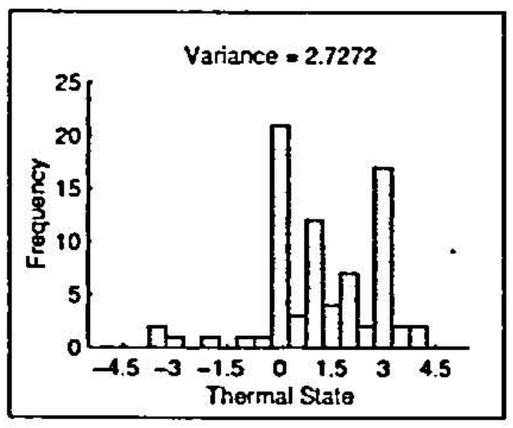 | 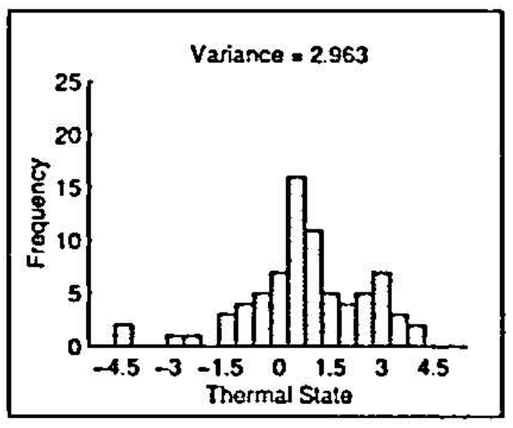 | 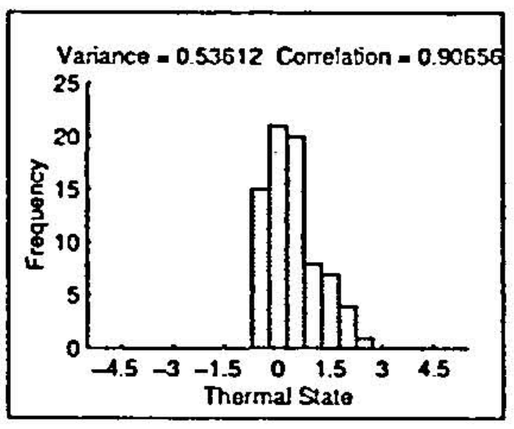 |
| 05 | 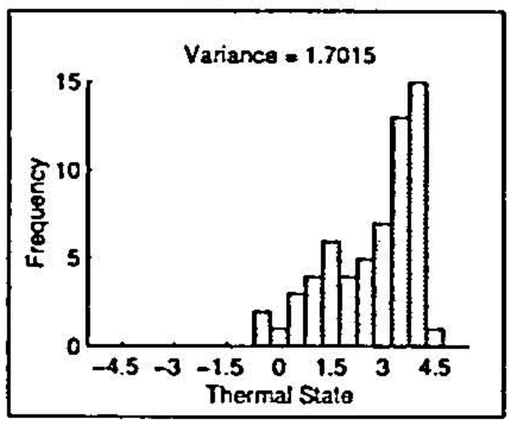 | 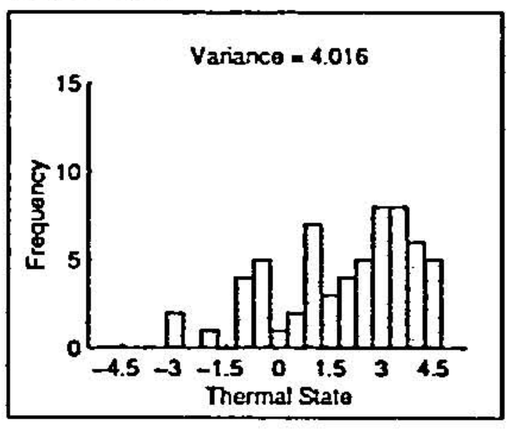 | 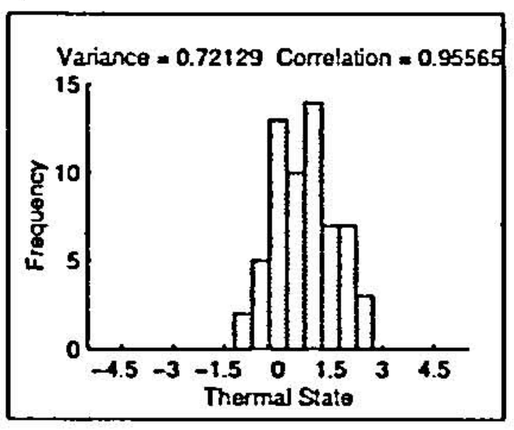 |
| 10 | 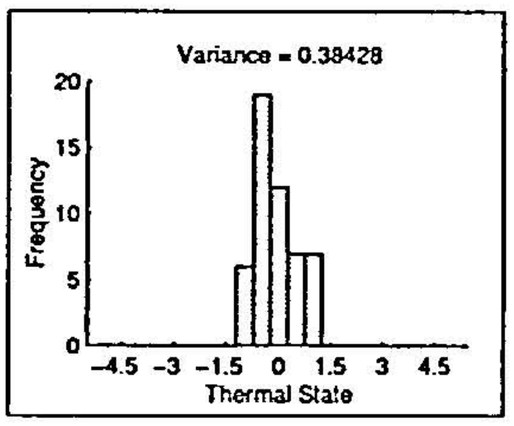 | 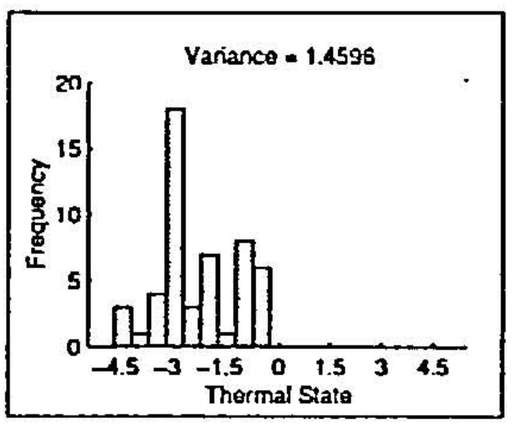 | 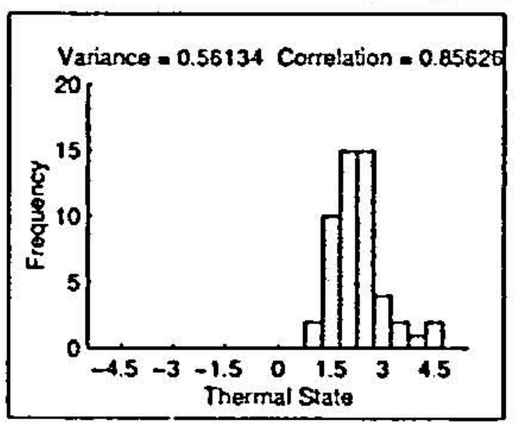 |
| 11 | 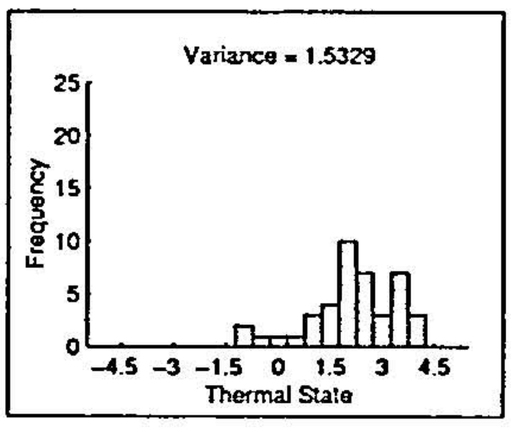 | 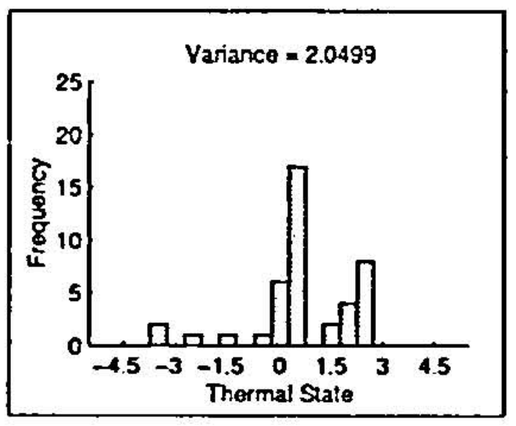 | 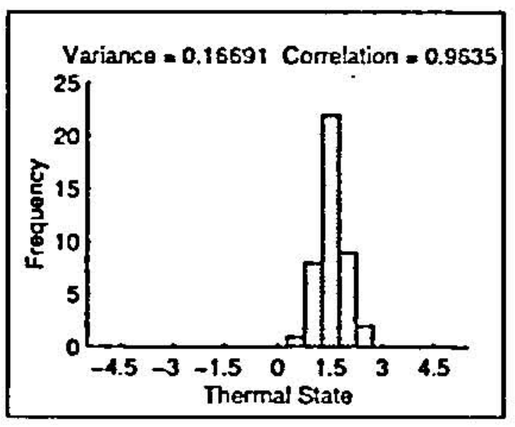 |
| 15 | 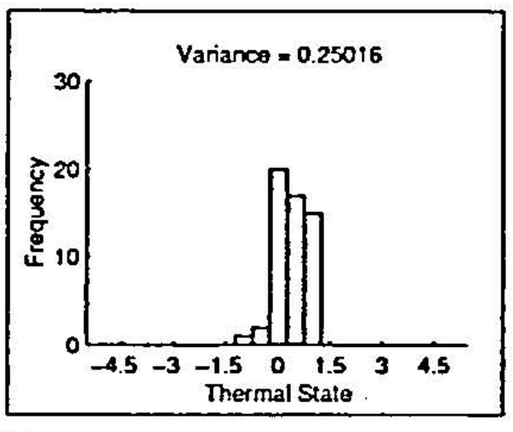 | 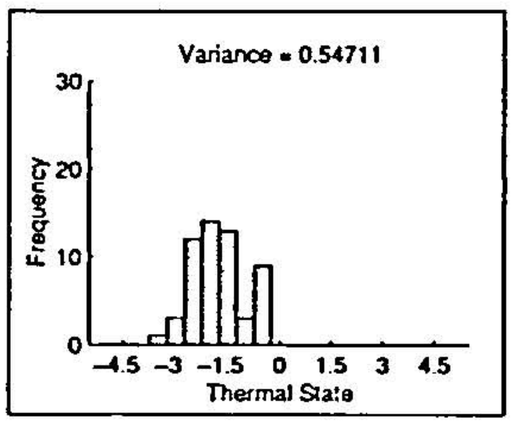 | 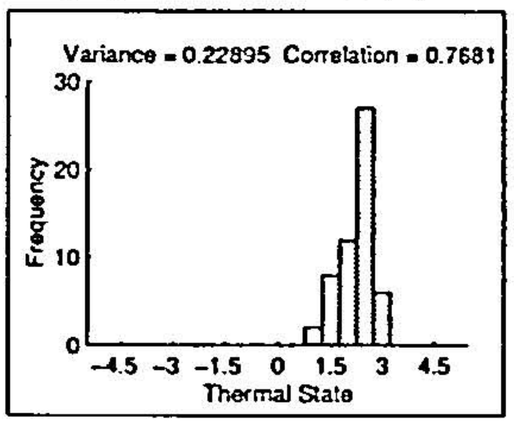 |

Table 3.3: Histogram results of the PMV Estimation Method

From the histogram results displayed in table 3.3 it can be seen from test 3 that this person preferred to stick to the integer values of thermal state (i.e. 0 1 2 and 3), which seem to have significantly more values than those between. This suggests that this person was less confident to interpolate between the suggested linguistic values. The shape of the histogram and the variance of the personal vote shows a fairly good spread of points over the warmer side of thermal state. A good spread is also indicated by the PMV variance. The variance of the

error is expected to be bad because of the poor thermal sensitivity of the subject. However, the variance is small which indicates that the PMV has been fairly effective in estimating the personal thermal vote. This is confirmed by the high value of correlation between the PMV estimate and the personal thermal vote.

Test 10 suffers from the problem of a poor variance of personal thermal state. The time domain data, displayed in Figure 3.1, shows that the subject was responding to the changes instigated by the experiment. The personal response just appears to have a smaller gain than the PMV system. The variance of the error is actually higher than the variance of the personal vote which is not a good sign. The value of the variance of the error is still in line with that of the other tests and the poor variance of personal votes does not detract too much from the confidence in the PMV as shown by the correlation value which has fallen slightly but is still practically good.

Test 15 also suffers from the same problem as test 10, i.e. a poor variance in personal thermal vote. The variance of the error however is in this case lower than the variance of the personal vote but the effect has reduced the correlation value.

Test 11 shows a very good result - a wide variance of personal vote and PMV values but a very small variance in the error which is complimented by a high correlation value. Perhaps this test has slightly fewer data points than the other tests. Nevertheless, the result is particularly good.

It is interesting to note that tests 3 and 5 have little or no offset errors but that the other three tests show some difference. The cause of the offset is not clear. Perhaps the error is a calibration fault or perhaps the error is a personal preference issue. The experiments were set up the same way, the temperature sensors were calibrated against an industrial standard thermometer before each test. Tests 5, 10 and 11 used the same test subject yet show different offset values. What is clear is that the offset can be approximated by the mean of the error and once this has been taken care of the PMV shows a good performance.

### Discussion of Method

The PMV is an established method described by the International and British Standards (BS-EN-ISO 7730) and has a few additional computational features such as the PPD (predicted percentage of dissatisfied) and a draught equation.

$$PPD = 100 - 95\,\mathrm{e}^{(0.03353PMV^4 + 0.2179PMV^2)} \tag{3.9}$$

The PPD is an estimation of the percentage of people subjected to the measured environment that will be unhappy with the environment. The votes of a group of people all subjected to the same environment will not all be exactly the same, as expected. It is the purpose of the PPD to predict the percentage of people within such a group that will be unhappy with the environmental conditions. Equation (3.9) is used for calculating the PPD and shows that it is just another representation of the PMV which tackles the control issue in a different way. Instead of aiming to maintain a high level of comfort the PPD is used to minimize the number of dissatisfied people. Table 3.4 gives a comparison between values of PMV and PPD.

| PMV | PPD | Percentage of persons predicted to vote | | |
|---|---|---|---|---|
| | | 0 | -1, 0 or +1 | -2, -1, 0, +1 or +2 |
| +2 | 75 | 5 | 25 | 70 |
| +1 | 25 | 27 | 75 | 95 |
| 0 | 5 | 55 | 95 | 100 |
| -1 | 25 | 27 | 75 | 95 |
| -2 | 75 | 5 | 25 | 70 |

Table 3.4: The predicted distribution of PMV and PPD votes

Unhappiness with the environmental conditions can be greatly affected by draughts – "an unwanted local area of cooling caused by the movement of air". The draught rating is expressed as a percentage of people dissatisfied due to draught, $DR$ in equation (3.10), and is expressed as a function of the local air temperature, $t_a$, the local mean air velocity, $v$, and the local turbulence intensity, $T_u$.

$$DR = (34 - t_a)\,(v - 0.05)^{0.62}\,(0.37v \cdot T_u + 3.14) \tag{3.10}$$

The British Standard presenting PMV also states acceptability of the environment for thermal comfort as maintaining the PPD under 10% which translates to the PMV being kept within $\pm 0.5$. The draught rate should also be kept lower than 15%, which can be done by controlling the local mean air velocity.

Recommendations for use of the PMV calculation in control of the thermal environment by the British Standard are as follows:

- PMV is derived from steady state conditions and so should only be used with minor

fluctuations in environmental disturbances.

- Time-weighted averages over the previous 1 hour should be applied to the variables involved.
- The use of the PMV index should be limited to between -2 and +2.
- Limitation of the 6 main variables:
  - $M = 46$ to $232 W/m^2 (0.8$ to $4 met)$
  - $I_{cl} = 0$ to $0.310 m^2\,^oC/W (0$ to $2 clo)$
  - $t_a = 10$ to $30\,^oC$
  - $\bar{t}_r = 10$ to $40\,^oC$
  - $v_{ar} = 0$ to $1 m/s$
  - $p_a = 0$ to $2700 Pa$
  - (Relative Humidity = 30% to 70%)

Note: the draught rate may limit the relative air velocity even further..

The PMV is designed for use with groups of people, typically working together, and so acceptability is defined in terms of a limit of satisfied people. This gives a problem in applying this approach to the automotive cabin occupants to whom the air conditioning system can assign individual control laws. The PPD could, however, be interpreted as the probability that a single occupant will be unhappy with the current environment and in this context the acceptability rating can be used as a control limit.

Several assumptions and approximations have been made in the experimental application of the PMV. For example, the $fcl$ value (ratio of surface area of clothed body to nude body) is approximated in the algorithm code from the value of the clothing resistance. Values of activity and clothing resistance are extracted from the tables of approximate values. The air velocity used in the experiments is high with regard to the recommended standards of use of the PMV calculation. However as the results show the PMV method has still proven to be quite accurate.

## 3.3 Linear Facial Skin Temperature Regression Equation

### 3.3.1 Background

The six principal variables used in the PMV method, with the exception of activity level, measure external conditions around the test subject. These are then used in a thermal balance

equation to evaluate the heat transfer between the subject and the environment. Fanger even states that thermal state can be reduced to an evaluation of skin temperature and sweat level. The two-node method by J. B. Pierce (see [18] and [19]) is also based on the thermal balance heat transfer process between the person and the environment. It seems then that a much more direct approach would be to base the thermal state on the skin temperature itself.

This approach has attracted researchers and tested techniques have been presented in the literature, such as the Hardy-DuPoint 7 point method in [32] in 1938, and the work of N. L. Ramamathan [33] in 1964. [34] gives a useful discussion on thermal comfort, skin temperature and thermoregulation. The problem with this approach is that there are few applications where it is practically possible to observe the skin temperature.

In the car cabin environment the non-contact measurement of skin temperature is not easy. With the current infrared technology it is possible to obtain facial skin temperatures, clothing temperatures and cabin wall temperatures however this is costly but methods and sensors are being developed, as in [35], [36] and [37]. The use of a thermal imaging device to look at the environment of the user has the advantage of a continuous temperature distribution across the field of view. This can be used to aim the vents as well as providing skin temperature.

There has been substantial research input from the Toyota Central Research & Development Labs in thermal comfort analysis in this area. In particular 5 papers have demonstrated significant accomplishment [25], [11], [27] [39] and [40]. The paper by Taniguchi et al [25] is the first of a 2-part study in which two sets of experiments were carried out in order to correlate the passenger facial skin temperatures with a thermal sensation vote. It was noted in the paper that thermal sensation evaluation by an overall average skin temperature had been studied for the application of building HVAC systems. In a car however, the close proximity of the air outlets causes a non-uniform temperature distribution and it was expected that the comfort of the user could be evaluated by observing the face skin temperature only.

A pre-test experiment involved blowing air at a subject's face and recording face temperature and overall body temperature and the thermal sensation vote of the subject. The test describes a very similar experimental setup to the one carried out in the investigation described in chapter 2. The test involved a single tube of variable air temperature directed towards the test subject's face and upper body and their facial skin temperatures were recorded. Additionally the experiment included a solar simulator to reproduce a sunshine load. The subjects indicated their thermal state by voting on a similar 11-point scale. The test started with the subject in a warm state and then the air was applied and the face was cooled. The results showed that the facial skin temperature was greatly reduced (since the air was directed at the face) and the overall skin temperature showed a slight increase. The thermal sensation

vote showed a decrease and it was hence presumed that the facial temperature could be used to determine the subject's thermal state. The authors explained that even when heating the subject by aiming the outlet at the feet, correlation between facial skin temperature and thermal sensation vote was still high.

The study then went on to produce a linear regression equation to equate thermal state votes to the corresponding mean facial skin temperature and rate of change of the mean facial skin temperature. It is the resulting equation from the first part of this study that will be examined next. The resulting equations were then tested in a car using the car's air conditioning system.

This paper gives rise to an interesting discussion concerning the use of facial skin temperature for thermal state evaluation even when heating air is supplied via the outlet vent by the feet. The paper explains that facial skin temperature may be particularly sensitive to thermal stimuli. This is an interesting assumption since it is the face that often turns red when undertaking physical exercise or even when blushing which are both examples of the body increasing heat loss.

### 3.3.2 How it Works

In the work carried out in [25] and [11], two important equations were presented. The first, equation (3.11), evaluates thermal state from the average facial skin temperature and rate of change of average facial skin temperature.

$$TSV = 0.81\left(\bar{tsk} - 33.9\right) + 39.1\bar{tsk}' \tag{3.11}$$

Here:

$TSV =$ Thermal Sensation Vote.

$\bar{tsk} =$ Average facial skin temperature in $^{o}$C.

$\bar{tsk}' =$ Rate of change of average facial skin temperature in $^{o}\mathrm{C}/s$.

The second, equation (3.12), reverses the process using a desired thermal state as an input to determine the required average skin temperature. In place of the normal user input for setting the temperature a desired thermal state input is required. Equation (3.12) is thus derived from equation (3.11) to calculate a target skin temperature from the desired thermal state input.

$$tsk^* = \frac{(TS + 27.5)\,\Delta\tau + 39.1tsk}{0.81\Delta\tau + 39.1} \tag{3.12}$$

Here:

$tsk^* =$ Target skin temperature after $\Delta\tau$ seconds in $^o$C.

$TS =$ Thermal sensation setting.

$\Delta\tau =$ Time interval in $s$.

This target skin temperature is then linked to the air temperature and air flow outputs from the HVAC system using a one-dimensional heat transfer model of the skin from the external surface to the body core (36.7 C). It was assumed that the air flow velocity was more likely to produce greater disturbance on the skin and provoke discomfort. Thus, setting of this parameter was left up to the user and the corresponding air temperature for the desired thermal state was calculated. The target skin temperature in steady state is found by solving equation (3.12) but with $tsk^* = tsk$.

Actually doing this reduces equation (3.12) to equation (3.13) which can be used to equate facial skin temperature with thermal state. This is an important step when discussing the implementation of thermal state (see chapter 6).

$$tsk = \frac{TS + 27.5}{0.81} \tag{3.13}$$

In the experiment described by [25], 7 facial skin temperature measurements were used to calculate a mean value. In the experiment conducted in chapter 2 only three measurements were taken due to a limitation of the number of available acquisition channels. From initial observation it was found that temperature differences between sensors that were within a centimetre or so of each other were negligible (except in the case when one happened to be over a vein). Thus by placing each sensor at the centre of different parts of the face (and avoiding veins) a mean value of facial skin temperature could be determined. A diagram of the facial skin temperature measurement points was presented earlier in figure 2.3.

### 3.3.3 TSV Experimental Results

Using the data collected in chapter 2 a TSV estimation was carried out. A detailed display of the results from tests 3 and 10 are provided in figures 3.3 and 3.4, respectively, and a summary of all the results is presented in table 3.5.

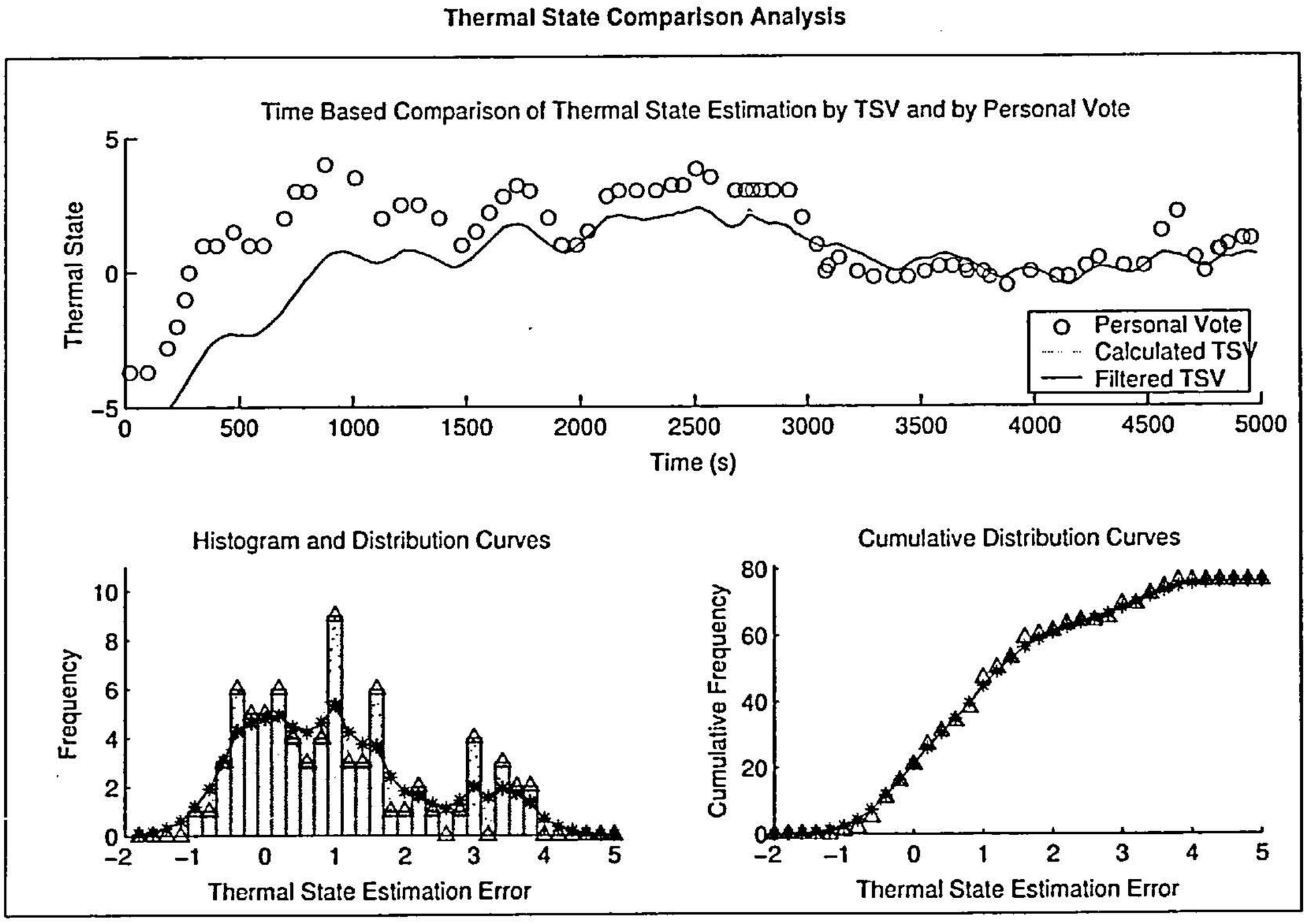


Figure 3.3: Comparison of the TSV thermal state estimate with the personal thermal state vote - test 03

From the time plot for data set 3, the results seem to get better and better as the test proceeds and the overall time plot seems to indicate a good correlation. The error between the TSV estimate and the thermal vote from the subject seems to slowly disappear and this disrupts the histogram and distribution curves. The initial value of the TSV estimate is extremely low (below -5) and so it is suspected that the test subject was uncomfortable in voting beyond or even on the limit of the suggested voting scale. Once the test had started previous votes may have influenced the estimate of subsequent votes and so the initial error is propagated, and dissipates slowly.

There is possibly a similar reason for the initial difference in test 10. The voting of this test subject with respect to the PMV approach has already been noted as being of a much lower gain and this is again confirmed with the TSV approach. What is interesting is that the poor initial response is not dissipated as smoothly as the error propagates through the data as in test 3. Instead there appears to be a jump as is evident in the histogram by the small peak at about 3.5 just to the right of the main peak, which without the smaller peak would look more like a normal distribution curve. This led to an analysis of part of data set 10, only considering the points after 1000 seconds, renamed data set 10b in table 3.5.

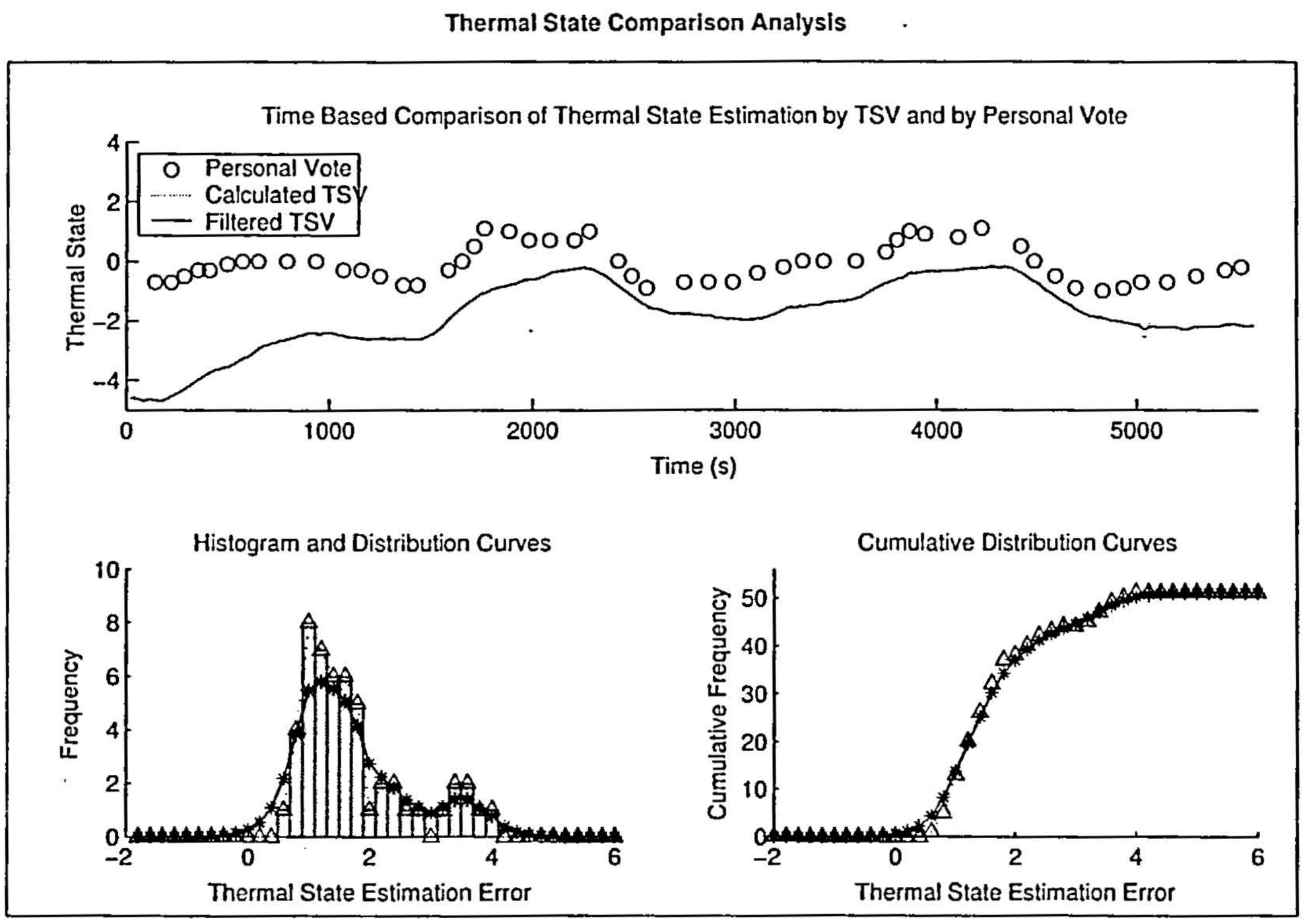


Figure 3.4: Comparison of the TSV thermal state estimate with the personal thermal state vote - test 10

### 3.3.4 Discussion of the TSV Method

#### Discussion of Results

The results presented in table 3.5 show that the worst correlated and highest error variances are data sets 3 and 10. Observations from the time plots in figures 3.3 and 3.4 suggest that these results are not as bad as they appear and that perhaps some initialization problems were the cause. The latter parts of both the time plots look very good. This is a good indication that the variance and correlation values on their own can make a data set appear worse than it actually is. In the case of data set 10 the results were re-evaluated and presented as data set 10b which shows a remarkable improvement in both error variance and correlation just by removing a small section at the beginning of the time plot. This could be done with data set 10 because there appeared to be a jump in the error early on, whereas with data set 3 the error seemed to slowly dissipate.

The rest of the results show good performance with low error variances with respect to the variances of the thermal votes and the TSV estimates and with high correlation values.

| Test Number | Personal Thermal Vote | TSV | Difference (Error) |
|---|---|---|---|
| 03 | 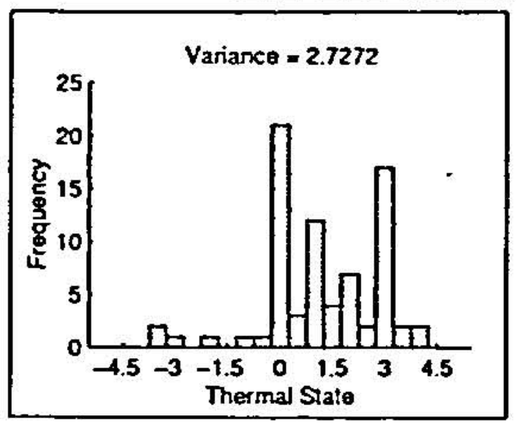 | 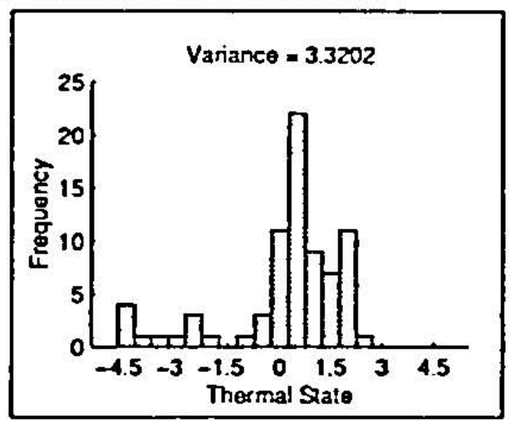 | 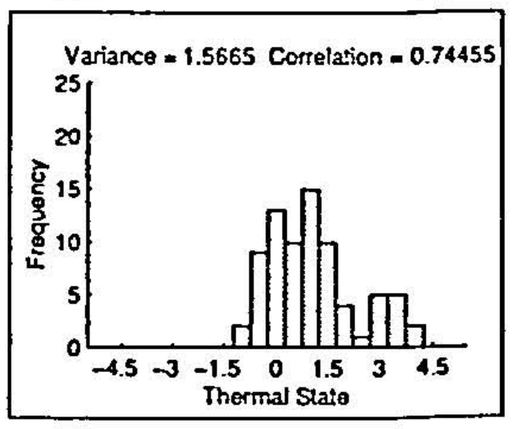 |
| 05 | 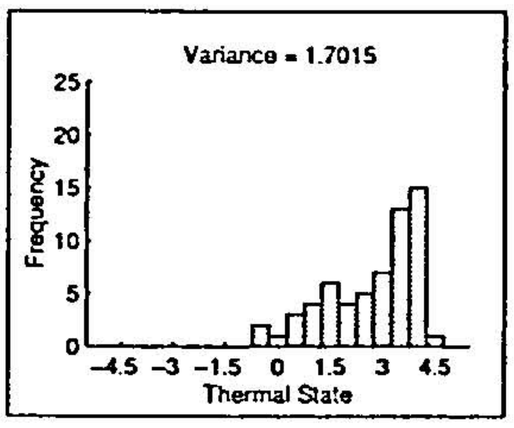 | 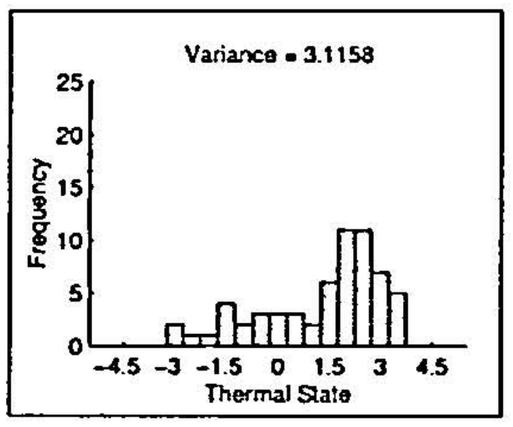 | 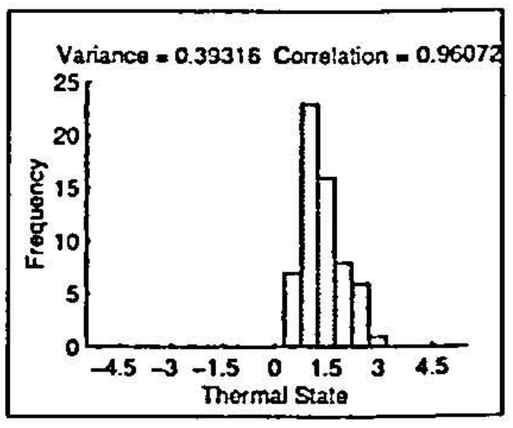 |
| 10 | 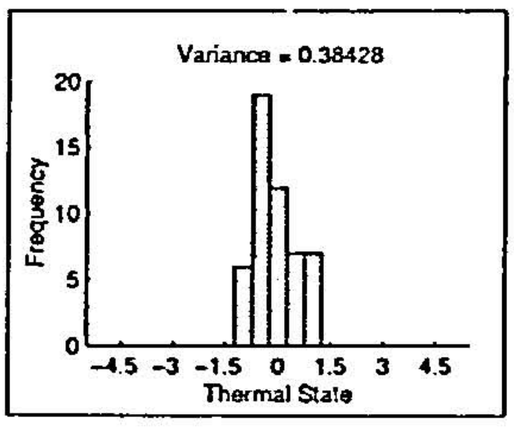 | 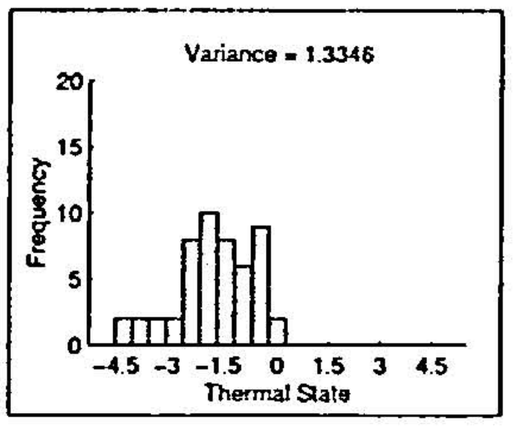 | 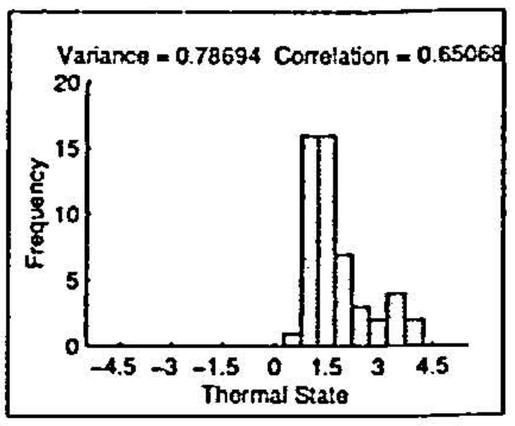 |
| 10b | 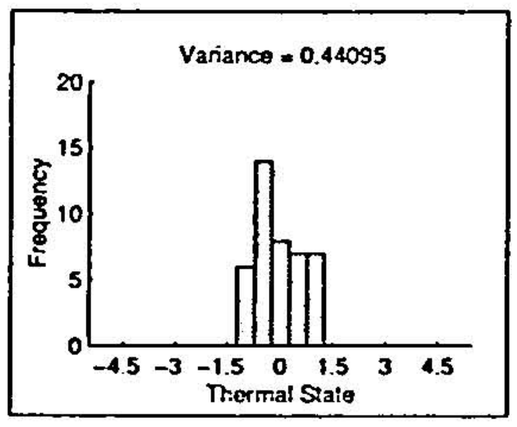 | 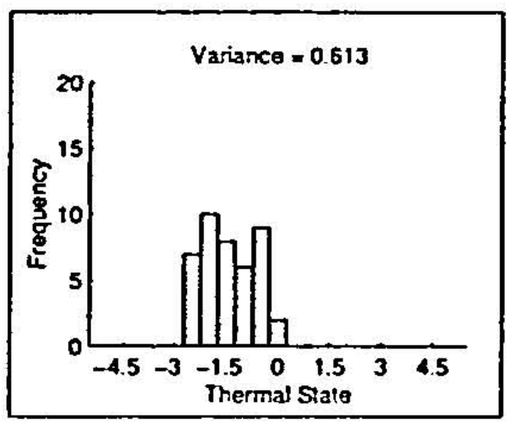 | 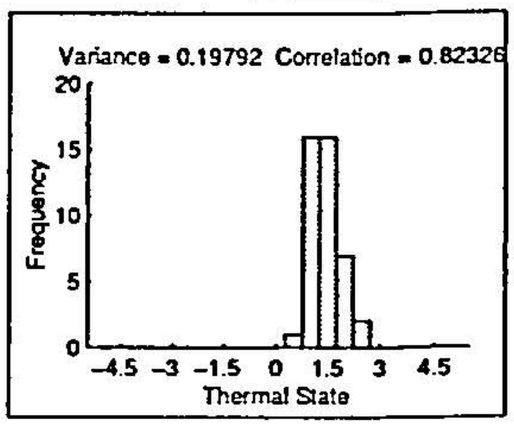 |
| 11 | 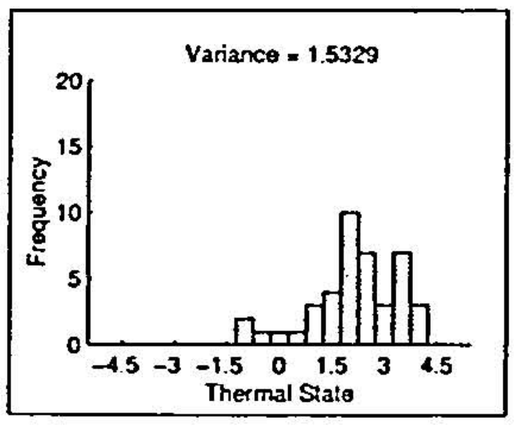 | 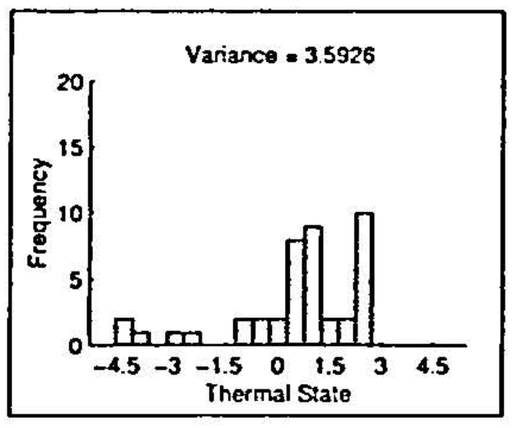 | 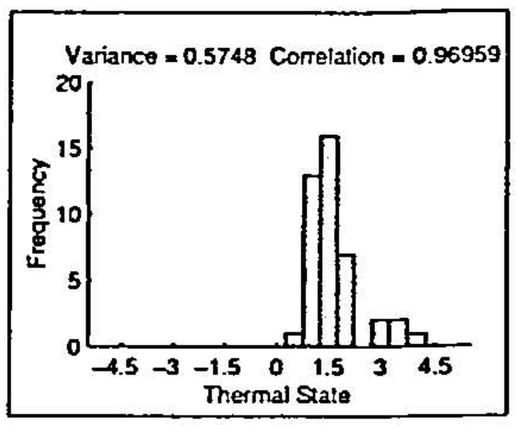 |
| 15 | 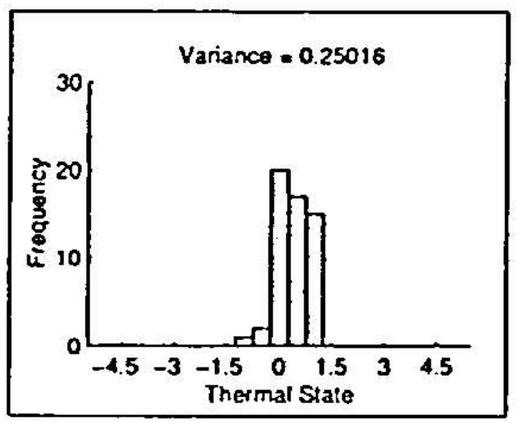 | 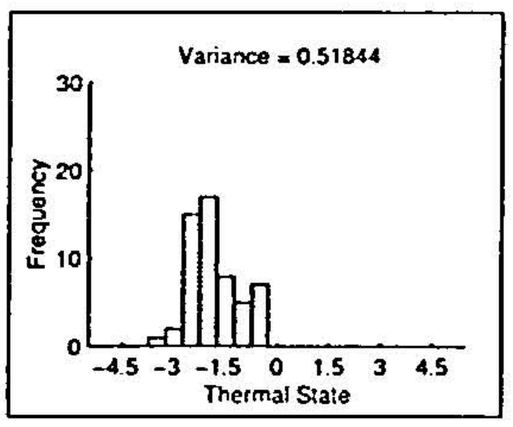 | 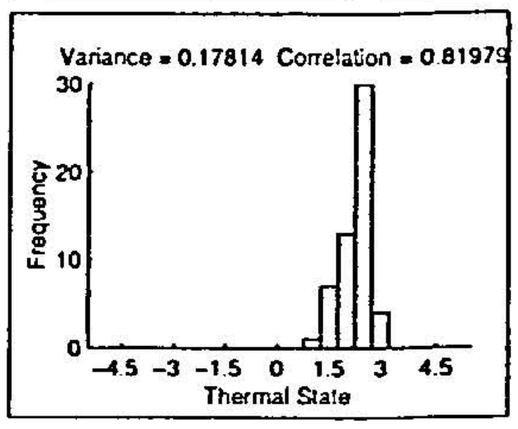 |

Table 3.5: Histogram results of the TSV Estimation Method

### Discussion of Method

The derivation of the second equation (3.12) and its use in calculating a skin temperature reference to control the environment has strong implications on the use of facial skin temperature as a feedback variable for the control of thermal state. This is demonstrated in the second part of the original paper [11]. Results presented in this paper show that the controller is able to maintain thermal state after an initial delay caused by the air conditioner reaching capacity. Tests also included varying the clothing level of the subjects, which did not prove to be a problem for the controller.

The benefit of basing the thermal sensation calculation on the skin temperature is that it is direct and avoids making assumptions about the fluid dynamics within the car and about the intensity of sunlight on the face, etc.

Obtaining the mean facial skin temperature is a prerequisite of this method, which in the automotive application is not yet available. However with the advancement of infrared technology the non-contact measurement of facial skin temperature is possible, yet expensive. The results shown above, from a simple equation and only 3 facial skin temperature measurements, are encouraging and imply the potential of this approach. Combining this method with other measurements from around the car might make this estimation even better.

## 3.4 Neural Network Evaluation

### 3.4.1 Background

Neural networks provide an other interesting approach that current researchers have applied to the task of thermal state estimation (see [38]).

Furuse and Komoriya [28] examined the relationship between thermal state and skin temperature. Mean skin temperature, calculated using the Hardy-Dubois 7 point method, and partial skin temperature were measured. It was found through comparison that outputs from a neural network were closer to the experimental results than a regression calculation. The paper explains that the neural network, with 15 skin temperature inputs, can make use of the temperature distribution pattern, in contrast to the regression calculation using a mean skin temperature only. The paper concludes that neural networks are suitable for the evaluation of thermal comfort and thermal state.

Ueda et al [39] presented a neural network method of predicting thermal sensation based on a mean facial skin temperature. By combining the facial skin temperature history measurement with a history of the internal cabin air temperature as inputs to a neural network structure their results proved that there was no need for measurement of the body skin temperature for accurate control. A plot of temperatures at different positions around the body showed that as the environmental temperature increases from a low value, the abdomen and thigh temperature did not rise with the face temperature but remained at a lower temperature for longer. This makes the subject feel colder and so facial temperature can not be used on its own to predict the thermal sensation. Results showed that with the setting of thermal state reference it was possible to keep the subject from becoming uncomfortable but to achieve a more comfortable state required knowledge about personal preferences.

Another approach to determining skin temperature was investigated in a paper from Ueda et al [40]. The method described in this paper used a neural network based on environmental data to estimate facial skin temperatures and thus avoided the use of thermocouples attached to the skin. This led to the control of thermal state estimated from facial skin temperature, which in turn was estimated from the environmental data. The results were presented in a separate paper [27]. This seems to be a roundabout solution. However, even the PMV method is based around the skin temperature and a heat transfer balance between the subject and the environment. If it is found that the neural network method provides better results in estimating thermal state than a regression equation then perhaps it might also be better at estimating the relationship between the skin temperature and the environmental parameters.

### 3.4.2 How it Works

There are many types of neural network structures with different properties. The predominant methods used in the literature in the prediction and estimation of thermal state is a feed-forward multi-layer perceptron network.

A perceptron consists of a set of weighted inputs which are summed and compared against an internal threshold function as described in figure 3.5.

The multi-layer perceptron structure normally follows a similar profile to the one shown in figure 3.6 where each circle represents an individual perceptron.

The network is a feed-forward network because none of the outputs are immediately returned as inputs. The system knowledge is held in the network via the input weights and it is by

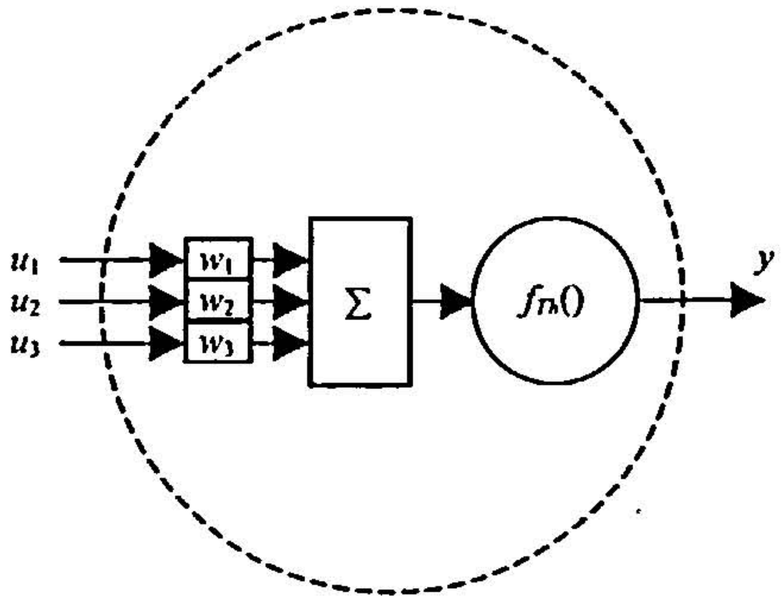


$$y = f_{Th}\left(\sum_i w_i u_i\right) \qquad (3.14)$$

Figure 3.5: The internal workings of a single perceptron

Here, $f_{Th}$ represents the threshold function, $y$ is the output, $u_i$ is the $i^{\text{th}}$ input and $w_i$ is the associated weight for that input.

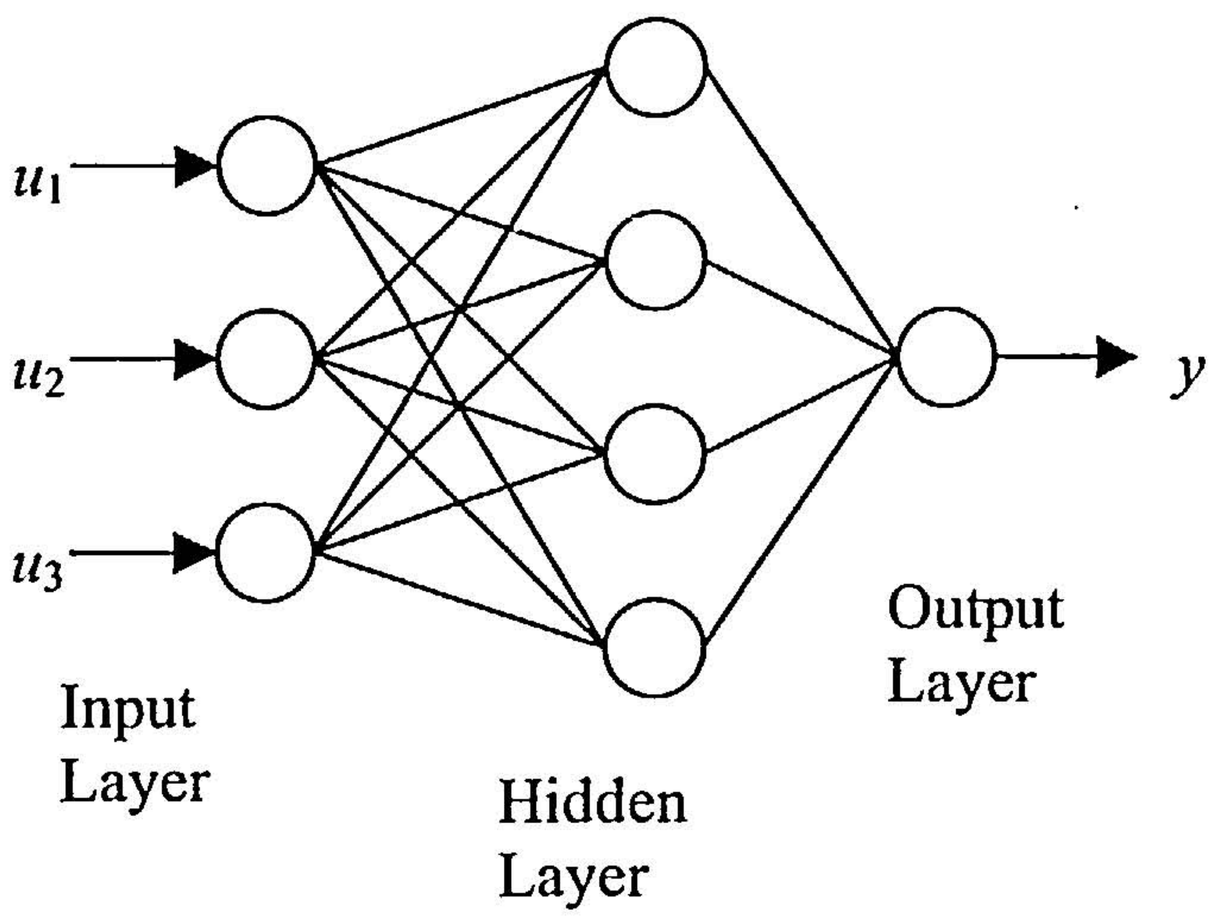


Figure 3.6: A feed-forward multi-layer perceptron with 3 inputs and 1 output

modifying these that the network can be taught. The most common method is called back-propagation. All the weights are initialized with a random value. The threshold functions in each perceptron need not all be the same and it is common to see linear functions in the output layer perceptrons and saturated sigmoid functions in the hidden layers.

The network that was formed to estimate the thermal state to provide results for this section had 5 input temperatures:

- Air temperature at the nozzle outlet
- Air temperature at the face
- Face temperature on the forehead.
- Face temperature on the left cheek under the eye.

- Face temperature on the side of the right cheek.

The network was constructed with one hidden layer with 15 perceptron and 1 output layer with 1 perceptron. The training data was run 500 times from a random selection of weights. The selected training algorithm was the Bayesian Regulation back-propagation method, which updates the weights according to Levenberg-Marquardt optimization and produces a good generalized network. The threshold functions in the hidden layer were hyperbolic tangent sigmoid functions and the threshold function in the output perceptron was a linear function.

The network was constructed, taught and simulated within the MATLAB neural network toolbox, which also provided analysis during training showing the perceived number of useful perceptrons within the network. This was used to iteratively optimize the size of the network.

### 3.4.3 Neural Network Experimental Results

The neural network method specializes in non-linear modelling of systems with certain repetitive pattern behaviour. It is possible to teach a network to estimate the thermal state of any member of the general population. However the correct set of teaching data would have to be compiled in order to provide a good representation of the expected patterns and to generalize out any individual idiosyncrasies. It would then perhaps become directly comparable with the other techniques. The neural network method can make use of parameter properties that other methods find difficult to use, such as the distribution in skin temperature across the face rather than just the mean value.

It is the advantage of the neural network method to find personalization within the teaching data that is of most interest. It is thus proposed that a neural network can be taught to be more accurate than the general methods discussed earlier by learning personal traits in the response. Because of this only 3 of the 5 data sets used earlier will be used in testing this method because the 3 data sets are from the same person.

The results for the neural network approach are presented in figures 3.7, 3.8 and 3.9 and in table 3.6. Data set 5 was used to teach the neural network and so it is obvious that the resulting correlation between the network's output and the measured data set will be good. The noise on the input sensors means that there will be some noise on the output of the neural network, even on the training data. The noise level can be reduced by reducing the number of perceptrons in the layers of the network. This will however mean that the network will have more difficulty in learning the desired behaviour.

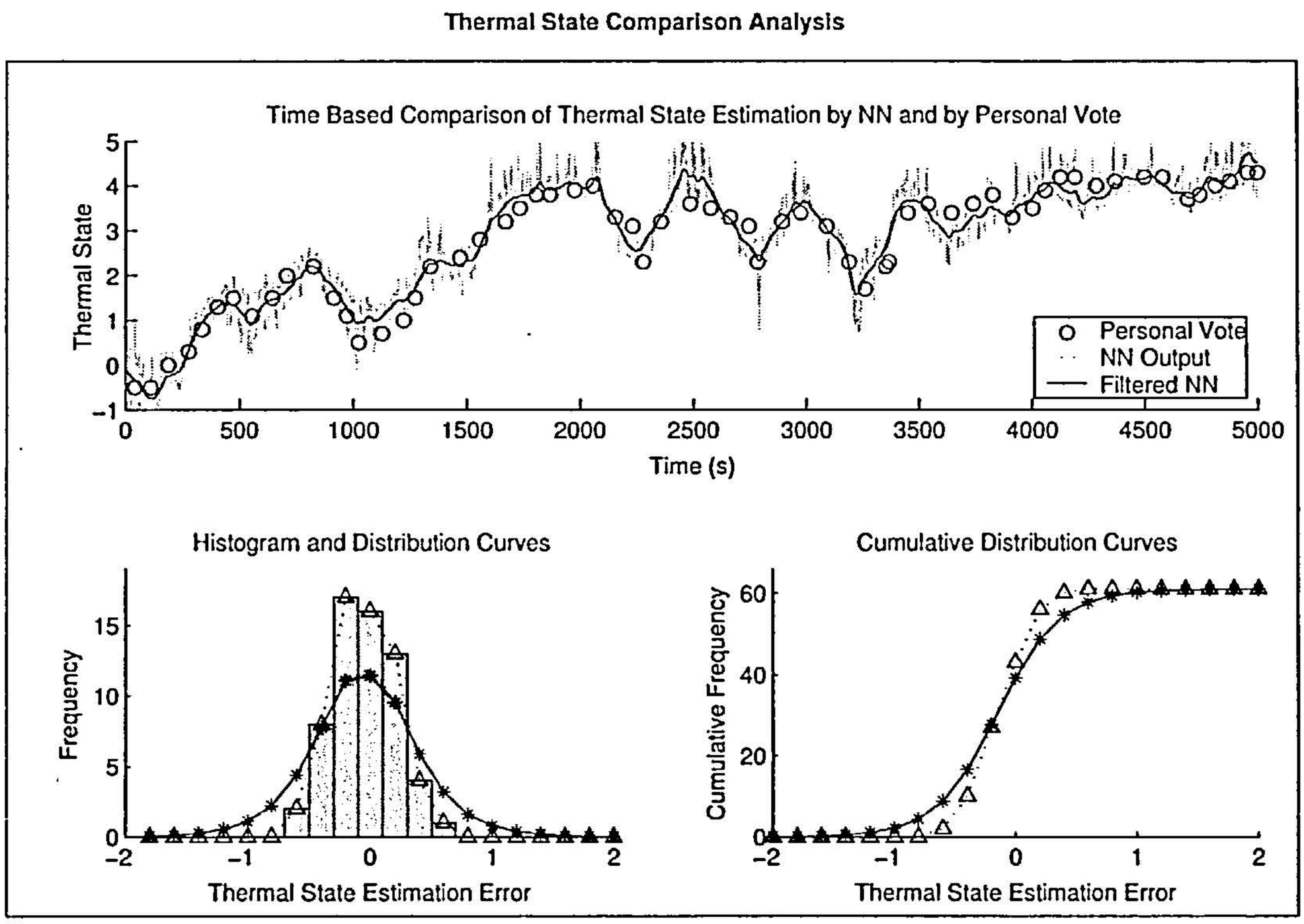


Figure 3.7: Comparison of the neural network thermal state estimate with the personal thermal state vote - test 05 (teaching data)

The small noise level shown in figure 3.7 is acceptable and could be reduced by filtering the noise on the temperature sensors first. Alternatively the output signal from the neural network can be filtered, as shown in the figure (dark line in top plot). The histogram and distribution curves are also less significant as it is expected that error in the signal is due to the noise on the sensors. If the noise is truly random then the curves should assume the normal distribution shape, which they do.

The teaching data (set 5) does not have good coverage of the thermal state estimation at low values. The network only has a few points of thermal state votes at around the 0 mark and nothing lower. It is expected that this will cause problems when applying the network with data set 10, which has many points at 0 and lower. This forces the neural network to extrapolate beyond its teaching data. The weights of the network were randomly selected and when encountering unlearnt inputs the network can not be expected to provide a good response. As can be seen in figure 3.8 the network's response seems to be reluctant to drop below the 0 mark which may be due to limitations in the teaching data.

The neural network response in figure 3.8 is quite interesting, especially in the later half of the test. The error reduces throughout the test the step change just after 3000 seconds is

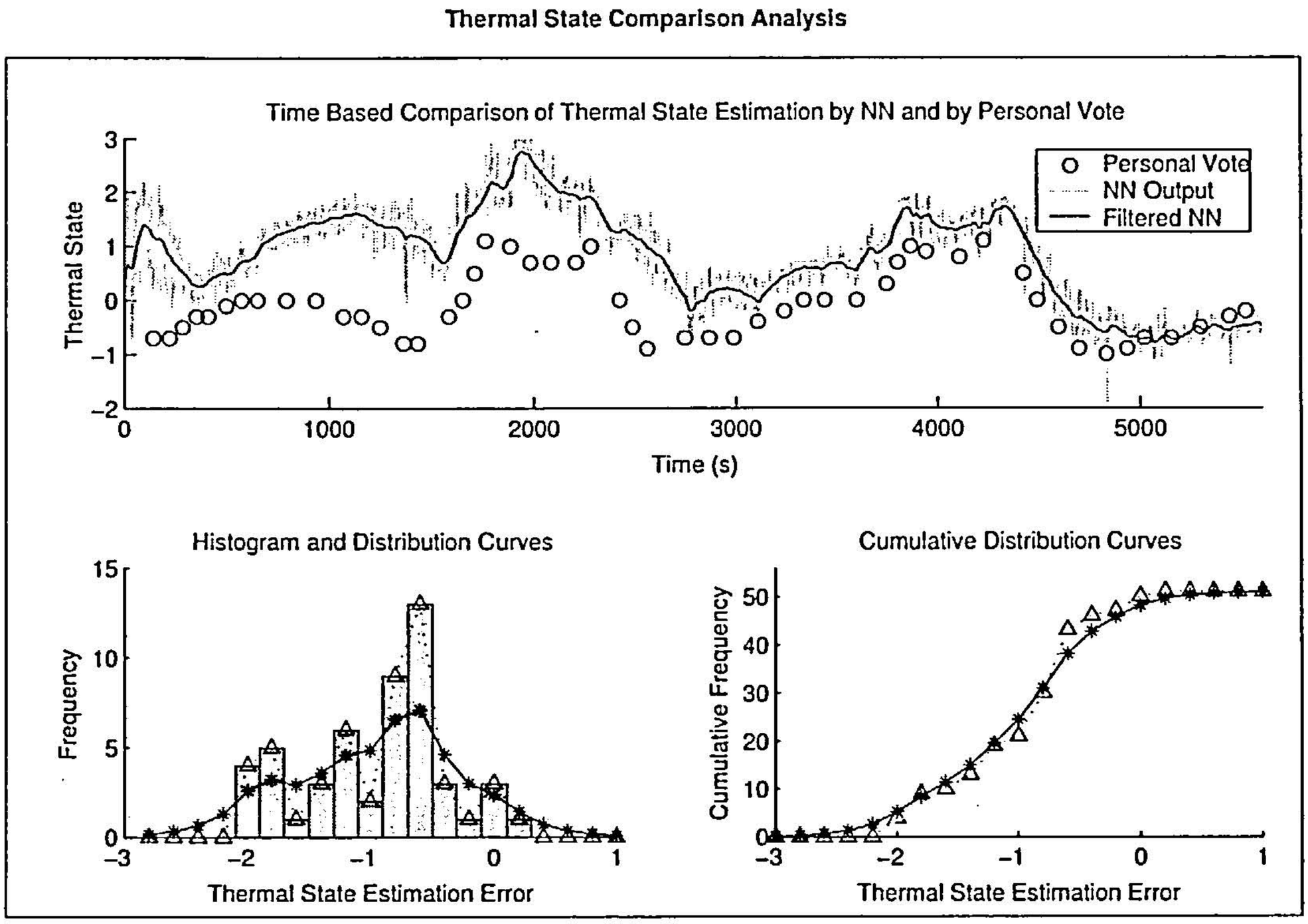


Figure 3.8: Comparison of the neural network thermal state estimate with the personal thermal state vote - test 10

identified and the shape of the second set of peaks, just before and after 4000s, is correctly identified. The network response then follows the thermal state well below the zero mark staying very close to the actual thermal votes.

The third data set provides a more realistic test of the neural network. The result shown in figure 3.9 demonstrate that the network can accurately track the thermal state votes of the subject. The noise levels are certainly worse than those in either the teaching data or in the results from data set 10. The noise on the sensors during this test were slightly worse. However the neural network seems to have been severely affected by the noise which does imply that it has be "over taught".

The histogram and distribution curves seem poor in comparison to the main plot. This is because for each step change in thermal state the neural network response has a different mean error. The fact that the test involves extended periods of similar environments followed by rapid jumps to the next means that the errors will build up and then jump to the next error. Three peaks are seen in the histogram because of this at -1, -0.2 and 0.4. Note that the histogram is based on the unfiltered neural network output.

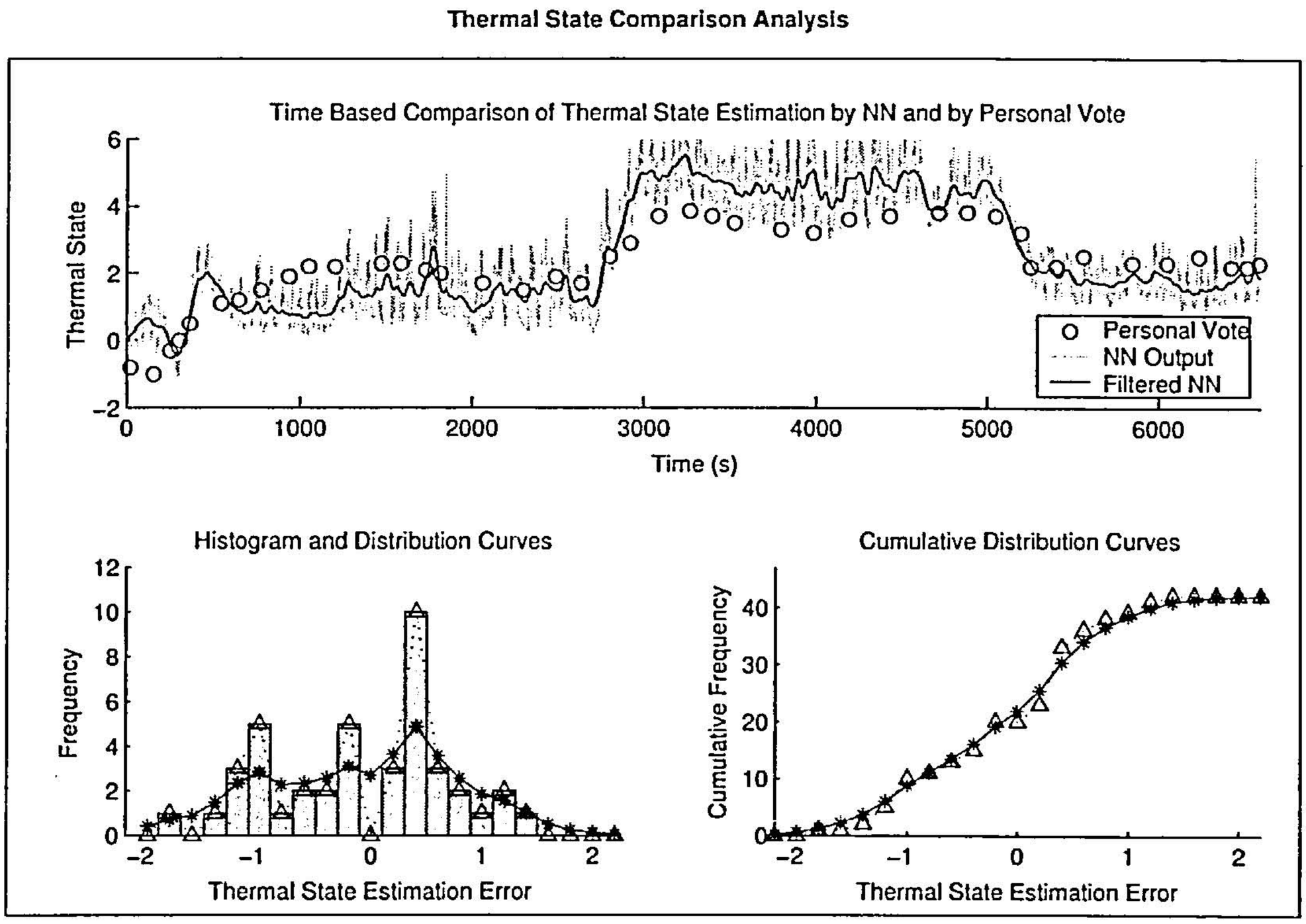


Figure 3.9: Comparison of the neural network thermal state estimate with the personal thermal state vote - test 11

Table 3.6 below helps to verify the discussion points. The histograms of the teaching data shows very few personal thermal votes and neural network votes at 0 and lower. The histograms of the thermal votes in data set 10 show a comparatively large number of votes at around 0. The histogram of the thermal votes in data set 10 is also quite narrow with a variance of less than 0.4. It is still surprising to find the correlation between the neural network output and the personal thermal votes to be as high as 70%. The correlation for the teaching data is expected to be high and at 98% it shows the extent of the teaching. As observed previously the network was prone to noise which is a symptom of over teaching. Perhaps by allowing a greater error in the acceptable correlation of the teaching data the correlation of the other 2 tests could have been improved.

The jumping around of the error in test 11 appears different in the summarised table because of the different sized histogram classes. The neural network response has a clear gap in the data points and the personal thermal votes also show spikes of data points with a gap at 3. The wider histogram classes means that the 3 spikes seen in the earlier error histogram have been reduced to 2 spikes, with offset errors at just above 0 and at -1. The spike at -1 is detrimental to the overall error variance and correlation.

| Test Number | Personal Thermal Vote | Neural Network | Difference (Error) |
|---|---|---|---|
| 05 | 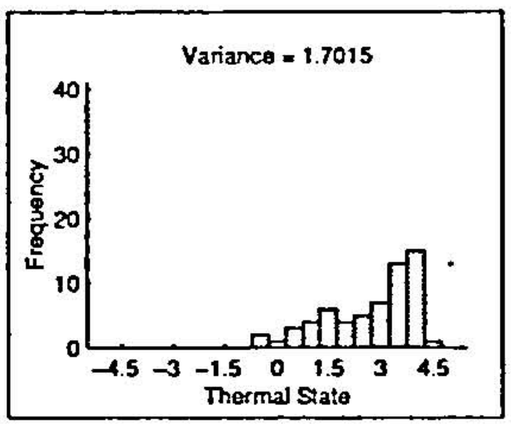 | 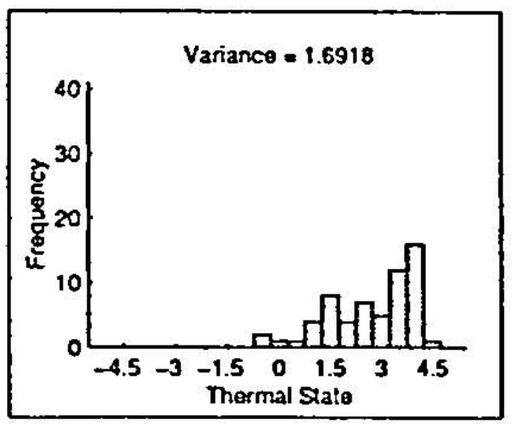 | 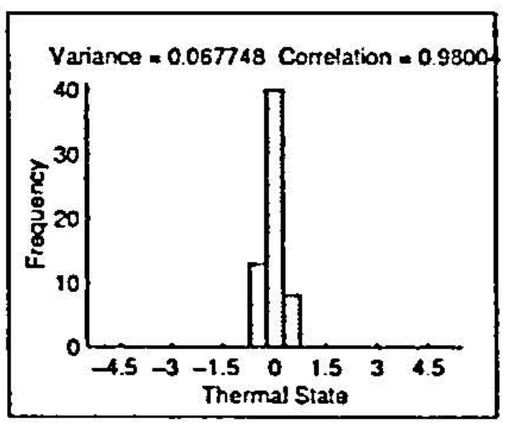 |
| 10 | 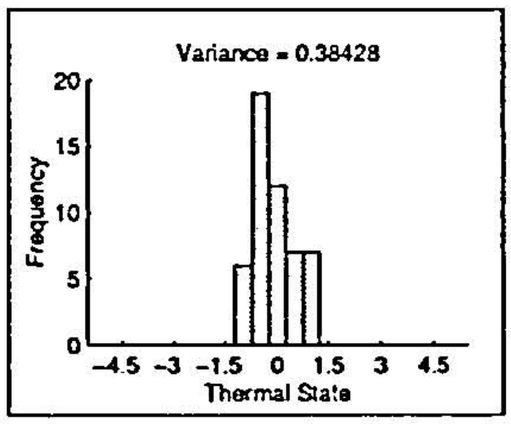 | 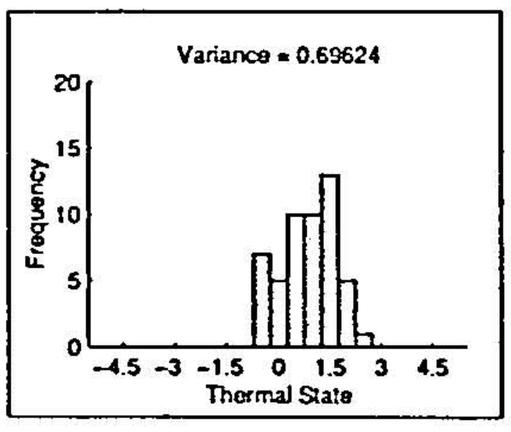 | 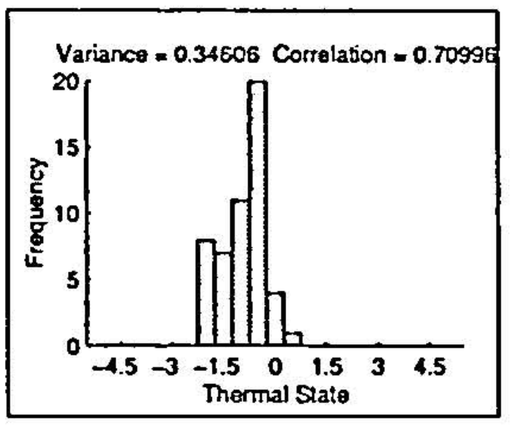 |
| 11 | 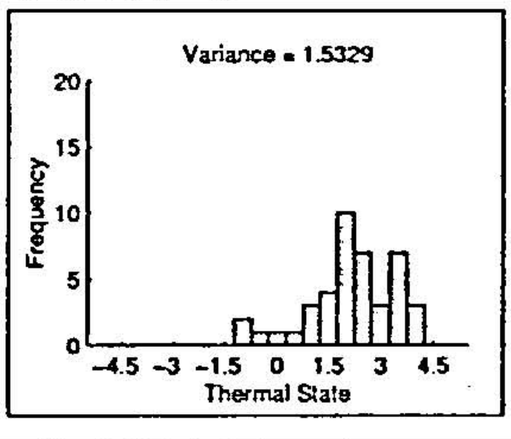 | 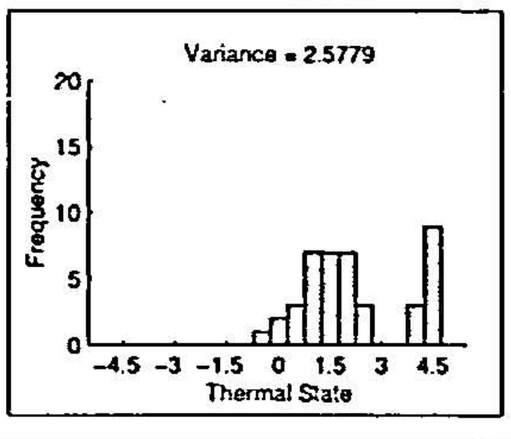 | 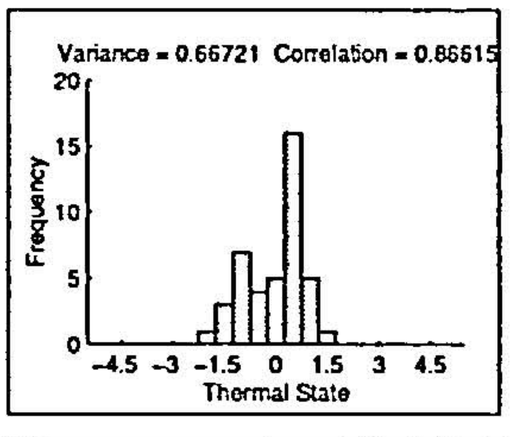 |

Table 3.6: Histogram results of the neural network Estimation Method

### 3.4.4 Discussion of the Neural Network Method

The neural network approach appears to give good results. The expected advantage of using the neural network approach is that it can identify personalization within the teaching data and thus should be more accurate than the other methods – as long as the subjects are consistent in the way they make their personal votes.

Problems with the method start to occur when the neural network is over-taught. The network can start to learn sensor noise behaviour and if the subject is not being consistent then learning the precise voting technique from the teaching data will not cause the network to be more accurate for subsequent tests, in fact this could make the network worse at estimating thermal state.

The general disadvantage of using neural networks is that they require a good teaching data set which will give the controller a basis for interpolation of future input signals. Choosing the correct network structure and relevant input variables is also important in obtaining a

good network. Finally, because the network training is done from an initial state of randomly selected weights, some solutions will be better than others given the same network structure and the same training conditions. All training must be carried out before the network can be used and so if personalization of the thermal state estimation is desired then networks will have to be taught with personalized data sets. This has consequences for its implementation in the automotive application.

## 3.5 Discussion: Direct Comparison of Techniques

### 3.5.1 Variance and Correlation Comparison

A direct comparison of the different thermal state estimation methods is presented in tables 3.7 and 3.8.

Table 3.7 shows the variances in the thermal states of the personal votes and in the thermal state estimation method outputs and the error between the vote and the method output. The variance of the thermal votes and the variance of the method outputs should be similar and the variance of the error of each method should be small.

| Test Number | Personal Vote | PMV | | TSV | | neural network | |
|---|---|---|---|---|---|---|---|
| | | Output | Error | Output | Error | Output | Error |
| 03 | 2.7272 | 2.963 | 0.53612 | 3.3202 | 1.5665 | | |
| 05 | 1.7015 | 4.016 | 0.72129 | 3.1158 | 0.39316 | 1.6918 | 0.067748 |
| 10 | 0.38428 | 1.4596 | 0.56134 | 1.3346 | 0.78694 | 0.69624 | 0.34606 |
| 10b | 0.44095 | | | 0.613 | 0.19792 | | |
| 11 | 1.5329 | 2.0499 | 0.16691 | 3.5926 | 0.5748 | 2.5779 | 0.66721 |
| 15 | 0.25016 | 0.54711 | 0.22895 | 0.51844 | 0.17814 | | |
| $Avg_{all} =$ | 1.172832 | | | 2.08244 | 0.616243 | | |
| $Avg_{prp1} =$ | 1.319208 | 2.207122 | 0.442922 | 2.376328 | 0.699908 | | |
| $Avg_{prp1b} =$ | 1.330542 | | | 2.232008 | 0.582104 | | |
| $Avg_{prp2} =$ | 1.206227 | 2.5085 | 0.48318 | 2.681 | 0.58497 | 1.655313 | 0.3603393 |
| $Avg_{prp3} =$ | 0.95859 | 1.75475 | 0.364125 | 2.4636 | 0.68087 | 1.63707 | 0.506635 |

Table 3.7: Direct comparison of the variance in different thermal state estimation methods

$Avg_{all}$ is the average of data sets 3, 5, 10, 10b, 11 and 15
$Avg_{prp1}$ is the average of data sets 3, 5, 10, 11 and 15
$Avg_{prp1b}$ is the average of data sets 3, 5, 10b, 11 and 15
$Avg_{prp2}$ is the average of data sets 5, 10, and 11
$Avg_{prp3}$ is the average of data sets 10 and 11

All but one of the thermal state method outputs shows a variance greater than that of the subject's personal vote and the exception is the neural network's response to its teaching data. This suggests that the thermal state estimation methods are all more sensitive to their inputs than the test subjects. This needs to be confirmed from the time domain plots but the variance is a good indication.

The variances of the errors in table 3.7 show that all but one are below 0.8. This gives a good indication of the overall accuracy of the methods and can be used to design performance criteria in future control strategies. In terms of using the variance of the errors to cross compare the different techniques there is no clearly superior method. The PMV method seems to be better on test 3 and 11 while the TSV method is better on test 15. The neural network approach shows good results on tests 5 and 10 but then test 5 was its training data. As discussed earlier the TSV approach does display good properties in part of test 10 (renamed test 10b) with a very low error variance.

The variance of the error was not the only calculated value and the correlation between the thermal state votes and the thermal state method outputs was also presented for each of the methods. These have been collected into table 3.8 below:

| Test Number | PMV Error | TSV Error | neural network Error |
|---|---|---|---|
| 03 | 0.90656 | 0.74455 | |
| 05 | 0.95565 | 0.96072 | 0.98004 |
| 10 | 0.85626 | 0.65068 | 0.70996 |
| 10b | | 0.82326 | |
| 11 | 0.9635 | 0.96959 | 0.86615 |
| 15 | 0.7681 | 0.81979 | |

Table 3.8: Direct comparison of the correlation in different thermal state estimation methods

The correlation results show a good overall performance from all the methods. The lowest PMV correlation is 77% which is higher than the lowest of the other 2 methods. In terms of the correlation, the PMV method was the best method for tests 3 and 10. The neural network only provided the best results from its training data and even then the other methods also provided excellent results. The TSV method gave the best results in tests 11 and 15 but also provided the worst correlation of the 3 methods at 65% in test 10. Only looking at part of test 10 (renamed test 10b) the TSV is improved but still is not better than the PMV method calculated for the whole of test 10. The overall comparison would suggest that none of the methods has a clear advantage but that the PMV method has provided marginally better results for the test data used.

### 3.5.2 Method Implementation Comparison

The neural network was expected to be the most accurate since it was expected to learn the personal thermal state estimation patterns of the test subject. It was found that the noise on the temperature sensors started to impair the results of the network before it could learn sufficiently to perform better than the other 2 methods. The neural network provided the smallest error offset and in that respect was the most accurate method. There is evidence that the network was slightly over-trained but the results indicate that its performance was still comparable. Perhaps by pre-filtering the sensor inputs and with additional fine tuning the performance could be increased. The main disadvantage with this technique, in comparison with the other methods, is that it requires a lot of off-line training with a suitable data set. It might be argued that the fact that the neural network was just as bad as the other methods on non-trained data sets might suggest that this is due to variance in personal thermal state estimation by the test subject.

The PMV is a standard method used mainly in buildings and is based on air temperature, air velocity, air humidity, solar gain, activity rate and clothing level. The PMV method was derived using assumptions of steady state and so is not so dependable in variant conditions. It also requires a lot of information about the environment which is not always available. In this test air humidity, solar gain and activity rate were assumed to be constant throughout the test and were given estimated values. The air velocity and clothing level were constant throughout the test which means that the PMV value depended entirely on the air temperature measured at the face of the subject. The is not a strong representation of the full method. However, the use of tables for estimating input parameters did result in fairly accurate correlation and variance results. The output offsets with the actual thermal votes were the largest for this method but then the documentation on this technique suggests that one hour averages should be taken (this was not done).

The TSV value relies on facial skin temperature only - it does not require a lot of previous knowledge about the subject (as the PMV method does) and it does not require training as the neural network method does. With the presented test results there are offset differences between thermal vote and the TSV output. However, the variance and correlation results suggest an acceptable level of accuracy.

## 3.6 Conclusions

Three methods of thermal state estimation have been tested on data collected from chapter 2. The test results show that none of the methods are better than the others in terms of performance. The average variance of the error is below 0.7 and is only this high because of one bad test result, which appears to be affected by some initialization problems. The average variance of error from the PMV is the lowest (below 0.5) which is good considering that it is being applied to a turbulent transient environment. It also means that it is possible with good control to maintain the British Standard of acceptability of the environment for thermal comfort (maintaining the PMV within $\pm 0.5$ of the neutral level).

The number of test results presented in this chapter is small and on there own are not enough to provide verification data for the methods involved. The aim of this chapter was not to test each of the methods individually. Each method has already been published and has been verified by the authors and by other researchers in the same field. The results presented here help to confirm and to complement these previous results. The main aim of this chapter was to compare the implementation of each of the methods. In this respect it is quite fortunate that the three methods provided similar performance. This means that the effort involved in setting each method up can be compared more directly.

In concluding this chapter it was found that the TSV method was the easiest to set up and to implement. It required a set of facial skin temperature sensors and consisted of a single regression equation which required no pre-test values. The PMV method was also fairly easy to program when given the code listing in the British Standard. The algorithm does use an iterative loop which is more processor demanding than the TSV method. The PMV method also required pre-test information such as the clothing resistance and activity level of the test subject. The PMV method uses a more diverse set of inputs, which may require a more extensive set of sensors (such as a humidity sensor and solar gain sensor). In some automotive applications, however, these required sensors may already exist for other applications. The neural network approach required the most work in setting it up due to the fact that it requires a training data set and then needed to be taught. The neural network can be set up in different ways with different sensors and in this respect is more flexible than the other methods. From the test results it appears that for the extra effort in applying the PMV and neural network methods there is no real gain in performance of estimation.

# 4 Control of Thermal Sensation Vote in a Car

The aim of this chapter is to address the application of climate control to the automotive cabin. This chapter extends the TSV thermal state estimation method, presented in chapter 3, in a novel way and introduces thermal state control in the automotive cabin. A plant model was identified between the desired air temperature input to the car's HVAC controller and the actual cabin air temperature. A second model was identified between the desired air temperature and the subject's calculated TSV value. A 3$^{rd}$ order model with a 30 second sample time was chosen for the air temperature model and a 3$^{rd}$ order model with a 20 second sample time was chosen for the TSV model. A state-space controller was synthesised using a pole-placement technique and used to control the air temperature and the test subject's calculated TSV value. The results show good control of the air temperature and the TSV value. The control model for the TSV controller was rigorously designed to be satisfactorily fast and, consequently pushed the system too hard resulting in saturation of the desired temperature signal. The local HVAC control, for the sake of thermal comfort, would not allow the foot area to become too cool and thus inhibited the cooling of the subject's feet.

This chapter contributes and verifies a thermal state control method using the TSV estimation. It proves feasibility of the control of thermal state using a linear state-space controller.

## 4.1 Introduction

### 4.1.1 Aim of the Chapter

In this chapter the the application of thermal state control in the automotive cabin environment will be directly addressed. Parallels can be assumed between the experiment in chapter

2 and the real application. However for a better realization of the aspects involved an experiment was set up using a Mercedes-Benz S-class test car. The experiments carried out in the test car were intended to extend the work of chapter 2 and include the TSV method described in chapter 3.

The aim of this chapter is to investigate the control of the Thermal Sensation Vote (TSV), using facial skin temperatures, developed by [25], in the automotive application. The linear relationship of the TSV to mean facial skin temperature and the intriguing prospects of determining facial skin temperature through infrared technology motivates the development of this control technique for the automotive application. The choice of using the TSV estimation is purely pragmatic and demonstration of the control of the TSV illustrates that control of thermal state, estimated by any means, is feasible.

Additionally, control issues will be examined for certain demands on the automotive HVAC system. Since the ultimate effect of a change in the outputs of the HVAC system is to modify the user's thermal state value, demands on the system can be interpreted as changes in desired thermal state of the person. It is very difficult to show the reasons why someone's personal desired thermal state changes since there are many trigger variables and most are abstract, non-measurable and have little, if any, influence on the estimates of thermal state. It is expected, however, that influencing factors will result in a desired shift in thermal state and thus what will be examined is not just the actions by the controller to maintain a neutral thermal state but the actions that move away from a neutral level also. Thus it is logical that the input to the controller should be a reference thermal vote.

It is believed that the control of the TSV in the manner presented in this chapter is a new approach and this work has been presented as a conference paper [41].

## 4.2 Experimental Setup

The test car was a Mercedes-Benz S-class with a built-in Power PC linked to the Control Area Network (CAN) bus on which the climate control elements communicated. Temperature sensors were connected to the input channels of the power PC's AD card. The temperature sensors were the same as those explained in section 2.2.2 and were set up in the same manner as described earlier. During the experiments data were recorded from the sensors and from the CAN bus every second. The temperature sensors were used to measure the 5 skin temperatures from the test subject's face, and an air temperature from close to the subjects face. Additional information from the car's own sensors was recorded from the CAN bus,

which included air temperature measured from a sensor located close to the rear-view mirror, outside air temperature, Engine coolant temperature and information from the solar sensor.

A photograph of the internal view of the front of an S-Class's passenger cabin is presented in figure 4.1. The photographs shows the central air vents and the side air vents.

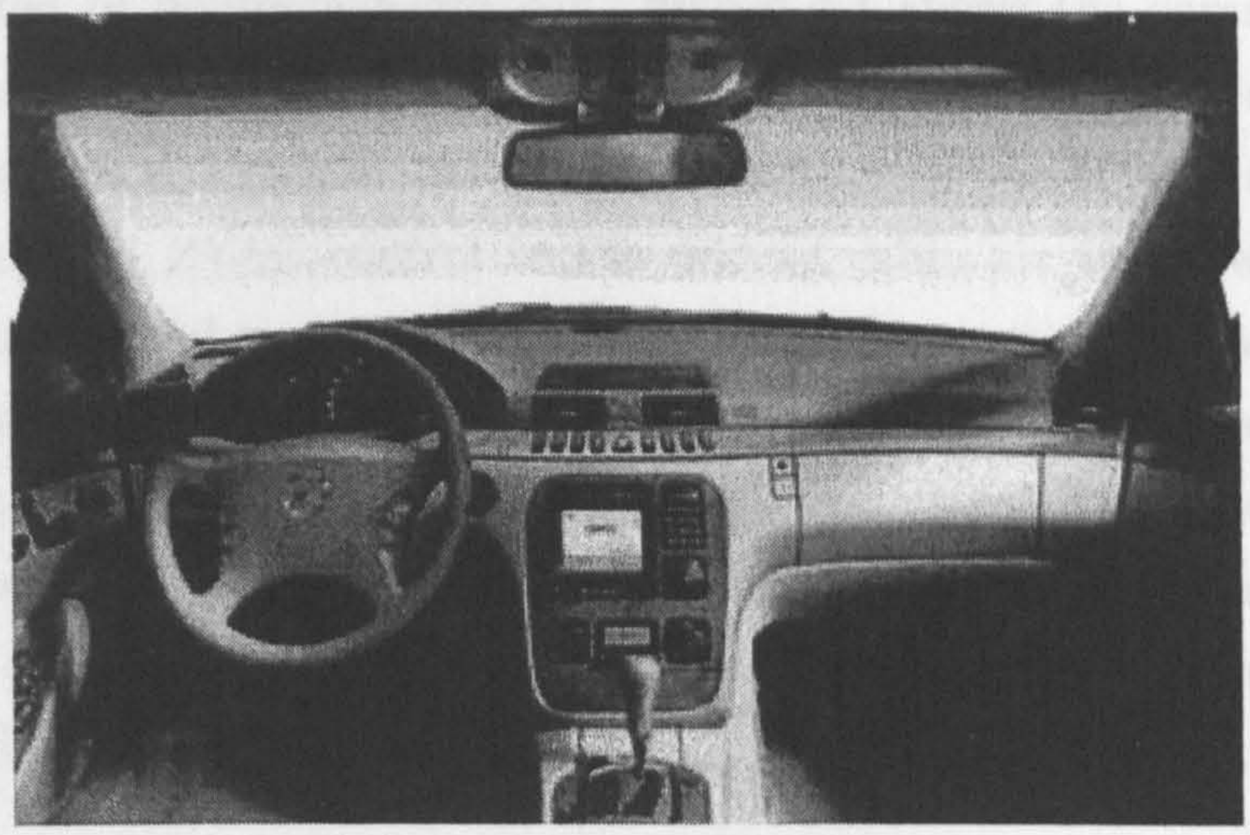

Figure 4.1: Inside the passenger cabin of a Mercedes S-Class

In addition to these there were air outlet vents for the driver and front passenger's foot compartments, an air outlet for the windscreen, and a side and central air vent for both the rear seated passengers. All 4 passenger could individually select different desired air temperatures and the passengers in the back of the car could select a different air flow rate to the people in the front of the car.

During the experiments in the car the rear air vents were deactivated and the driver and passenger's desired air temperature were tied and operated as one value. The test subjects sat in the drivers seat and were asked to adjust the seat position as they would in order to drive the car. The test subjects were all male aged between 22 and 30 and in good health. A test administrator sat in the front passenger seat. The car's engine was switched on but the car remained stationary for all the tests.

During all of the experiments the subjects were quizzed on their thermal sensation and asked to vote for themselves. Their inputs were recorded by use of a touch screen display which was directly linked to the power PC. The display was programmed to allow a value with one decimal place to be submitted and the test subjects were asked to be as accurate as they could be. Each submission was logged by the power PC with the corresponding time value.

## 4.3 Method

This part of the investigation consisted of two main stages: identification experiments and closed loop control experiments using a linear state-space controller. In this chapter 2 models will be presented and used to synthesize controllers. A diagram of the 2 closed loop control systems is presented in figures 4.2 and 4.3. Figure 4.2 shows the control of the cars air temperature (measured at the rear-view mirror). The desired air temperature value is the same as the value selected by the user at the interface of the HVAC system and is not interpreted by the local HVAC control as the desired cabin air temperature thus a state-space controller was needed to control this. This control test was done for comparison with the work from chapter 2. The diagram in figure 4.3 shows the identification of everything between the input of desired air temperature and the calculated TSV value. Looking at the amount of disturbance injected into the air temperature controlled system will give a good indication of the amount of disturbances that come from the HVAC block (and the cabin environment) in the control of the TSV system.

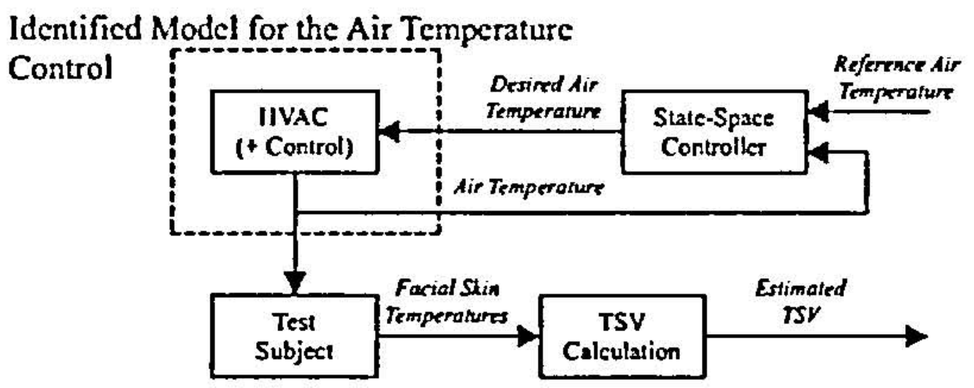


Figure 4.2: Components of the closed-loop systems for controlling the air temperature

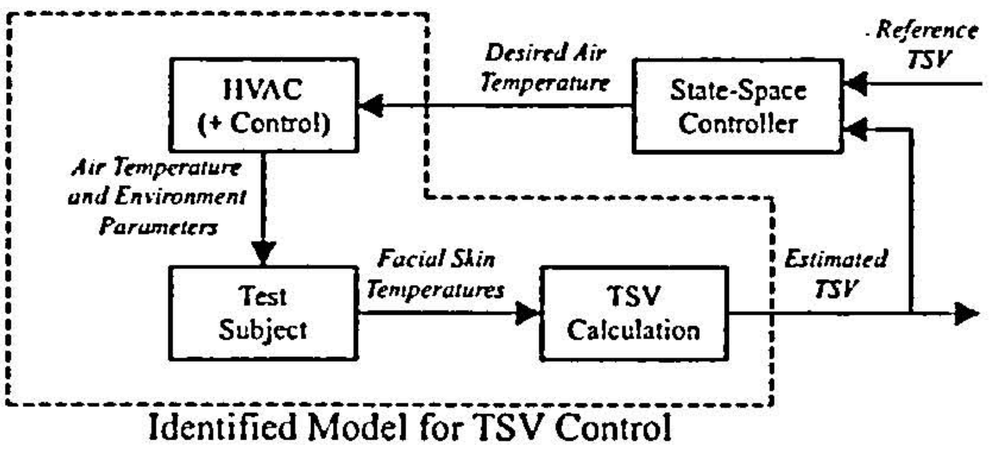


Figure 4.3: Components of the closed-loop systems for controlling the TSV

Skin temperature measurements were used to calculate an on-line TSV estimation which was then fed back in to a state-space controller. The state-space controller output a desired air temperature which was controlled by the local HVAC controller.

The HVAC control algorithm is a sophisticated technology that determines which vents are

open or closed, the actual outlet temperature and the air flow rate at each vent. The algorithm interprets interactions and decides on the best way to achieve the desired effect. The automatic channelling and mixing of the air to different outlets by the car's own controller was left on to reduce the non-linear aspects of the overall system. The desired air temperature to the local HVAC control unit is not meant as a reference for the temperature of the cabin air. The local HVAC control unit does not take this input literally and interprets the desired air temperature (along with the current value of the other HVAC settings) as a desire for a particular type of environment. Thus the local HVAC control unit delivers different air temperatures to different vent outlets in an attempt to provide the driver or passenger with the desired environment.

To speed the experiment up and to avoid variations in dead-time and rise-time the automatic flow rate control was deactivated and set as a constant (level 3).

### 4.3.1 TSV Calculation

The on-line TSV calculation was based on the method described in section 3.3. However, in this experiment more sensors were available for measuring the facial skin temperature and so 5 measurements around the face, as illustrated in figure 4.4, were used in the estimation.

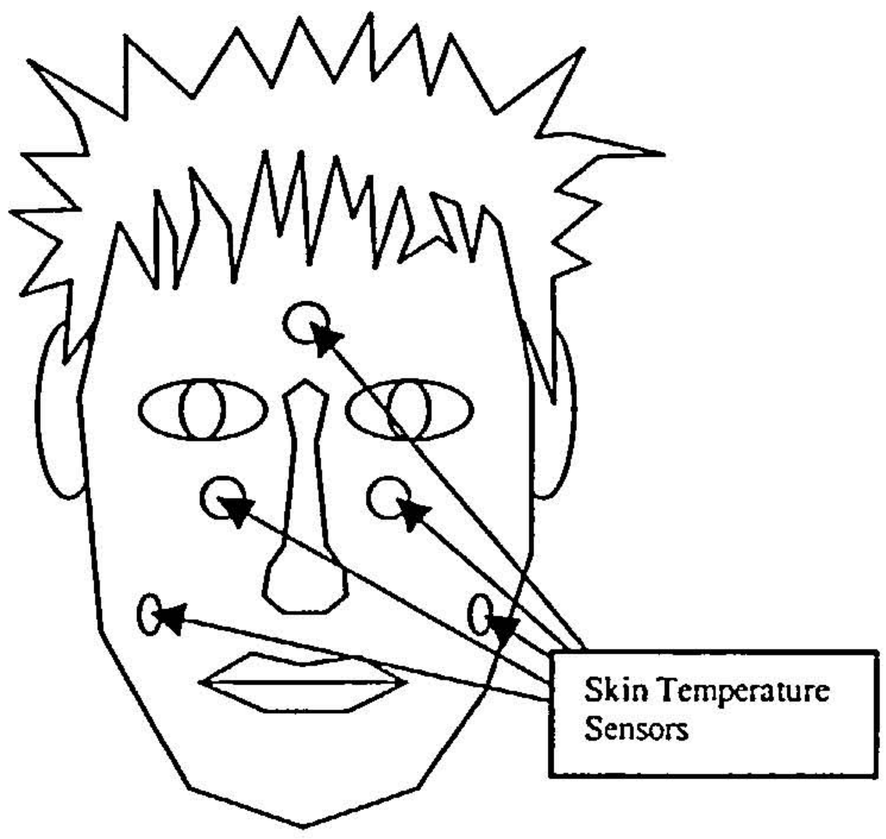


Figure 4.4: Placement of the facial skin temperature sensors

### 4.3.2 Identifying A Model

A PRBS input was used to identify the dynamics of the plant. There are 2 models of interest. The first is the internal air temperature of the car cabin to compare with the experiment

done in chapter 2. The air temperature was measured from the car's own sensor located in the rear-view mirror housing. The second model to be identified is the TSV estimate directly which includes the air dynamics and human physiology.

As seen in figure 4.5, a maximum length PRBS was used as the input of the open loop system. The input is the desired temperature setting - upper plot, dotted line. The internal air temperature in the cabin was measured, upper plot black line, and the skin temperature of the user's face was recorded, upper plot grey line. The TSV value, lower plot grey line, was calculated on-line from the facial temperature measurements and was validated by the thermal votes submitted by the user, lower plot circles.

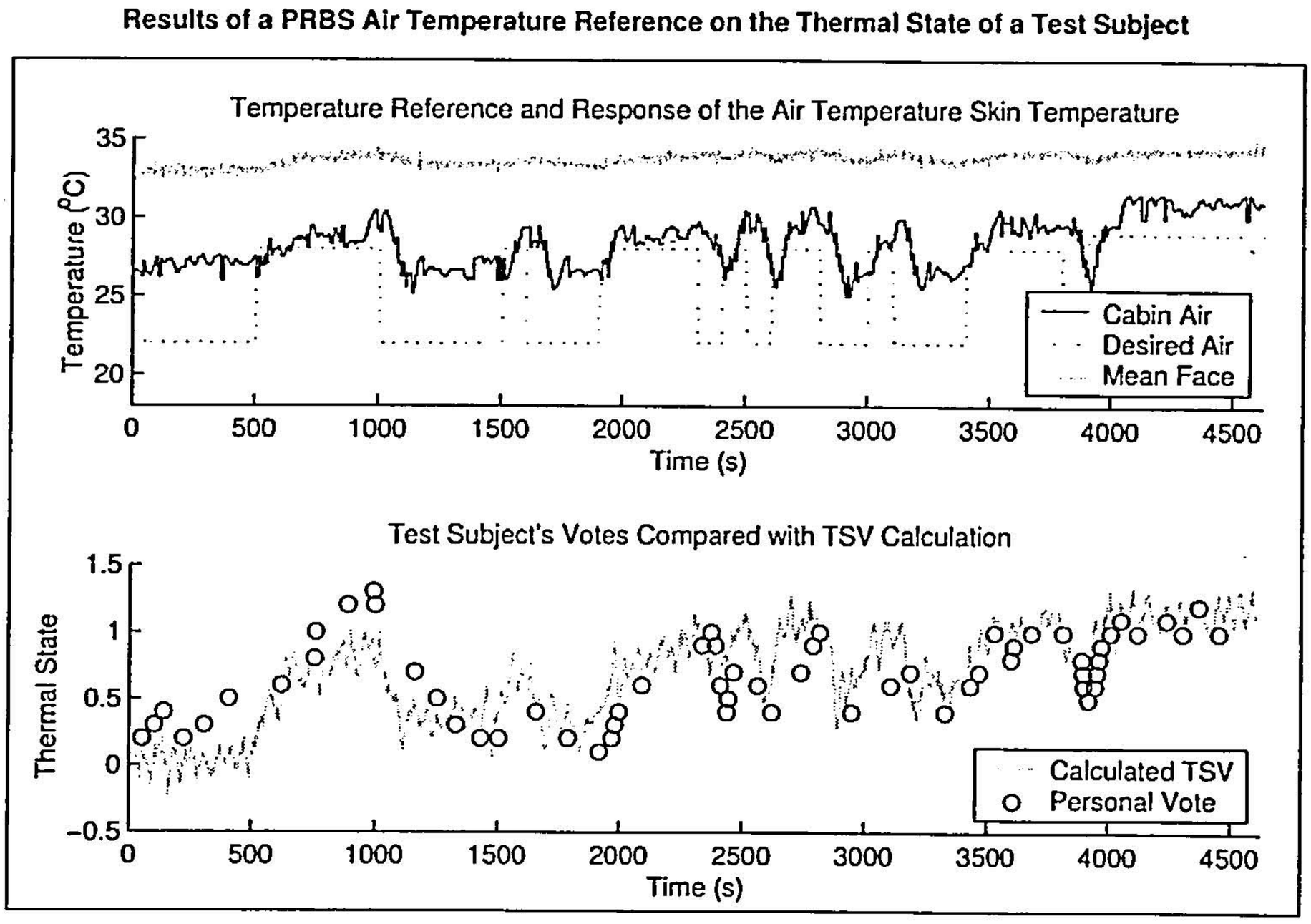


Figure 4.5: Identification of TSV from HVAC air temperature reference with a maximum length PRBS input

The means and trends were removed from the data and again the "ident" tool in MATLAB was used to find an ARX model by the least squares method. Models were compared and cross-referenced with data from different subjects to find the best model overall. A 3rd order model with a 30 second sample time was selected for the air temperature sensor and a 3rd order model with a 20 second sample time was selected for the TSV output.

By representing the identified models by polynomials as in equation (4.1)then equation set (4.2) represents the model identified for the air temperature and equation set (4.3) represents the model identified for the TSV value:

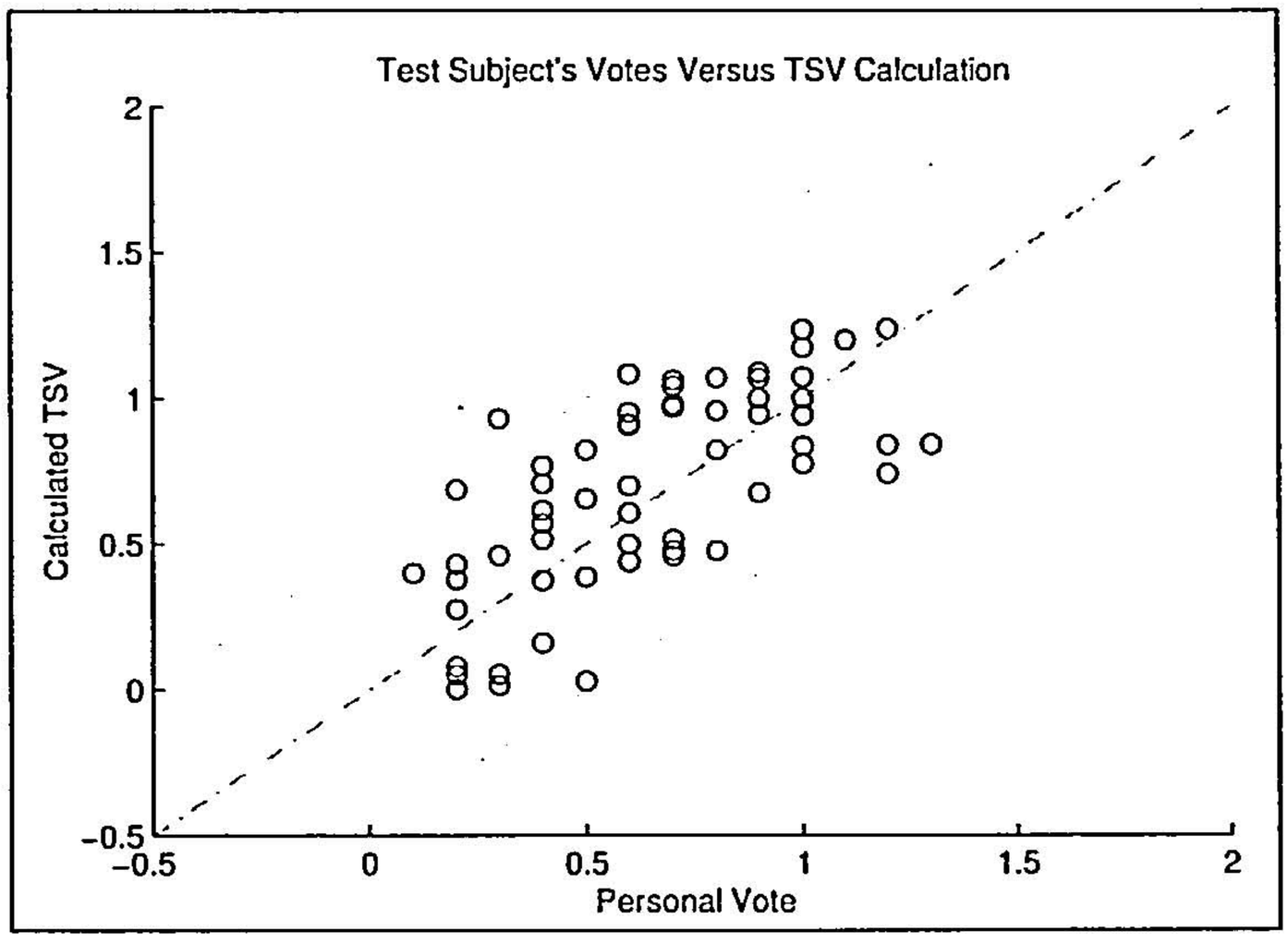


Figure 4.6: Comparison of thermal sensation estimated by the subject and calculated during identification

$$A(z^{-1})y_p(t) = B(z^{-1})u_p(t) + e(t) \tag{4.1}$$

Equation (4.1) is the same as equation (2.3) presented earlier but with an error term added. Thus $A(z^{-1})$ and $B(z^{-1})$ are polynomials with a z-transform argument, such that the transfer function of the system is $\frac{B(z^{-1})}{A(z^{-1})}$. The plant input and output at time $t$, are $u_p(t)$ and $y_p(t)$ respectively.

$$\begin{aligned} A(z^{-1}) &= 1 - 0.5283z^{-1} + 0.03598z^{-2} + 0.05264z^{-3} \\ B(z^{-1}) &= 0.5283z^{-1} - 0.03598z^{-2} - 0.05264z^{-3} \end{aligned} \tag{4.2}$$

$$\begin{aligned} A(z^{-1}) &= 1 - 0.2928z^{-1} - 0.2927z^{-2} - 0.2236z^{-3} \\ B(z^{-1}) &= 0.006119z^{-1} + 0.01921z^{-2} + 0.005697z^{-3} \end{aligned} \tag{4.3}$$

## 4.4 Controller Synthesis

The control design is standard state-space theory and is taken from [29]. Consider the plant described in discrete state-space format (in the reachable canonical form):

$$\begin{aligned} x_p(k+1) &= \Phi_p x(k) + \Gamma_p u_p(k) \\ y_p(k) &= C_p x_p(k) \end{aligned} \tag{4.4}$$

Here $x_p(k)$ is the state vector of the plant a time sample $k$ and $\Phi_p$, $\Gamma_p$ and $C_p$ are the discrete versions of the state-space Matrices.

A simple closed loop control method can be described by:

$$u_p(k) = L_c u_c - L_p x_p \tag{4.5}$$

Here $u_c$ is the controller reference, $L_c$ is a scalar multiplier and $L_p$ is a vector multiplier. It is the aim of the control synthesis to determine the values for $L_c$ and $L_p$. This control law can be visualized in figure 4.7:

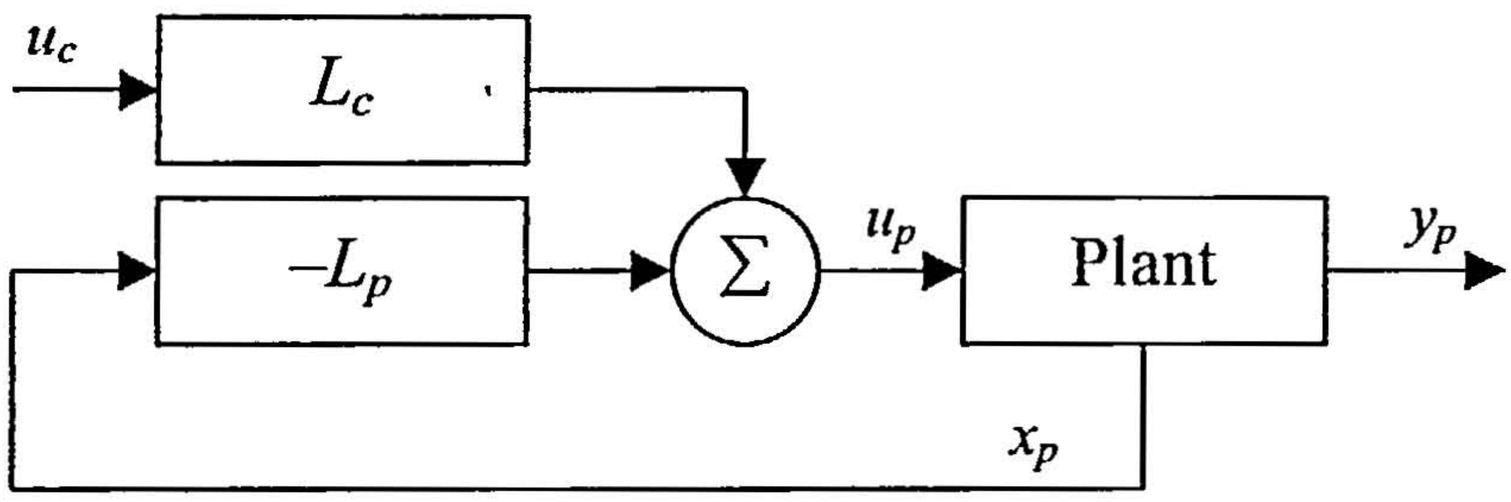


Figure 4.7: A simple state-space controller

$L_c$ is a scalar value and is chosen to force the steady state gain of the closed loop system to be 1 by solving the difference between the final value theorem and the desired final value $u_c$.

In order to find $L_p$ the plant must be reachable - the Controllability Matrix needs to have a rank $= n$, where $n$ is the order of the system.

Controllability Matrix of the plant: $W_{cp} = \begin{bmatrix} \Gamma_p & \Phi_p\Gamma_p & \dots & {\Phi_p}^{n-1}\Gamma_p \end{bmatrix}$

The vector $L_p$ can be found using Ackermann's Formula:

$$L_p = \begin{bmatrix} 0 & \dots & 0 & 1 \end{bmatrix} {W_{cp}}^{-1} P_p(\Phi_p) \tag{4.6}$$

Where the function $P_p()$ is a polynomial with roots representing the poles of the desired characteristic polynomial of the plant response.

When the internal states of the plant are unmeasurable then an observer has to be used to estimate the state values. The observer can be formed with an extra state $\nu(k)$ to provide integral action, see equation (4.7) - a hat is used to indicate an estimated state.

$$\hat{z}(k+1) = \Phi_{op}\hat{z}(k) + \Gamma_{op}u_p(k) + K_{op}\left(y_p(k) - C_{op}\hat{z}(k)\right) \tag{4.7}$$

Here $z(k) = \begin{bmatrix} x_p(k) \\ \nu(k) \end{bmatrix}$, $\Phi_{op} = \begin{bmatrix} \Phi_p & \Gamma_p \\ 0 & 1 \end{bmatrix}$, $\Gamma_{op} = \begin{bmatrix} \Gamma_p \\ 0 \end{bmatrix}$, $C_{op} = \begin{bmatrix} C_p & 0 \end{bmatrix}$ and $K_{op} = \begin{bmatrix} K_p \\ K_w \end{bmatrix}$.

In the calculation of the observer Ackermann's Formula is applied in a rearranged form to find $K_{op} = P_p\left(\Phi_{op}\right) {W_{op}}^{-1} \begin{bmatrix} 0 & \dots & 0 & 1 \end{bmatrix}^{\mathsf{T}}$ using the same $P_p()$ function that was used to calculate $L_p$ and where $W_{op}$ is the observability matrix of the plant model. (Note that the plant is only observable if $W_{op}$ has rank $n$).

Observability Matrix of the plant: $W_{op} = \begin{bmatrix} C_p & C_p\Phi_p & \dots & C_p{\Phi_p}^{n-1} \end{bmatrix}^t op$

Finally a reference model can be applied to the input of the controller with a direct feed-forward of the model states. A diagram of this is presented in figure 4.8:

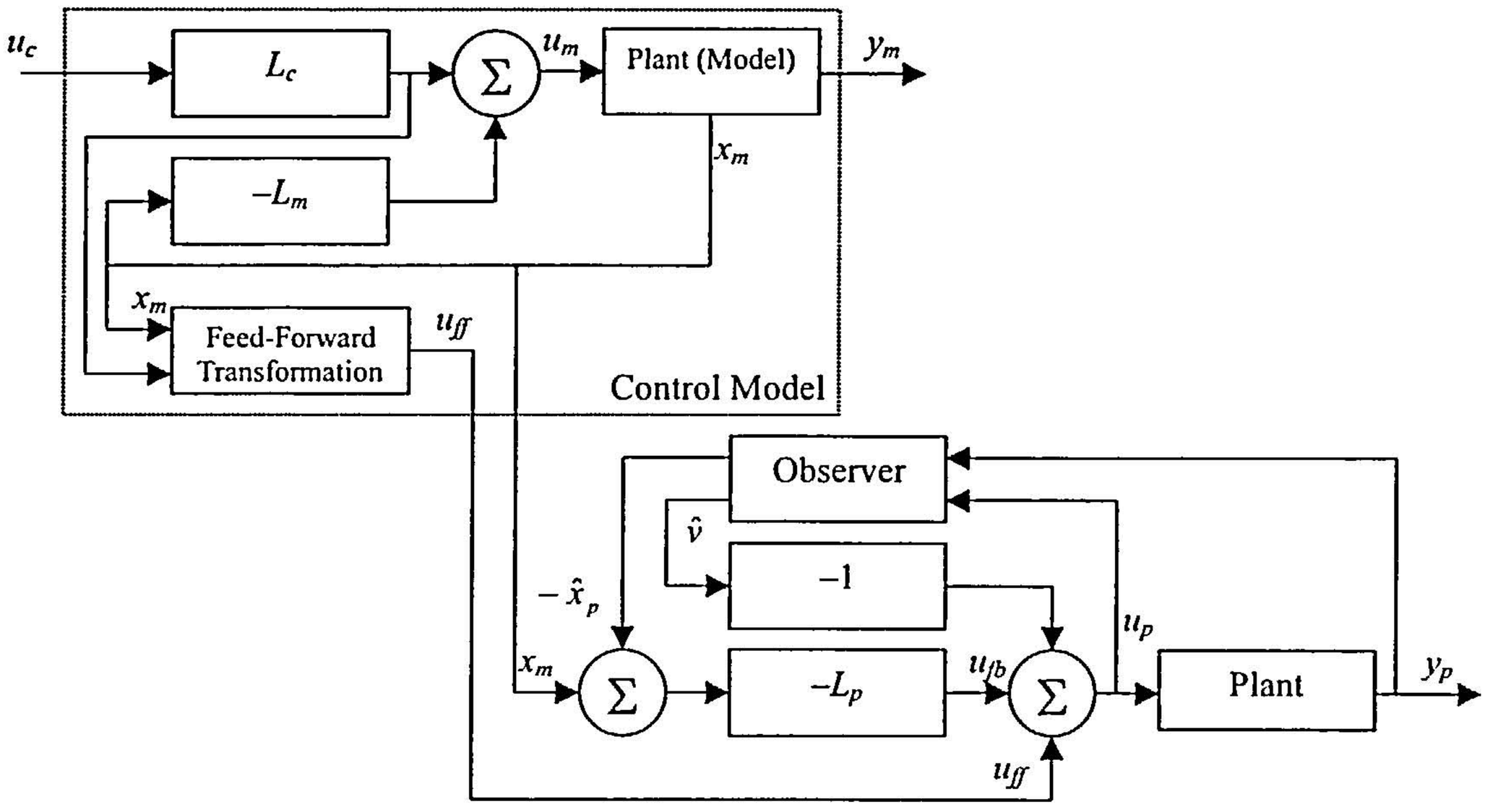


Figure 4.8: A state-space 2-D.O.F. Model Reference Controller

The closed loop system of the control model can be represented simply in the form:

$$\begin{aligned} x_m(k+1) &= \Phi_m x(k) + \Gamma_m u_m(k) \\ y_m(k) &= C_m x_m(k) \end{aligned} \tag{4.8}$$

Where $\begin{aligned} \Phi_m &= \Phi_p - \Gamma_p L_m \qquad \Gamma_m = \Gamma_p L_c \\ C_m &= C_p \qquad\qquad\quad u_m(k) = u_p(k) \end{aligned}$

The values of $L_m$ can be obtained by applying Ackermann's Formula again as

$$L_m = \begin{bmatrix} 0 & \dots & 0 & 1 \end{bmatrix} {W_{cp}}^{-1} P_m(\Phi_p) \tag{4.9}$$

Here the function $P_m()$ is a polynomial with roots representing the poles of the desired characteristic polynomial for the reference model.

The feed-forward term is defined as:

$$u_{ff}(k) = L_c u_c(k) + C_{ff} x_m(k) \tag{4.10}$$

Here $C_{ff} = \begin{bmatrix} (a_{p1} - a_{m1}) & (a_{p2} - a_{m2}) & \dots & (a_{pn} - a_{mn}) \end{bmatrix}$ and the elements $a_{pi}$ and $a_{mi}$ are the $i^{\text{th}}$ elements of the first row of the $\Phi_p$ and $\Phi_m$ matrices respectively (when in reachable canonical form).

The functions $P_p()$ and $P_m()$ were designed with two dominant poles with the excess poles forced to the origin in the discrete time plane. It was expected that by setting the excess poles to zero their influence would be too quick to have any real effect on the actual system. The dominant poles were evaluated via prescribed damping and natural frequencies.

For the Air Controller these values were chosen as:

- Plant Control Damping = 1.0
- Plant Natural Frequency = 0.05
- Model Control Damping = 0.8
- Model Natural Frequency = 0.05

For the TSV Controller these values were chosen as:

- Plant Control Damping = 0.7

- Plant Natural Frequency = 0.7
- Model Control Damping = 1.1
- Model Natural Frequency = 0.05

The performance was examined using a simulation (see figure 4.9), with a random noise on the simulated plant output, before being tested on the actual system.

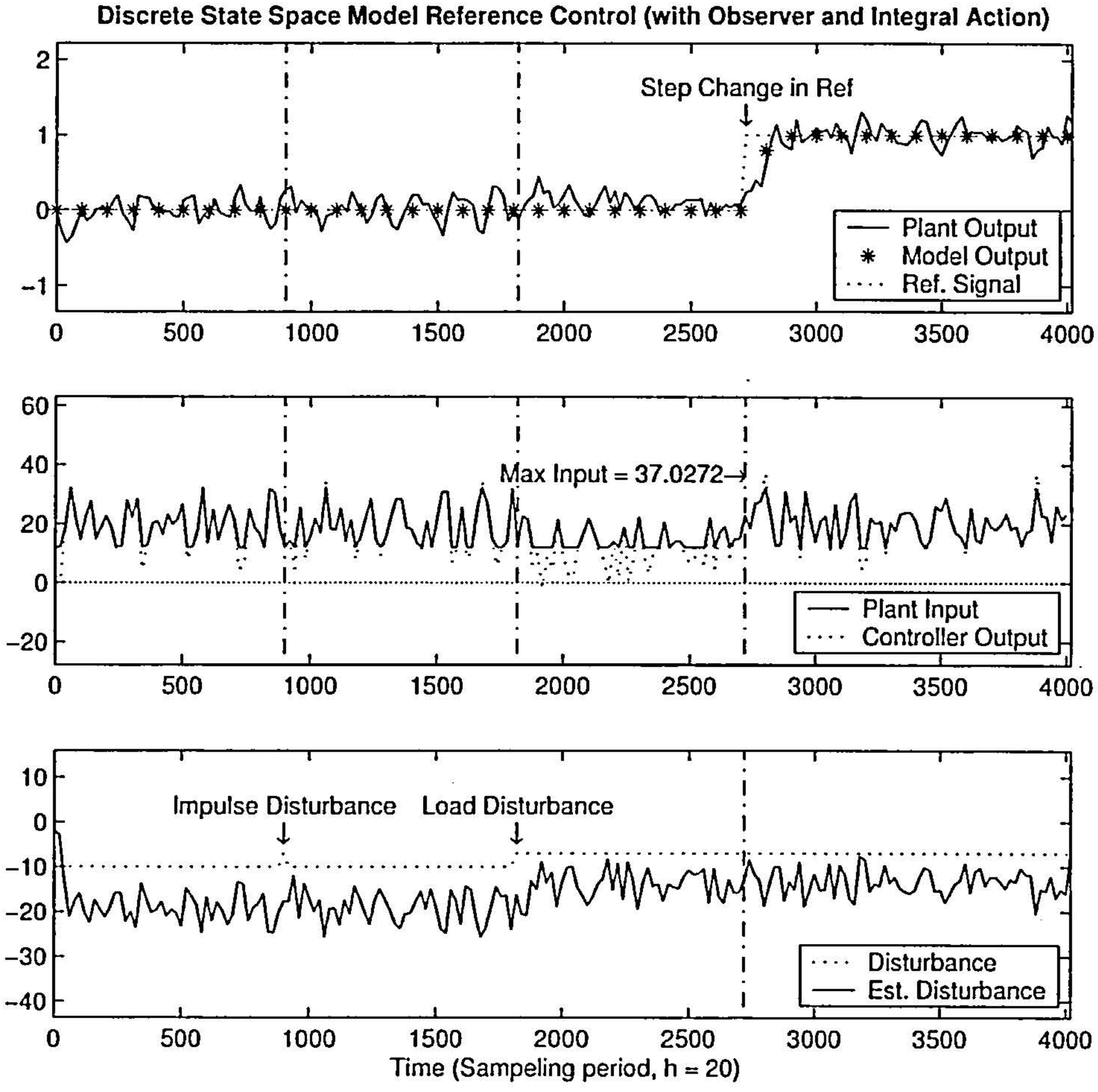


Figure 4.9: Simulation of the control of an identified model

The simulation shows that the controller seems to be able to cope with significant noise on the actuator sensors and can handle step changes and disturbance changes (changes in load) adequately. There does seem to be slight saturation when the load change is applied.

## 4.5 Experimental Results

### 4.5.1 Control of the Air Temperature

As a first step in the experiment the air temperature was controlled and the results in figure 4.10 show good performance apart from a slight oscillation at the higher temperature level. As described earlier the input for the controller, desired air temperature, is interpreted by the local HVAC control unit and thus gives a different cabin temperature. This can be seen in figure 4.10 by the difference between the measured air temperature and the input to the controller in steady-state conditions.

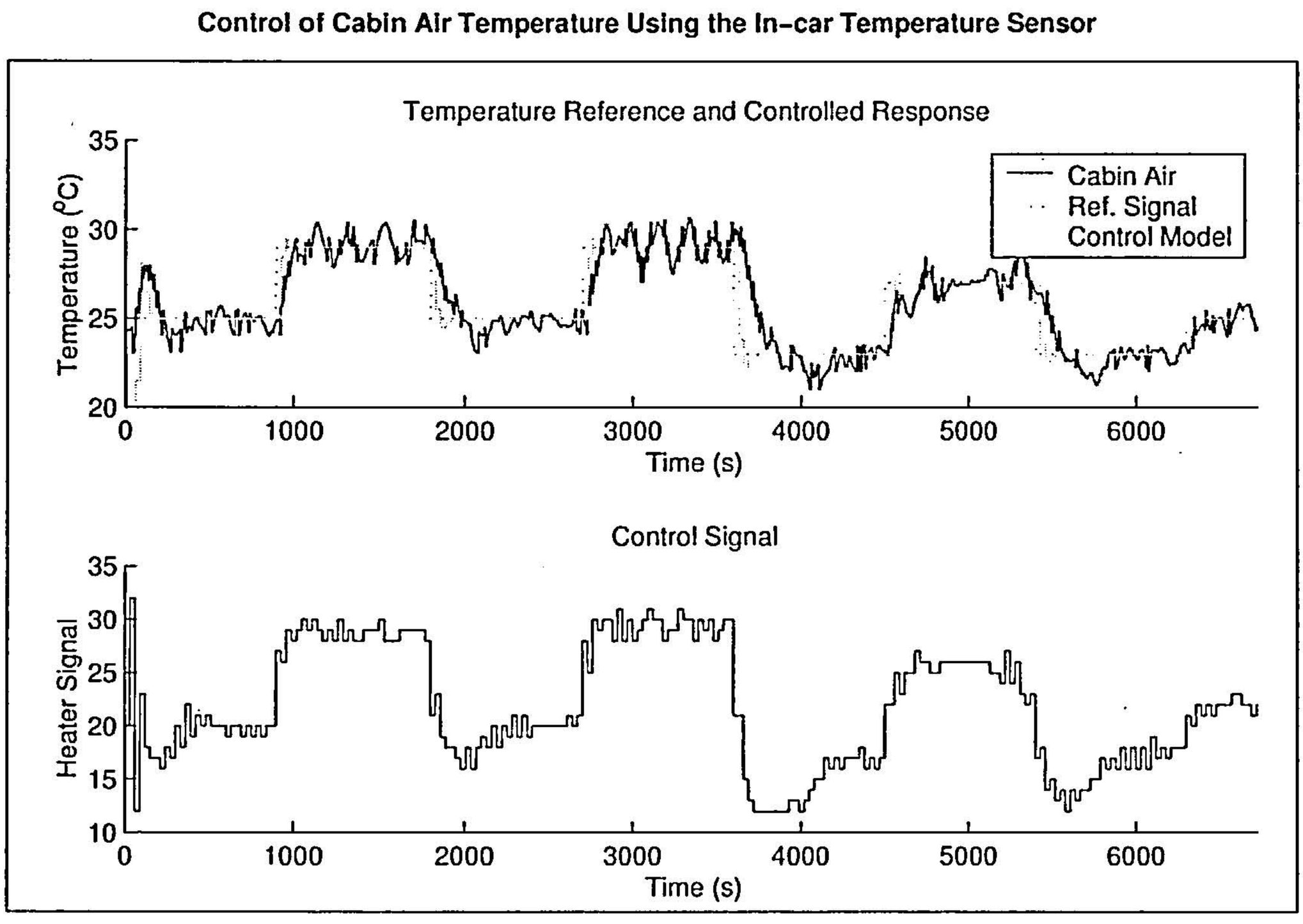


Figure 4.10: Control of the Internal Air Temperature

### 4.5.2 TSV Control Results

A suitable 3rd order model was identified and an acceptable controller was formed with a control model damping of 1.1 and natural frequency of 0.05 and with plant control damping of 0.7 and a natural frequency of 0.7.

Results of the control experiment from 2 subjects are presented in figures 4.11 and 4.12. The controlled on-line calculation of TSV is shown as the solid black lines in the upper plots and is compared with the command signal, upper plots dotted line, used as the controller reference. The control model output, upper plots grey line, shows the attempted change in TSV due to the step response of the command signal. The controller model, however, does not take into consideration the saturation of the command signal. The lower plots show the command signal - direct from the controller, lower plot dotted grey line, and the command signal read into the HVAC system, lower plot solid line, which has been rounded to the nearest degree and has saturation limits. The middle plot shows the result of the command signal (desired air temperature) on the actual cabin air temperature.

The personal thermal vote of the subjects is also displayed on the upper plots of figures 4.11 and 4.12 as circles. This is used to compare the effectiveness of the TSV estimation and the perceived personal thermal state.

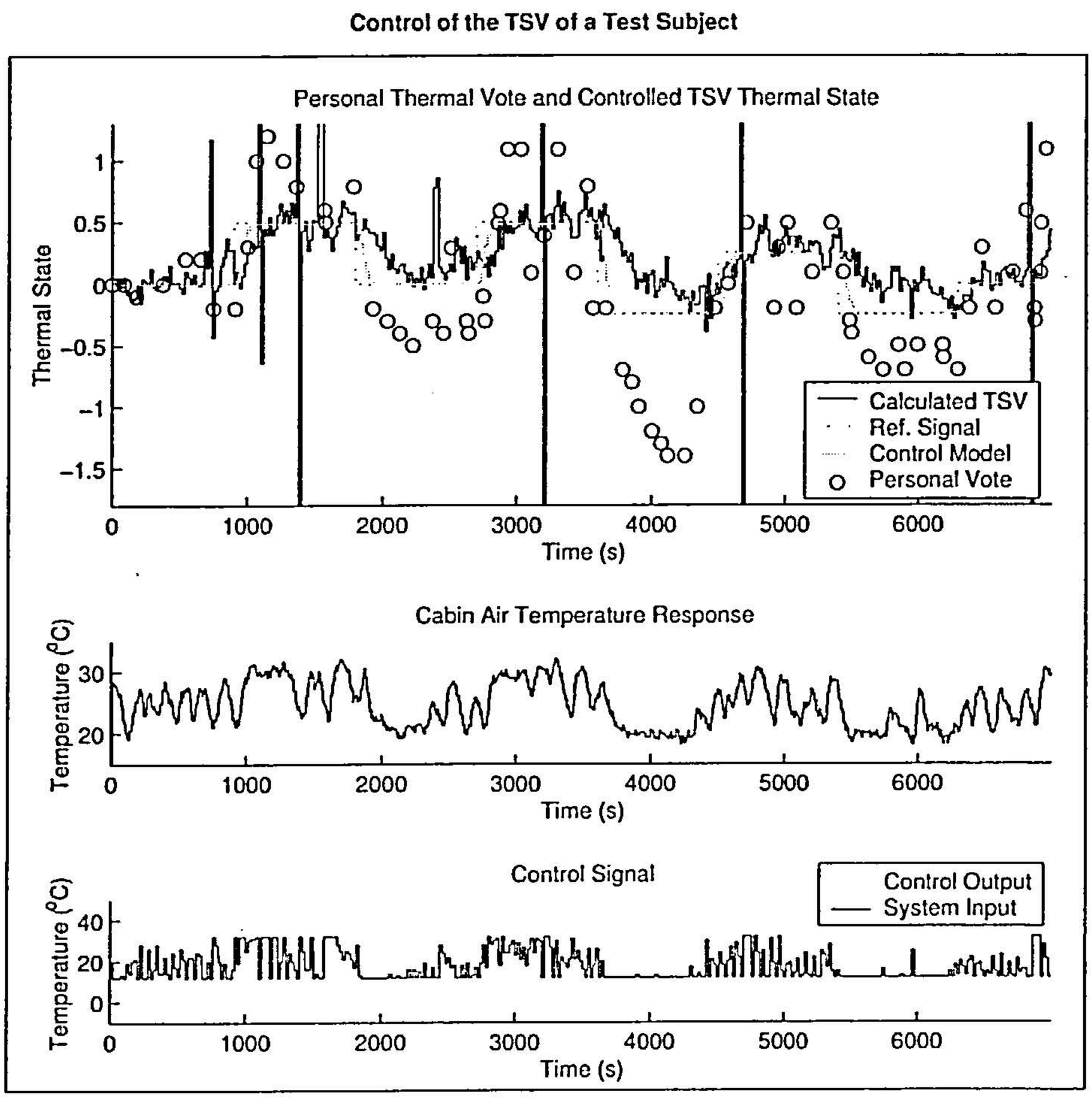


Figure 4.11: Reference control of TSV results with Test Subject 1

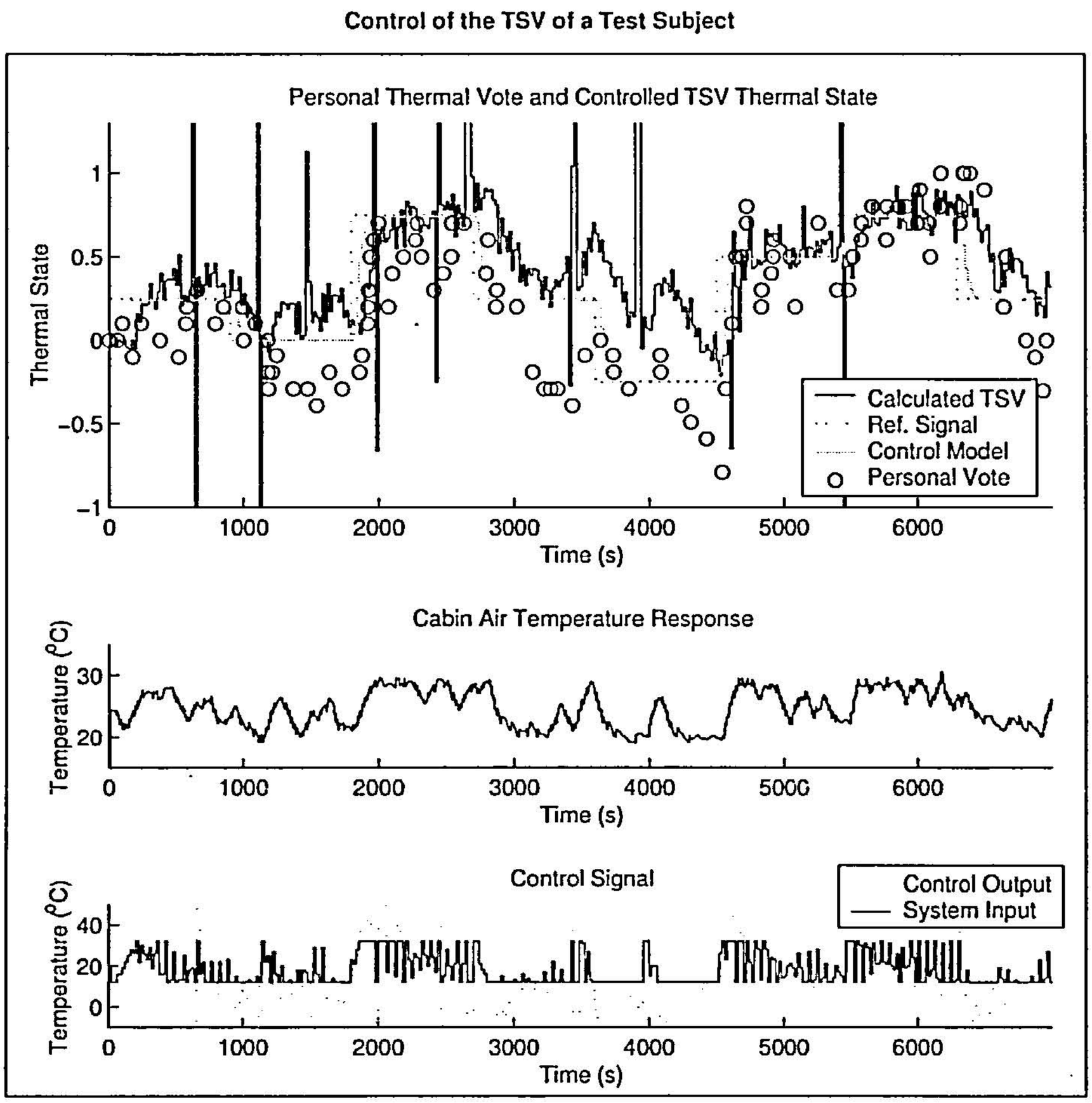


Figure 4.12: Reference control of TSV results with Test Subject 2

There is significant noise on the sensor readings. However, the results shows good response during heating up, tracking the model reference signal well.

## 4.6 Discussion of Results

The noise to signal ratio of the TSV seems quite high as a result of high noise levels on the facial skin temperature sensors. The sensors are accurate to $\pm 0.5\,^{o}$C on each sensor but were constantly noisy over a $0.4\,^{o}$C range. The 5 sensor readings were averaged over the 30 seconds between control samples.

In addition to the noise there is also an interference impulse disturbance that was not tracked down. This was left in the measured signal to test the controller. The rejection of impulse disturbances in the simulation showed a quick attenuation of the disruption to the signal.

However, the interference impulse disturbances in the real plant were much greater than those in the simulation and resulted in a large perturbation of the signal after the disturbance. The impulses were large and could have easily been filtered out with a crude "if signal is greater than last value + 0.5 then ignore" statement in the algorithm code.

The controller is designed for a discrete time system but no provision is given for a discrete output setting. The output from the controller had to be rounded to the nearest degree before being sent to the HVAC actuator. The effect of this rounding error was expected to be negligible, overpowered by the noise on the sensors.

Setting the excess (non-dominant) poles to zero in the discrete complex plane is not always the best strategy and does not minimize the control energy. The inherent high frequency components of the controller caused by the excess poles is perhaps a reason why the actuator signal is particularly sensitive to noise and to interference impulse disturbances.

The control model was rigorously designed to be satisfactorily fast and, consequently pushed the system too hard resulting in saturation of the actuator signal. The results show, however, that the system dynamics allow rapid heating of the subject but made the cooling process much slower. When designing the controller the focus had been on the heating up phase. It is interesting to note that the local HVAC control favoured using the foot air outlet for heating and the dashboard air outlets for cooling. The air temperature measurement in figure 4.5 reacts faster to a drop in temperature than to an increase because it is closer to the dashboard. The local HVAC control, for the sake of thermal comfort, would not allow the foot area to become too cool and thus inhibited the cooling of the subject's feet. Even though the subject's face is in the cooler air, supplied from the dashboard, the subject's thermal state does not respond significantly which supports the use of facial skin temperature as a indicator of global thermal state.

The subject's perception of thermal state did seem to disagree with the TSV estimate more during the cooling down phases, but this is probably because the sensation of the air on the face and hands is more noticeable when thermal state is consciously considered and in an uncomfortable environment is more easily exaggerated.

## 4.7 Conclusions

It has been demonstrated in this chapter that control of the TSV is feasible and it is suggested that better control performance could be generated with certain improvements. These would

include proper filtering of the noise and interference impulse disturbances and reduction of the control energy through optimal placement of the poles to reduce the demand on the actuator. Combining the local HVAC control with the TSV controller did inhibit performance during cooling, which was unexpected and should be planned for, or even bypassed in future investigations.

The TSV calculation has been successfully used and for the most part it seems to have been fairly accurate in estimating the thermal state. However, some questions arise from the cooling phase data. The replacement of the TSV calculation with any other method of thermal state estimation is not expected to cause any additional control problems.

We have successfully demonstrated the feasibility of feedback control of TSV. We believe this to be an important novel contribution.

# Part II

# Learning User Interactions

# 5 Fuzzy Logic Estimation and User Reference Learning

It is the aim of this chapter to examine the use of information supplied during the user's interactions to personalize the control response. Fuzzy logic fits well with the idea of thermal state and the fuzzy logic knowledge base or rule base matrix can be used to remember user interactions. The method is a new variation on the adaptive theory using on-line interactions to represent the reference model and inverse controller.

The control methodology is then applied in two different ways: Firstly to learn and then to estimate a user's thermal state votes, and secondly to learn and to automate the interactions of a user with an automotive HVAC system. The fuzzy method is shown to learn and interpolate thermal state and is better than the neural network solution after only one pass through the training data. The controller learns on-line and can use sporadic input from a human operator. It was shown that, used as a controller with a feedback input, the fuzzy method can quickly start to interact for the user.

This chapter contributes a new method of learning user interactions and shows how this could be implemented in the automotive cabin.

## 5.1 Introduction

### 5.1.1 Background (State of the Art)

In the previous chapters thermal state estimation from environmental and skin temperature sensors has been evaluated and used in a control strategy. Most of the scientific literature

has been based on related techniques and relatively little attention has been given to the interactions that the user has with the HVAC interface. In some cases the aim of the automation of the environmental control has been to reduce the amount of interface required in the car, as in [42]. This paper presents work carried out by Valeo Thermal Systems and PSA Peugeot-Citron in the development of two fuzzy logic controllers used to control the thermal environment inside a car. The first regulates the internal temperature fixed by the user on the climate control panel. The new interface only requires the user to input their desires either to be made hotter or cooler and not, as previously, an absolute temperature. The fuzzy temperature regulation controller only manipulates the blend door, the distribution and air intake doors and the blower voltage. The second part of this paper considers a thermal balance regulation (comparable to the PMV estimation method) using the temperature regulating fuzzy controller with a supervisor program that calculates the thermal balance of the user. The thermal balance is calculated from 6 parameters: internal cabin temperature, operative temperature, metabolic rate, thermal resistance of clothing, humidity and air flow velocity. It is assumed that the best thermal comfort is accomplished when the thermal balance of the user is around zero and hence the target temperature is calculated for the temperature regulator. The modified instrument panel only allows the user to ask to be heated or to be cooled, successive presses on the particular button representing intensity of the demand. The consequence of user input is to modify the clothing resistance value in the thermal balance calculation. This modification uses a fuzzy logic system with 3 inputs: the original value of the clothing resistance, the value of thermal balance and the magnitude of the demand.

Although this strategy assumes that the most desirable thermal balance of a user will be a zero heat transfer balance, the interaction of the user, which causes a modification to the clothing resistance variable, will inherently adapt the system to the preferred desired thermal state. It is the use of the personal interaction to personalize the response that is of particular interest. However, in the case described above the interface was simplified whereas left in its original form the user interactions can provide much more information.

There has been little research into algorithms for learning user preference for automotive HVAC systems. Federspiel and Asada [43] aimed to provide a neutral thermal state in steady state conditions, but also illustrated an interesting approach for mapping the function of thermal state for individual users. The method demonstrated by Ritter and Holdgrew [44] categorized the environmental and driver information into "situations" and learnt user preferences for these situations. They also suggested learning from the user the relationship between the situations.

### 5.1.2 Aim of the Chapter

It is the aim of this chapter to examine the use of information supplied during the user's interactions to personalize the control response. This can be achieved by introducing personalization into the thermal state estimation method or by directly adapting the control output. The framework for such a control strategy is presented in figure 5.1.

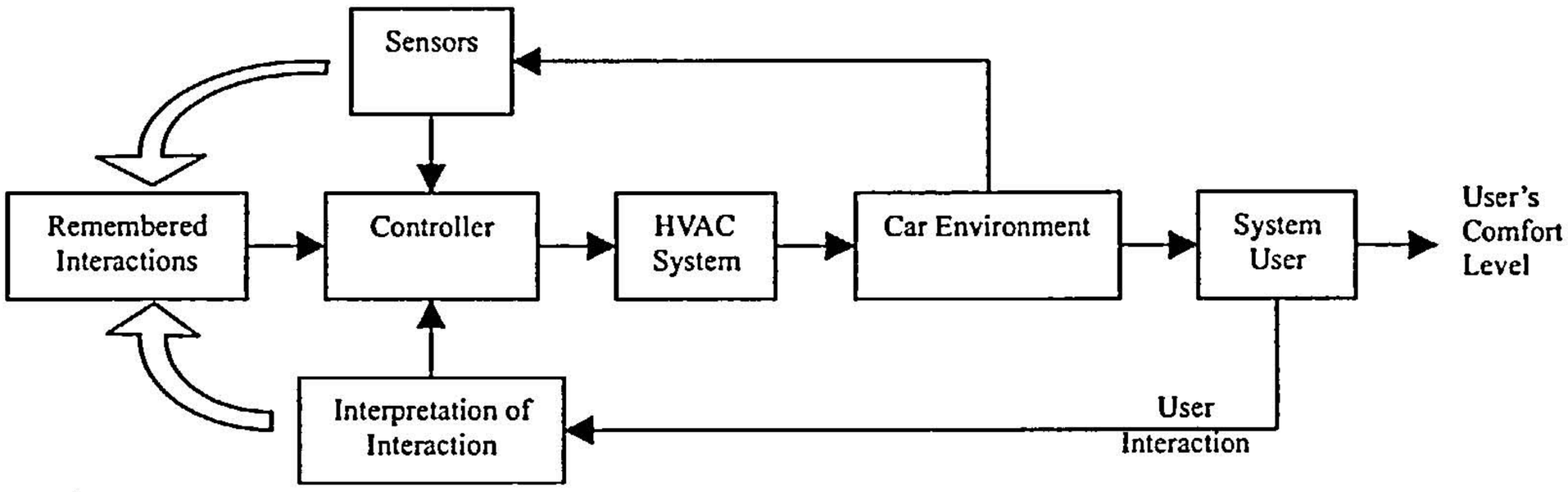


Figure 5.1: Block diagram of a learning control structure

The controller uses information from the user and their environment to suggest the best output by the HVAC plant. The aim of the controller is not to rely on feedback, rather to remember user interactions with the system to build a feed-forward database. Hence it needs to remember what it has learnt for different environments. Thus the controller is shown with a "Remembered Interactions" memory. Additionally, the controller may have to interpret the user interaction.

Fuzzy logic fits well with the idea of thermal state and thermal comfort because both already make use of linguistic variables. It is thus a natural choice for developers (see [45], [46] and [42]). In addition fuzzy controllers contain a memory in the form of the knowledge base or rule base matrix. The concept of utilizing this memory to learn user interactions comes from a consideration of the methods used in Fuzzy Model Reference Learning Control (FMRLC). A diagram of FMRLC is presented in figure 5.2, (this figure is taken from [47], page 304).

The plant is unknown and may change without the controller realizing. The solution is to use a reference model - a representation of what is expected from the controller and plant for a given input. The difference between the reference model and the real plant is then put though an inverse plant model to determine the actual properties of the real controller.

However, if the output of the plant ($y$) is thermal comfort then it can not be easily measured for feedback. Without measuring $y$ a reference model can not be used to compare the different outputs. Instead user interaction stands in for the reference model. This interaction not only

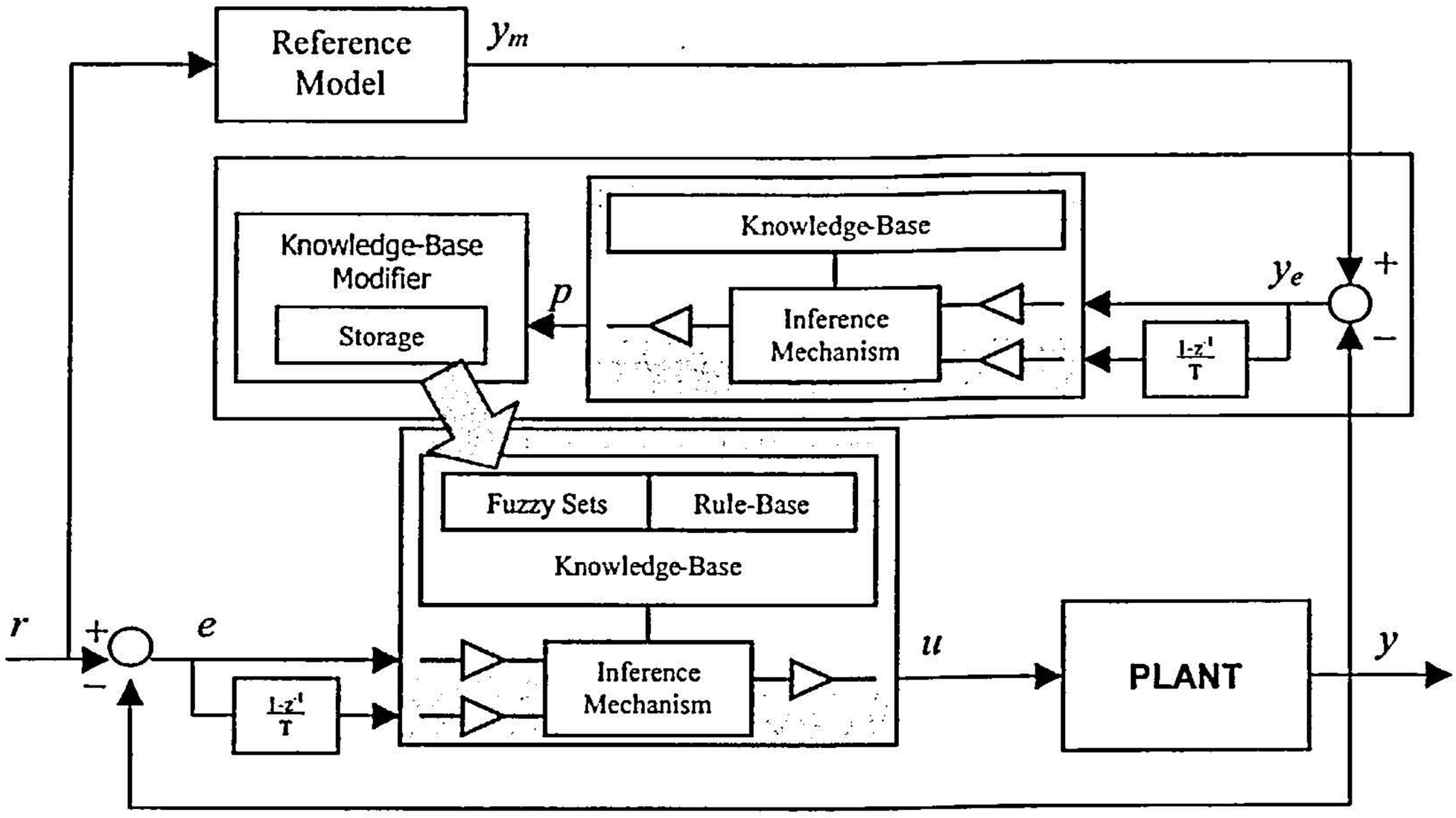


Figure 5.2: Block diagram of a Fuzzy Model Reference Learning Controller (FMRLC) from [47]

acts as a reference model but also eliminates the need for an inverse plant model since there is now a direct comparison between the output of the controller and what the output of the controller should be. Hence the new control strategy is more simple than FMRLC and is termed Fuzzy User Reference Learning Control (FURLC), figure 5.3 represents this.

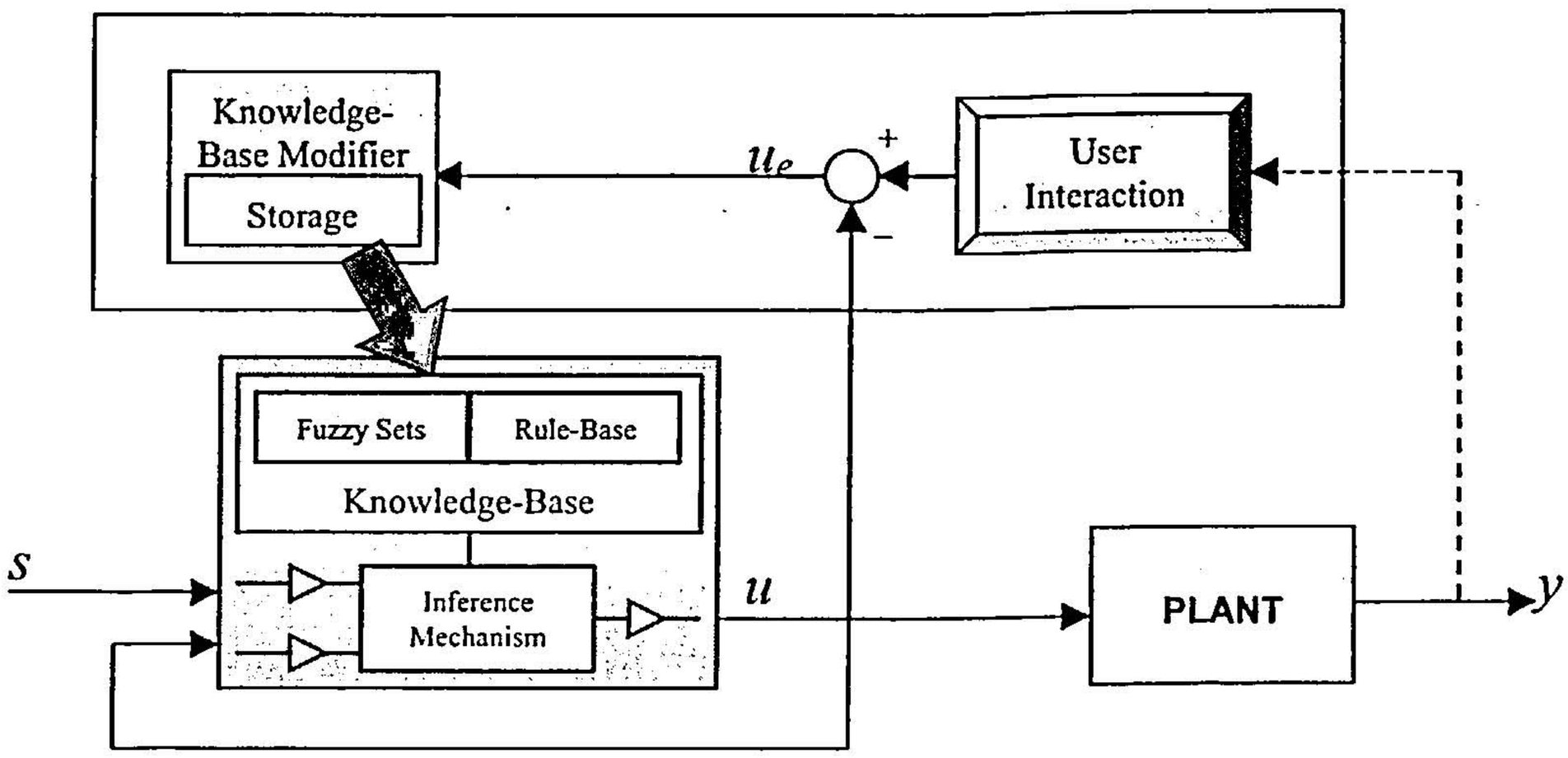


Figure 5.3: Block diagram of a Fuzzy User Reference Learning Controller (FURLC)

To examine the properties of such a method, two control objectives were set:

1. To learn and then estimate thermal state from varying facial skin temperature conditions.

2. To learn the correct interactions for modifying the thermal state of the user.

For the second objective a specific set of experiments were conducted in the Mercedes-Benz S-class test car. The aim of the experiment was to examine the interaction of the user with the system and to show that it is possible for a controller to learn from the user and then to automate the system reducing the need for the user to interact with the system.

## 5.2 Basics of Fuzzy User Reference Control

The following section describes the authors own interpretation of fuzzy logic theory. [47] provides a good reference to the standard techniques used in fuzzy logic.

A MISO fuzzy controller can be represented by figure 5.4. The input is a vector $c_i = \left[ \begin{array}{cccc} c_1 & c_2 & \dots & c_n \end{array} \right]^\top$ or in the linguistic form $\tilde{c_i}$ and associated with this linguistic vector are the set of linguistic membership functions for each element of the vector $\tilde{A}_{i,j}$, (the $j^{th}$ membership function for the $i^{th}$ input).

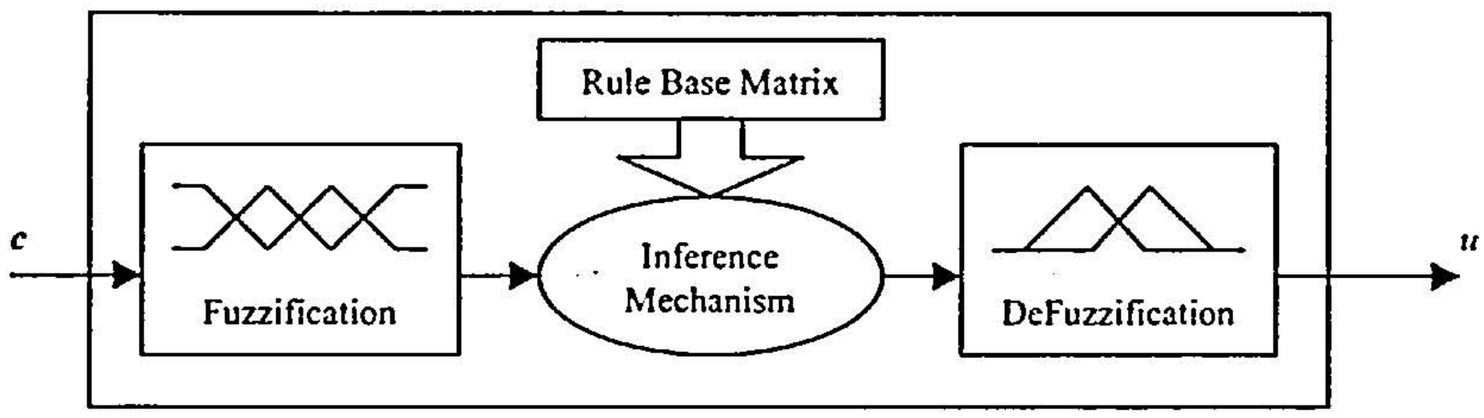


Figure 5.4: Internal workings of a fuzzy controller

Thus the input element $c_i$ has the set of membership functions:

$$A_{i,j} = \left[ \begin{array}{cccc} A_{i,1} & A_{i,2} & \dots & A_{i,MAXMBR_i} \end{array} \right]$$

These are defined as being bounded on the universe of discourse between $MIN_i$ and $MAX_i$. For symmetrical triangular membership functions that are equally spaced to cover the bounded universe of discourse, for any value of $c_i$ within the bounds, the active membership functions can be simply calculated using equation (5.1).

$$
\begin{aligned}
j_{active_1} &= \text{fix}\left(\frac{(c_i - MIN_i)(MAXMBR_i - 1)}{(MAX_i - MIN_i)}\right) + 1 \\
&\text{and} \\
j_{active_2} &= j_{active_1} + 1
\end{aligned}
\tag{5.1}
$$

Here the function fix() rounds down to the next integer. The argument of the fix() function can be used again to calculate the corresponding value of the membership function using equation (5.2):

$$
\begin{aligned}
A_{i,j_{active_1}} &= j_{active_1} - \left(\frac{(c_i - MIN_i)(MAXMBR_i - 1)}{(MAX_i - MIN_i)}\right) \\
&\text{and} \\
A_{i,j_{active_2}} &= \left(1 - A_{i,j_{active_1}}\right)
\end{aligned}
\tag{5.2}
$$

To clarify the notation consider an example of the $1^{mathrmst}$ element of the input vector ($i = 1$) with 5 triangular membership functions ($MAXMBR_1 = 5$) described by the diagram in figure 5.5:

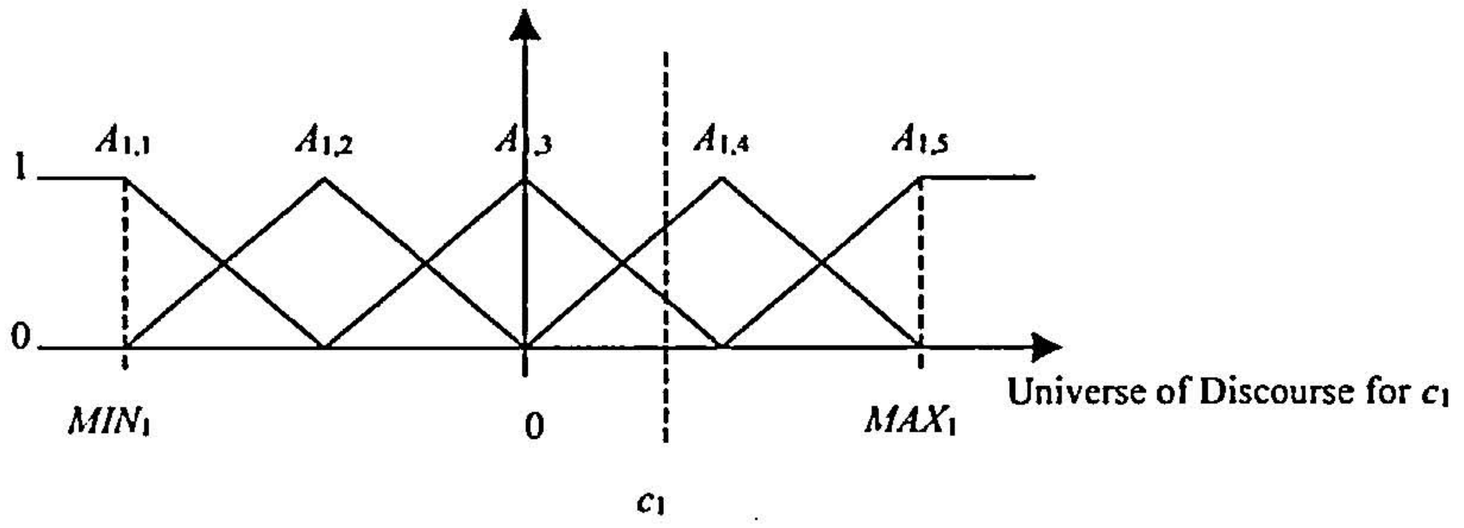


Figure 5.5: Example of an input on the universe of discourse with input membership functions

If $c_1 = 0.75$, $MIN_1 = -2$ and $MAX_1 = +2$ (with the centres of the membership function at -2 -1 0 1 2) then the 2 active membership functions $\left(j_{active_{1|2}}\right)$, where the subscript (1 | 2) means 1 or 2, are calculated using equation (5.1) and the values of the membership functions are calculated using equation (5.2):

$$
\begin{aligned}
j_{active_1} &= \text{fix}\left(\frac{(0.75+2)(5-1)}{(2+2)}\right) + 1 = \text{fix}\,(2.75) + 1 = 3 \\
&\text{and} \\
j_{active_2} &= j_{active_1} + 1 = 4
\end{aligned}
$$

Thus

$$A_{i,j_{active_1}} = 3 - (2.75) = 0.25$$

and

$$A_{i,j_{active_2}} = (1 - 0.25) = 0.75$$

This is done for all the elements in the input vector.

The output of the controller is $u$ or in the linguistic form $\tilde{u}$ which has the linguistic membership functions $B_{[\ j_1\ \ j_2\ \ \dots\ \ j_n\ ]}$. Where $j_1$ is the same as the $j$ index from the membership function set $A_{1,j}$, and $j_2$ is the same as the $j$ index from the membership function set $A_{2,j}$ etc. Thus for all possible combinations of $A_{1,j}\ \dots\ A_{n,j}$ there is a corresponding output membership function as an element of the matrix $B_{[\ j_1\ \ j_2\ \ \dots\ \ j_n\ ]}$. Thus the size of $B$ is $MAXMBR_1 \cdot MAXMBR_2 \cdot \dots \cdot MAXMBR_n$ .

With this notation the linguistic interpretation of the rule base "If Premise Then Consequence" statement can be expressed in a general form by the following:

$$\textbf{If } \tilde{c}_1 = \tilde{A}_{1,j_1} \textbf{ And } \tilde{c}_2 = \tilde{A}_{2,j_2} \textbf{ And } \dots \tilde{c}_n = \tilde{A}_{n,j_n} \textbf{ Then } \tilde{u} = \tilde{B}_{[\ j_1\ \ j_2\ \ \dots\ \ j_n\ ]}$$

The purpose of the inference mechanism is to evaluate the premise. The aim of evaluating the premise is to find a value that represents how closely the premise describes the actual inputs. The premise for each rule can be evaluated in different ways but the simplest is to treat the **And** as a minimum operator thus the premise for each rule, $P_{[\ j_1\ \ j_2\ \ \dots\ \ j_n\ ]}$, takes the form of equation (5.3).

$$P_{[\ j_1\ \ j_2\ \ \dots\ \ j_n\ ]} = \min\left(A_{1,j_1}, A_{2,j_2}, \dots, A_{n,j_n}\right) \tag{5.3}$$

The process of fuzzification using symmetrical triangular membership functions will result in only 2 active input membership functions per input. Hence there is a maximum of $2^n$ premise rules with non-zero values and so equation (5.3) is thus modified to give equation (5.4) where $r = 1, 2, \dots, 2^n$

$$P_r = \min\left(A_{1,j_{1_{active_{1|2}}}}, A_{2,j_{2_{active_{1|2}}}}, \dots, A_{n,j_{n_{active_{1|2}}}}\right) \tag{5.4}$$

The corresponding activated elements of the rule base matrix from the consequence of the rules can also be referenced in terms of $r$ as in equation (5.5):

$$B_{act_r} = B_{[\ j1_{active_{1|2}} \quad j2_{active_{1|2}} \quad \cdots \quad jn_{active_{1|2}}\ ]} \tag{5.5}$$

The inference mechanism then relates the premise to the element of the rule base matrix (output membership functions), which again can be done in a variety of ways. If the premise closely resembles the actual situation then we want the corresponding output membership function to be more strongly weighted. Maintaining consistency the minimum operator will be used again to do this and the resulting output membership functions are called the implied membership functions, $B_{imp_r}$ in equation (5.6):

$$B_{imp_r} = \min\left(P_r, B_{act_r}\right) \tag{5.6}$$

Note that all $B_{imp_r}$ are still functions as shown in figure 5.6 as the shaded parts of the output membership functions $B_{act_r}$ for $r = 1$ and 2.

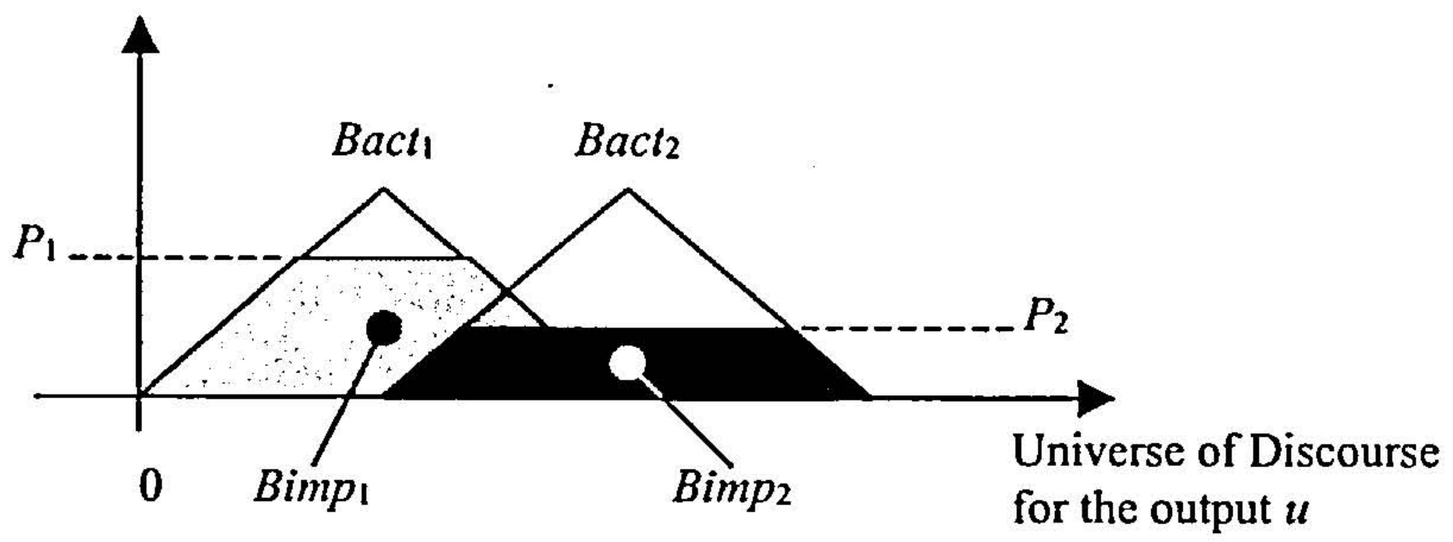


Figure 5.6: Formation of implied output membership functions

The defuzzification process takes the implied output membership functions and calculates a value for the actual output $u$. There are many methods for doing this but the most common is the Centre Of Gravity (COG) method. The equation for the COG method is quite straightforward and is defined by:

$$u = \frac{\sum_r b_r \cdot \int B_{imp_r}}{\sum_r \int B_{imp_r}} \tag{5.7}$$

Here $b_r$ is the central position of the membership function on the output universe of discourse. The integral represents the shaded area under the implied membership functions $B_{imp_r}$ and is easily calculated for the truncated form of the symmetric triangular membership functions, with width $w$ by equation (5.8).

$$\int B_{imp_r} = w\left(P_r - \frac{P_r^2}{2}\right) \tag{5.8}$$

When using this method it is important that the denominator of equation (5.7) does not become zero. It can be seen from rearranging equation (5.8) that $\int B_{imp_r}$ becomes zero only when $P_r = 0$ or 2. $P_r$, however, is confined between 0 and 1 and as long as at least one of the active premises is greater than 0 then this anomaly is avoided. This will be true as long as for every point on the universe of discourse for each input there is a membership function greater than zero. This explains why it is necessary for the membership functions on the extremities to saturate and remain saturated out past the limits (see Figure 5.5).

It is noted that $u$ is calculated only from $P_r$ and from $b_r$. $P_r$ is obtained from the inputs, equation (5.4), equation (5.5) is not used at all and so the Rule Base Matrix can be used to store the values of $b_r$ directly. Hence, equation (5.5) is replaced with:

$$b_r = B_{\left[\, j1_{active_{1|2}} \quad j2_{active_{1|2}} \quad \cdots \quad jn_{active_{1|2}} \,\right]} \tag{5.9}$$

Thus $B_{\left[\, j_1 \quad j_2 \quad \cdots \quad j_n \,\right]}$ becomes a matrix of centres of the output membership functions to be used with equation (5.8) in the COG calculation.

## 5.3 Learning By Modification to The Rule Base Matrix

The output from the controller depends on two values, $P_r$ derived from the inputs, and $b_r$ the values stored in the rule base matrix. The rule base matrix does not necessarily have to remain constant and there are fuzzy logic methods for modifying it on-line such as the "knowledge-base modifiers" used in adaptive fuzzy control. One such approach states that if $e$ is the difference between the actual controller output, $u$, and the desired output, $u^*$, equation (5.10), then the elements of $B_{\left[\, j_1 \quad j_2 \quad \cdots \quad j_n \,\right]}$ representing the active output membership functions (i.e. $b_r$ from equation (5.9)) can be modified by simply adding $e$ as in equation (5.11).

$$e = u - u^* \tag{5.10}$$

$$b_r \rightarrow b_r + e \tag{5.11}$$

This simple addition in conjunction with the COG method of defuzzification will guarantee that the next time the same inputs are applied $e$ will be zero. However there are variations that can be investigated such as weighting the addition by the premise value so that modifications are relative to the contribution of the output membership function to the final value of $u$. Hence the learning rule in equation (5.11) becomes that in equation (5.12). This ensures that only elements that contributed significantly are modified significantly.

$$b_r \rightarrow b_r + P_r \cdot e \tag{5.12}$$

Alternatively the effects of both equation (5.11) and equation (5.12) can be combined with an independent coefficient, the "Convergence Factor" $CvFc$ as in equation (5.13):

$$b_r \rightarrow b_r + (P_r + CvFc(1 - P_r))\, e \tag{5.13}$$

This will reduce the error, $e$, in the output of the controller at a faster rate of adaptation than equation (5.11) but is a more damped version than equation (5.12) and makes it possible, by varying $CvFc$ on-line, to modify the learning rate for different events. It may be more desirable to start with the effects of equation (5.11) ($CvFc = 1$) for a quicker convergence but then later to follow the effects of equation (5.12) ($CvFc = 0$) for fine tuning.

## 5.4 Implementation of Learning from User Interactions

User interaction is an ideal source of reference for the controller. In adaptive control using the knowledge-base modifier techniques the error in control action, $e$, is obtained indirectly, through an inverse fuzzy model. However the user of a system can be given access to the output of the controller to make overriding commands and so when the controller makes a bad output the user can correct the output when it happens. This means $u^*$ can be measured directly.

The user is not expected to input a correct action for every new element of the rule base that the controller encounters. When the controller encounters an element of the rule base matrix that has no previously learnt value then the last controller output is stored in the

new element. (This is when it is desirable for the convergence factor to be 1 to speed up the learning process at the beginning). This will spread the previously learnt output over situations that are similar to each other initially.

It is now left to recognize when the controller has no previously learnt data to use for a specific set of inputs. There are at least 2 solutions:

- To initialize the $B_{[\ j_1 \quad j_2 \quad \cdots \quad j_n\ ]}$ matrix with values that are outside the possible range of controller outputs (i.e. a value that can not be learnt at any time). Thus when that value is seen within the controller it is known that it could not have been learnt and so must be an area of empty memory. If implementing this method with an initial value that is far outside the possible values of $u$ it is appropriate to use equation (5.11) for learning with since it immediately learns the correct value and will not result in $u$ being outside the possible range after learning has taken place.
- To use a second matrix of the same dimensions as a record of where learning has taken place. This is a more comprehensive method since information about how much data has been learnt to a particular place can be stored. It also gives a greater opportunity for development of the algorithm (see equation (5.14) below). The cost of these advantages is in memory requirement, especially for controllers with many inputs, as the memory rises exponentially with each input (of similar dimensions).

Following on from the second solution, the matrix used to record learning is noted as $LB_{[\ j_1 \quad j_2 \quad \cdots \quad j_n\ ]}$ where a value of 0 in the corresponding element indicates that nothing has been learnt and a value of 1 indicates a fully learnt element. Equation (5.13) can thus be modified so that learning is not just based on the premise but also on the previous amount of learning that has take place in that element. This can be done by replacing the convergence factor with $(1 - LB_{[\ j_1 \quad j_2 \quad \cdots \quad j_n\ ]})$ and after rearranging:

$$b_r \to b_r + \left(1 - (1 - P_r)\, LB_{[\ j_1 \quad j_2 \quad \cdots \quad j_n\ ]}\right) e \tag{5.14}$$

There are many more opportunities for development. For example, a distinction in the matrix $LB$ between user learning and auto learning could be used so that user learning overrides surrounding elements and automatic learning will be implemented only until the element reaches a certain value after which the algorithm interacts instead of learning.

When updating the $LB$ matrix the learning rules can be used again. For example, $LB$ can

be updated by using equation (5.13) but with an $e$ of 1 so that the $LB$ matrix correctly represents the quantity of adaptation of the $B$ matrix which uses the same learning rule.

The error $e$ calculated from equation (5.10) could be replaced by a specifically calculated error for each element of the $B$ matrix. In this case $e$ would be calculated as in equation (5.15) below:

$$e = b_r - u^* \tag{5.15}$$

An implementation of the control method is provided in appendix C.

## 5.5 Experimental Work and Results

Two scenarios will be used to demonstrate the performance of the FURLC method. First the data collected in chapter 2 of this thesis will be used to examine the interpolation characteristics. A fuzzy estimator will be taught to predict thermal state based on the same inputs as the Neural Network approach in Chapter 3, facial skin temperature and the air temperatures at the face and nozzle outlet. The second scenario, using the Mercedes S-class test car, teaches a FURLC the user interactions directly. The inputs into this controller were the thermal state of the subject, calculated using the TSV method (see Chapter 3) and a reference thermal state.

### 5.5.1 Learning Thermal State Votes from User Estimates

This test was done off-line to examine the feasibility of the method. It has already been mentioned that fuzzy logic is a good method for the interpretation of thermal state and thermal comfort. In order to evaluate the ability of the FURLC method to learn and to interpolate between learnt values, it was thus conceived to teach an estimator to predict the thermal state of a subject. The method could then be compared to the results of chapter 3.

The biggest advantage of FURLC is that it learns on-line. This test, however, was done off-line but used the data collected in chapter 3 in a simulation as if the estimator was being implemented on-line. This allows the examination of the estimator's output as it learns and adapts. The convergence factor, $Cv_{FC}$, the number of membership functions and the learning rules can be modified and the simulation can be re-run. Training data can also be retaught

many times to the same estimator.

In order to compare the estimator to the other methods, the inputs into the estimator, from which it learns the correct response, must be appropriate. It has already been demonstrated that a neural network was able to learn a fairly accurate response with inputs of facial skin temperature and air temperature and so the same inputs were selected for use with the fuzzy method. The estimator was set up with 5 membership functions for each input with MAX and MIN values on the universe of discourse the same as the max and min values of the inputs in its training data set (Data Set 05). The rule base matrix was initialized with zeros.

The first result in figure 5.7 compares results using different convergence factors. The plots show the actual thermal votes of the test subject as the black dots, the 2 grey lines on each plot are outputs from the estimator. The dark grey binary output represents when the estimator is able to use previously learnt data to interpolate the thermal state (high) and when it does not have enough data (low). The light grey line is the calculated thermal state. When the estimator does not have enough information to confidently calculate a value of thermal state the last confidently calculated value is used. This is why at the beginning of each of the plots in figure 5.7 the estimator's output seems to rise in steps. A comparison between the estimator's estimate of thermal state and the personal thermal vote is presented in the form of a histogram of the error. Note that it is on the next time sample that the learnt data is applied and so the error between the estimator's output and the personal thermal vote is calculated prior to learning.

It can clearly be seen from figure 5.7 that the estimator can quickly learn. The start of the plots show a stepping shaped output from the estimator but later the output becomes more active. As stated before the convergence factor is a tool to be used on-line to adapt the rate of learning. Thus it is not unexpected that the result when using a convergence factor of 1.0 shows a much closer fit to the personal thermal votes (a faster learning approach) and a higher correlation value. The results with the convergence factor set to 0.1 do show a slight deterioration in estimation, however the result is still fairly accurate. The binary knowledge signal is the same for all the plots because the teaching data is the same and the number of membership functions is the same in each of the cases.

Figure 5.7 just proves that the estimator has the ability to interpolate. In order to test its ability to learn thermal state it should be tested on data other than the learning set. In reality the learning algorithm would be left on continuously to constantly keep the rule base matrix up to date. However in order to compare the effectiveness of the learning in estimating thermal state the learning rule was turned off and the estimator was applied to other data sets to examine the performance. Continuing the comparison with the neural network approach it

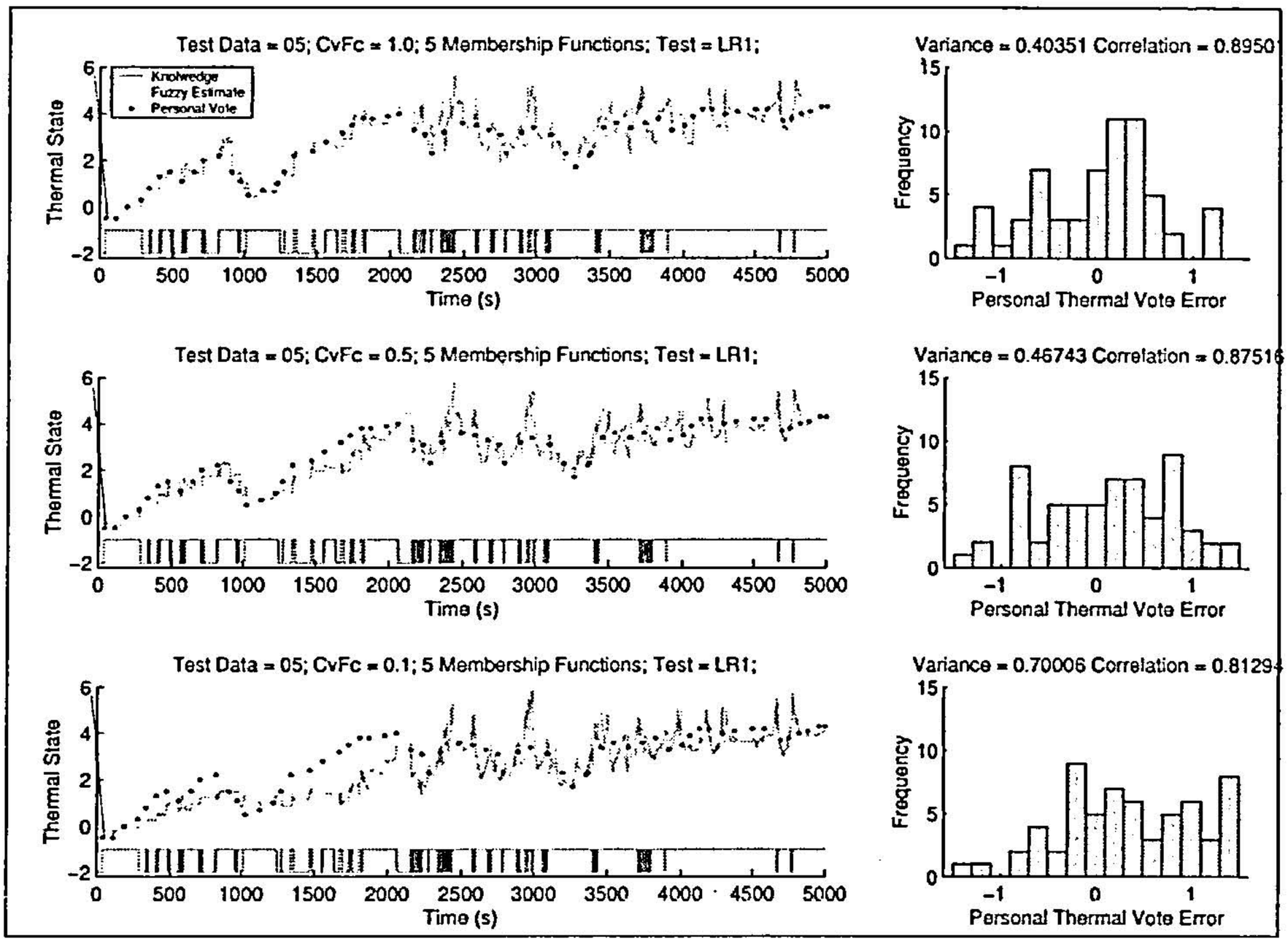


Figure 5.7: Comparison of results using different convergence factors

should be noted that the teaching data in figure 5.7 was the same as the teaching data for the neural network. The other data sets from the same test subject are used as the verification data - as was done with the neural network approach. These results are presented in figure 5.8.

The results in figure 5.8 show that the teaching data (in the top plot) provides a poorly distributed set of teaching points for estimating the thermal state in data set 10 (middle plot). This is observed from the binary knowledge signal which shows large areas with a low output. Even from observing the thermal votes given in the teaching data there are relatively few points with values around 0 from which to learn from, in comparison to the many points around 0 in data set 10. The way the estimator was set-up, in terms of the MIN and MAX values on the universes of discourse, means that it is quite likely that the estimator is operating close to the saturation limits. The peak values at around 2000s and 4000s do show fairly accurate evaluation. The lower plot, data set 11, does not have the same problems as data set 10 and the estimator's estimate of thermal state is much more accurate.

The results from figure 5.8 are very encouraging, especially from data set 11. This was after passing the estimator through the teaching data only once, compared to the neural network which was trained 500 times on the same data. However, in the simulation environment it is possible to take the same estimator and pass the same teaching data back through it. The

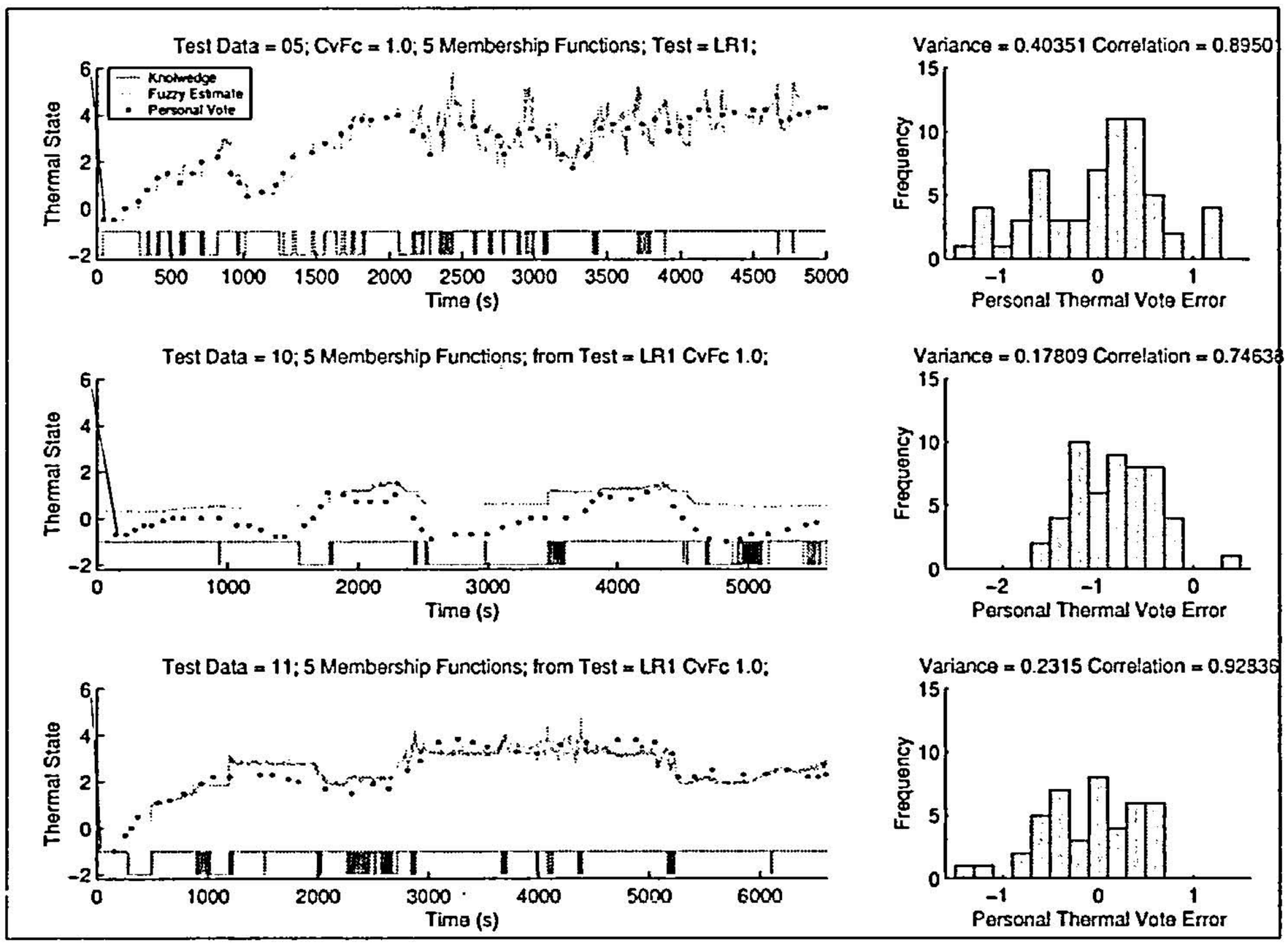


Figure 5.8: Interpolation of a taught thermal state estimator on unlearnt data sets

advantage of this is that data points that contradict each other when using a convergence factor of 1.0 can be separated out slightly by applying a lower convergence factor. Thus after training an estimator speedily using a convergence factor of 1.0 the estimator can be retrained (with the same data) using a lower convergence factor to fine tune the response. This is demonstrated in figure 5.9. After teaching the estimator with a convergence factor of 1.0 it is re-taught using a convergence factor of 0.5 and then re-taught again using a convergence factor of 0.1.

The benefit of relearning with a lower convergence factor is clearly seen from figure 5.9. The large noise of the estimator's output in the upper plot is reduced in the lower plot. The variance of the error is reduced and the correlation is increased. The final estimator, after being passed through the teaching data three times, seems to provide a much more desirable estimation. However this also needs to be tested on the verification data. Again the learning rule is turned off and the "over-trained" estimator is applied to data sets 10 and 11, see figure 5.10.

The extra learning the estimator has received has seemed to increase its accuracy in estimating the thermal state, even with data set 10. The middle plot in figure 5.10 still shows that data set 10 is suffering from a lack of representation in the teaching data. Both the results of data sets 10 and 11 in figure 5.10 are improved from those shown in figure 5.8.

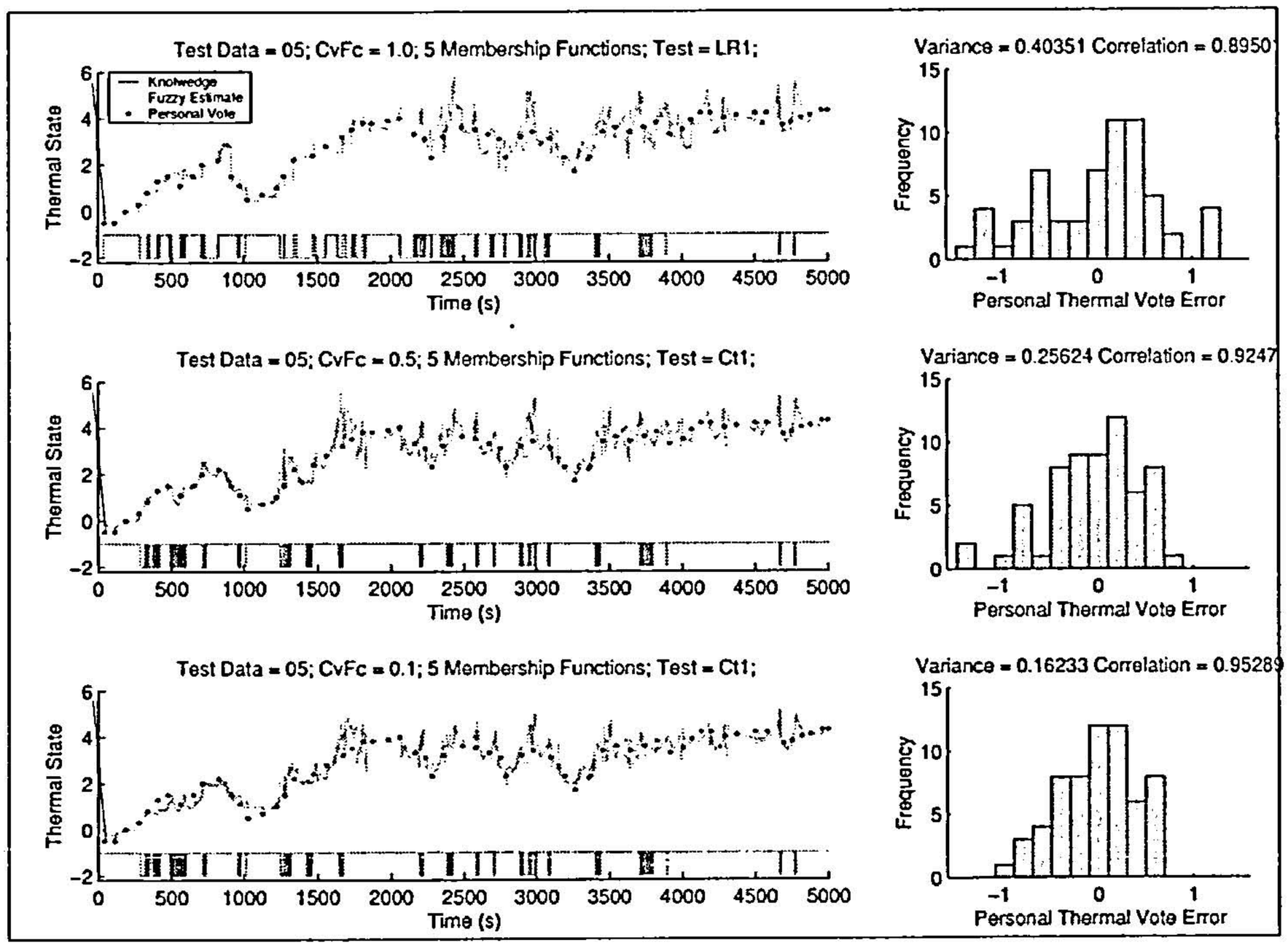


Figure 5.9: Demonstration of relearning with reduced convergence factor

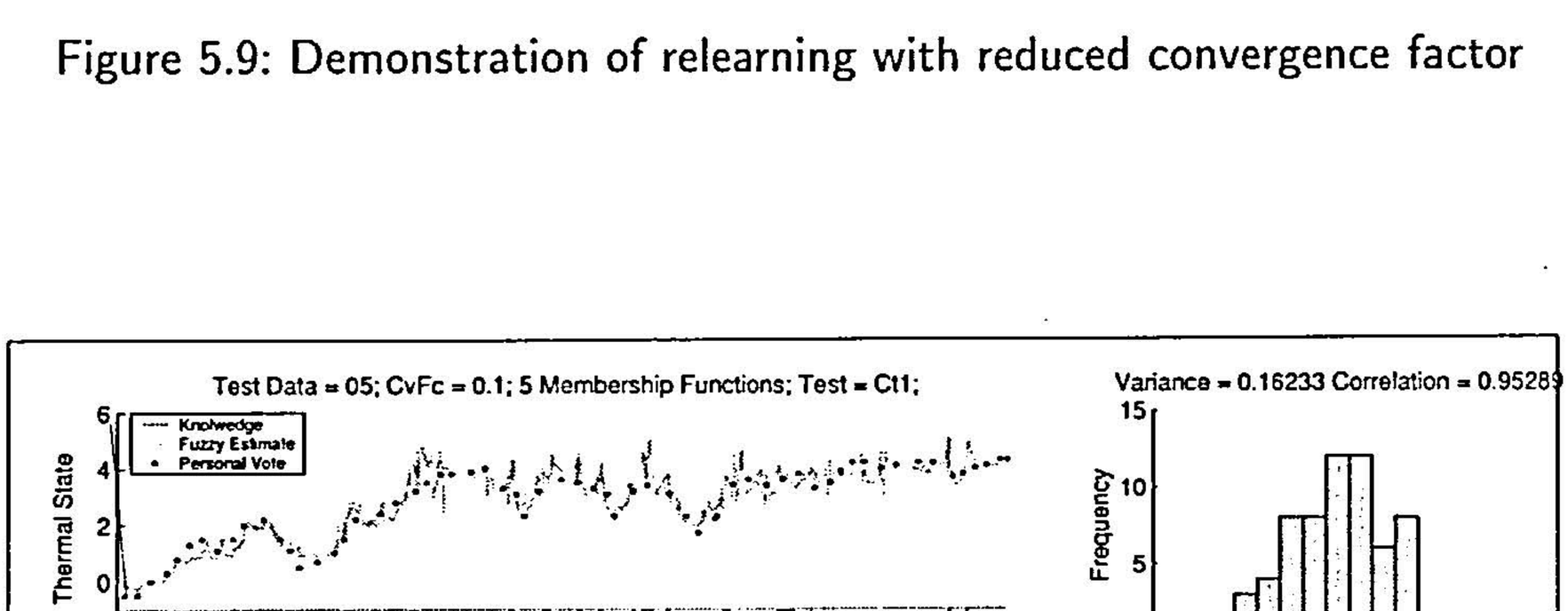


Figure 5.10: Interpolation of an over trained estimator on unlearnt data sets

The results from data set 10 in figure 5.10, although showing an improvement, still contain large areas of data where the estimator has no information on which to base an estimate. The teaching data can be stretched to cover more states by reducing the number of membership functions. This will, however, have a converse effect on the maximum operational performance due to the competition between points, for the same elements in the rule base matrix. The simulation was run again but with an estimator that was initialized with three membership functions on each universe of discourse. The teaching performance is presented in figure 5.11 and the verification is presented in figure 5.12.

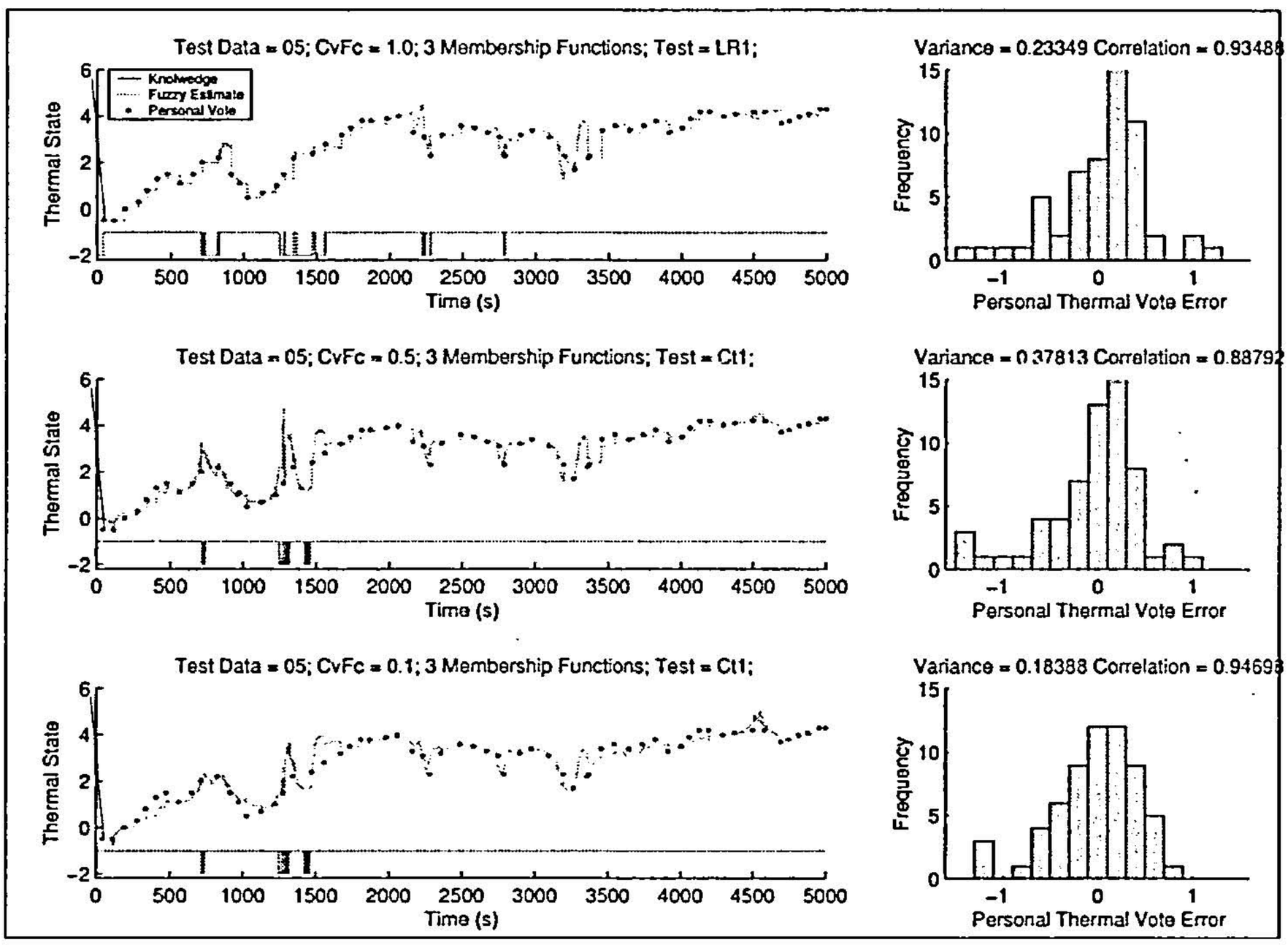


Figure 5.11: Demonstration of relearning with reduced convergence factor and fewer membership functions

An advantage of reducing the number of membership functions is that it reduces the required memory size of the estimator. This will reduce the hardware cost of implementation. However, as seen in figure 5.11 the correlation figures are not as good as those presented in the same test but with 5 membership functions, figure 5.9. An interesting result from the estimator with only 3 membership functions during learning is that the second learning phase (middle plot, figure 5.12) seems to have made the correlation worse. It should be realized that because the estimator started with no knowledge of the interactions the correlation of the upper plot is very much dependent on the spacing between the points. The stair pattern at the beginning shows that the estimator was unsure of the correct response but that the error was never very great. Because the estimator has only 3 membership functions due to the choice of symmetrical triangular input membership functions at least 2 will be active for

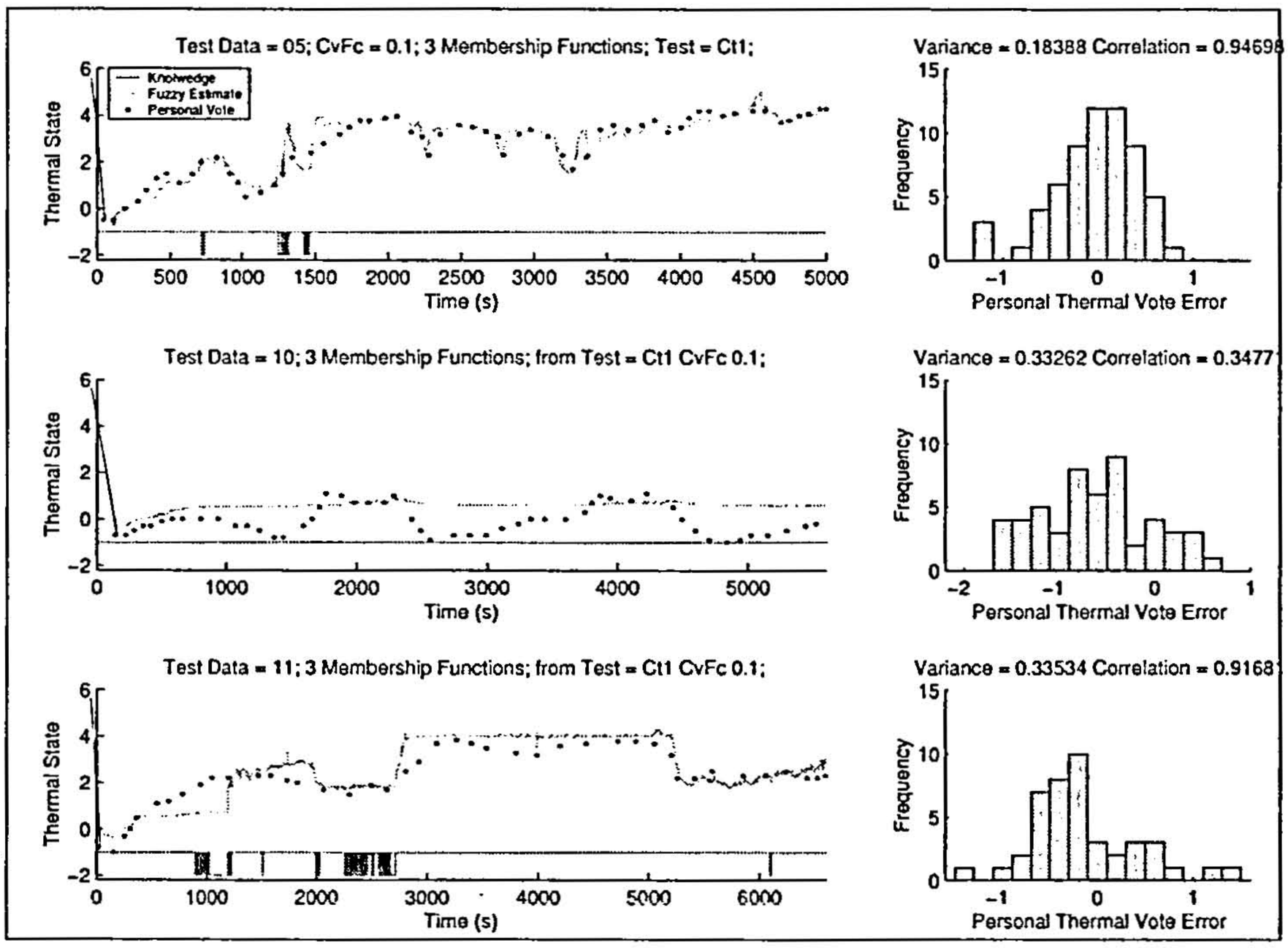


Figure 5.12: Interpolation of an over taught estimator with fewer membership functions on unlearnt data sets

each input. With the convergence factor set to learn at a fast rate both active membership functions will be fully modified, irrespective of premise values, corresponding to the error. This leads to a lot of modifications many contradicting the others. The result in the middle plot of figure 5.11 shows the effect of this. Once the estimator is relearnt with the smaller convergence factors the correlation is improved again. The distribution shape of the final histogram in figure 5.11 is more like that of the normal distribution than any other.

To finish the analysis some results were gathered using a modified learning rule. Up until now the learning rule that has been applied has been the rule expressed in equation (5.13) with the error term calculated from equation (5.10). The results so far have been good and equation (5.13) has proved to be a very versatile learning rule. The error term however is not so specific to the location of the rule base matrix and so for the next set of results was replaced by equation (5.15). Five input membership functions are used again across the input universes of discourse. The results are illustrated in figures 5.13 and 5.14.

The results show a less noisy output in the learning data in figure 5.13 and in the verification data in figure 5.14. In terms of the correlation values the results are the best yet both in the learning performance and the verification plots. The modification to the error calculation has the same effect as reducing the convergence factor, i.e. making the learning rule more specific

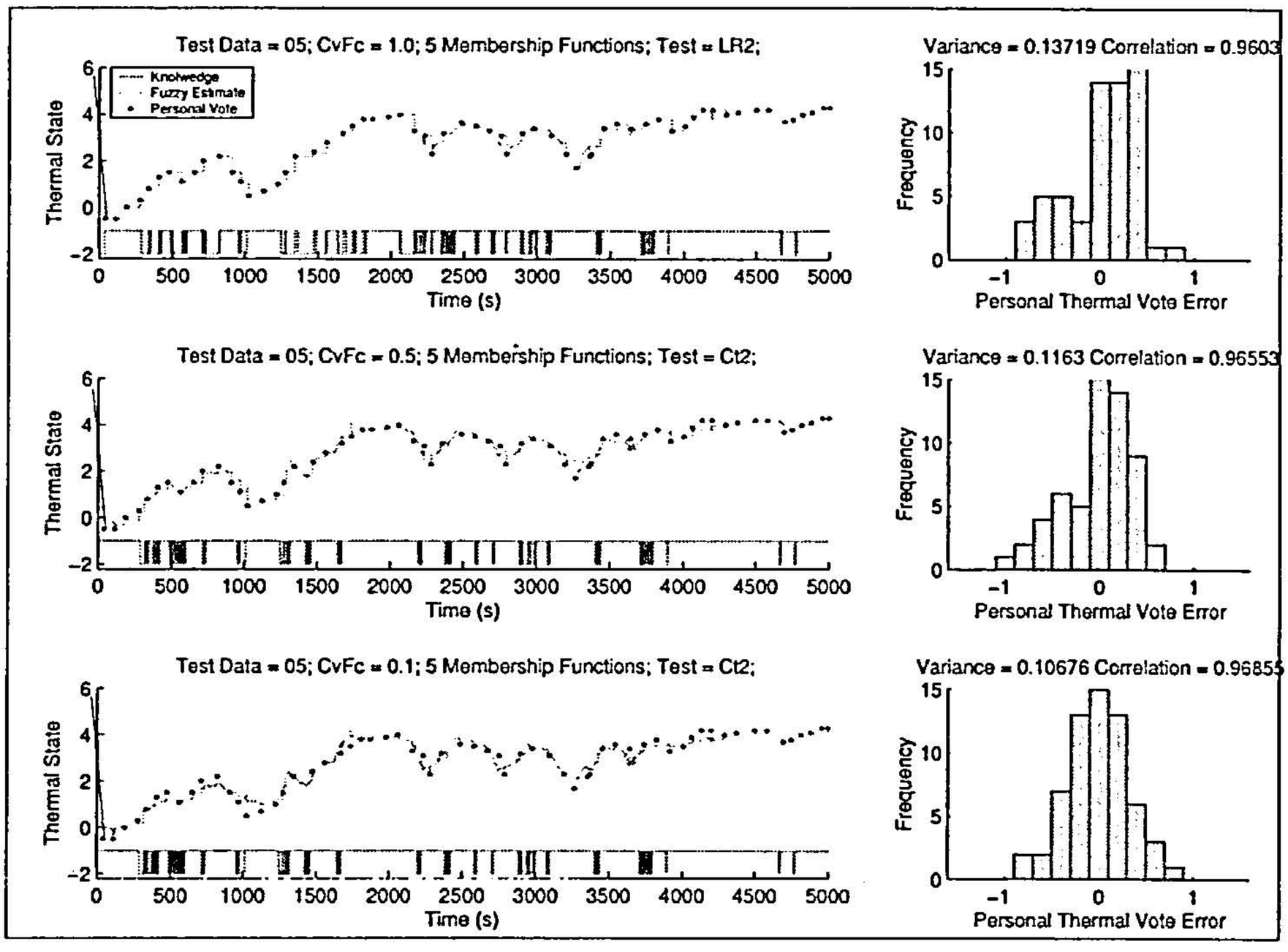


Figure 5.13: Demonstration of relearning with reduced convergence factor using a modified learning rule

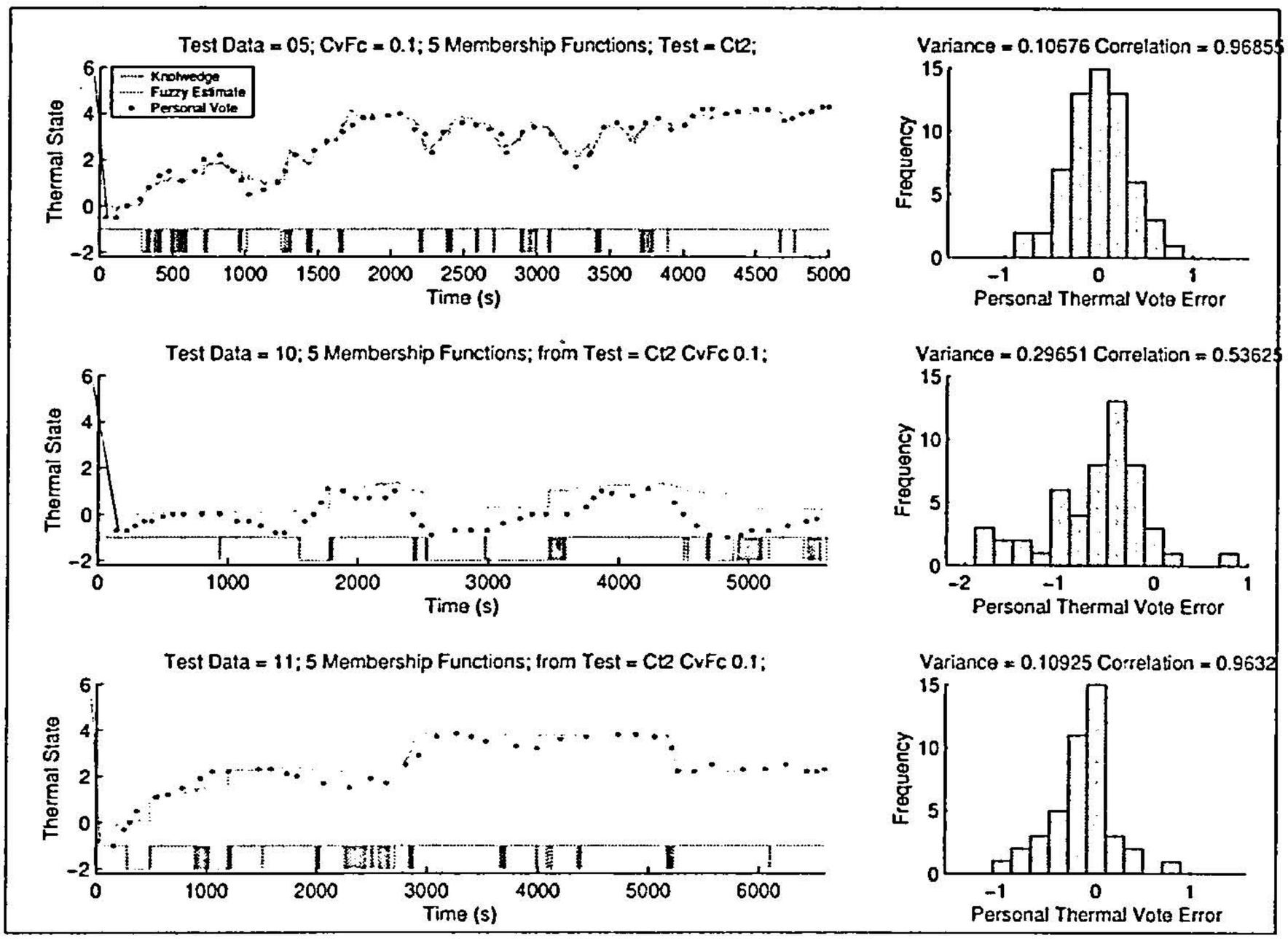


Figure 5.14: Interpolation of an over taught estimator with a modified learning rule on unlearnt data sets

to individual rule base elements, but without the disadvantage of slowing the learning process down. However, in the application of thermal state prediction, it may be more desirable not to make the learning rule too specific. Since the estimates of the test subject are susceptible to an error band relating to how accurately the user can interpret thermal state, the estimator should not assume to be too specific and a certain amount of competition between data points should be allowed.

#### Discussion

The effectiveness of the test subjects in estimating their own thermal state may start a discussion on how refined the estimator should be. This is more of an issue about the number of membership functions than about making the learning rule more individual. Reducing the number of membership functions will reduce the number of elements in the rule base matrix and will increase competition from teaching data points for those elements. This will help to even out rogue data points and reduce the need for the user to be as accurate in estimating thermal state. Reducing the number of membership functions also has the added advantage that it reduces memory size requirement in the hardware. The disadvantage is that the maximum obtainable operational performance is reduced by compromising the estimator's accuracy.

The input data to the estimator was unfiltered and contained a lot of noise which can be seen to have affected the output of the controller. The additional passes through the teaching data has helped to make this noise less significant and it is suggested that an even better performance could be achieved by filtering the inputs.

### 5.5.2 Learning Desired Outlet Temperature from User Interactions

#### Aim

So far the FURLC method's ability to learn and interpolate thermal state has been demonstrated. This verifies, by using an on-line learning approach, that the method can be applied to learning user interactions. The second part of the experimental work is to confirm that the FURLC method can use feedback inputs, in the automotive cabin.

## Methodology

The experimental setup described in chapter 4 using the Mercedes-Benz S-Class was also used to test the FURLC method. As with the previous experiments the TSV method was used to estimate the thermal state of the subject and was used as an input into a fuzzy controller. Thus, the TSV estimation was used as a feedback term in the controller. Additionally the cabin air temperature was used as an input into the controller and was thus a second feedback term.

The controller output was the temperature setting of the car's HVAC system. The local control of the car's HVAC system was left on, as with the experiments in chapter 4. The test subjects were also given access to the temperature setting of the HVAC system through the interface panel. A diagram of the set up is presented in figure 5.15 which shows the inputs into the fuzzy controller. The diagram also shows the direct link between the user's interaction and the car's local HVAC control system.

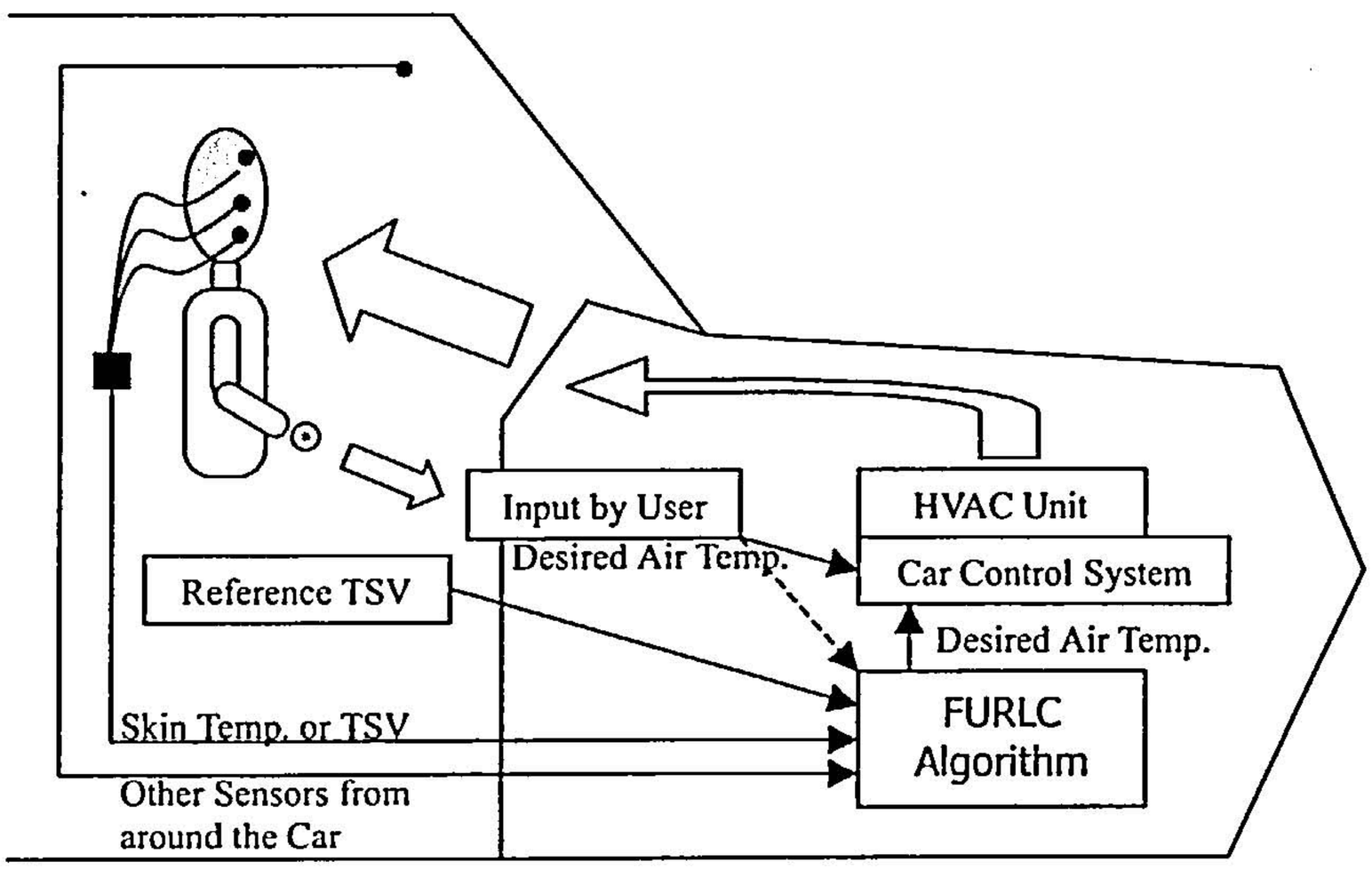


Figure 5.15: Diagram of the FURLC experiment in the car

The use of the TSV is a compact way of expressing the changes to the actual thermal state of the driver. The experiments in chapter 4 used a desired thermal state reference as the control signal. The reasons for this were explained in the chapter and for the same reasons a pre-determined reference thermal vote is used as an input to the FURLC. This reference thermal vote is also shown to the test subject who is asked to change the HVAC settings (after the algorithm has been given time to react) to feel the same as the desired personal thermal state. The reference thermal state is just a temporary replacement for a thermal comfort indicator which represents a desired shift in thermal state.

The experiment was run as follows:

1. A reference thermal vote is displayed to the user.
2. The driver is asked to adjust the HVAC settings in order that his thermal vote matches the reference as closely as possible.
3. The algorithm learns the interaction.
4. The next reference thermal vote is loaded.
5. The new reference thermal vote is shown to the algorithm first.
6. The algorithm is allowed time to react automatically and to adjust the HVAC settings.
7. Once the algorithm settles down the user is shown the new reference thermal vote.
8. The process is repeated from step 2.

### Results

Two sets of results are presented in this thesis from two different test subjects. The results are presented in figures 5.16 and 5.17. In each figure there is an upper plot with the desired air temperature as the black line and the actual measured air temperature as the light grey line. Along the bottom of the upper plots there are a series of dark grey spikes which indicate the modifications to the desired air temperature. The spikes pointing up were interactions by the controller and the spikes pointing down were interactions by the user. In the lower plots in each figure there is a black line showing the reference thermal state, the circles are the personal votes from the test subject and the grey dotted line is the calculated TSV estimate of thermal state.

The data presented in the two figures is relatively short and for each test the controller started with a blank memory. This makes it difficult to compare the results from different thermal state reference steps. One step in thermal state reference for which the algorithm knows how to interact may be followed by a step for which the algorithm does not know how to interact. Thus important observations have been highlighted by tall ellipses placed on the upper plots.

The test subjects were asked to make their interaction so as to cause their thermal state to converge with the reference thermal state as quickly as possible. It is interesting to see that in figure 5.16, at about 2200s, the initial drop in desired temperature made by the test subject is attenuated by the next interaction by the algorithm (the user then confirms this action with another slight increase in desired air temperature just after). The response by the algorithm is a cause of the feedback in the system. As the subject's TSV estimate and the internal air temperature drops the FURLC algorithm stabilizes the thermal state. The

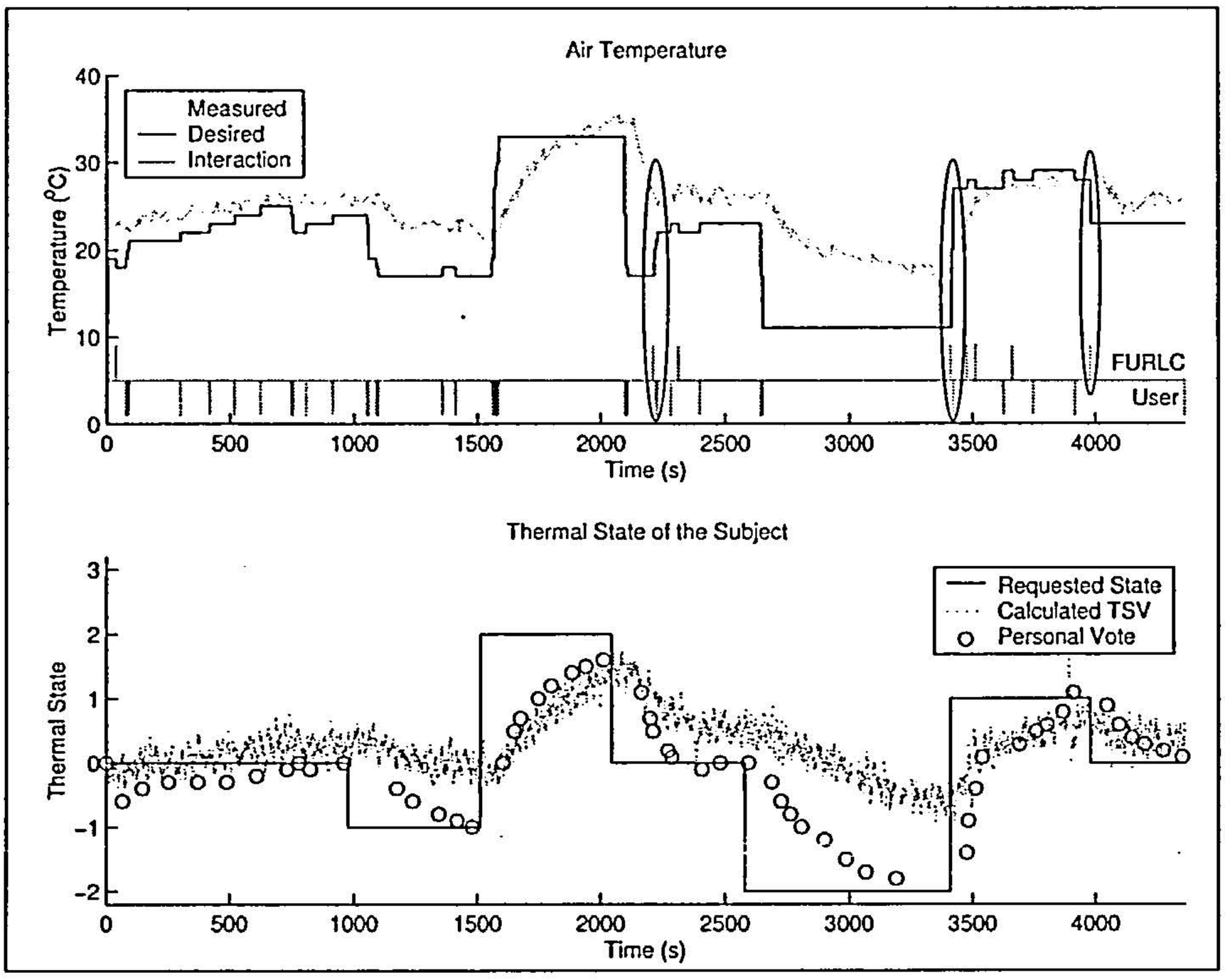


Figure 5.16: FURLC applied with feedback to learn desired temperature from test subject B

algorithm increases the temperature to the value that was learned from interactions during the initial thermal state reference.

The second elliptical highlight in figure 5.16 shows that the algorithm made the first major interaction and the third elliptical highlight shows an interaction that was entirely carried out by the FURLC algorithm. This shows the ability of the controller to learn user interactions and then to apply the interaction to major changes in thermal state in the automotive cabin.

Figure 5.17 confirms the observations in the results presented in figure 5.16. The thermal state reference follows the same path and the same three observations can also be seen in the results. This test subject make slightly more interactions and as a result so does the FURLC algorithm. The first elliptical highlight in figure 5.17 shows a similar response to the first elliptical highlight in figure 5.16 but not as obviously. The difference is because the controller is using a different set of user interactions to learn from. It is obvious from the lower plots that the second test subject is more thermally sensitive than the first test subject. This will also affect the performance of the FURLC method.

The two other elliptical highlights in figure 5.17 show that the fuzzy controller starts to

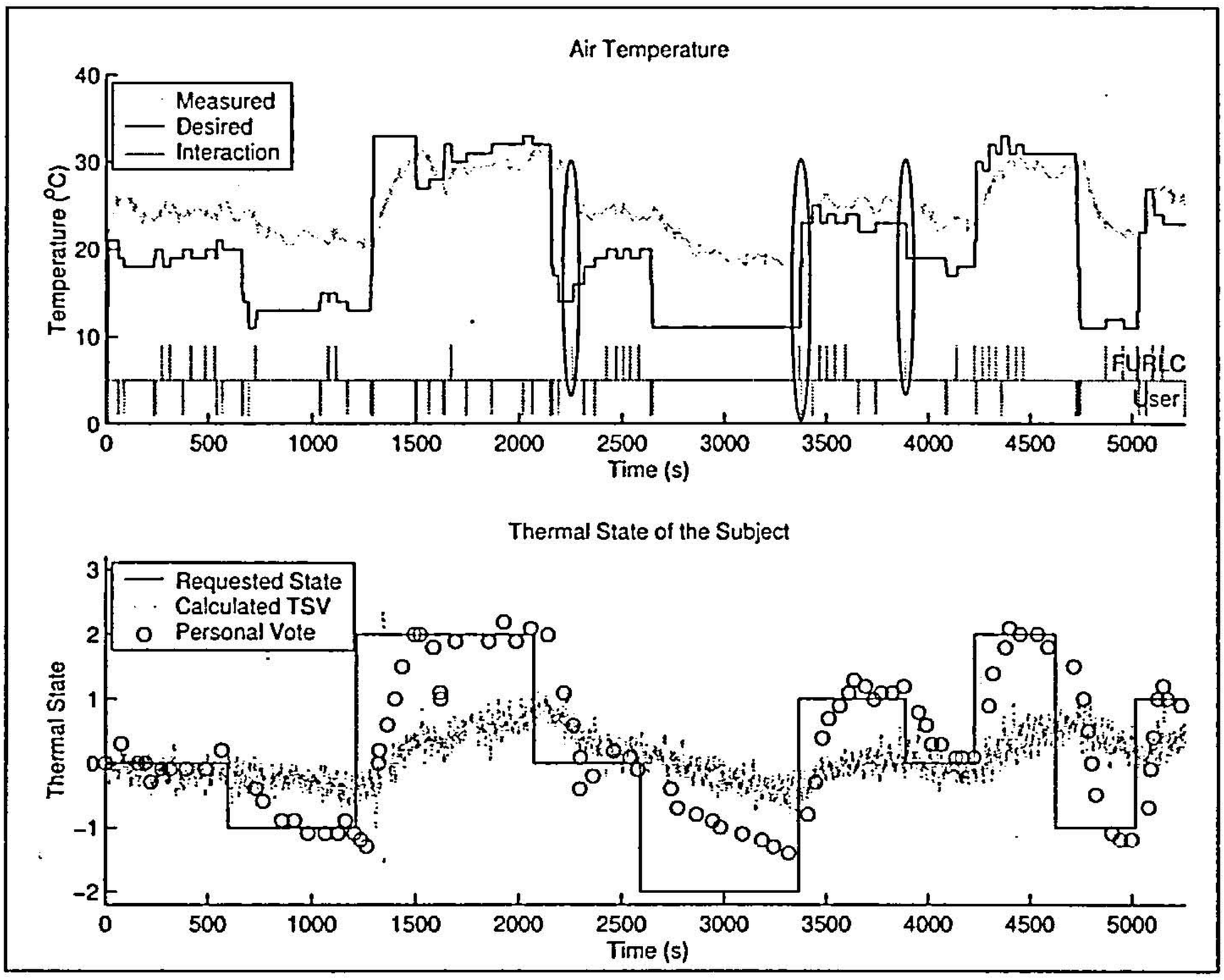


Figure 5.17: FURLC applied with feedback to learn desired temperature from test subject C

interact for the user and eventually manages to entirely make the interactions, as with figure 5.16. Note that in the cases where the algorithm makes the only interaction (highlighted by the third ellipse) the scenario is similar to the third step change in thermal state reference, and it is from interactions during this previous step that the controller learnt how to interact.

### Discussion

The reference signal, which the test subject and the controller are asked to follow, is designed to help speed up the learning of the controller so that results can be seen within the allocated experimental time frame. The number of interactions by the user provide far less data points than those used to teach the controller to estimate thermal state. The controller performance can not be expected to be as good as those seen with the thermal state estimator, however, the use of feedback variables can be seen to activate learnt control actions.

Because the controller is attempting to learn the interactions by the test subject to modify their own thermal state, the inputs to the controller also need to represent the changes in thermal state. This could be carried out by including the same inputs into this controller

that were used by the thermal state estimator. However, this would require too many inputs into the controller and so the TSV, as a compact alternative, was used.

It can also be seen by comparing the results that although the reference thermal state followed the same sequence for both test subjects the actual values of desired air temperature selected (once in steady state) are different for each person. The way the controller learns helps to preserve the individual user preference.

## 5.6 Discussion on FURLC

The benefit of using a fuzzy controller is that it allows for the specific localization of data learning. Since only stimulated rules are on at any one time then only these (and perhaps the surrounding rules) are used to modify specific parts of the rule base matrix.

In most forms of control synthesis a plant model is required such as the models identified in chapters 2 and 4. Even neural networks have a representation of the plant dynamics encoded into the weights of the network during learning. Considering the fuzzy logic controllers in general one might think that, in a similar way to the neural networks, the plant dynamics are encoded into the rule-base knowledge. This could be a valid assumption in the case of controllers that are synthesized off-line. However, the FURLC method seems a little deceptive because exactly the same on-line control algorithm and same control structure can be used to estimate thermal state or to learn user interactions. Because the user updates the rule base and is in essence a separate entity to the controller it may erroneously appear as if the controller is in absence of need of a representation of any plant dynamics at all. The truth is that in attempting to make the control method diversifiable and relying on the ability of the user to teach the controller, the supply of plant dynamic behaviour is made more difficult. The controller relies on the chosen inputs, and the user's recognition between the desired output and those inputs. The inputs then must correlate to the output and thus the inputs must transfer information about the plant. Not only this but the user must also recognize the relationship between the inputs and what the output should be. Thus the information about plant dynamics are encoded into the controller by the choice of inputs and the user teaches the relationship, as the user sees it. If the user starts to react to a variable that is not represented by an input, the controller's performance will start to deteriorate. An input that has no relation to the output will not cause the controller's accuracy to fall but it will slow down the learning process because it will increase the size of the rule base matrix making more elements to fill up.

The choice of membership functions used for each input is also an important decision made by the control engineer in designing the controller. Too few and the controller performance is compromised, too many and then it takes longer for the controller to learn enough to be useful. The choice of how many membership functions to use is also dependent on the choice of the expected range of the input and on the expected reaction by the users for that input. For example, humidity only really affects thermal comfort at extreme levels and so this input could probably consist of only three membership functions representing high, low and normal. A thermal state input such as TSV which is highly related to the change in thermal comfort may be better having a larger number of membership functions.

Note that when dealing with personal feelings such as thermal state there are additional disturbances from within the human body that may lead to a choice of extra inputs such as a "time of day" variable.

## 5.7 Conclusions

This chapter aimed to examine the use of information supplied during the user's interactions to personalize the control response. Previous work on this topic has given some results to suggest that it is possible. The motivation of this chapter led to the innovation of applying a variation on Fuzzy Model Reference Control (FMRLC), the new method was termed Fuzzy User Reference Control (FURLC) and was investigated through experiments.

The FURLC method has been shown to learn and then interpolate thermal state and is better than the neural network solution after only one pass through the training data. Subsequent passes through the training data make it even better. The effects of modifying the convergence factor shows improved performance as has modifications to the learning rule.

The FURLC algorithm learns on-line and can use sporadic input from a human operator. A second verification experiment in a Mercedes-Benz S-class test car showed successful use of the FURLC method with feedback inputs. It was demonstrated that the controller can learn to interact for the user. The way the controller operates also shows that it preserves individual user preferences.

It was also expressed through discussion that the inputs into the controller and the number of membership functions for each input needs careful consideration when designing a specific controller. The experimental results show that this can be done, certainly in the application of the control over the desired air temperature of an automotive HVAC system for control

of the thermal state. To extend this functionality to the control over the air flow rate of the same HVAC system is not expected to cause any additional problems.

# Part III

# Systems Level Analysis

# 6 Systems Level – Design of a T.S. Gizmo

The aim of this chapter is to investigate the microprocessor performance of the implementation of the TSV and PMV thermal state estimation methods and the state-space control and FURLC methods. The performance is measured in terms of the time taken to complete one loop of the methods algorithm code together with the size of the code and the memory required by the methods for local variables.

The fuzzy algorithm took the least amount of time to execute. The TSV method had the least amount of code being only a linear regression equation. The PMV code needs the most space. The active memory needed by each method showed that the TSV is again the best with the fuzzy model the worst when including the size of the rule base matrix.

This chapter contributes a systems level performance comparison between the thermal state estimation methods. It also provides a realization of the typical amount of resources required at the systems level for thermal state estimation and control.

## 6.1 Introduction

### 6.1.1 Aim of the Chapter

This chapter will investigate the implementation issues involved and inspire some systems level appreciation by examining the operation of thermal state estimation algorithms and control methods in a microprocessor. The hardware is housed in a small hand held device called the "Thermal State Gizmo" or TS Gizmo.

The purpose of the TS Gizmo is for sensor acquisition and estimation of thermal state, in most environments but in particular in the automobile. Thermal state estimation of the driver and passengers is a common evaluation and is used to help provide reference signals to the heating and air-conditioning systems. The performance of the microprocessor in the TS Gizmo will be measured.

The aim of this chapter is to examine the requirements for thermal state acquisition in terms of system hardware. Performance measurements will be made on the functions used and on the CPU to determine the workload demanded by the algorithms.

### 6.1.2 Background

Previous attempts at thermal state estimation devices have been presented in the literature such as [48] by Kang et al, which provided a PMV evaluation device. Utilizing only the PMV thermal state approach means that the device is inhibited by the same disadvantages as the PMV thermal state approach. It has already been stated that the PMV approach has no direct measurement from the person involved and with assumptions of steady state the device is only really useful in slowly changing environments using sensor data averaged over the previous hour. It has been shown in chapter 3 that these requirements can be relaxed while maintaining fairly accurate results in a dynamic environment and Kang et al [48] stated in their paper that their device is suitable for the automotive application as well as for home and office space.

As stated in [49], the fundamental motivations for the integration of microelectronics into automotive systems are:

- Increasing functionality and performance.
- Decreasing cost.
- (Political sanctions and requirements such as emission restrictions).

> "Performance can be defined as the ability to perform a specified function with increased precision, as well as the ability to perform a larger number of functions in a given time period."

The paper goes on to explain that better microelectronics can help improve performance by:

- More complex and accurate interpolation methods.

- Acquisition and evaluation of a greater number of sensors.
- Allowing a larger database to search from.

Alternatively the number of sensors can be reduced by relying on computationally derived data. For a more expensive microprocessor the reduction in sensors may provide a less expensive solution. Software implementation of hardware components can also reduce cost and allow standardization of system components throughout vehicle models reducing system development time and cost.

There exists an optimal compromise between using more sensors and computing derived data using less sensors. The solution will be unique for individual applications and thus a TS Gizmo can help to find this solution for car manufacturers.

## 6.2 Description of the TS Gizmo

The usefulness of the TS Gizmo, with the advantage of being portable, is that it can be used to test the appropriateness of the observation of thermal state and can then be used to compare different thermal state estimation techniques with different setups of sensor types and positions. The TS Gizmo is designed to be more versatile than the device proposed by [48]. Currently the TS Gizmo is programmed with the PMV, TSV and fuzzy logic thermal state estimation methods and is more flexible in terms of functionality with programmable input channels. The state space control algorithm used in chapter 4 was also programmed into the device.

To start the design of the TS Gizmo a list of specifications was conceived:

- Should be a hand held device → Small
- Should run from battery and mains → Power efficient.
- Should give accurate measurements from the sensors → good resolution on AD conversion and good specification on the sensors.
- Should be applicable to the experimentation in the automotive application → Link to CAN and serial port.

### 6.2.1 Selection of Hardware and Hardware Issues

Main Components:

- CPU MC9S12DP256 of the HCS12 family running at 8 MHz
- Keyboard / On-Off Switch
- Display
- Power Supply / Battery Compartment
- Sensor Input Interface
- (AD Conversion unit – Part of CPU)
- Output Control Signal
- Serial Port and CAN Port Communication with the TS Gizmo

The display chosen was a Powertip Alphanumeric dot matrix LCD with a 2 row x 16 character display area. The display has a standard 8 bit ASCII interface utilizing Chip-on-Board technology. The display has a variable LCD brightness and an LED back light however the back light was disabled to reduce power consumption. The display could be programmed to activate only when needed so as to save battery life.

The keypad is a 4x4 grid of keys that operate 8 pins, as shown in figure 6.1 below:

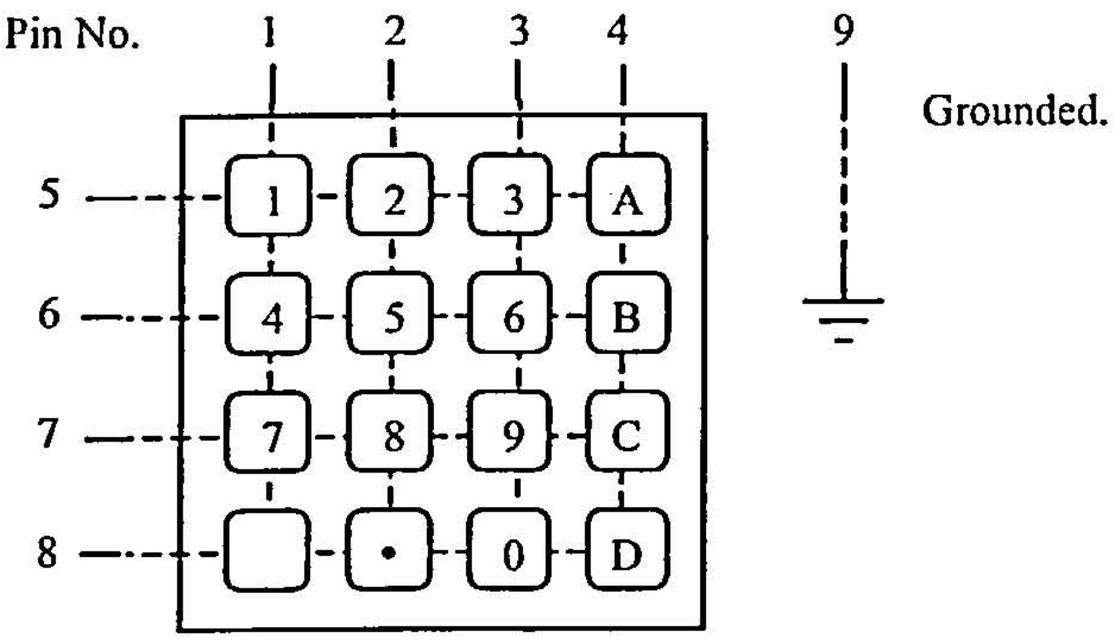


Figure 6.1: Illustration of Keyboard and association of output pins

To test for a key press pins 1 to 4 are turned high and pins 5 to 8 are scanned for a high. If a high is found then this initiates a more detailed search for the correct key. Pins 1 to 4 are sequentially made high and pins 5 to 8 are scanned for each case. When a high is found then the combination of which pin was turned high (1 to 4) and which pin reads a high (5 to 8) corresponds to the key that is pressed. This operation is done so quickly that the keyboard can be fully scanned many times during even the briefest touches by a human user.

The temperature sensors are the same as those used in the experiments described in chapters 2, section 2.2.2, consisting of up to 5 skin temperature sensors and 3 air temperature sensors. The temperature sensors are in the form of thermistors, which relate resistance to

temperature, so it is thus necessary to determine the resistance of the sensor from the voltage measured across it (see equation (2.1) in chapter 2). The evaluated resistance is then cross-referenced with a look-up table to determine the temperature (see table 2.1 in chapter 2). All the reference resistors are housed in the same casing block and have been, are, and will be, exposed to similar environments.

Note that although the TS Gizmo is being set up to read thermistor resistances it should not be too difficult to connect alternative sensors to the TS Gizmo in such a way that the resistance can represent the property being measured.

Previous experiments with these temperature sensors has suggested that filtering of the sensors may be required and this can be done with hardware or software. The sensors are interfaced through an AD conversion module to provide the inputs into the TS Gizmo, alternatively a CAN connection allows direct access to the automotive communication bus which could allow the Gizmo to use the car's own sensors.

With the set up suggested the voltage across the reference resistor will be a constant drain on the power supply, thus wasting power. This is improved by connecting each resistor with its own power supply which can be switched on when a sensor is connected or even only when the sensor is being read. There is also an internal drain on the power supply which means that it is not at maximum when it is pulled across the sensor and reference resistance. The supply voltage can be measured by switching it across the AD converter directly.

Insight into the choice and set-up of the AD converter can be obtained from an equation presented in Chapter 3, equation (3.13) restated below as equation (6.1). The equation was derived from the TSV thermal state estimation method and equates facial skin temperature to a thermal state estimate. As the TSV method is implemented in the TS Gizmo the equation can be used appropriately.

$$tsk = \frac{TS + 27.5}{0.81} \tag{6.1}$$

Limiting the range of thermal state values between $\pm 2$ will result, from equation (6.1), in a skin temperature range between $31.48\,^{o}$C and $36.42\,^{o}$C. From the data about the skin temperature sensors given in section 2.2.2 in chapter 2 and by applying a $5^{th}$ order polynomial interpolation to table 2.1 this results in a range of resistances between $7565.79\Omega$ and $6158.75\Omega$. Using a reference resistance of $1000\Omega$ and a supply voltage of 5 volts gives a voltage range between 0.5837 and 0.6984 volts from equation (6.2) below, which is a rearranged version of equation (2.1) in chapter 2.

$$V_m = \frac{V_s \cdot R_r}{R_T + R_r} \tag{6.2}$$

For skin temperature sensors that are accurate to $\pm 0.2\,^oC$ the minimum AD resolution required for the most accurate reading is $\pm 0.0044$ volts (using the difference between $31.48\,^oC$ and $31.68\,^oC \Rightarrow 0.5881$ volts). Conversely if the acquisition resolution is set then the maximum sensor accuracy could be calculated so that more sensitive (more expensive) sensors need not be bought. The reference resistance and supply voltage are chosen to maximize the voltage range from the sensors to that allowed by the acquisition card. For example using a reference resistance of $10000\Omega$ and a supply voltage of 10 volts gives a 0.496 volts voltage range with a minimum resolution of 0.0194 volts (using the difference between $36.22\,^oC$ and $36.42\,^oC$). Using equation (6.2), table 6.1 was created which shows different set up configurations:

| Temperature ($^oC$) | 31.48 | 31.68 | $\Leftrightarrow$ | 36.22 | 36.42 |
|---|---|---|---|---|---|
| $R_T$ ($\Omega$) | 7.5658 | 7.5022 | $\Leftrightarrow$ | 6.2096 | 6.1588 |
| With $V_s = 5$ and $R_r = 1000$ | | | | | |
| $V_m$ in volts | 0.5837 | 0.5881 | $\Leftrightarrow$ | 0.6935 | 0.6984 |
| Difference | 0.0044 | | $\Leftrightarrow$ | 0.0049 | |
| With $V_s = 5$ and $R_r = 10000$ | | | | | |
| $V_m$ in volts | 2.8464 | 2.8568 | $\Leftrightarrow$ | 3.0846 | 3.0943 |
| Difference | 0.0103 | | $\Leftrightarrow$ | 0.0097 | |
| With $V_s = 10$ and $R_r = 10000$ | | | | | |
| $V_m$ in volts | 5.6929 | 5.7136 | $\Leftrightarrow$ | 6.1692 | 6.1886 |
| Difference | 0.0207 | | $\Leftrightarrow$ | 0.0194 | |

Table 6.1: Operational resolutions by choice of $V_s$ and $R_r$

The AD converter can be optimized to save power by regulating operation to run only when required rather than all the time. Similarly algorithm code can be optimized to save power by running only when required. This will optimize processor bandwidth and reduce the power consumption. Knowledge about the software demands on the processor can help in deciding the correct CPU frequency speed to use.

The serial connection was included to allow uploading experimental results to an external storage device. The CAN link also allows a control algorithm to interact with the car's own systems.

### 6.2.2 Functionality and Issues of Software Architecture and Configuration

The software was written in C and optimized by a pre-compiler. Some of the options on the optimizer were turned off because of "over optimization" errors.

The software architecture can be described in terms of functionality. The software was divided into separate groups classified as follows:

- Keyboard Drivers
- AD Drivers
- Gizmo Functions
- Menu Functions
- Display Drivers
- Output Drivers

The keyboard drivers and menu functions ran on separately configured interrupt routines. A high frequency interrupt was used for the keyboard drivers, which have a simple job of testing the keyboard for a pressed key. When it finds a pressed key it stores the key identification. The AD drivers are used to get the most recent values stored in the AD buffer.

Gizmo functions contain the main computational algorithms for the thermal state estimations and the controller outputs. The results from these functions are stored into a shared memory. The gizmo functions ran in a continuous loop, apart from when being interrupted. Temperature interpretation was coded into the gizmo functions group. The sensor look-up table was interpolated with a 3rd order polynomial. The TSV and PMV thermal state estimation methods were coded into the Gizmo functions. A State-Space controller was also programmed into the gizmo functions group, the same controller that was used in chapter 4. The output of the controller was not used, and the function was only used to test the required processing power. For a similar reason the FURLC method was also programmed into the gizmo functions group.

The Menu functions used a less frequent interrupt routine in comparison to the Keyboard drivers. The menu functions are used to interpret the keyboard input and provide the desired display information. The Display drivers are called by the menu functions and are used to write the desired message to the display. The dot matrix display drivers required a lot of time, relative to other operations, in order to update the display and this limited the effective speed of the menu functions interrupt.

Communication between the groups of functions takes place via the shared memory. The format for the shared memory is a single C structure variable, which comprises of substructures each representing the results of different functions. Each substructure contains a semaphore for write-operation protection.

In addition to the main operational functions a timer function was also included in order to examine the performance of the other functions. This timer will be explained later when discussing the performance experiments.

Most of the computations programmed contain floating point calculations. Floating point calculations are not 100% accurate and it is apparent that at some stage the floating point value has to be rounded when converting for binary calculations. This is a well discussed problem and has been given special attention by the IEEE in the form of a set of standards to which floating points should be represented.

## 6.3 Experimental Work

### 6.3.1 Examination of System Performance - Timing of Functions

Deciding on the type of hardware to use will depend on the desired performance-cost combination. Slower, smaller components will be cheaper but obviously performance will be reduced and vice-versa. The choice of components is usually application based. Information on issues that affect the choice of components is of interest to both the automotive manufacturer and the supplier of the system components. The aim of this experiment is to provide some useful information about the demands on the system hardware.

#### Methodology

In order to investigate the speed of computation a method for timing individual function routines was programmed into the TS Gizmo. An internal clock timer was the preferred method and involved setting up an extra interrupt function to increment an integer counter. A value could be read from the counter before the start of a function call and read again after the end of the function and the difference would be the time taken during the calculation of the function. A separate function, called a stopwatch, was programmed to do this. The stopwatch function returned 2 integer values to represent the number of elapsed milliseconds and elapsed microseconds.

The internal clock interrupt was actually set to increment the counter after slightly more time than the counter value represented. The difference was the time taken by the clock interrupt itself so that the counter represented the total time that the processor was engaged in the real computation without measuring the time taken by the clock interrupt.

Because the software includes a few other interrupts these had to be disabled before starting the stopwatch and then enabled once the stopwatch had been stopped.

**Results**

The stopwatch function was designed to capture the time between the "StartWatch" and "ReadWatch" commands and not to include any time taken by these commands. When using multiple stopwatches however no account of the others is taken and so the time for the "StartWatch" and "ReadWatch" commands of other stopwatches had to be subtracted. The time taken by these commands was found by overlapping 2 stopwatches with no other commands in between:

- StartWatch(1)
- StartWatch(2)
- ReadWatch(1)
- ReadWatch(2)

Results:

- Watch(1) = 0.005 ms : Time taken for the "StartWatch" command
- Watch(2) = 0.010 ms : Time taken for the "ReadWatch" command

The stopwatch commands were used to time the functions. Because processor times can vary depending on operational events (such as iterative loops), the functions were timed 10 times and the averages were calculated. The results are presented below:

- StartUp() = 33.307 ms
- Recorded from within StartUp():
  - GetChVal() = 4.619 ms

  - FURLC_Out() = 4.588 ms

- ReInitialize() = 39.937 ms
- Recorded from within ReInitialize():
  - GetChVal() = 4.929 ms
- Main Loop (with StartUp) = 140.152 ms
- Main Loop (without StartUp) = 66.770 ms
- Recorded from within the Main Loop
  - GetChVal() = 4.929 ms
  - GetTSV() = 7.280 ms
  - GetPMV() = 20.300 ms
- Controller() = 5.543 ms
- FURLC_Out() = 4.586 ms

The StartUp() function and the ReInitialize() functions have similar purposes and involve initializing or re-initializing parts of the shared memory which included the large matrices used in the fuzzy logic method. It takes almost 5 ms to extract a sensor value (GetChVal()). The PMV method (GetPMV()), with its iterative algorithm took the most processor time, 20.3 ms. The TSV function (GetTSV()) took 7.3 ms but most of this is due to the calculation of the rate of change of the skin temperature from a history of values of the skin temperature. The main FURLC function (FURLC_Out()) took the least amount of time of 4.6 ms. The state-space controller function (Controller()) needed 5.5 ms.

### Measuring function times with a scope on an output pin

Because the stopwatch commands relied on an interrupt call, they were not easily implemented within other interrupt functions and so the timing of these functions needed to be done in another way.

Another method of measuring the time taken by a function is to directly wire an oscilloscope to an output pin and to set the pin high when the function is on and low when the function is not running. The time taken by the function can then be directly read off the oscilloscope screen. With this method the smaller the time taken by the measured function the more

accurately the duration can be read. This approach can only be used while measuring time within loops because the oscilloscope that was used could only show measurements in real time (could not pause the screen). This is suited to the measurements of code within the interrupts which are frequency dependent.

The UserInterface() function updates the display with the correct menu display. The UserInterface() is the main calling function for the display and so recording the time of this function will also be the total time used to update the display. The display functions are very time dependent on specific displays and on the number of changing digits, some will take longer than others. This also means that swapping between displays (where a lot of digits are changed) will be quite time consuming. Thus timing the UserInterface() function will result in a variation in times depending on what is happening to the display.

Time measured for the UserInterface() function: min time $\approx$ 160 $\mu$s: max time $\approx$ 4 ms. Usually, when left idle the routine will take between 160 $\mu$s and 600 $\mu$s.

After taking out the actual display routine to leave just the menu finder (Menu_Main), the time measured for the Main_Menu() function was: min time $\approx$ 9 $\mu$s; max time $\approx$ 260 $\mu$s.

Measuring the other functions with the oscilloscope gave the following results:

- GetTSV() $\approx$ 7.4ms (7.2ms to 7.5ms)
- GetPMV() $\approx$ 20ms to 21ms
- Controller()$\approx$ 5.6ms
- FURLC() $\approx$ 4.6ms

These confirm the results measured by the stopwatch function.

### 6.3.2 Memory Requirements

Memory requirements covers 2 meanings: the storage of the function code and constant variables on the chip's flash memory, and the amount of RAM type memory needed by a function to handle its local variables. The storage requirements of the whole TS Gizmo code are stored for reference in a memory map file generated by the compiler after optimization of the code. From this file the relevant data have been summarised in table 6.2, along with the global variable requirements (which are local with respect to the file they are in).

| Files | Storage Memory | File local Variable Memory |
|---|---|---|
| Gizmo.c | 75 | 326 |
| display.c | 500 | 19 |
| adc.c | 241 | 0 |
| serial.c | 76 | 0 |
| timer.c | 90 | 44 |
| dac.c | 58 | 0 |
| keyb.c | 277 | 1 |
| menu_functions.c | 4426 | 1553 |
| gizmo_functions.c | 8435 | 1718 |
| ( | | S = 817) |
| ( | | FURLC.BMx = 320) |
| (Start_Up | 613 | ) |
| (Gizmo_Main | 185 | ) |
| (ReInitialize | 151 | ) |
| (StrWrt | 16 | ) |
| (GetChVal | 1887 | ) |
| (GetTSV | 507 | ) |
| (GetPMV | 2229 | ) |
| (Controller | 1538 | ) |
| (FURLC_Out | 1309 | ) |
| Total | 17645 | 3694 |
| Total Downloaded | 19457 (10 blocks) | |

Table 6.2: Memory requirements read from the compiler memory map file

From table 6.2 it can be seen that the TSV function (GetTSV()) requires the least storage memory whereas the PMV algorithm requires the most. The size of the shared memory, S, and the main FURLC rule base matrix, FURLC.BMx, is also shown.

The variables used locally within each function are presented in table 6.3. The list of the types of variables used can be quoted as a total amount of memory by referencing the list of variable allocation sizes:

- Char = 8 bit
- Short = 16 bit
- Int = 16 bit
- Float = 16 bit
- Pointers = 16 bit

These variable size allocations are not always the same and depend on the platform being used.

| Function | Char | Short | Int | Float | Structure | Memory |
|---|---|---|---|---|---|---|
| StartUp() | | 2 | | | | 32 |
| Gizmo_Main() | | 2 | | | | 32 |
| ReInitialize() | | 2 | | | | 32 |
| StrWrt() | 2* | | | | | 32 |
| GetChVal() | | 4 | 1 | 23 | | 448 |
| GetTSV() | | 4 | | 2 | TSVstruct* | 112 |
| GetPMV() | 1 | 2 | | 30 | PMVstruct* | 536 |
| Controller() (total) | | 2 | | 67 | | 1104 |
| Controller() (control) | | | | 51 | | 816 |
| FURLC_Out() | | 16 | | 18 | FURLC_Struct* | 560 |
| FURLC_Learn() | | 5 | | 3 | FURLC_Struct* | 144 |
| FURLC_Check() | | 4 | | | FURLC_Struct* | 80 |

Table 6.3: Number of local variables used in each function

From table 6.3 the controller function seems to require a lot of floating point values. The table shows two entries for the controller function, a total count of all the variables used and then a separate count for the variables that are used in the actual control method itself. The reason this is quite high is because the actual control model is stored as a variable array of floats. This could be re-coded to use defined constants which would take up only storage memory.

### 6.3.3 Discussion

The PMV estimate worked on an iterative solution and varied the most in terms of the processor time taken. The iterative loop was limited to a maximum number of iterations so that there was a hard maximum time the function would take. The PMV function only hit this hard limit when the air temperature sensor that it was using was disconnected. The times shown in the results are for normal working conditions.

Due to the reduced available time for programming, the algorithms were not written for optimal CPU performance but were written in such a way as to simplify programming and reduce debugging time. An optimizing pre-compiler was used but it is expected that a revamp of the algorithm code with the aim of better CPU performance could improve the times taken for the different functions. The results presented in this chapter, however, demonstrate a case study from which a first consideration of hardware design can be initiated. It is often the case that styles of production code also aim to increase readability and understandability of the code and reduce development time and debugging time and CPU optimization is post-development consideration.

Only the main FURLC function was tested, FURLC_Out. This is the bulk of the computation and the learning function is only activated when there is something to learn. The microprocessor that is being used does have fuzzy logic support built in. This comprises of 4 fuzzy assembly language commands. The use of these commands has been documented as being as much as 15 times faster than a program with conventional programming commands. There are some restrictions with using the built in functions, e.g. the defuzzification has to use singleton output membership functions. Nevertheless, it is expected that the FURLC functions could be speeded up using these in-built functions.

## 6.4 Conclusions

The final times indicate the amount of computation required to estimate thermal state and to provide a foundation control structure. This helps in decisions about how much extra capacity is left in the chip for other functions. For example the fastest desired sampling rate for the thermal state estimation and thermal state control may be 4 times a second, with a maximum computational time of 100ms on an 8MHz processor. This leaves a maximum of 600ms for other functions, or a slower chip could be used.

The experimental results show exactly how much more computation is required by the PMV method compared to the TSV method of thermal state estimation and the PMV iterative solution means that it is not certain exactly how long it requires, which makes real-time programming less predictable. The main code of the fuzzy controller took the least amount of time to execute. The TSV method is the shortest code and takes up the least amount of storage memory being only a linear regression equation. The PMV code needs the most space. The active memory needed by each method showed that the TSV is again the best with the fuzzy model the worst when including the size of the rule base matrix.

The FURLC method seems to compare well against the TSV and the PMV thermal state methods and it also compares well against the state-space controller. Both were used to control the thermal state in conjunction with the TSV method.

# 7 Conclusions

## 7.1 Thesis Summary and Final Discussion

The motivation for the current study is to provide an information base on which to predict the implementation of future automotive HVAC systems. The work in this thesis was carried out in cooperation with a key provider of microprocessor and data communication components of the automotive HVAC system, and with a major automotive company. Thermal state has been identified as the key technology in the future development of comfort control, which is the goal of modern day automotive HVAC control.The aim of this thesis is to provide a detailed review of the requirements involved in estimating thermal state, to investigate the control of thermal state via the cabin environment and to examine user interactions as a source of personalizing the control response.

Chapter 1 discusses the meaning of thermal state and offers the author's opinion on the definitions of some of the more frequent terms. In the discussion on thermal comfort it is recommended that a satisfaction scale should be used similar to the one in table 1.4. This is essentially an evaluation of thermal comfort based on a thermal state estimation. The two concepts are linked.

The future requirements of climate control will depend on the processes and equipment used to measure thermal state and already most luxury cars use some sort of thermal state calculation in the control of the cabin environment. This clearly sets the aims of the first part of this thesis to investigate more closely the methods and implementations used in thermal state estimation. The aim of chapter 3 was to investigate three of the more popular methods of thermal state estimation and to compare the results. The set-up and experimental design for the data acquisition used to calculate the thermal state was presented in chapter 2. Although the three methods of thermal state estimation are not new methods the results presented in chapter 3 give a detailed comparison and overview of thermal state estimation that has not been found in the research literature. In this respect this chapter provides a

novel contribution.

The experimental work continued in chapter 4 with the control of thermal state via a state-space controller designed using a pole-placement technique. This work uses one of the methods of thermal state estimation, outwith its original context, in a new way to control the thermal state of a test subject. Chapter 4 is also important because it introduces the application of thermal state control within the automobile cabin. The state of the test car's control over its HVAC system did not include any form of feedback control from the driver or passenger. However, the operation of the system was sensitive to the comfort of the occupants. This was found to have a detrimental effect on the test results. It is however an interesting consideration in the implementation of the control of thermal state and highlights added restriction in maintaining comfort.

The control of thermal state is, after all, only part of the solution. Thermal comfort is a much more difficult condition to quantify. Chapter 5 marks the beginning of the second part of this thesis because it aims to tackle thermal comfort in a new way. The idea of using the interactions from the user to identify personal preferences in thermal comfort control is only just starting to be investigated. This thesis provides a new approach to this concept in the form of a fuzzy logic method that has been designed to learn.

The method was tested by applying it to the task of learning thermal state. Because this task has a lot of background research and results from three methods were already presented in chapter 4 it was a good task for performance analysis. The fuzzy algorithm proved to be very effective. The algorithm was then applied, in a verification task, to learn user interactions for specific demands on the automotive HVAC system. The demands on the system were interpreted by a thermal state reference signal. Note that the fuzzy algorithm is not controlling the thermal state according to a reference but is learning the interactions, from a user, that depend on the difference between the current thermal state and the reference thermal state, i.e. the comfort according to table 1.4.

The final chapter provides a case study of the implementation of the algorithms used. This thesis is not just about new methods of investigating thermal state but about the types of information that are, and will be, needed and about the types of calculations used to estimate and control thermal state.

Even though the sample times of the controllers are quoted in tens of seconds and the computation times are given in milliseconds, what is important is the bandwidth required on the processor and on the data transfer bus that communicates the sensor signals with the main algorithm. The discussions on thermal state in chapter 3 also allow the contemplation of

extra sensors that might be required. The case study demonstrates that there are significant differences in computational time and hardware resources between the methods implemented.

## 7.2 Overall Conclusions

The aim of this thesis was to investigate methods of estimating thermal comfort for the passengers of an automobile with particular interest in using passenger feedback information from the HVAC system in predicting individual preferences. This has been carried out. The objective of this work was to provide an information base on which to predict future automotive HVAC system requirements from an implementation perspective. It is not the job of this thesis to predict the future requirements of implementing automotive climate control, but to provide an overview of the state of the art to show the direction that the research is going, and to provide several novel contributions in these areas.

The current state of the art in automotive climate control is centred around estimating the feelings of the user of the system. Thermal state estimation has already been shown to be quantifiable and provides a good basis on which to control the climate. The results presented in chapter 3 show the accuracies and performance of the three thermal state estimation methods, which can be used to determine future controller and computational specifications. Only a few data sets were used but the values comply with results in the literature. The types of measurements needed and the implementation issues for each method are also described. All three methods provided fairly accurate results and the PMV method seemed to have marginally better performance. This seems a little strange since it is not recommended for use in such a turbulent environment and all the input variables, except air temperature, were estimated. The TSV method was the most direct to implement and to calculate.

The control of the automotive cabin environment was demonstrated in chapter 4. The approach taken is an original contribution. However, the processes involved are standard techniques and the results from this chapter help to clarify the current ability and capacity of the automotive HVAC control systems. The results show that the thermal state of a test subject, estimated using the TSV method, was successfully controlled. It is suggested that better control performance could be achieved with certain improvements to the experiment.

One possible future development in the control of the automotive environment is adaptation via user interactions. This idea is explored in this thesis and a new concept of applying knowledge base modifiers to fuzzy logic control mechanism in order to learn user interactions is presented in chapter 5. The new idea performs well on estimating thermal state and

outperforms the neural network approach presented in chapter 3. The fuzzy control method was also tested with feedback variables. However, limited test resources meant that each test contained few data points to learn from and only a few tests could be made. The results show that the controller was able to effectively learn user interactions and automate learnt actions in a feedback control loop. User preferences were also preserved.

The final part of this thesis concludes the analysis of the implementation of control of the automotive cabin climate based on thermal state with a chapter on algorithm performance. Algorithm performance is an important issue in system level implementation and ultimately has a direct influence on the overall cost of the system. In the conclusions from this chapter the fuzzy logic approach introduced in chapter 5 is shown to maintain competitiveness with the other methods tested.

This thesis achieves its aim of providing an overview of the current state of the art in automotive climate control based on thermal state estimation. New approaches have been presented and validation results prove the methods.

## 7.3 Recommendation for Further Research

Apart from the obvious extensions of chapter 2 to include the additional sensors required for the PMV such as humidity and air flow, the draught equation could be integrated into the PMV calculation to provide a more transient solution.

Investigations into controlling the air temperature input together with the air velocity is an important step that was not possible with the equipment supplied in chapter 2. This would have made a valuable contribution to the conclusions of this thesis.

The results presented in Chapter 2 presented an interesting observation of facial skin temperature relative to the air temperature and the thermal state vote. The phenomenon observed showed the facial skin temperature of the test subjects, which were individual values at the beginning of the test, converge to the same value as the air temperature increased above the mean facial skin temperature. At the same time the thermal state jumped from a warm level to a hot level. This was briefly discussed and it was hypothesised that it had something to do with the body physiology however this observation could be investigated further.

More thermal state estimation methods could be included in the comparison in chapter 3. However, the three methods chosen together with the fuzzy method described in chapter 5 cover all the main types of successful methods presented in the literature.

Given more time with the test car used in chapters 4 and 5 might have allowed some of the problems to be overcome. The large impulse disturbances were an unexpected interference and, although it provided a good test of the controller's robustness to disturbances, it should have been removed. The unexpected effect that the car's own HVAC controller had on the experimental results could also have been investigated further. During the experiments the test car remained stationary. An experiment that was not included in this study but that had been considered was to measure the thermal state of the driver of the test car during a test drive. The aim of this experiment would have been to examine the range of thermal state feelings and the rate of change of thermal state during a typical driving session. The TS Gizmo described in chapter 6 would be the perfect tool for this job.

# Appendices

# A : Thermodynamics of HVAC

The system theory for automotive heating, ventilation and air conditioning (HVAC) has been extensively covered and consists of textbook thermodynamics, however many papers are still produced based on this application. Development of this automotive feature has been proliferate and will continue to expand for many years in the future.

In the modern day air-conditioning systems there are 6 main components. The air fan, the evaporator, the compressor, the condenser, the expansion valve and the heater. Simplistically these components fit together as shown in figure A.1.

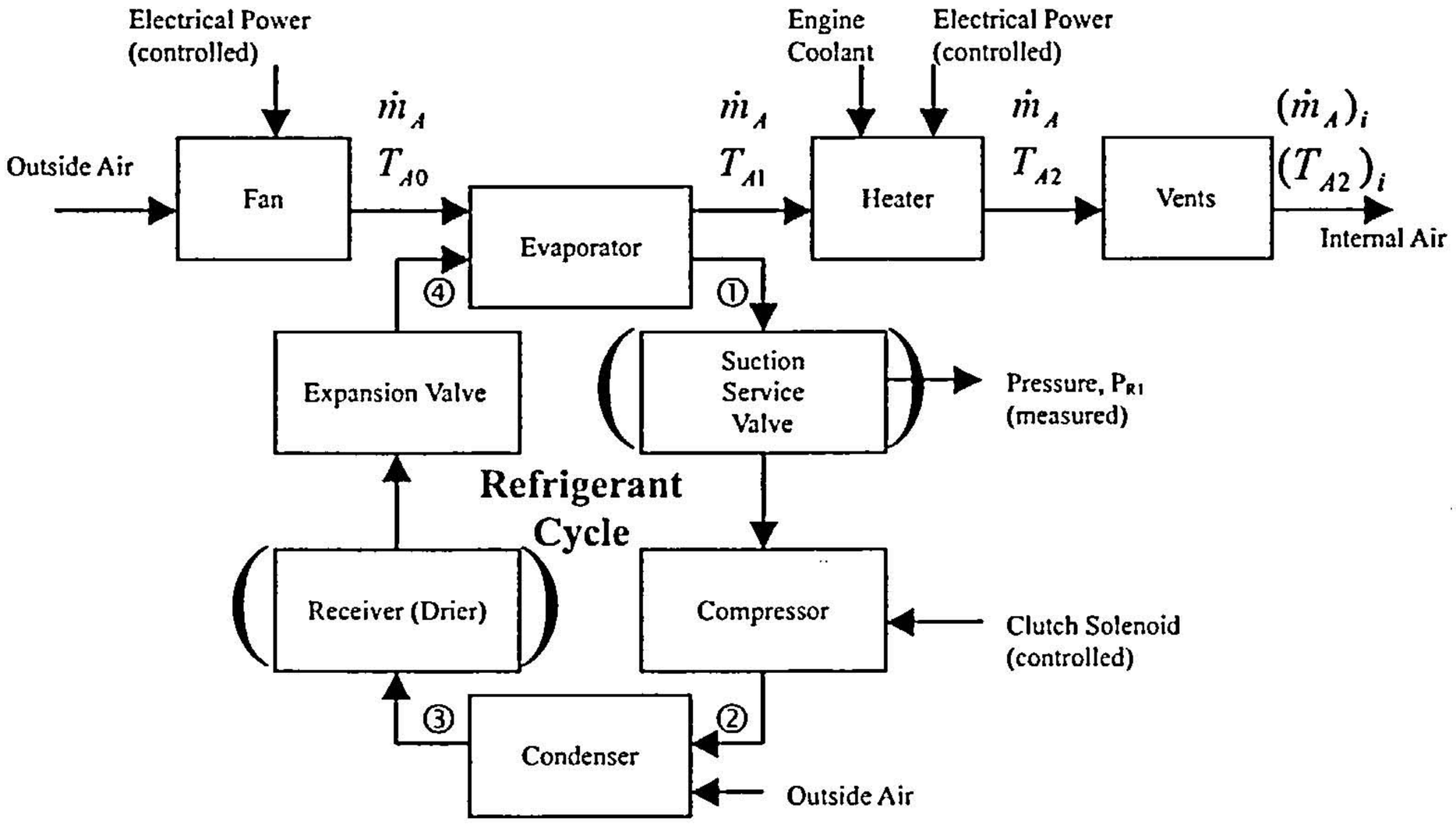


Figure A.1: Components of an automotive heating, ventilation and air conditioning system

The refrigerant is pumped around the cycle by the compressor. The most popular compressors used are the two cylinder reciprocating type, the four cylinder RADIAL and the six cylinder AXIAL types. Refrigerant is sucked in to the compressor at low pressure and is forced out at a higher pressure. The compressor supplies work to the refrigerant and is powered by means

of a drive belt from the engine. The drive belt is connected to the compressor clutch, which can either engage the compressor or not. With a solenoid actuator the compressor clutch can control the refrigerant flow with a two-position (or on-off) control action, however in most cases the clutch is only used to switch the refrigerant cycle on or off (linked to the economy switch). The state of the art in compressor design and control is ever increasing as evident in papers [50] and [51].

The refrigerant used in the system was originally a substance called R12 however with the abolition of CFC's and a general move away from using ozone unfriendly materials, a replacement for R12 was necessary. This provided an interesting problem since R12 is still the best engineering solution as a refrigerant and suggested replacements require system retrofitting and operational changes. Additional costs and efficiency reduction have supplied good motivation for research in this area and many papers have been issued under this topic such as [52].

Considering the refrigerant cycle starting at the point 1 and moving around to 4: If assuming an adiabatic process with negligible kinetic energy differences between input and output then the work of the compressor, $\dot{W}$ in $(J/s)$, can be described by equation (A-1). If $h_n$ is the enthalpy at position $n$ shown on figure A.1 then $h_2$ should be greater than $h_1$ and thus $\dot{W}$ is positive.

$$\dot{W} = \dot{m}\,(h_2 - h_1) \tag{A-1}$$

The high pressure refrigerant is then condensed to a lower enthalpy. Simplistically the kinetic energy differences between input and output become negligible and the fluid does no work. This reduces the steady flow energy balance to equation (A-2), where $\dot{Q}_{Condenser}$ is the heat transferred to the refrigerant and $h_2 > h_3$ making $\dot{Q}_{Condenser}$ negative.

$$\dot{Q}_{Condenser} = \dot{m}\,(h_3 - h_2) \tag{A-2}$$

Next the refrigerant is throttled through the expansion valve which reduces the pressure. Heat transfer into the valve can be ignored and again the kinetic differences are negligible. No work is done and so the energy equation (A-3) is simply an equality.

$$h_4 = h_3 \tag{A-3}$$

Finally the refrigerant undertakes the evaporation process before starting the cycle again. The evaporator pulls in heat energy to evaporate the refrigerant. The pressure of the refrigerant is kept constant, the fluid does no work and with the assumption that the kinetic energy differences between input and output become negligible, the energy equation can be written as equation (A-4), with $\dot{Q}_{Evaporater}$ being the heat transferred to the refrigerant with $h_1 > h_4$ and $\dot{Q}_{Evaporater}$ being positive.

$$\dot{Q}_{Evaporater} = \dot{m}\,(h_1 - h_4) \tag{A-4}$$

The coefficient of performance of a refrigerator is defined as the useful output over the input. The effectiveness of the system is dependent on how much heat is taken away by the evaporator. Hence the coefficient of performance of the refrigeration is shown in equation (A-5). This is not termed as efficiency since the coefficient of performance could have a value greater than 1.

$$CP_{Refrigerator} = \frac{Q_{Evaporater}}{W} \tag{A-5}$$

The refrigerant cycle T-s diagram will look similar to figure A.2.

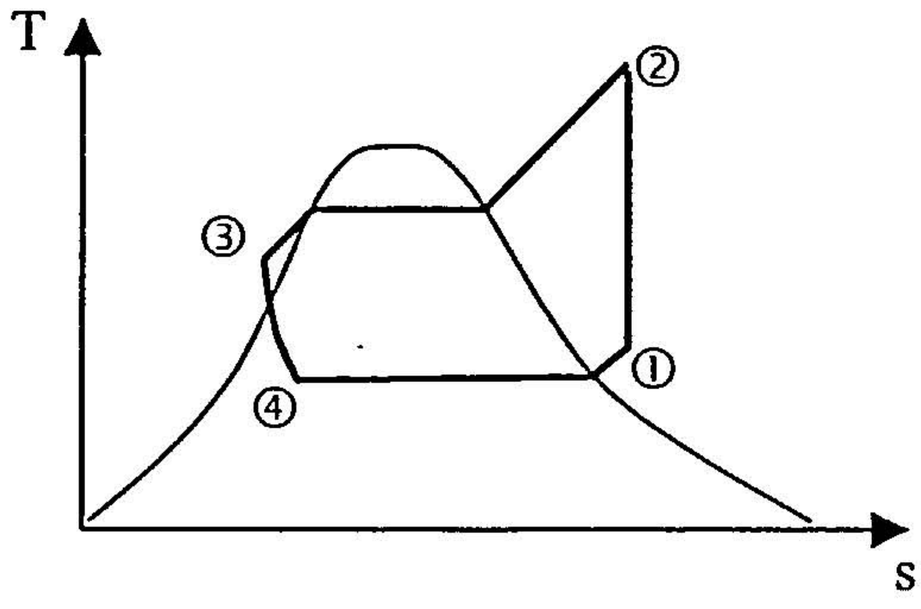


Figure A.2: Example of thermodynamic refrigerant cycle T-s diagram

Note that expansion through the throttling valve is not isentropic which results in a smaller coefficient of performance. However the alternative is to use an expansion machine which could extract work from the system and would give a better refrigeration effect i.e. heat extracted per unit mass of refrigerant. In the automotive application the benefits of using an expansion machine are not worth the complication to the system. It can also be seen from figure A.2 that the refrigerant is superheated before entering the compressor and although this gives the compressor more work, which reduces the coefficient of performance, it avoids liquid

refrigerant washing the compressor's lubricating oil into the evaporator. If the evaporator does superheat the refrigerant as shown in the diagram then this ideal cycle will have an increased refrigeration effect over other cycles with non-superheated regions (such as the reverse Carnot cycle).

When describing the 2 regions (2-phase and superheated) each will have different evaporator properties but this is only taken in to consideration for more advanced simulations. Another addition for more advanced simulations is the condensation from the air on the outside wall of the evaporator. This will take place if the temperature of the evaporator wall becomes lower than the 'Due Point' or value of formation. An indication of the value of formation for air at 1 bar, 28 $^{o}$C and with a relative humidity * of 30% is 8.8 $^{o}$C. Condensation will affect the convection heat transfer coefficient in a way that is difficult to predict and will depend on materials and surface geometry.

The suction service valve is used to empty and fill the system with refrigerant and can also be used to measure the system pressure. The receiver-drier is used to separate the superheated vapour and the liquid but can also be used to filter out dirt and moisture. The heater and the evaporator are similar in nature and provide hot and cold surface areas respectively for conditioning the air flowing through the system. Engine coolant is diverted into the heater system to provide a heat source. The flow of coolant can be controlled by the use of a valve and the temperature of the coolant is dependent on the speed of the engine.

* "Relative Humidity is the ratio of the actual partial pressure of the vapour to the partial pressure of the vapour when the air is saturated at the same temperature" as defined by [53]

# B : Properties of the HVAC Unit and Development of a Physical Model

## Plant Parameters and Properties of Air for Approximate Calculations

The parameters of the HVAC plant were measured approximately by conventional methods and are listed below:

$Vol_{all} = 0.9242\ m^3$ : Volume of air in the HVAC plant from the heaters to the outlet nozzel.

$Vol_{cool} = 0.6742\ m^3$ : Volume of air in the HVAC plant from the point where the heater walls were heated (taking heat from the air).

$A = 7.12168\ m^2$ : Area of the heated HVAC walls.

$W_{thk} = 0.002\ m$ : Wall thickness.

$ExtDim = 0.22\ m$ : Exit diameter of nozzle.

$EquDim = 0.47\ m$ : Equivalent diameter of HVAC plant when assumed as a tube duct.

$I_H = 8.5\ Amps$ : Maximum electrical current through heaters.

$V_H = 240\ Volts$ : Maximum electrical voltage in the heaters.

The Properties of Air for Approximate Calculations:

$c_{p(Air)} = 1.005 \cdot 10^3\ J/(Kg\ ^oC)$ : Specific Heat Capacity, (constant pressure).

$c_{v(Air)} = 0.718 \cdot 10^3\ J/(Kg\ ^oC)$ : Specific Heat Capacity, (constant volume).

$R = 287\ J/(Kg\ ^oK)$ : Specific Gas Constant.

$P_{(Atm)} = 1.01325 \cdot 10^5\ N/m^2$ : Atmospheric Pressure.

Properties of Air at Low Pressure and at 310 $^o$K:

$\mu = 1.892 \cdot 10^{-5}\ Kg/(m\ s)$ : Viscosity of Air

$k = 0.027\ W/(m\ ^oC)$ : Thermal Conductivity

$\rho_{(Air)} = 1.1415\ Kg/m^3$ : Density of Air

Properties of Steel for Approximate Calculations:

$c_p = 0.46 \cdot 10^3\ J/(Kg\ ^oC)$ : Specific Heat Capacity

$\rho_{(St)} = 7800\ Kg/m^3$ : Density of Steel

Using the measured parameters of the HVAC plant and the properties of air and steel for approximate calculations, more useful values can be calculated:

$m_{all} = \rho_{(Air)} \cdot Vol_{all} = 1.0550\ Kg$ : Mass of air in the HVAC plant.

$m_{cool} = \rho_{(Air)} \cdot Vol_{cool} = 0.7696\ Kg$ : Mass of air being cooled by the heater wall.

$u_m = \frac{(3.2+2.5)}{2} = 2.85\ m/s$ : Air velocity, average of the velocity at the outlet nozzle center and edge respectfully, (see below).

$\dot{m} = \pi \cdot \frac{ExtDim^2}{4} \cdot u_m \cdot \rho_{(Air)} = 0.12367\ Kg/s$ : Air mass transfer rate.

$C_H = C_{p(steel)} \cdot thick \cdot A = 51105.3192\ J/^oC$ : Heat Capacity of Heater Walls

$h = 9.68459$ or $10.0302\ W/(m^2\ ^oC)$ : Heat Transfer Coefficient for heating and cooling respectfully, (see below for the calculation).

$Q_{f(max)} = 6I_H V_H = 12,240\ W$ : Maximum Power Output from HVAC heaters (2 3-phase-heater hence the multiplier of 6).

In deriving these calculations certain assumptions have been made

1. The estimated area of the heater wall is assumed to be the same for the inside as for the outside, i.e. $A = A_{in} = A_{out}$.
2. The value of the gravitational constant $g$ is assumed to be $9.80665 m/s^2$.

## Calculation of Air Velocity

Although the air flow rate through the HVAC system is an input variable it was not varied and was thus thought of as a constant system parameter. The control unit for the fan setting was not electronically variable and had to be set by hand as a percentage setting of the

fan power. To relate the chosen percentage to actual air velocity some measurements were recorded by an electronic manometer.

The traditional manometer is a simple "U" tube with water resting at the bottom, see figure B.1. The pressure difference between the different sides is equivalent to the mass of water that has been displaced or the difference in height between the different water levels. This can be represented as equation (B-1).

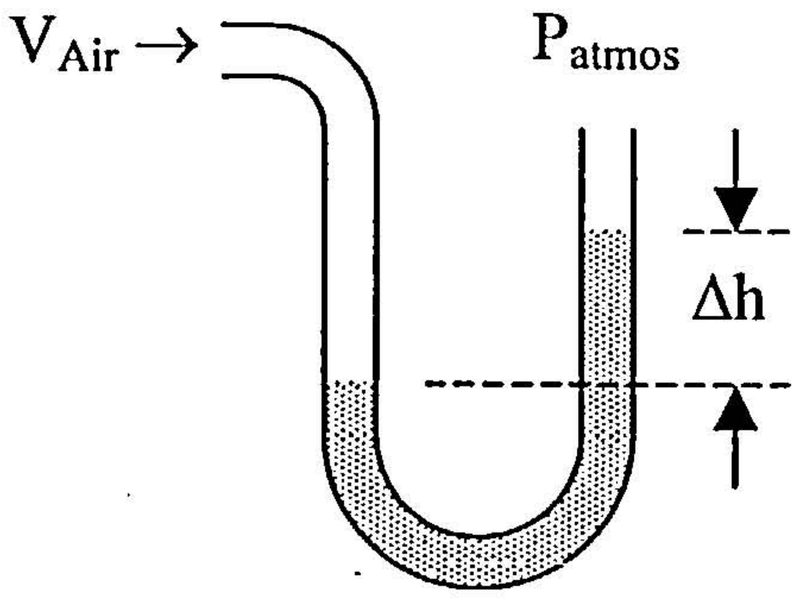


$$\Delta P = \rho_{(H_2O)} g \Delta h \qquad \text{(B-1)}$$

If one end is open to atmospheric pressure and relating pressure to air velocity:

$$\frac{1}{2}\rho_{(Air)} V^2_{(Air)} = \rho_{(H_2O)} g \Delta h \qquad \text{(B-2)}$$

Figure B.1: Explanation of a simple "U" tube manometer

Taking $\rho_{(H_2O)} \approx 1000$ and rearranged equation (B-2) to form equation (B-3).

$$\Rightarrow V_{(Air)} = \sqrt{\frac{2}{\rho_{(Air)}} g \Delta h_{(mm)}} \qquad \text{(B-3)}$$

The electronic manometer displayed results in terms of mm as equivalent difference in height of water in a "U" tube. The readings were taken at the HVAC system nozzle outlet, at the edge of the nozzle outlet, at the face (the same positions as the air temperature measurement (3)) and at the neck area. The results are shown in table B.1. From these results and using equation (B-3) the velocity of the air was calculated and is presented in table B.2.

### Calculation of the Heat Transfer Coefficient

The heat transfer coefficient is calculated for flow within a tube of diameter *EquDim* using equation (B-4) (Ref. J.P. Holman, Heat Transfer, McGraw Hill, 1989.p.274 Example p.283) recommended by Dittus and Boelter relevant for fully developed turbulent flow in smooth tubes for fluids with a Prandtl number between 0.6 and 100 and with moderate temperature differences between the wall and the flow:

| Fan Speed Setting (%) | Manometer measurement (in $mm$) at: Nozzle Outlet | Edge of Nozzle | Center of Face | Neck | Calibration Error |
|---|---|---|---|---|---|
| 20 | 0.08 | 0.02 | 0.05 | 0.00 | 0.01 |
| 23 | 0.18 | 0.10 | 0.12 | 0.07 | 0.01 |
| 25 | 0.25 | 0.20 | 0.23 | 0.15 | 0.02 |
| 27 | 0.40 | 0.25 | 0.25 | 0.15 | 0.01 |
| 30 | 0.60 | 0.30 | 0.35 | 0.25 | 0.01 |
| 32 | 0.78 | 0.35 | 0.48 | 0.30 | 0.01 |
| 35 | 1.10 | 0.70 | 0.65 | 0.50 | 0.01 |
| 40 | 1.60 | 0.80 | 1.05 | 0.75 | 0.01 |
| 50 | 3.00 | 1.50 | 2.00 | 1.20 | 0.03 |

Table B.1: Measurements taken from an electronic manometer to calculate air velocity

| Fan Speed Setting (%) | Velocity (in $m/s$) at: Nozzle Outlet | Edge of Nozzle | Centre of Face | Neck |
|---|---|---|---|---|
| 20 | 1.1724 | 0.5862 | 0.9269 | 0.0000 |
| 23 | 1.7586 | 1.3108 | 1.4359 | 1.0967 |
| 25 | 2.0726 | 1.8538 | 1.9879 | 1.6054 |
| 27 | 2.6216 | 2.0726 | 2.0726 | 1.6054 |
| 30 | 3.2108 | 2.2704 | 2.4523 | 2.0726 |
| 32 | 3.6609 | 2.4523 | 2.8718 | 2.2704 |
| 35 | 4.3474 | 3.4681 | 3.3419 | 2.9310 |
| 40 | 5.2432 | 3.7075 | 4.2475 | 3.5898 |
| 50 | 7.1796 | 5.0767 | 5.8621 | 4.5408 |

Table B.2: Air velocity for different settings of fan power

$$\mathrm{Nu}_{EquDim} = 0.023 \cdot \mathrm{Re}_{EquDim}^{0.8} \cdot \mathrm{Pr}^{n} \tag{B-4}$$

$\mathbf{Nu}_{EquDim} = \frac{h_t c \cdot EquDim}{k}$: Nusselt number
$\mathbf{Re}_{EquDim} = \frac{\rho_{(Air)} \cdot u_m \cdot EquDim}{\mu}$: Reynolds number
$\mathbf{Pr} = \frac{c_{p(Air)} \cdot \mu}{k} \approx 0.70424$: Prandtl number

Where $n$ is 0.3 for cooling or 0.4 for heating. Note that equation (B-4) is for flow along a smooth cylindrical tube. The actual plant consists of ducting with a cross-section of varying shape and contains components which cause disturbance and turbulence to the air flow. Thus equation (B-4) is a gross approximation.

## A Physical Model

A simple physical model of the system can be described by a set of 3 control volumes, see figure B.2. The output of the system is the temperature $T_{A2}$ and the inputs are the energy supplied from the heaters, $\dot{Q}_f$, and the ambient air temperature entering the plant, $T_{A0}$. Mass flow rate is kept constant during the experiments and is assumed to be constant throughout the plant. 'Lumped Heat Capacity Systems' are assumed for the 3 control volumes so that the rates of temperature change within each can be equated to the summation of the energy terms entering. < As stated before it is assumed that the inside surface area of the plant wall is equal to the outside area of the plant wall, $A_{in} = Aout = A$ >.

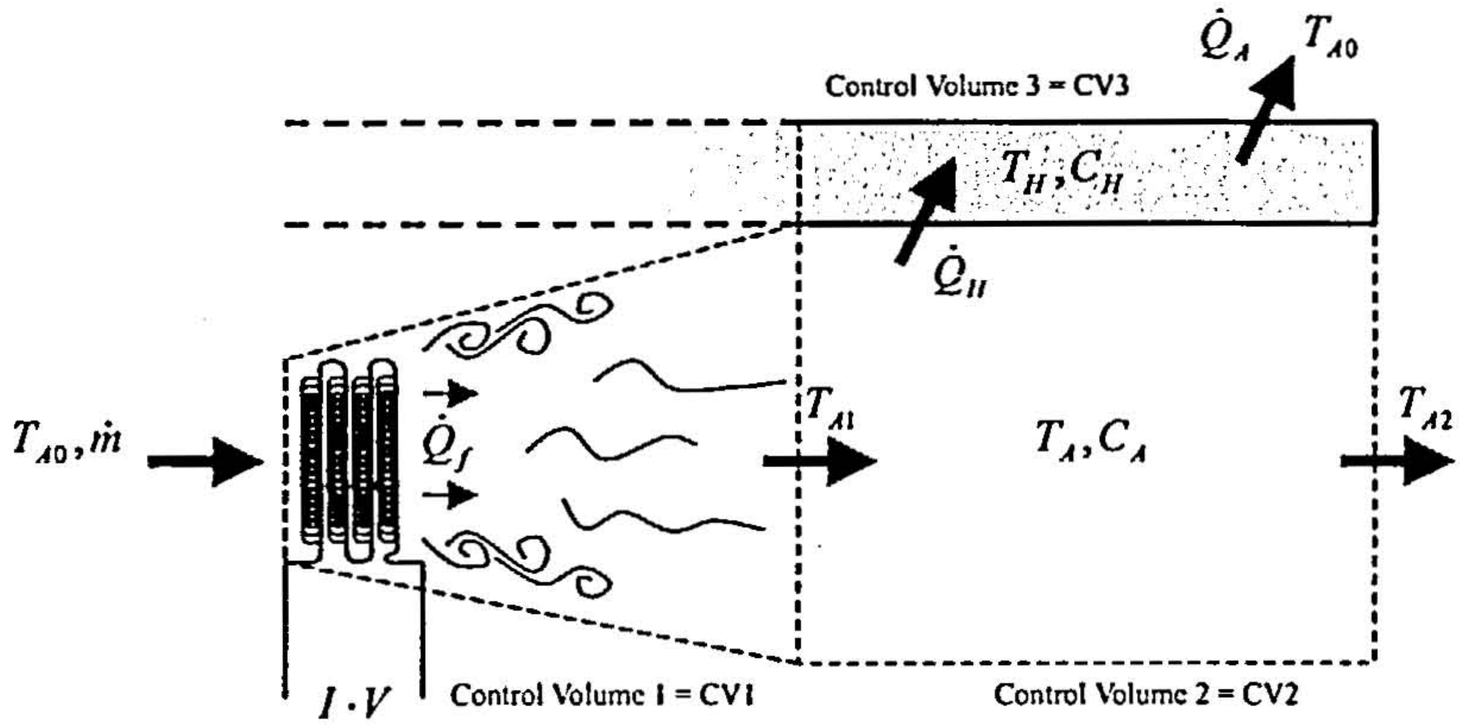


Figure B.2: Block diagram of a simple representation of the HVAC system

The first control volume surrounds the heating elements and the air flowing passed the heating elements to the point where the warm air starts to come in contact with the plant wall. The mass of air in the control volume is thus given as $m_{CV1} = m_{all} - m_{cool} = 0.28537Kg$. It is assumed that the air is mixed and of uniform temperature at this final point and that all the electrical energy has been transferred into thermal energy in the air. The energy transfer for this control volume can be expressed by equation (B-5).

$$\frac{dE_{CV1}}{dt} = m_{CV1} \cdot c_A \frac{dT_{CV1}}{dt} = \dot{m} \cdot c_A \left(T_{A0} - T_{A1}\right) + \dot{Q}_f \qquad \text{(B-5)}$$

The second control volume contains the air flow from the end of the first control volume to the outlet nozzle of the plant. The mass of air in this control volume is just simply $m_{CV2} = m_{cool}$. Energy is lost from the air into the heater walls, $\dot{Q}_H = h \cdot A \left(T_{CV1} - T_{CV3}\right)$, reducing the air temperature thus forming the energy transfer equation (B-6). Note that $\dot{Q}_H$ uses $T_{CV1}$ and not, as might be expected, $\frac{(T_{CV1}+T_{CV2})}{2}$ because it was too low and did not allow the heater

wall to heat up enough which then lead to $T_{CV2}$ not heating up enough. The justification for using $T_{CV1}$ is that the cross-sectional temperature distribution of the air was not constant throughout the plant as assumed by the model thus a hotter channel of air did pass further through the plant in the centre of the ducting.

$$\frac{dE_{CV2}}{dt} = m_{CV2} \cdot c_A \frac{dT_{CV2}}{dt} = \dot{m} \cdot c_A \left(T_{A1} - T_{A2}\right) - h \cdot A \left(T_{CV1} - T_{CV3}\right) \tag{B-6}$$

The third control volume contains the plant wall that is heated by the air flow in control volume 2, $\dot{Q}_H = h \cdot A \left(T_{CV1} - T_{CV3}\right)$. The heater wall is also cooled by the ambient air temperature on the outside, $\dot{Q}_A = h \cdot A \left(T_{CV3} - T_{A0}\right)$. This gives equation (B-7).

$$\frac{dE_{CV3}}{dt} = C_H \frac{dT_{CV3}}{dt} = h \cdot A \left(T_{A0} + T_{CV1} - 2T_{CV3}\right) \tag{B-7}$$

Assuming $T_{CV1} = T_{A1}$, $T_{CV2} = T_{A2}$ and $T_{CV3} = T_H$ and using equations (B-5), (B-6) and (B-7) in the MATLAB SIMULINK environment with the properties of the plant described in section previously a model was simulated. As is seen in figure B.3 the simulation using the parameters evaluated directly show very different dynamics. The method for calculating $h$ was not expected to be sufficient since equation (B-4) is relavent for a smooth tube of constant cross-section. The measured results show no indication of such a difference between the dynamics due to the heaters and those due to the plant walls as is shown by the model. No thought was given to the heater elements warming up as it was expect that this would be so quickly that it would be negligible. Whatever the cause of the slower dynamics the "fix" was to increase the size of the first control volume and hence the mass. The dynamics of the heater wall was altered by changing the thickness value of the wall. As the actual plant consists of ducting with a cross-section of varying shape the thickness of the plant wall was difficult to estimate and yet very sensitive to the model simulation. By re-evaluating the values of $h$ as 17 $W/(m^2\,^oC)$, the size of control volume 1 by an extra 2 $m^3$ and the thickness of the plant wall to 5 $mm$ the model was tuned to the measured data and re-simulated, as shown by the modified simulation line in figure B.3.

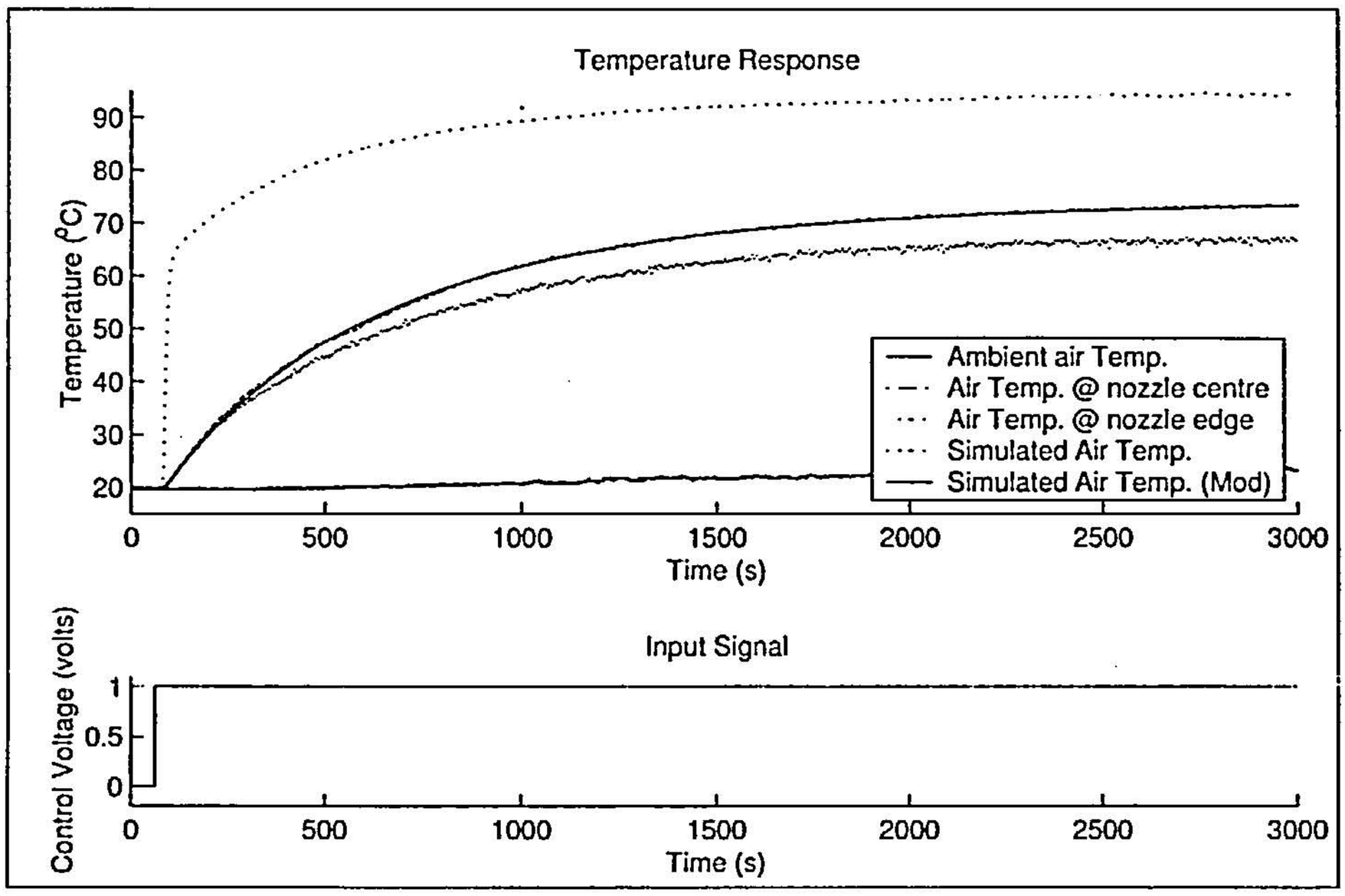


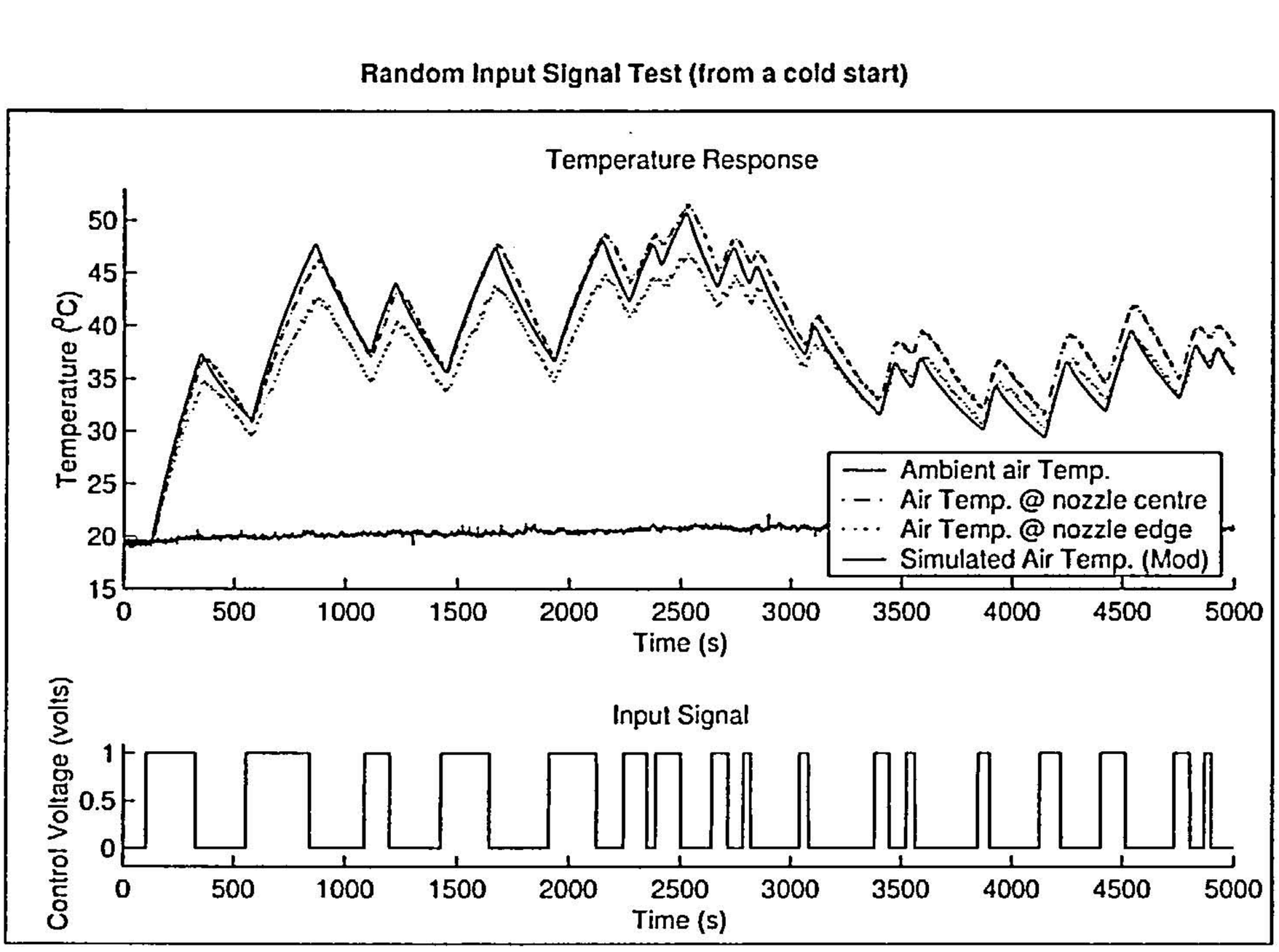


Figure B.3: Measured response and simulated response of a physical model of the HVAC plant

# C : Fuzzy User Reference Learning Controller Structures and Algorithm Diagrams

The method outlined in chapter 5 has been kept general and this is a great advantage when programming the algorithm. The benefit is that general functions can be written without being specific to individual controllers. The controllers themselves are actually the variables that are passed through the general functions. It then makes sense to collect together the variables and parameters of each controller in a structure format. The "control-structure" is then passed through the general functions, which performs the general calculations using the control-structure's parameters, and the control-structure's variables are thus modified.

Consider the control-structure *CtlStr* with the following fields:

CtlStr.In[i] = Latest values of the controller inputs
CtlStr.MAX[i] = Largest allowable value of the input
CtlStr.MIN[i] = Lowest allowable value of the input
CtlStr.MAXMBR[i] = Number of input membership functions
CtlStr.W = Width of output membership functions
CtlStr.CvFc = Convergence factor
CtlStr.BMx[..] = Rule base matrix
CtlStr.LBMx[..] = Memory of learning
CtlStr.Out_Old = Last calculated output
CtlStr.Out_Msrd = Measured output
CtlStr.Out_Calc = Output calculated from inputs
CtlStr.MPrm_Calc = Premise values $P_r$
CtlStr.ActMbr_Calc = Activated output membership functions
CtlStr.Ctr_UIuse = Counter used after a user interaction
CtlStr.Ctr_Learn = Counter used to delay learning
CtlStr.Chck_Flg = Operation flag

There are 3 main functions that need to be carried out on the control-structures:

1. Evaluated the output of a controller for a given set of inputs.
2. Teach the controller by modifying the controllers rule base matrix.
3. Update the counters to operate the control action of the previous 2 functions.

The general functions fit together like so:

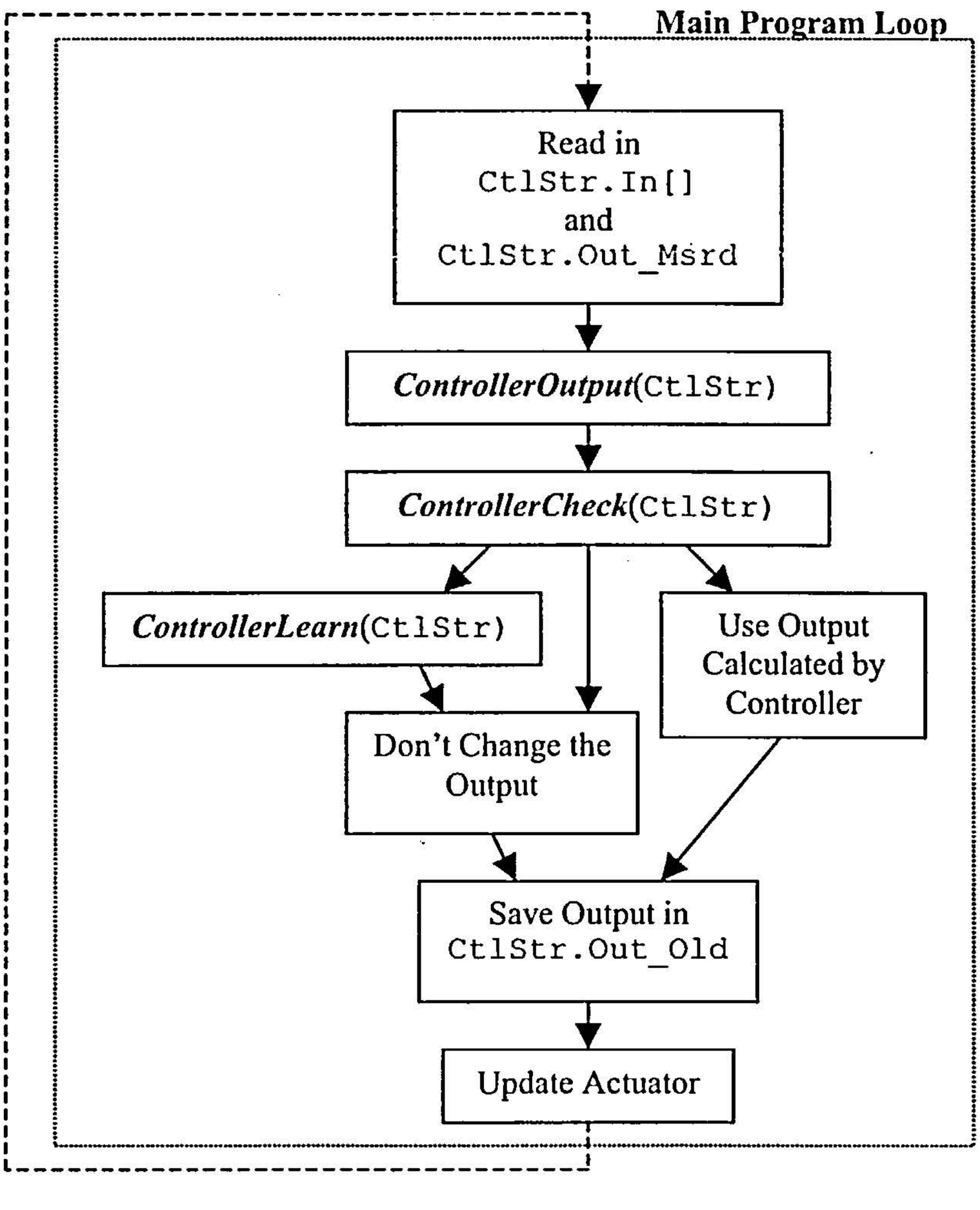


Figure C.1: Main control algorithm loop

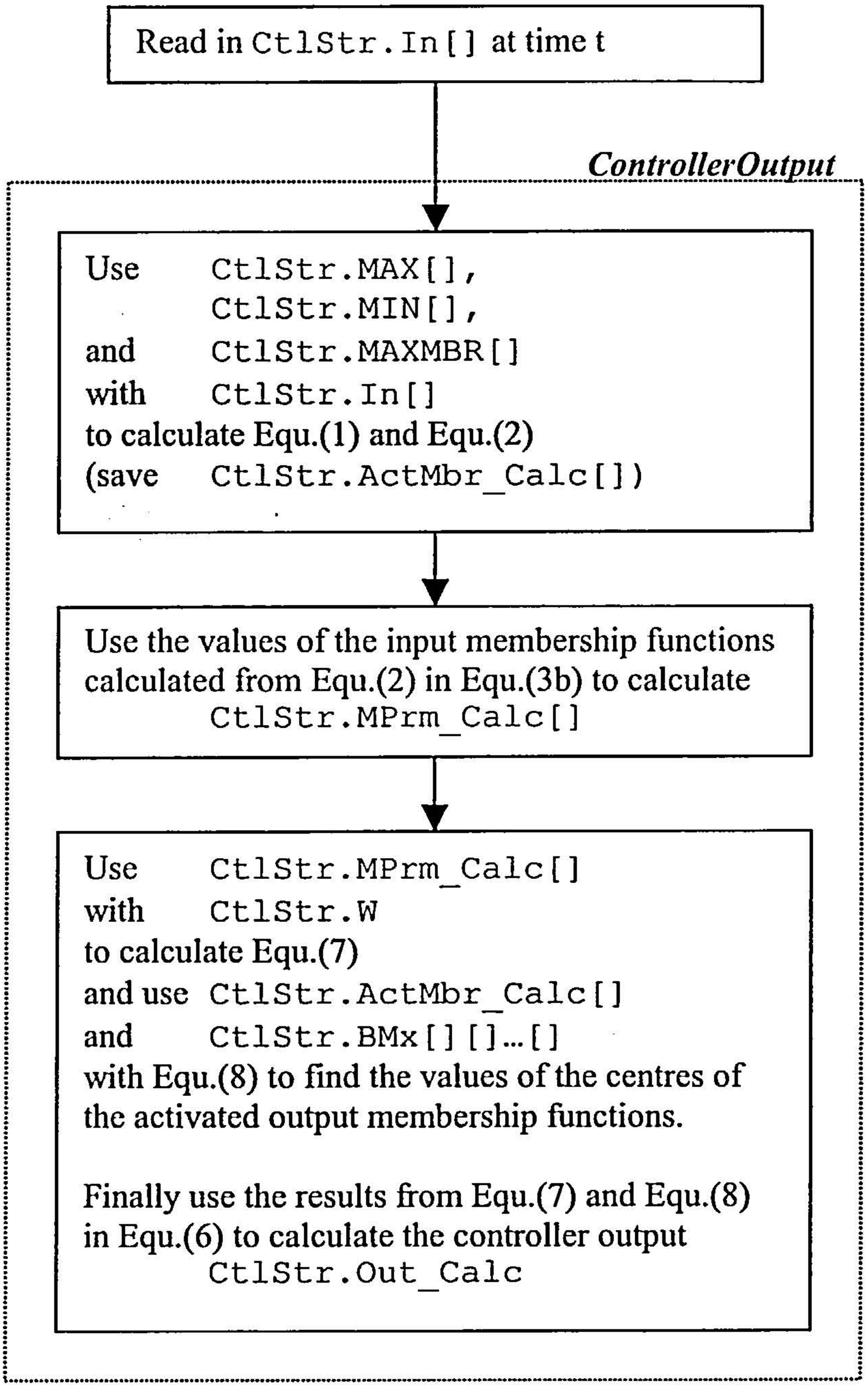


Figure C.2: Diagram of the output function operation

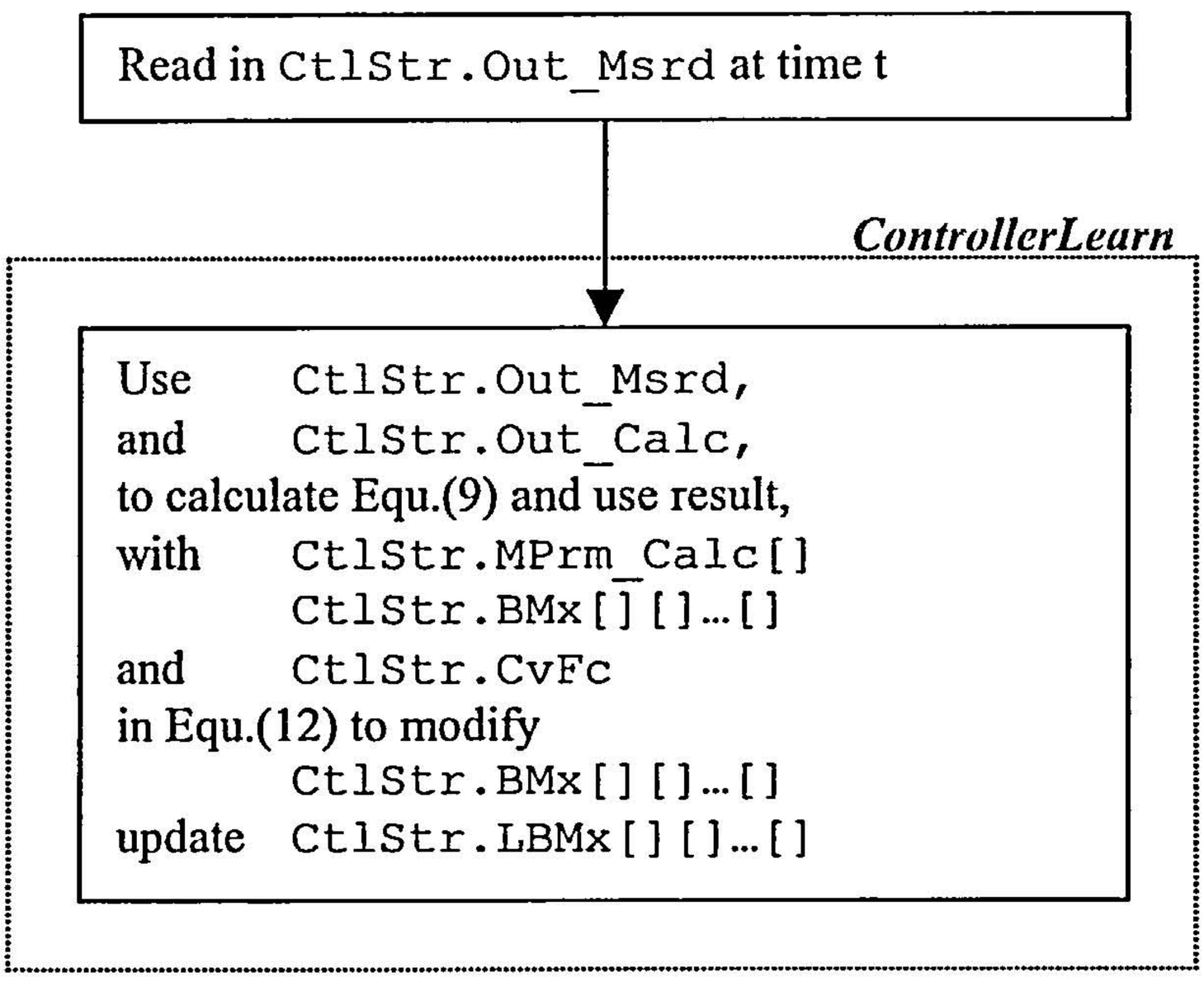


Figure C.3: Diagram of the Learning function operation

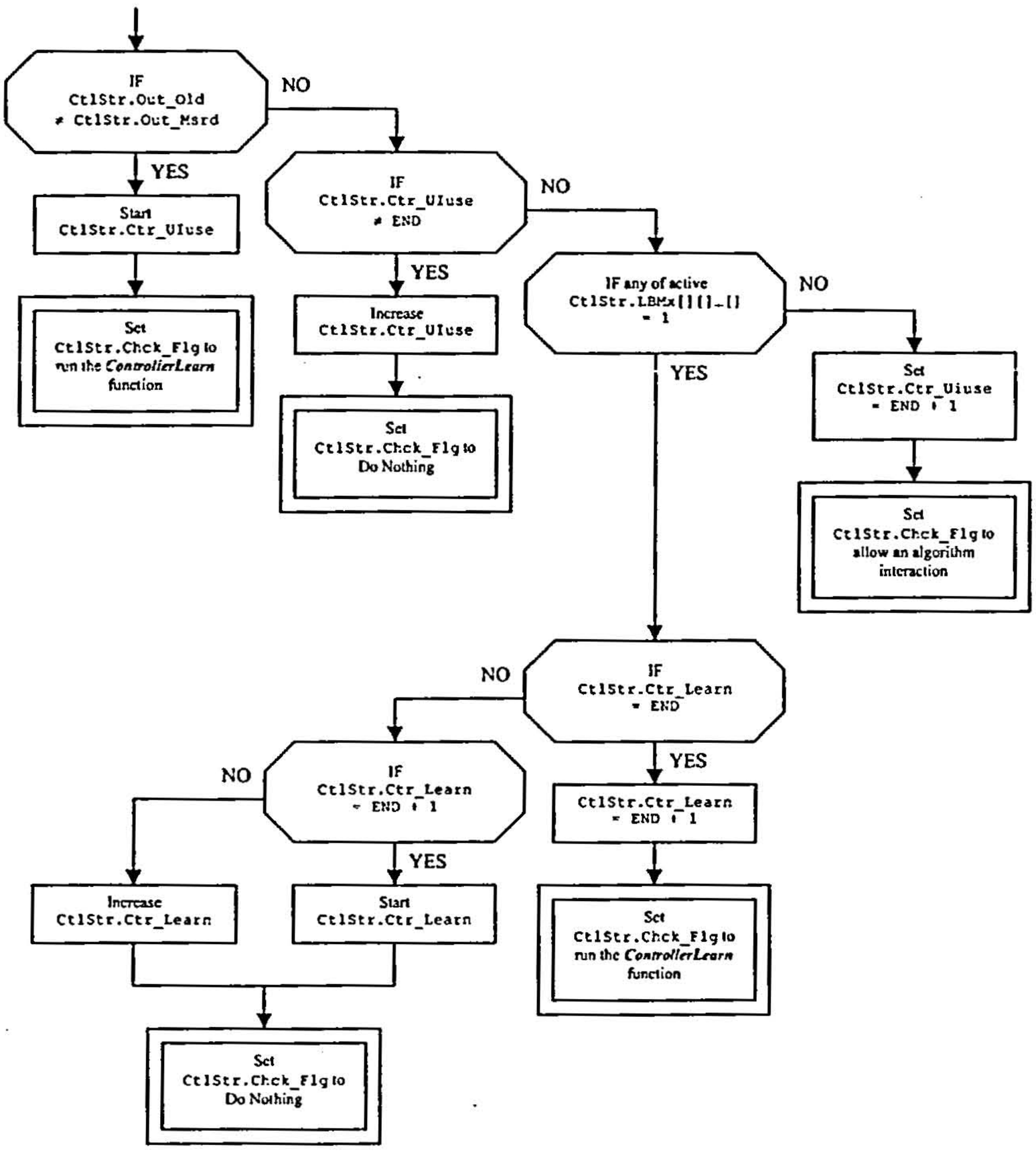


Figure C.4: Flow diagram of the decision function operation

# Bibliography


[1] O. Gaveau and D. Clodic
"Test Bench for Measuring the Energy Consumption of an Automotive Air Conditioning System"
*SAE*, Paper No. 980291, (1998).

[2] W. Chakroun and S. Al-Fahed
"Thermal Comfort Analysis Inside a Car"
*International Journal of Energy Research*, Vol. 21, No. 4, pp. 327-340, (1997).

[3] M. S. Bhatti
"Open Air Cycle Air Conditioning System for Motor Vehicles"
*SAE*, Paper No. 980289, (1998).

[4] D. A. Cobb and T. C. Edwards
"Climate Control System for Electric Vehicles"
*Southcon Conference Record*, pp. 37-41, (1994).

[5] T. Suzuki and K. Ishii (Information supplied by)
"Electric Vehicle Air conditioning"
*Automotive Engineering (Warrendale, Pennsylvania)*, Vol. 104, No. 9, pp. 113-117, (1996).

[6] I. Holmer, H. Nilsson, M. Bohm and O. Noren
"Thermal Aspects of Vehicle Comfort"
*Journal of Physiological Anthropology*, Vol. 14, Part 4, pp. 159-165, (1995).

[7] B. W. Olesen and J. Rosendahl
"Thermal Comfort in Trucks"
*Proceedings - Society of Automotive Engineers*, pp. 349-355, (1990).

[8] P. O. Fanger
"Calculation of Thermal Comfort: Introduction of a Basic Comfort Equation"
*ASHRAE* $74^{th}$ *Annual Meeting (Minneapolis)*, No. 2051, (1967).

[9] D. P. Mehta
"Modeling of Thermal Dynamic Responses of Occupants in Controlled Environments"
*American Society of Mechanical Engineers, Bioengineering Division (Publication) BED*, Vol. 17, pp. 281-284, (1990).

[10] T. M. Chung and W. C. Tong
"Thermal Comfort Study of Young Chinese People in Hong Kong"
*Building and Environment*, Vol. 25, No. 4, pp. 317-328, (1990).

[11] H. Tanaka, M. Kitada, Y. Taniguchi, Y. Ohno, T. Shinagawa and H. Aoki
"Study on Car Air Conditioning System Controlled by Car Occupants' Skin Temperature - Part 2:

Development of a New Air Conditioning System"
*SAE Technical Paper Series*, Paper No. 920170, (1992).

[12] E. H. Wissler
"The Use of Finite Difference Techniques in Simulating the Human Thermal System"
*Physiological and Behavioral Temperature Regulation*, Pub: Charles C. Thomas, pp. 367-388, (1970).

[13] D. Mitchell
"Measurement of the Thermal Emissivity of Human Skin"
*Physiological and Behavioral Temperature Regulation*, Pub: Charles C. Thomas, pp. 25-33, (1970).

[14] G. M. Rapp
"Convective Mass Transfer and the Coefficient of Evaporative Heat Loss from Human Skin"
*Physiological and Behavioral Temperature Regulation*, Pub: Charles C. Thomas, pp. 55-80, (1970).

[15] A. P. Gagge and Y. Nishi
"Standard Humid Operative Temperature - A Single Temperature Measure of Environmental Stress"
*Biology and Medicine*, No. 188, pp. 2051-2061.

[16] J. A. J. Stolwijk
"Mathematical Model of Thermoregulation"
*Physiological and Behavioral Temperature Regulation*, Pub: Charles C. Thomas, pp. 703-721, (1970).

[17] J. L. M. Hensen
"Literature Review on Thermal Comfort in Transient Conditions"
*Building and Environment*, Vol. 25, No. 4, pp. 309-316, (1990).

[18] A. P. Gagge
"Rational Temperature Indices of Man's Thermal Environment and Their use with a 2-Node Model of his Temperature Regulation"
*Federation Proceedings American Soc. Exp. Biol.*, Vol. 32, No. 5, pp. 1572-1582, (1973).

[19] A. P. Gagge, A. P. Fobelets and L. G. Berglund
"A Standard Predictive Index of Human Response to the Thermal Environment"
*ASHRAE Trans.*, 92:2B, pp. 709-731, (1986).

[20] B. W. Jones and Y. Ogawa
"Transient Interaction Between the Human and the Thermal Environment"
*ASHRAE Transactions, Winter Meeting Anaheim*, Vol. 98, No. 1, pp. 189-195, (1992).

[21] E. Arens, R. Gonzalez and L. Berglund
"Thermal Comfort Under an Extended Range of Environmental Conditions"
*ASHRAE Transactions, Winter Meeting San Fransisco*, Vol. 92, No. 1B, pp. 18-26, (1986).

[22] F. Mingrino and G. T. Rivalta
"An Automatic Climate Control Based on the Concept of Equivalent Temperature"
*SAE International Conference*, SP-950022, (1995).

[23] Y. Khamsi, C. Petitjean and V. Pomme
"Modeling of Automotive Passenger Compartment and Its Air Conditioning System"
*SAE Special Publications*, Vol. 1347, pp. 35-43, (1998).

[24] W. Liu and Z. Chen
"Dynamic Simulation of HFC134a Automobile Air Conditioning System"
*Proceedings of the International Conference on Energy and Environment (ICEE)*, pp. 315-320, (1996).

[25] Y. Taniguchi, H. Aoki, K. Fujikake, H. Tanaka and M. Kitada
"Study on Car Air Conditioning System Controlled by Car Occupants' Skin Temperature - Part 1:

Research on a Method of Quantitative Evaluation of Car Occupants' Thermal Sensations by Skin Temperatures"
*SAE Technical Paper Series*, Paper No. 920169, pp. 13-19, (1992).

[26] "Determination of the PMV and PPD indices and specification of the conditions for thermal comfort"
*British Standard BS-EN-ISO 7730*, (1995).

[27] M. Ueda, Y. Taniguchi, A. Asano, M. Mochizuki, T. Ikegami and T. Kawai
"An Automobile Heating, Ventilating and Air Conditioning (HVAC) System with a Neural Network for Controlling the Thermal Sensations Felt by a Passenger"
*JSME International Journal, Series B: Fluids and Thermal Engineering*, Vol. 40, No. 3, pp. 469-477, (1997).

[28] K. Furuse and T. Komoriya
"Study of Passenger's Comfort in Non-Uniform Thermal Environments of Vehicle Compartment"
*JASE Review*, Vol. 18, No. 4, pp. 411-414, (1997).

[29] K. J. Åström and B. Wittenmark
"Computer-Controlled Systems: Theory and Design"
*Prentice-Hall Inc.*, Ed. 3, (1997).

[30] D. McK. Kerslake
"Factors Concerned in the Regulation of Sweat Production in Man"
*Jour. Physiology*, Vol. 127, pp. 329-346, (1955).

[31] T. H. Benzinger, C. Kitzinger and A. W. Pratt
"The Human Thermostat"
*Temperature, Its Measurement and Control on Science and Industry*, Vol. 3, Part III, Ch. 56, pp. 637-665.

[32] J. D. Hardy and E. F. DuBois
"The Technic of Measuring Radiation and Convection"
*Journal of Nutrition*, Vol. 15, No. 5, pp. 461-475, (1937).

[33] N. L. Ramanathan
"A New Weighting System for Mean Surface Temperature of the Human Body"
*Journal of Applied Physiology*, Vol. 19, No. 3, pp. 531-533, (1964).

[34] J. D. Hardy
"Thermal Comfort: Skin Temperature and Physiological Thermoregulation"
*Physiological and Behavioral Temperature Regulation* Pub: Charles C. Thomas, pp. 856-873, (1970).

[35] T. J. Love, J. E. Francis and J. D. Haberman
"A Comparison of Predicted Skin Temperatures with Thermographic Measurements"
*Biology and Medicine*, No. 189, pp. 2065-2072.

[36] K. C. Wei and G. A. Dage
"Intelligent Automotive Climate Control Systems"
*Proceedings of the IEEE International Conference on Systems, Man and Cybernetics*, Vol. 4, pp. 2977-2982, (1995).

[37] G. L. Ghiardi
"Occupant Thermal Comfort Evaluation"
*SPIE Conference on Thermosense XXI*, Vol. 3700, pp. 324-331, (1999).

[38] T. Takemori, N. Miyasaka and S. Osaka
"Thermal Comfort Sensor Based on Probabilistic Energy Neural Network"
$90^{th}$ *International Joint Conference on Neural Networks (IJCNN)*, (1990).

[39] M. Ueda, Y. Taniguchi and H. Aoki
"A New Method to Predict the Thermal Sensation of an Occupant Using a Neural Network and Its Application to the Automobile HVAC System"
*JSME International Journal, Series B: Fluids and Thermal Engineering*, Vol. 40, No. 1, pp. 166-174, (1997).

[40] M. Ueda, Y. Taniguchi, A. Asano and M. Mochizuki
"Prediction of Automobile Passenger's Skin Temperature using a Neural Netwotk"
*JSME Int. Journal, Series B*, Vol. 40, No. 2, pp. 328-336, (1997).

[41] B. A. Saunders
"Automatic Control of Thermal Sensation in the Automotive Cabin"
*European Control Conference*, Porto, (2001).

[42] B. Gach, M. Lang and J-C. Riat
"Fuzzy Controller for Thermal Comfort in a Car Cabin"
*SAE Special Publications*, Vol. 1239, pp. 9-16, (1997).

[43] C. C. Federspiel and H. Asada
"Transfer of Human Preference to Smart Machines: A Case Study of Human Thermal Comfort Control"
*Proceedings of the American Control Conference*, pp. 2833-2839, (1990).

[44] C. Reitter and K. Holgrew
"Basics of User Adaptive Interfaces for Air Conditioning Control"
*Computational Intelligence for Modelling, Control & Automation, M. Mohammadian (Ed.), IOS Press*, pp. 244-248, (1999).

[45] L. I. Jr. Davis, T. F. Sieja, R. W. Matteson, G. A. Dage and R. Ames
"Fuzzy Logic for Vehicle Climate Control"
*IEEE International Conference on Fuzzy Systems*, Vol. 1, pp. 530-534, (1994).

[46] L. F. D. Antoni, S. Pasini and P. Vercesi
"Simulation of a Fuzzy Controller, in Personal Set Up of Environmental Characteristics"
*Proceedings of the Intersociety Energy Conservation Engineering Conference*, Vol. 3-4, pp. 1613-1617, (1997).

[47] K. M. Passino and S. Yurkovich
"Fuzzy Control"
*Addison Wesley Longman, Inc.*, (1998).

[48] J. Kang and S. Park
"Development of Comfort Sensing System for Human Environment"
*Mechatronics*, Vol. 8, No. 5, pp. 459-466, (1998).
See also:
J. Kang, Y. Kim, H. Kim, J. Jeong and S. Park
"Comfort Sensing System for Indoor Environment"
*International Conference on Solid State Sensors and Actuators*, Vol. 1, pp. 311-314, (1997).

[49] L. S. Davidson and R. M. Kowalczyk
"Microcontroller Technology Enhancements to Meet Ever-Increasing Engine Control Requirements"
*Proceedings - Society of Automotive Engineers*, No. P-260, pp. 67-69, (1992).

[50] R. H. King
"Rotary Vane Compressor Improves AC Efficiency"
*Design News (Boston)*, Vol. 51, No. 10, pp. 65-66, (1996).

See also:
http://www.manufacturing.net/magazine/dn/archives/1996/dn0520.96/10d1401.htm

[51] A. Bartlett, D. Standaert and E. Ratts
"A Real-Time Computer System for the Control of Refrigerant Flow"
*SAE Special Publications*, Vol. 1239, pp. 17-28, (1997).

[52] T. Kiatsiriroat and T. Euakit
"Performance Analysis of an Automobile Air-Conditioning System with R22/R124/R152a Refrigerant"
*Applied Thermal Engineering*, Vol. 17, No. 11, pp. 1085-1097, (1997).

[53] G. C. F. Rogers and Y. R.Mayhew
"Engineering Thermodynamics Work and Heat Transfer"
*Longman Group UK Ltd*, Ed. 4, (1992).

## Other Interesting Publications

[54] R. T. Wilkinson, R. H. Fox, R. Goldsmith, I. F. G. Hampton and H. E. Lewis
"Psychological and Physiological Responses to Raised Body Temperature"
*Journal of Applied Physiology*, Vol. 19, No. 2, pp. 287-291, (1964).

[55] T. Bedford
"The Effective Radiating Surface of the Human Body"
*Journal of Hygiene*, Vol. 35 No. 3, pp. 303-306, (1935).

[56] T. Bedford
"Skin Temperature in Relation to the Warmth of the Environment"
*Journal of Hygiene*, Vol. 35, No. 3, pp. 307-317, (1935).

[57] W. H. Teichner
"Assessment of Mean Body Surface Temperature"
*Journal of Applied Physiology*, Vol. 12, No. 2, pp. 169-176, (1958).

[58] M. Lipkin and J. D. Hardy
"Measurement of Some Thermal Properties of Human Tissues"
*Journal of Applied Physiology*, Vol. 7, pp. 212-217, (1954).

[59] T. Horikoshi, Y. Kobayashi and T. Tsuchikawa
"Indicies of Combined and Independent effect of Thermal Environmental Variables Upon the Human Body"
*ASHRAE Transactions, Winter Meeting New York City*, No. 1, pp. 228-238, (1991).

[60] F. C. Houghten and C. P. Yaglou
"Determination of the Comfort Zone"
*ASHVE Trans.*, Vol. 29, p. 361, (1923).

[61] S-J. Lee, J-H. Yoon and K-W. Kim
"Simultaneous Measurement of Temperature and Velocity Fields of Ventilation Flow in a Passenger Compartment"
*SAE*, Paper No. 980292, (1998).

[62] C-E. A. Winslow, L. P. Herrington and A. P. Gagge
"Physiological Reactions and Sensations of Pleasantness Under Varying Atmospheric Conditions"
*ASHVE Trans.*, Vol. 44, pp. 179-194, (1939).

[63] W. Koch, B. H. Jennings and C. M. Humphreys
"Environmental Study II: Sensation Responses to Temperature and Humidity Under Still Air Conditions in the Comfort Range"
*ASHRAE Trans.*, Vol. 66, p. 264, (1960).

[64] A. P. Gagge, J. D. Hardy and G. M. Rapp
"Exploratory Study of Comfort for High Temperature Sources of Radiant Heat"
*ASHRAE Trans.*, Vol. 71, Part II, pp. 19-26, (1965).

[65] R. G. Nevins, F. H. Rohles, W. Springer and A. M. Feyerherm
"A Temperature Humidity Chart for Thermal Comfort of Seated Persons"
*ASHRAE Trans.*, Vol. 72, Part I, pp. 283-291, (1966).

[66] P. E. McNall, J. Jaax, F. H. Rohles, R. G. Nevins and W. Springer
"Thermal Comfort (Thermally Neutral) Conditions for Three Levels of Activity"
*ASHRAE Trans.*, Vol. 73, Part I, (1967).

[67] A. P. Gagge, C-E. A. Winslow and L. P. Herrington
"The Influence of Clothing on Physiological Reactions of the Human Body to Varying Environmental Temperatures"
*American Journal of Physiology*, Vol. 124, pp. 30-50, (1938).

## Web Page Links

[68] ASHRAE (The American Society of Heating Refrigerating and Air Conditioning Engineers) Home Page
http://www.ctashrae.org/

[69] SAE (Society of Automotive Engineers) Home Page
http://turboguide.com/data2/cdprod1/doc/cdrom.frame/006/881.pub.Society.of.Automotive.Engineers.Inc.SAE.html

[70] ISO (International Organization for Standardization) Home Page
http://www.iso.ch/

[71] T. Olcott
"The History of Automotive Air Conditioning"
wysiwyg://119/http://vintagecars.tqn.com/library/weekly/aa050898.htm

[72] C. Bede
"Air Conditioning Systems"
http://www.familycar.com/ac1.htm

[73] R. H. King
"Rotary Vane Compressor Improves AC Efficiency"
http://www.manufacturing.net/magazine/dn/archives/1996/dn0520.96/10d1401.htm